

Aus dem Institut für Parasitologie und Tropenveterinärmedizin  
des Fachbereichs Veterinärmedizin  
der Freien Universität Berlin  
in Kooperation mit dem  
Forschungszentrum Borstel  
Leibniz-Zentrum für Medizin und Biowissenschaften  
Laborgruppe Veterinär-Infektiologie und -Immunologie

The Role of Heat Shock Protein 90 (HSP90) in the Transformation of *Theileria annulata*-  
infected Cells and the Parasite Stage Differentiation

Inaugural-Dissertation  
zur Erlangung des Grades eines  
Doktors der Veterinärmedizin  
an der  
Freien Universität Berlin

vorgelegt von  
Sara Basher Taha Mohammed  
Tierärztin  
aus Algzeira, Sudan

Berlin 2015

Journal-Nr.:3784

## **Gedruckt mit Unterstützung des Deutschen Akademischen Austauschdienstes**

Gedruckt mit Genehmigung des Fachbereichs Veterinärmedizin  
der Freien Universität Berlin

Dekan: Univ.-Prof. Dr. Jürgen Zentek  
Erster Gutachter: Prof. Dr. Jabbar S. Ahmed  
Zweiter Gutachter: Univ.-Prof. Dr. Hafez Mohamed Hafez  
Dritter Gutachter: Prof. Dr. Peter-Henning Clausen

*Deskriptoren (nach CAB-Thesaurus):*

cattle, buffaloes, *Theileria annulata*, heat shock proteins, apoptosis, transformation, differentiation, antibodies, immunofluorescence, polymerase chain reaction, cell proliferation (MeSH)

Tag der Promotion: 06.08.2015

Bibliografische Information der *Deutschen Nationalbibliothek*

Die Deutsche Nationalbibliothek verzeichnet diese Publikation in der Deutschen Nationalbibliografie; detaillierte bibliografische Daten sind im Internet über <http://dnb.ddb.de> abrufbar.

ISBN: 978-3-86387-632-6

**Zugl.: Berlin, Freie Univ., Diss., 2015**

Dissertation, Freie Universität Berlin

**D 188**

Dieses Werk ist urheberrechtlich geschützt.

Alle Rechte, auch die der Übersetzung, des Nachdruckes und der Vervielfältigung des Buches, oder Teilen daraus, vorbehalten. Kein Teil des Werkes darf ohne schriftliche Genehmigung des Verlages in irgendeiner Form reproduziert oder unter Verwendung elektronischer Systeme verarbeitet, vervielfältigt oder verbreitet werden.

Die Wiedergabe von Gebrauchsnamen, Warenbezeichnungen, usw. in diesem Werk berechtigt auch ohne besondere Kennzeichnung nicht zu der Annahme, dass solche Namen im Sinne der Warenzeichen- und Markenschutz-Gesetzgebung als frei zu betrachten wären und daher von jedermann benutzt werden dürfen.

This document is protected by copyright law.

No part of this document may be reproduced in any form by any means without prior written authorization of the publisher.

Alle Rechte vorbehalten | all rights reserved

© Mensch und Buch Verlag 2015

Choriner Str. 85 - 10119 Berlin

verlag@menschundbuch.de – [www.menschundbuch.de](http://www.menschundbuch.de)

## *D.E.D.I.C.A.T.I.O.N*

*This thesis is dedicated to my children, Hussam and Muram  
and my family members, who offered me unconditional love and  
support throughout the years.*

*Thanks for everything.*



---

# Table of Contents

	Page
<b>List of figures.....</b>	<b>iv</b>
<b>List of tables.....</b>	<b>vii</b>
<b>List of abbreviations .....</b>	<b>viii</b>
<b>1 Introduction .....</b>	<b>1</b>
<b>2 Literature review.....</b>	<b>3</b>
2.1 Genus <i>Theileria</i> .....	3
2.2 <i>Theileria</i> in bovine .....	3
2.2.1 <i>T.annulata</i> .....	3
2.3 Life cycle of <i>Theileria</i> .....	4
2.4 Clinical signs .....	5
2.5 Pathogenesis and immunity to <i>Theileria</i> infection.....	5
2.6 Host parasite interaction.....	6
2.6.1 Invasion process .....	7
2.6.2 Induction and maintenance of transformation and proliferation.....	7
2.7 Apoptosis.....	9
2.7.1 Pathways leading to apoptosis.....	10
2.7.2 Inhibition of apoptosis.....	11
2.8 Stage differentiation .....	11
2.9 HSPs.....	12
2.9.1 HSPs and parasitic infection .....	13
2.10 HSP90.....	13
2.10.1 Structure of HSP90.....	14
2.10.2 HSP90 and parasitic infection.....	15
2.11 Aim of this study .....	15
<b>3 Materials and Methods .....</b>	<b>16</b>
3.1 Materials.....	16
3.1.1 Cells and Cell lines.....	16
3.1.2 Chemicals, reagents and Kits .....	16
3.1.3 Buffers, solutions and media .....	18
3.1.4 Primers .....	20
3.1.5 Antibodies .....	21
3.1.6 Bacteria, vectors and enzymes .....	22
3.1.7 Lab supplies.....	23
3.1.8 Equipment .....	23
3.1.9 Software .....	24

---

3.2	Methods.....	25
3.2.1	Cell culture.....	25
3.2.2	Sub-culturing and cell counting.....	25
3.2.3	Molecular biological methods.....	26
3.2.4	Expression and purification of recombinant <i>T. annulata</i> HSP90.....	32
3.2.5	Protein analysis.....	34
3.2.6	Generation of rabbit anti- <i>T. annulata</i> HSP90 antiserum.....	36
3.2.7	Isolation of <i>T.annulata</i> schizonts.....	38
3.2.8	Cytospin slides.....	38
3.2.9	Immunocytochemistry.....	39
3.2.10	HSP90 inhibitors.....	41
3.2.11	Statistical analysis and data management.....	45
3.3	Plan of work.....	46
<b>4</b>	<b>Results.....</b>	<b>47</b>
4.1	Functional analysis of HSP90 in <i>T.annulata</i> Ankara 288-infected cells.....	47
4.1.1	Assessment of apoptosis.....	47
4.1.2	Quantitative assessment of the proliferation of <i>T. annulata</i> Ankara 288-infected cells.....	56
4.1.3	Quantitative assessment of the stage progression in <i>T. annulata</i> Ankara 288-infected cells treated with GA.....	59
4.2	The regulation of HSP90 in <i>T. annulata</i> Ankara 288-infected cells.....	62
4.2.1	The regulation of bovine HSP90 in GA-treated cells.....	62
4.2.2	The regulation of <i>T. annulata</i> HSP90 in GA-treated cells.....	65
4.2.3	Comparison between the expression of bovine HSP90 and <i>T.annulata</i> HSP90 during the parasite differentiation.....	67
4.3	Detection of the bovine HSP90 protein.....	68
4.4	Identification and characterization of <i>T. annulata</i> HSP90.....	71
4.4.1	Detection of <i>T. annulata</i> HSP90 and cDNA cloning.....	71
4.4.2	Sequencing and sequence analysis.....	72
4.4.3	Phylogenetic analysis.....	75
4.5	Expression and purification of recombinant <i>T. annulata</i> HSP90.....	76
4.5.1	Bioinformatic analysis of TaHSP90-Chr1 and TaHSP90-Chr4.....	76
4.5.2	Expression and purification of TaHSP90-Chr1 and TaHSP90-Chr4 recombinant protein.....	76
4.6	Detection of <i>T. annulata</i> HSP90 protein.....	79
4.6.1	Antigenic determinants of TaHSP90-Chr1 and TahSP90-Chr4.....	80
4.6.2	Detection of <i>T. annulata</i> HSP90 in cell lysates prepared from <i>T. annulata</i> Ankara 288-infected cells.....	81
4.7	Assessment of the effect of Novobiocin on <i>T. annulata</i> Ankara 288-infected cells.....	83

---

<b>5</b>	<b>Discussion</b> .....	<b>85</b>
5.1	The role of HSP90 in apoptosis and cell proliferation in <i>T.annulata</i> -infected cells	85
5.2	HSP90 and stage progression of the parasite .....	88
5.3	The regulation of HSP90 in <i>T. annulata</i> Ankara 288-infected cells.....	90
5.4	Identification and characterization of <i>T. annulata</i> HSP90.....	92
5.5	Detection of <i>T.annulata</i> HSP90 and bovine HSP90 .....	93
5.6	Novobiocin.....	94
5.7	Conclusion.....	95
<b>6</b>	<b>Summary</b> .....	<b>96</b>
<b>7</b>	<b>Zusammenfassung</b> .....	<b>99</b>
<b>8</b>	<b>Reference</b> .....	<b>102</b>
<b>9</b>	<b>Appendix</b> .....	<b>115</b>
9.1	Flow cytometric analysis of apoptosis in <i>T. annulata</i> -infected cells incubated with GA 0.05 $\mu$ M at 41°C .....	115
9.2	Quantitative assessment of the stage progression in <i>T. annulata</i> Ankara 288-infected cells treated with GA using TamS1 and TamR1 .....	116
9.3	Quantitative real-time polymerase chain reaction (qRT-PCR).....	116
9.4	The alignment of bovine HSP90 with HSP90 $\beta$ of human .....	118
9.5	FastDigest® restriction enzymes of purified plasmids from <i>E. coli</i> DH5 $\alpha$ competent cell .....	119
9.6	Alignment of the amino acid sequence of TaHSP90-Chr1 and TaHSP90-Chr4 ....	119
9.6.1	Comparison of the deduced amino acid sequences of the clones .....	119
9.6.2	Comparison of the deduced amino acid sequences of TaHSP90-Chr1 with TaHSP90-Chr4 .....	127
9.7	Bioinformatic analysis of TaHSP90-Chr1 and TaHSP90-Chr4.....	129
<b>10</b>	<b>List of publications</b> .....	<b>130</b>
<b>11</b>	<b>Acknowledgements</b> .....	<b>131</b>

## List of figures

	Page
Figure 1: The life cycle of <i>Theileria</i> .....	4
Figure 2: Pathogenesis and protective immunity in <i>T. annulata</i> infection.....	6
Figure 3: Three pathways leading to apoptosis.....	10
Figure 4: Schematic of the domain structure of yeast HSP90. ....	14
Figure 5: Preparation of the wet blot system. ....	36
Figure 6: Diagram shows the plan of work.....	46
Figure 7: The percentages of dead cells (%) in <i>T. annulata</i> Ankara 288-infected cells.....	48
Figure 8: Flow cytometric analysis of apoptosis using Annexin V -FITC and PI staining in <i>T. annulata</i> Ankara 288-infected cells treated with GA $\geq 0.5$ $\mu$ M and incubated at 37°C. ....	49
Figure 9: Flow cytometric analysis of apoptosis using Annexin V -FITC and PI staining in <i>T. annulata</i> Ankara 288-infected cells treated with GA $\leq 0.5$ $\mu$ M and incubated at 37°C. ....	51
Figure 10: Flow cytometric analysis of apoptosis using Annexin V-FITC and PI staining in <i>T. annulata</i> Ankara 288-infected cells treated with GA $\leq 0.1$ $\mu$ M and incubated at 41°C. ....	53
Figure 11: Subcellular localization of host cell p53 within <i>T. annulata</i> Ankara 288-infected cells treated with GA or DMSO.....	55
Figure 12: Quantitative assessment of the cell proliferation of <i>T. annulata</i> Ankara 288-infected cells incubated at 37°C.....	57
Figure 13: Quantitative assessment of the cell proliferation of <i>T. annulata</i> Ankara 288-infected cells incubated at 41°C.....	58
Figure 14: The percentages of the cells undergoing merogony in <i>T. annulata</i> Ankara 288-infected cells. ....	60
Figure 15: Immunostaining of the cells undergoing merogony in <i>T. annulata</i> Ankara 288-infected cells. ....	61
Figure 16: Relative expression of TamR1 mRNA in <i>T.annulata</i> Ankara 288-infected cells. 62	
Figure 17: Relative expression of BHSP90-alpha mRNA and BHSP90-beta mRNA in <i>T.annulata</i> Ankara 288-infected cells at 37°C.....	64
Figure 18: Relative expression of BHSP90-alpha mRNA and BHSP90-beta mRNA in <i>T.annulata</i> Ankara 288-infected cells incubated at 41°C. ....	65
Figure 19: Relative expression of TaHSP90-Chr1 mRNA and TaHSP90-Chr4 mRNA in <i>T.annulata</i> Ankara 288-infected cells.....	66

Figure 20: Relative expression of BHSP90-alpha mRNA, BHSP90-beta mRNA, TaHSP90-Chr1 mRNA, TaHSP90-Chr4 mRNA and TamR1 mRNA in <i>T.annulata</i> Ankara 288-infected cells at 37°C.....	67
Figure 21: Relative expression of BHSP90-alpha mRNA, BHSP90-beta mRNA, TaHSP90-Chr1 mRNA, TaHSP90-Chr4 mRNA and TamR1 mRNA in <i>T.annulata</i> Ankara 288-infected cells at 41°C.....	68
Figure 22: Detection of bovine HSP90.....	69
Figure 23: Subcellular localization of bovine HSP90.....	70
Figure 24: PCR amplification of mRNA transcripts of <i>T. annulata</i> HSP90 isoforms using <i>T. annulata</i> HSP90 specific primers. ....	71
Figure 25: M13 PCR selection of positive pDrive clones of TaHSP90-Chr1 and TaHSP90-Chr4 construct.....	72
Figure 26: Alignment of the nucleotide sequence of TaHSP90-Chr1 and TaHSP90-Chr1 ...	74
Figure 27: Phylogenetic relationship of <i>T. annulata</i> TaHSP90-Chr1 and TaHSP90-Chr4....	75
Figure 28: Plating and screening of the clones expressing the His-tagged protein using the colony blot method.....	77
Figure 29: PQE-PCR and selection of recombinant pQE30 clones (TaHSP90-Chr1).....	77
Figure 30: PQE-PCR and selection of recombinant pQE30 clones (TaHSP90-Chr4).....	78
Figure 31: Recombinant expression and detection of <i>T. annulata</i> HSP90 proteins.....	79
Figure 32: Distribution of the antigenic determinants sequence in the TaHSP90-Chr1 and TaHSP90-Chr4.....	80
Figure 33: Dot blot testing the reactivity of anti- <i>T. annulata</i> HSP90 antiserum with peptide.....	81
Figure 34: Recombinant expression and detection of TaHSP90-Chr1 protein.....	82
Figure 35: Alignment of the amino acid sequence of bovine HSP90 with novobiocin binding site.....	83
Figure 36: Alignment of the amino acid sequence of <i>T.annulata</i> HSP90 with novobiocin binding site.....	83
Figure 37: The effect of Novobiocin (Nb) on <i>T.annulata</i> Ankara 288-infected cells.....	84
Figure 38: Model: The potential biological role of HSP90 (bovine/ parasite HSP90) in <i>T.annulata</i> Ankara 288-infected cells.....	91
Figure 39: Flow cytometric analysis of apoptosis using Annexin V-FITC in <i>T. annulata</i> Ankara 288-infected cells treated with GA 0.05 $\mu$ M and incubated at 41°C for 5, 6 and 7 days.....	115
Figure 40: An increase in the number of the cells undergoing merogony after treatment with GA.....	116

Figure 41: Specificity of the qRT-PCR primers used to detect TaHSP90-Chr1, TaHSP90-Chr4, BHSP90-alpha and BHSP90-beta.....	117
Figure 42: Specificity of the qRT-PCR primers used to detect TaAct1 and TamR1. ....	118
Figure 43: The alignment of bovine HSP90 with amino acids 610-723 of HSP90 $\beta$ of human origin. ....	118
Figure 44: FastDigest® restriction enzymes of purified plasmids from E.coli DH5 $\alpha$ competent cell. ....	119
Figure 45: Alignment of the amino acid sequence of the clones of TaHSP90-Chr1 and TaHSP90-Chr4.....	126
Figure 46: Alignment of the amino acid sequence of TaHSP90-Chr1 with TaHSP90-Chr4.	128

## List of tables

	Page
Table 1: List of cells and cell lines .....	16
Table 2: List of primers.....	20
Table 3: List of qRT-PCR primers and probes .....	21
Table 4: List of primary antibodies. WB: Western blotting, IF: Immunofluorescence .....	21
Table 5: List of secondary antibodies. WB: Western blotting, IF: Immunofluorescence .....	22
Table 6: The RT-PCR program.....	29
Table 7: Composition of resolving and stacking gel .....	35
Table 8: Primary and secondary antibodies used for western blot analysis. ....	37
Table 9: Primary and secondary antibodies used for immunofluorescence staining.....	39
Table 10: Staining procedure for cover slip to detect merozoites. ....	40
Table 11: FACS Calibur settings for flow cytometry used to assess apoptosis .....	41
Table 12: FACS Calibur settings for flow cytometry used to assess cell proliferation.....	41
Table 13: Treatment conditions for <i>T.annulata</i> Ankara 288-infected cells to assess the cell viability using trypan blue.....	42
Table 14: Treatment conditions for <i>T.annulata</i> Ankara 288-infected cells to assess apoptosis using FACS Calibur flow Cytometry, covering GA concentrations $\geq 0.5 \mu\text{M}$ . ...	42
Table 15: Treatment conditions for <i>T.annulata</i> Ankara 288-infected cells to assess apoptosis using FACS Calibur flow Cytometry, covering GA concentrations $\leq 0.5\mu\text{M}$ . ....	43
Table 16: Treatment conditions for <i>T.annulata</i> Ankara 288-infected cells to assess apoptosis by using immunofluorescence staining.....	43
Table 17: The concentration of GA and DMSO and the incubation times used to induce merogony in <i>T. annulata</i> Ankara 288-infected cells.....	43
Table 18: The concentration of GA and DMSO and the incubation time used to assess proliferation in <i>T. annulata</i> Ankara 288-infected cells.....	44
Table 19: Showing the GA or DMSO concentrations used to analyse the expression of bovine HSP90 genes. ....	44
Table 20: Showing the GA or DMSO concentrations used to analyse the expression of <i>T. annulata</i> HSP90 and Tamr1 genes. ....	44
Table 21: Bioinformatic analysis of TaHSP90-Chr1.....	129
Table 22: Bioinformatic analysis of TaHSP90-Chr4.....	129

**List of abbreviations**

<u>Abbreviation</u>	<u>Term</u>
17-AAG	17-N-allylamino-17-demethoxygeldanamycin
ADP	Adenosine diphosphate
Akt/PKB	Protein Kinase B
AP buffer	Alkaline phosphatase buffer
AP-1	Activator protein-1
Apaf -1	Apoptotic protease activating factor 1
APS	Ammonium persulfate
ATF-2	Activating Transcription Factor 2
ATP	Adenosine triphosphate
Bad	Bcl-2-associated death promoter
Bax	Bcl-2-associated X protein
BCIP	5-Bromo-4 chloro-3-indolyl phosphate
Bcl-2	B-cell lymphoma 2
BHSP90-alpha	Bos taurus heat shock protein 90kDa alpha
BHSP90-beta	Bos taurus heat shock protein 90kDa beta
BoMac	Bovine macrophage cell line
BSA	Bovine serum albumin
CD4+ T cells	T helper cells
CD8+ T cells	T cytotoxic cell
cdc2	Cyclin-dependent kinase 1
cDNA	Complementary DNA
CFSE	Carboxyfluorescein succinimidyl ester
CO <sub>2</sub>	Carbon dioxide
DABCO	1,4 Diazabicyclo (2,2,2) octane
DAPI	4',6-Diamidine-2',phenylindole dihydrochlorid
ddH <sub>2</sub> O	Double-distilled water
DMEM	Dulbecco's Modified Eagle's Medium
DMSO	Dimethyl sulphoxide
DNA	Deoxyribonucleic acid
dNTP	deoxyribonucleotide
DTT	Dithiothreitol
<i>E. coli</i>	<i>Escherichia coli</i>
EDTA	Ethylenediaminetetraacetic acid
EGTA	Ethylene glycol tetraacetic acid
FACS	Fluorescence-activated cell sorter

---

FADD	Fas-associated death domain
Fas/CD95	FAS receptor
FasL	Fas ligand
FITC	Fluorescein isothiocyanate
GA	Geldanamycin
GAPDH	Glyceraldehyde 3-phosphate dehydrogenase
GM-CSF	Granulocyte-monocyte colony-stimulating factor
GyrB	gyraseB
HSF1	Heat shock factor 1
HSP27	Heat shock protein 27-kDa
HSP60	Heat shock protein 60-kDa
HSP70	Heat shock protein 70-kDa
HSP90	Heat shock protein 90-kDa
HSP90 $\alpha$	Heat shock protein 90 alpha
HSP90 $\beta$	Heat shock protein 90 beta
HSPs	Heat shock proteins
IFN- $\gamma$	Interferon- $\gamma$
IKK	I $\kappa$ B kinase
IL-2	Interleukin 2
IPTG	Isopropyl-beta-D-thiogalactopyranoside
I $\kappa$ Bs	Inhibitor of $\kappa$ B
JNK	c-Jun NH2-terminal kinase
LB medium	Lysogeny broth or Luria-Bertani
LDH1	Lactate dehydrogenase 1
LDH2	Lactate dehydrogenase 2
MAPK	Mitogen-activated protein kinases
MCS	Multiple cloning site
MHCI	Major histocompatibility complex class I
MHCII	Major histocompatibility complex class II
mRNA	Messenger RNA
NBT	Nitro blue tetrazolim chloride
NF- $\kappa$ B	Nuclear factor kappa B
NK	Natural killer
NO	Nitric oxide
OD	Optical density,
ORF	Open reading frame
p27 <sup>Kip1</sup>	Cyclin-dependent kinase inhibitor 1B
P53	Tumour suppressor protein
PBL	Peripheral Blood Leukocyte

PBL	Peripheral Blood Leukocyte
PBS	Phosphate buffered saline
PCR	Polymerase Chain Reaction
PFA	Paraformaldehyd
PH	Phase contrast
PI	Propidium iodide
PI-3k	Phosphoinositide-3 kinase
PPA2	Protein phosphatase 2
PVA	Polyvinyl alcohol
qRT-PCR	Quantitative real-time polymerase chain reaction
RNA	Ribonucleci acid
RPMI	Roswell Park Memorial Institute (culture medium)
RT	Room temperature
RT-PCR	Reverse transcription polymerase chain reaction
S.D	Standard deviation
SDS	Sodium dodecyl sulfate
SDS-PAGE	Sodium dodecyl sulfate (SDS), Polyacrylamide gel electrophoresis (PAGE)
SOC medium	Super Optimal broth with Catabolite repression (glucose)
SPSS	Statistical Package for the Social Sciences
SSC	Saline-Sodium Citrate buffer
TaAct1	<i>Theileria annulata</i> actin 1
TaHSP90-Chr1	<i>T. annulata</i> HSP90 located in chromosome one
TaHSP90-Chr4	<i>T. annulata</i> HSP90 located in chromosome four
TamR1	<i>Theileria annulata</i> merozoite rhoptry protein
Tams1	<i>Theileria annulata</i> major merozoite surface protein
Tash 1 and 2	<i>Theileria annulata</i> macroschizont specific antigen 1 and 2
TaSP	<i>T. annulata</i> surface membrane
TBE	Tris/Borate/EDTA
TEG	Trypsin EGTA
TEMED	N,N,N',N'-Tetramethylethylenediamine
TGF- $\beta$	Transforming growth factor- $\beta$
TNF	Tumor necrosis factor
TNFR1	TNF receptor type 1
TNF- $\alpha$	Tumor necrosis factor $\alpha$
TRADD	TNF receptor-associated death domain
X-gal	5-bromo-4-chloro-3-indolyl- $\beta$ -D-galactopyranoside
$\beta$ -ME	$\beta$ -mercaptoethanol

---

<u>Symbol</u>	<u>Term</u>
°C	Degree Celsius
µg	Microgram
µl	Microliter
µM	Micromol
bp	Base pairs
h	Hour
IU	International Unit
kDa	Kilodalton
L	Liter
M	Molar
m	Meter
mA	Milliamperere
min	Minute
ml	Milliliter
mM	Millimol
mm	Millimeter
ng	Nanogram
nm	Nanometer
P	P-value
s	Second
T <sub>m</sub>	Melting Temperature
U	Unit
V	Volume
V	Volt
W	Watt
xg	Gravity force
Σ	Sum



## 1 Introduction

The protozoan parasites *Theileria* infect wild and domestic Bovidae and they occur in tropical and subtropical regions. The diseases they cause are among the most serious constraints to the livestock production. *Theileria* spp are transmitted by ixodid ticks and have a complex life cycle in both vertebrate host and vector, with sexual reproduction occurring in the tick (Mehlhorn and Schein, 1984; Dolan, 1989). During tick feeding, the sporozoites are inoculated into the bovine host by the tick and shortly thereafter they invade host's leukocytes surrounded by the host cell membrane. This membrane is dissolved by the sporozoite, which then resides free in the host cell cytoplasm. After 2-3 days, the nucleus of the parasite starts to divide which results in a multinuclear syncytium named the schizont. The infected host cell acquires many characteristics of cancer cells such as uncontrolled proliferation and immortalization. However, the elimination of the schizont by using buparvaquone results in growth arrest and induces apoptosis in the host cell (Dobbelaere and Heussler, 1999; Dobbelaere *et al.*, 2000; Heussler, 2002). This indicates that *Theileria* parasite regulates the expression of anti-apoptotic protein and induces continuous host cell proliferation.

In the last decade, it has been found that a number of genes are involved in the regulation of cell proliferation and / or apoptosis such as NF- $\kappa$ B (Dobbelaere and Küenzi, 2004), PI-3k/Akt (Leirião *et al.*, 2005) and Heat shock proteins (HSPs) (Samali and Cotter, 1996; Parcellier *et al.*, 2003).

The synthesis of HSPs increases upon a sudden elevation in temperature or after exposure to other type of stress. Based on their molecular weight, HSPs are classified as: HSP90 (approximately 90 kilodaltons (kD)), HSP70 (approximately 70 kD), HSP60 (approximately 60 kD), etc. HSP90 is one of a chaperone proteins responsible for managing protein folding and preventing aggregation of abnormal proteins (Grover *et al.*, 2011). Although HSP90 is involved in the triage of misfolded proteins under stress conditions, it plays also a key role under normal conditions in regulating the stability, maturation and activation of a wide range of 'client' proteins, many of which are critical for signal transduction. Moreover, HSP90 plays a significant role in disease states, especially in cancer, where the chaperoning of mutated and overexpressed oncoproteins is crucial (Pearl *et al.*, 2008).

HSP90 is involved in the regulation of apoptosis on one hand, through its ability to inhibit cytochrome c-mediated oligomerization of Apaf-1 and thereby inhibits apoptosis (Pandey *et al.*, 2000a) and on the other hand, HSP90 is required as a regulator of NF- $\kappa$ B signalling by its general participation in the activation and homeostasis of I $\kappa$ B kinase (IKK) (Broemer *et al.*, 2004). It is known that NF- $\kappa$ B participates in regulating the expression of genes that are involved in cell survival such as Bcl-2 (Zong *et al.*, 1999). In addition, the functional role of HSP90 is essential for cell proliferation specifically in cancer cells (Wu *et al.*, 2009).

Numerous studies have confirmed the role of HSP90 in the development of protozoan parasites using Geldanamycin (GA), a drug known to interfere with HSP90 function. The addition of GA inhibited the parasite differentiation in *Plasmodium falciparum* (*P.falciparum*) (Banumathy *et al.*, 2003) and also in *Toxoplasma gondii* (*T.gondii*) (Echeverria *et al.*, 2005). Moreover, the treatment of different *Trypanosoma cruzi* (*T.cruzi*) stages with GA showed that HSP90 is essential for parasite cell cycle control (Graefe *et al.*, 2002). In addition, when GA was added to *Leishmania donovani* (*L. donovani*) culture, promastigotes exhibited apoptotic morphological changes (Li *et al.*, 2009). All these findings show that HSP90 can be a drug target and GA as a potential anti-parasitic drug (Pallavi *et al.*, 2010; Meyer and Shapiro, 2013).

Since no work has been reported regarding the functional role of HSP90 in *T.annulata* Ankara 288-infected cells, the main aims of this study were: (a) To investigate the role of HSP90 in the cell viability and proliferation as well as stage progression of the parasite. (b) To analyse the differential expression profile of HSP90 by *T.annulata* Ankara 288-infected cells during stress conditions (treatment with GA and/or high temperature) as well as during different developmental stages of the parasite by using qRT-PCR. (c) To identify and characterize *T.annulata* HSP90.

## **2 Literature review**

### **2.1 Genus *Theileria***

*Theileria* are obligate intracellular parasites that cause great health problems in domestic and wild animals in tropical and subtropical areas (Shaw, 2002). They are transmitted by ixodid ticks of the genera *Rhipicephalus*, *Amblyomma*, *Hyalomma* and *Haemaphysalis* (Bishop *et al.*, 2004). The genus *Theileria* is classified under family *Theileriidae*, order *Piroplasmida*, subclass *Piroplasmia*, class *Sporozoea*, phylum *Apicomplexa* (Levine *et al.*, 1980; Norval *et al.*, 1992). This phylum includes a number of species of both medical, such as *Plasmodium*, *Toxoplasma*, and veterinary, such as *Babesia* and *Theileria*, importance (Shaw, 1997).

### **2.2 *Theileria* in bovine**

The main *Theileria* (*T.*) species infecting cattle in Africa are *T. parva*, *T. annulata*, *T. mutans*, *T. velifera* and *T. orientalis/sergenti/buffeli* group (Norval *et al.*, 1992). The most virulent and economically important of which are *T. parva* and *T. annulata* (Norval *et al.*, 1992; Bishop *et al.*, 2004) and their geographical distribution is correlated with that of their vectors (Morzaria, 1989).

#### **2.2.1 *T.annulata***

*T. annulata* causes tropical theileriosis in cattle and domestic buffalo and it is transmitted by several species of *Hyalomma spp* like *H. anatolicum* and *H. detritum* (Uilenberg, 1981). The disease exists in large parts of the Mediterranean coast of North Africa, extending to northern Sudan, southern Europe, south-eastern Europe, Middle East, India, China and Central Asia (Dolan, 1989). This disease threatens around 250 million cattle and acts as a major limitation of livestock production and development in many developing countries. The mortality rate varies from 5% to 90% in the local breeds and imported breeds, respectively (d' Oliveira *et al.*, 1995).

### 2.3 Life cycle of *Theileria*

Generally, the life cycle of all *Theileria* species involves several developmental stages in the transmitting tick and vertebrate hosts (Fawcett *et al.*, 1987; Shaw, 2003). The life cycle of the *Theileria* is shown in Figure 1.

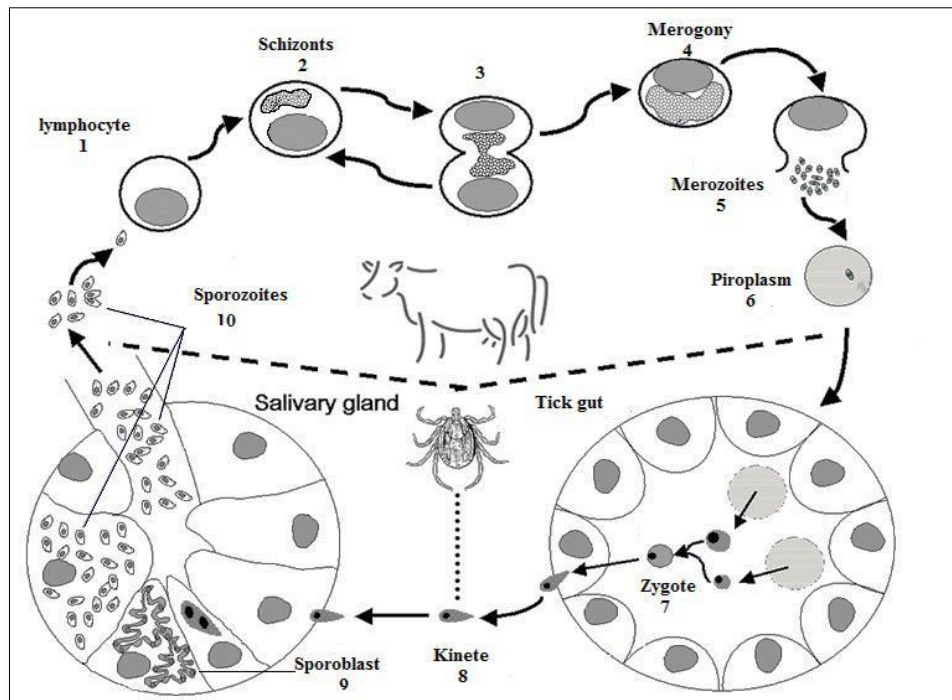


Figure 1: The life cycle of *Theileria* (Modified from <http://www.theileria.org/ahdw/background.htm>).

When infested ticks attack animals, the life cycle of *Theileria* in vertebrate hosts begins. (1) The sporozoites are released into the vertebrate host with saliva and enter lymphoid cells (Dolan, 1989). Sporozoites invade different leukocyte sub-types depending upon the *Theileria* species. *T. parva* sporozoites can invade and survive in all subpopulations of lymphocytes. In contrast, *T. annulata* sporozoites invade bovine MHC class II positive cells of the macrophage/monocyte lineage and at lower efficiency, they can invade B cells (Spooner *et al.*, 1989; Morrison *et al.*, 1996; Shaw, 2003). (2) The sporozoites differentiate into multinucleate schizonts. (3) The infected lymphocytes become larger and at the same time the schizonts inside the lymphocytes divide. (4, 5) The schizonts undergo differentiation to produce numerous merozoites (Fawcett *et al.*, 1987; Shaw and Tilney, 1992). (6) The merozoites are released from the lymphocytes and invade erythrocytes of the host where they develop into piroplasms (Mehlhorn and Schein, 1984; Shaw and Tilney, 1995). Ticks become infected after feeding on erythrocytes containing the piroplasm stage. (7) In the tick gut, the erythrocytes are rapidly destroyed and the piroplasm differentiates into male and female gametes (Norval *et al.*, 1992; Bishop *et al.*, 2004). The zygote is formed by the fusion of two similarly sized and structured gametes. (8) Zygote invades a gut epithelial cell and differentiates into a motile kinete (Mehlhorn and Schein, 1984). (9, 10) The motile kinetes invade salivary gland in which sporogony occurs. The sporozoites are introduced with the tick saliva during the tick feeding into a new bovine host.

## 2.4 Clinical signs

The severity of the disease is influenced by a number of parameters like breed, age, virulence of the parasite and the number of sporozoites that are transmitted to the animal (Preston *et al.*, 1992). Consequently, the clinical signs may vary from per-acute, acute or sub-acute to chronic. The typical clinical symptoms are enlargement of lymph nodes in areas of tick infestation, fever, anorexia, lacrimation and nasal discharge may occur, decreased milk and meat production, diarrhea and anemia. Terminally, dyspnea is common with an increasing respiratory rate. Death usually occurs within 10–25 days after the onset of clinical signs (Preston *et al.*, 1992; Forsyth *et al.*, 1999; Mehlhorn, 2008).

## 2.5 Pathogenesis and immunity to *Theileria* infection

The pathogenesis of theileriosis is dependent on the stage of the parasite and the type of affected cells. Concerning infection with *T. annulata*, the massive, uncontrolled cell proliferation during infection with schizonts is the most important pathogenic aspect (Ahmed *et al.*, 2008). The schizont-infected cells produce high levels of pro-inflammatory cytokines, especially TNF- $\alpha$  (Brown *et al.*, 1995; Glass *et al.*, 2003). Moreover, the infected cells stimulate naive T cells leading to the production of IFN- $\gamma$ , which in turn stimulates the macrophages to produce more TNF- $\alpha$  (Brown *et al.*, 1995). TNF- $\alpha$  is a potent inducer of fever and has also been connected to the production of anaemia, muscle wasting and necrosis (Bielefeldt Ohmann *et al.*, 1989).

During the course of *Theileria* infection, both T- and B-lymphocytes are activated (Ahmed *et al.*, 2008). It is known that both antibody-dependent and antibody-independent mechanisms participate in the protection against theileriosis. However, T- cells play the major role in the induction and maintenance of the immunity (Glass, 2001; Ahmed *et al.*, 2008). Both CD4+ and CD8+ T cells are involved in the mediation of this immunity (Campbell *et al.*, 1995). Helper and cytotoxic-T cells recognize parasite antigens, which are presented on the surface of the infected cell via MHC II and MHC I, respectively (Ahmed *et al.*, 2008). The activated helper T-cells produce IL-2 and IFN- $\gamma$  (Campbell *et al.*, 1995, 1997). Cytotoxic T-cells use IL-2 for their clonal expansion and subsequent killing of their target cells in an MHC class I restricted manner (Innes *et al.*, 1989; Ahmed and Mehlhorn, 1999), whereas IFN- $\gamma$  activates uninfected macrophages (Preston *et al.*, 1993; Ahmed *et al.*, 2008). The activation of natural

killer cells (NK) by microbes could induce NK cells to become lytic and produce more IFN- $\gamma$  (Preston *et al.*, 1999; Glass, 2001; Ahmed *et al.*, 2008) (Figure 2).

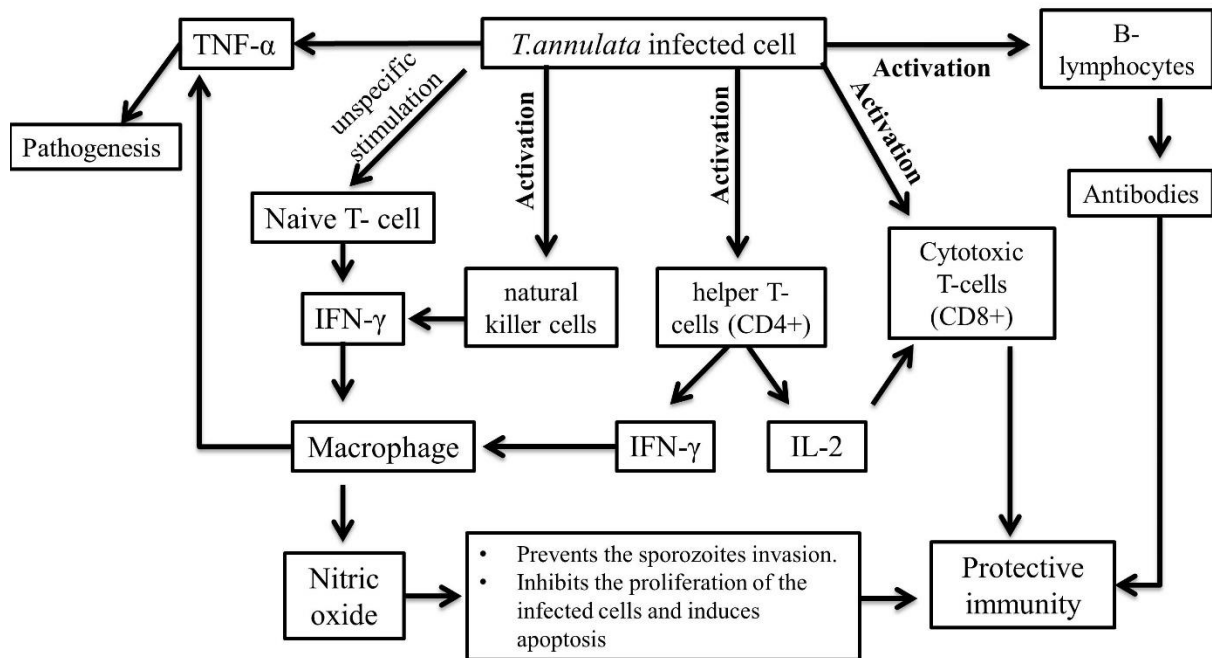


Figure 2: Pathogenesis and protective immunity in *T. annulata* infection.

(Explained in detail above).

## 2.6 Host parasite interaction

The parasites have developed a wide range of strategies that help them to survive and persist in their hosts. These strategies include molecular mimicry, antigenic variation, modulation of host immune responses and interfere with normal processes that regulate the functioning of the host cell (Dobbelaere *et al.*, 2000).

After their inoculation into the host, the sporozoites invade host leukocytes, where they become free in the host cytoplasm but associated with the host microtubules (Chaussepied and Langsley, 1996). Two days later, the sporozoite differentiates into the macroschizont (Shiels *et al.*, 2006). The infected cells become transformed and acquire the ability to proliferate in an uncontrolled manner (Dobbelaere and Heussler, 1999).

The proliferation results in an increase in the number of infected cells in lymphoid and non-lymphoid tissues of the infected host (Eichhorn and Dobbelaere, 1994). Elimination of the parasite by using buparvaquone (theilericidal drug) results in growth arrest and subsequently

cell death. This finding suggests that the host cell transformation is completely parasite-dependent (Eichhorn and Dobbelaere, 1994; Dobbelaere and Heussler, 1999; Heussler, 2002).

**How dose *Theileria* parasites transform the host cell and maintain this transformation to ensure their own survival?** In order to achieve a successful transformation of the host cell, the parasites undertake the following steps:

- 1- Invasion of the host cell.
- 2- Induction and maintenance of transformation and proliferation

### **2.6.1 Invasion process**

*T. annulata* sporozoites are non-motile, so that the attachment to a susceptible host cell is a random event. The attachment between the sporozoite and host cell results in irreversible binding. Once attached, the sporozoite is entered into the host cytoplasm by progressive circumferential (zippering) of the host and parasite membranes. Inside the host cell, the sporozoite is completely surrounded by the host cell membrane. Through the discharge of the rhoptries and microspheres, the parasite dissolves the host cell membrane and becomes free in the host cytoplasm. By escaping into the host cytoplasm, the parasite can avoid many of the problems associated with living in a parasitophorous vacuole (Shaw, 1997, 2003).

### **2.6.2 Induction and maintenance of transformation and proliferation**

After the invasion, the free sporozoites become permanently associated with the host cell microtubules. Within 24-48 hours, the sporozoite differentiates into the macroschizont form and also during this time the transformation of the infected leukocyte begins (Chaussepied and Langsley, 1996; Shiels *et al.*, 2006). The mechanism of the transformation process is still not fully understood. However, a number of molecules have been described to be involved in this mechanism.

#### a) Nuclear factor-kappaB (NF- $\kappa$ B)

In unstimulated cells, NF- $\kappa$ B is regulated by cytoplasmic inhibitor proteins called Inhibitor of NF- $\kappa$ B (I $\kappa$ Bs); the latter is sequestered with NF- $\kappa$ B and prevents NF- $\kappa$ B translocation to the host cell nucleus. When the cells are exposed to external or internal stimuli, I $\kappa$ Bs becomes phosphorylated by an upstream kinase complex called I $\kappa$ B kinase (IKK), which leads to dissociation of NF- $\kappa$ B from I $\kappa$ Bs (Heussler *et al.*, 1999; Dobbelaere and Küenzi, 2004). The

activation of NF- $\kappa$ B in *Theileria*-infected cells depends on the permanent degradation of NF- $\kappa$ B inhibitor (Palmer *et al.*, 1997), which in turn allows the NF- $\kappa$ B translocation from the cytoplasm to the nucleus, where it plays a key role in regulating the expression of genes that control the cell survival (Dobbelaere and Küenzi, 2004). One of the target genes regulated by NF- $\kappa$ B is Bcl-2, which plays a role as anti-apoptotic factor (Lee *et al.*, 1999; Zong *et al.*, 1999). Constitutive activation of NF- $\kappa$ B seems to be mediated by a direct parasite-dependent activation of the IKK complex (Heussler, 2002).

b) Tumor suppressor factor 53 (P53)

P53 is one of the most important proteins involved in the regulation of proliferation and apoptosis and plays a major role in protecting the integrity of the genome. Thus, in case of stress or DNA damage, p53 initiates cell-cycle arrest and apoptosis. When this protein fails to work properly, uncontrolled growth ensues as a defining feature of cancer cells (Vogelstein *et al.*, 2000).

As mentioned above, *T.annulata* schizont induces transformation of bovine leukocytes. Interestingly, Haller and co-workers demonstrated that due to the presence of parasite, p53 is sequestered in the host cell cytoplasm. Furthermore, they could demonstrate that the elimination of the parasite by anti-theileria drug, buparvaquone, leads to the translocation of p53 into the host cell nucleus resulting in the upregulation of the pro-apoptotic Bax and Apaf-1. The close association of the parasite membrane with host cell p53 suggests that the parasite interacts with p53, which in turn negatively affects the regulation of apoptosis (Haller *et al.*, 2010).

c) c-Jun NH2-terminal kinase (JNK)

Another factor that contributes to the survival of the parasite is JNK pathway. JNK belongs to the family of mitogen-activated protein kinases (MAPK). This pathway is activated in response to a wide range of stimuli such as heat shock (Heussler, 2002). Dobbelaere and co-workers demonstrated that the JNK pathway is constitutively activated in *Theileria*-infected cells (Dobbelaere *et al.*, 2000). Later, it was found that JNK plays a major role in the survival of *T.annulate*-infected cells (Lizundia *et al.*, 2005). To this end, constitutive activation of JNK results in a permanent activation of the transcription factors, Activator protein-1 (AP-1) and Activating Transcription Factor 2 (ATF-2), which in turn control a

number of cellular processes including proliferation and apoptosis (Botteron and Dobbelaere, 1998; Ameyar *et al.*, 2003).

d) Phosphoinositide 3-kinase (PI-3k)

PI-3K pathway is involved in the regulation of several cellular processes, including cell proliferation and survival (Morgensztern and McLeod, 2005). In response to the stimulating effect such as growth factors, PI-3k is activated and recruited to the cell membrane, resulting in the activation of Protein kinase B (PKB also called Akt) (Heussler *et al.*, 2001a; Dobbelaere and Küenzi, 2004), which in turn inactivates pro-apoptotic regulators such as Bad (Datta *et al.*, 1997).

Indeed Akt/PKB is constitutively activated in *Theileria*-infected cells (Heussler *et al.*, 2001a). Therefore, it seems that PI-3K is essential for the proliferation of *Theileria*-transformed leukocytes and most probably through the induction of a granulocyte-monocyte colony-stimulating factor (GM-CSF), which is known as a growth factor (Baumgartner *et al.*, 2000). Nevertheless, blocking the constitutive Akt/PKB activation by PI-3k inhibitor, LY294002, results in growth arrest and prolonged treatment of infected cells with this substrate finally leads to apoptosis (Heussler *et al.*, 2001a, 2001b).

## 2.7 Apoptosis

Programmed cell death or apoptosis is a normal process that has an important role in the development and in the conservation of homeostasis in multicellular organisms. The apoptotic cell is characterized by highly morphological changes such as blebbing of the plasma membrane, cell shrinkage, nuclear fragmentation, chromatin condensation and loss of mitochondrial function (Kerr *et al.*, 1972). Normally, the main function of apoptosis is to maintain homeostasis in multicellular organisms by elimination of tumour and damaged cells during development. Additionally, apoptosis serves as a defence mechanism against viruses, intracellular bacteria and parasites (Heussler *et al.*, 2001b). Consequently, a defect in apoptosis leads to the progress of a number of diseases including viral infection, autoimmune disease and, in particular, cancer (Thomson, 2001).

### 2.7.1 Pathways leading to apoptosis

In the last decade, the molecular mechanisms responsible for apoptosis have been extensively investigated. It was found that caspases play a central role in apoptosis (Wong, 2011). There are three pathways known to be involved in the activation of caspases and thus cell death. For further details, see Figure 3.

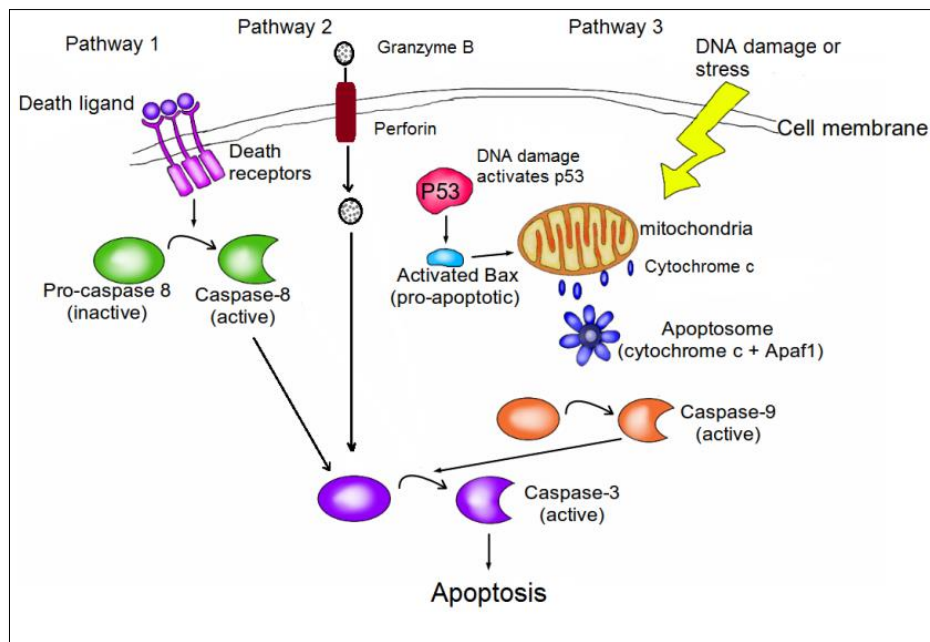


Figure 3: Three pathways leading to apoptosis (Modified from <http://blogs.scientificamerican.com/guest-blog/hallmarks-of-cancer-3-evading-apoptosis>).

The first pathway is the external death receptor pathway. The two most prominent members of the death receptors are the Fas (CD95) and TNF receptor type 1 (TNFR1) and their ligands are named Fas ligand (FasL) and TNF, respectively. The engagement of the death receptor with the death ligand results in the formation of an attaching site for an adaptor protein such as Fas-associated death domain (FADD) and TNF receptor-associated death domain (TRADD), which in turn start to stimulate pro-caspase 8. The latter starts directly to activate the other members of the caspase family (Kischkel *et al.*, 1995; Wong, 2011). The second pathway is granzyme B/ perforin-mediated pathway. Granzyme B is a serine protease which is found in the granules in the cytotoxic T cells and NK cells (Shi *et al.*, 1992a, 1992b). Upon signalling via the T cell receptor, cytotoxic T cells secreted granzyme B together with the pore forming protein perforin, the latter facilitates granzyme B to enter the target cell. Inside the target cell granzyme B can cleave and stimulate a number of the caspases particular caspases 3 (Atkinson *et al.*, 1998). The third pathway is mitochondrial-mediated pathway. The main signals activate this pathway are stress and DNA damage. These events lead to activate and accumulate of p53 (Vousden and Vande Woude, 2000), which in turn recruits Bax (a pro-apoptotic member of the Bcl-2 gene family). Bax facilitates the mitochondrial permeability and then release cytochrome c into the cytoplasm. The presence of the cytochrome c in the cytoplasm leads to the activation of caspase 9 via the formation of a complex called apoptosome (Kroemer *et al.*, 2007; Wong, 2011).

### 2.7.2 Inhibition of apoptosis

The suppression of apoptosis is one of the distinctive features of the interaction of intracellular pathogens with their host cells. Some parasites have developed different mechanisms to inhibit apoptosis.

For example, it has been reported that infection with *T.gondii* stimulates the activation of NF- $\kappa$ B, which in turn induces the expression of anti-apoptotic genes (Molestina *et al.*, 2003; Kim *et al.*, 2006). In addition, *T. gondii* has the ability to decrease Fas/CD95-triggered apoptosis in Hela cells by suppressing the activities of caspases 8 (Hippe *et al.*, 2008). Moreover, *T. gondii* also increases the resistance of host cells to apoptosis caused by granzyme B (Yamada *et al.*, 2011).

Akarid and co-workers explained that the ability of *Leishmania major* (*L.major*) to suppress apoptosis in the infected macrophages is associated with a repression of mitochondrial release of cytochrome c (Akarid *et al.*, 2004).

*T. cruzi* inhibits the host cell apoptosis via the action of a secreted enzyme named trans-sialidase. Trans-sialidase activates PI-3k pathway, which in turn leads to the inactivation of pro-apoptotic genes and to the recruitment of the pro-survival members of the Bcl-2 family (Downward, 1998; Chuenkova and Pereira, 2000). Also, NF- $\kappa$ B plays a crucial role in the protection of *T.cruzi*-infected cells from apoptosis (Petersen *et al.*, 2006).

Both NF- $\kappa$ B and PI-3k/Akt pathways also play a protective role against apoptosis in *Plasmodium* (Leirião *et al.*, 2005; Tripathi *et al.*, 2009).

In addition to the above mentioned molecules there is a strong evidence that members of HSPs are also involved in the protection of cells from apoptosis (for more details see section 2.9, 2.9.1 and 2.10.2).

## 2.8 Stage differentiation

Stage differentiation is crucial for survival and development of a number of parasites. Thus, at a certain period the intracellular parasites have to make a decision to differentiate to the next stage (Shiels, 1999). However, the ability of the parasite to convert from one stage to another requires dramatic transcriptional changes (Saksouk *et al.*, 2005). In 2001, Swan and co-workers investigated the regulation of two genes in *T.annulata* parasite during their stage

differentiation. They found that the mRNA levels of *T. annulata* macroschizont specific genes (Tash1 and Tash2) decreased during differentiation from macroschizont to merozoite coinciding with a major increase in the levels of the merozoite gene encoding the surface antigen TamS1 (Swan *et al.*, 2001).

In *T.gondii*, the expression level of two genes named lactate dehydrogenase one and two (LDH1, LDH2) respectively, was investigated also during the parasite's life cycle. These genes encode polypeptides similar to the enzyme lactate dehydrogenase. It has been shown that the mRNA of LDH2 is only detected in the bradyzoite stage, while the mRNA of LDH1 was detected in both bradyzoite and tachyzoite stages (Yang and Parmley, 1997).

Moreover, the regulation of HSPs has also been linked with the parasite differentiation (reviews in section 2.9.1 and 2.10.2).

## 2.9 HSPs

All organisms respond to high temperature by inducing the synthesis of a group of proteins named heat-shock proteins (HSPs) (Lindquist and Craig, 1988). The expression of these proteins is also increased when the cell is exposed to other stress such as high concentration of ethanol, arsenite and heavy metals (Parsell and Lindquist, 1993). Moreover, the aggregation of abnormal protein and denatured protein in cells increases the expression of HSPs (Parsell and Lindquist, 1993; Schmitt *et al.*, 2007).

HSPs include a large group of proteins that are often categorized based on their molecular weight: ubiquitin (~8kDa), HSP28 (~25-30kDa), HSP60 (~60kDa), HSP70 (~70kDa) and HSP90 (~90kDa) (Welch, 1992; Li and Srivastava, 2004). These proteins play a key role as molecular chaperone helping in folding of misfolded proteins, preventing their accumulation and promoting the proper refolding of denatured protein. Moreover, they perform essential functions by facilitating proper interaction between various other proteins (Welch, 1992; Gupta, 1995).

HSPs are overexpressed in a wide range of human cancers and are essential for the cancer cell survival (Ciocca and Calderwood, 2005; Schmitt *et al.*, 2007). For example, the high level of HSP27 and HSP70 expressions has been associated with drug resistance in breast cancer patients treated with combination chemotherapies (Vargas-Roig *et al.*, 1998). Mehlen and co-workers demonstrated that constitutive expression of human HSP27 in murine

fibrosarcoma cells blocks the apoptotic process generated by Fas receptor (Mehlen *et al.*, 1996). In pancreatic carcinoma and breast cancer, the expression level of HSP90 mRNA was higher compared with the control tissue. This finding suggests that the overexpression of HSP90 may be essential for cell proliferation in cancer cell (Conroy and Latchman, 1996; Ogata *et al.*, 2000). Therefore, the pharmacological inhibition of HSPs can offer therapeutic opportunities in the area of cancer treatment (Zagouri *et al.*, 2012).

### 2.9.1 HSPs and parasitic infection

HSPs have been shown to play a crucial role in parasite mobility, migration, ability to invasion of their host cell and ensuring the cell survival. For example, Montagna and co-workers showed that HSP20 plays a major role in *Plasmodium* motility and thus migration of the parasite. Consequently, loss of HSP20 function impairs the migration of *Plasmodium* in the host (Montagna *et al.*, 2012). In mice infected with *T.gondii*, the expression of high levels of HSP70 during the differentiation of bradyzoite to tachyzoite was observed (Silva *et al.*, 1998). Additionally, use of specific inhibitors of HSP90, HSP70, and HSP27, suppresses the induction of bradyzoite development in vitro (Weiss *et al.*, 1998). Furthermore, HSP70 plays a crucial role in the pathogenicity of *T.gondii* by inhibiting the induction of nitric oxide (NO) release by macrophages of IFN- $\gamma$  knockout mice infected with *T.gondii* during lethal as well as acute infection (Mun *et al.*, 2000).

Regarding the viability of the parasite and HSPs, Hisaeda and co-workers showed an increase in the expression level of HSP65 correlated with decreased levels of apoptosis in macrophages infected with *T. gondii* (Hisaeda *et al.*, 1997).

### 2.10 HSP90

HSP90 is one of the most abundant molecular chaperone proteins in eukaryotic cells. It amounts 1-2% of cellular proteins under non-stress condition (Johnson and Brown, 2009). However, this may increase up to tenfold under stress condition (Buchner, 1999). In coordination with other co-chaperones, HSP90 plays an essential role in folding of new synthesized proteins and in refolding of denatured proteins (Sreedhar *et al.*, 2004). Moreover, HSP90 has been shown to be necessary for the maturation of a wide range of client proteins such as steroid receptors, other classes of transcription factors, serine/ threonine and tyrosine kinases (Picard, 2002; Workman *et al.*, 2007; Johnson and Brown, 2009).

### 2.10.1 Structure of HSP90

In mammalian cells, there are two major cytoplasmic isoforms of HSP90: HSP90 $\alpha$  and HSP90 $\beta$  (Csermely *et al.*, 1998). Structurally, HSP90 consists of three highly conserved domains:

- a 25 kDa N-terminal ATP-binding domain.
- a 35 kDa middle domain.
- and a 12 kDa C-terminal dimerization domain (Figure 4).

HSP90 of eukaryotic cells, a charged region exists between the N-terminal domain and middle domain (Terasawa *et al.*, 2005; Xu *et al.*, 2012). The N-terminal domain contains the ATP/ADP binding site with ATPase activity. HSP90 shows conformational changes in the presence of ATP, which leads to signal transduction and protein folding. Additionally, mutation analysis demonstrated that ATPase activity was essential for the biological functions of HSP90. Some natural derivatives, such as GA closely bind to this site to interfere with HSP90 functions resulting in the degradation of many HSP90 client proteins (Young *et al.*, 2001; Terasawa *et al.*, 2005). The function of HSP90 depends not only on the N-terminal domain, but also on the involvement of the middle domain. The middle domain is implicated in the binding to p53 (Müller *et al.*, 2004) and Akt kinase (Sato *et al.*, 2000). The C-terminal domain is necessary for HSP90 dimerization (Pearl and Prodromou, 2006).

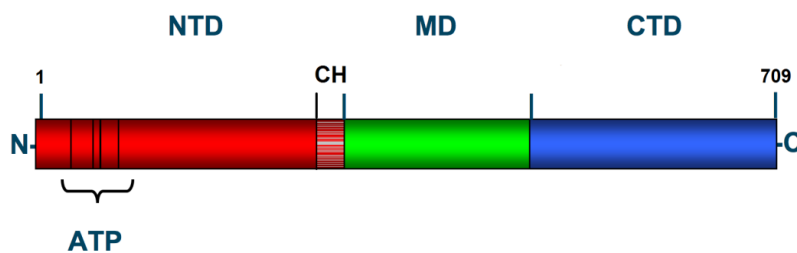


Figure 4: Schematic of the domain structure of yeast HSP90.

NTD= N-terminal domain, MD = middle domain, CTD = C-terminal domain and CH= a charged region. Modified from [http://upload.wikimedia.org/wikipedia/en/thumb/3/3b/Hsp90\\_schematic\\_2cg9.png/675px-Hsp90\\_schematic\\_2cg9.png](http://upload.wikimedia.org/wikipedia/en/thumb/3/3b/Hsp90_schematic_2cg9.png/675px-Hsp90_schematic_2cg9.png).

### 2.10.2 HSP90 and parasitic infection

The ability of HSP90 to affect the important cellular transformations was reported in various species of the intracellular parasites. For example, it has been observed that the inactivation of HSP90 by GA induces growth arrest in *L. donovani* (Wiesgigl and Clos, 2001), and in *T. cruzi* (Graefe *et al.*, 2002), while in *Plasmodium* and *T. gondii* the addition of GA results in inhibition of their stage progression in a dose-dependent manner (Banumathy *et al.*, 2003; Echeverria *et al.*, 2005). In *Eimeria tenella* (*E.tenella.*), the inhibition of HSP90 using GA leads to attenuation of the capacity of parasite to invade host cells (Péroval *et al.*, 2006). In addition, the possible protective role of HSP90 against apoptosis was observed in *L. donovani*, where treatment of *L. donovani* with GA induced their apoptosis (Li *et al.*, 2009).

### 2.11 Aim of this study

#### Hypothesis:

Based on the data generated for HSP90, I postulate that HSP90 may represent a potential target drug or vaccine candidate against *Theileria*.

Accordingly, the main objectives of my doctoral thesis are:

- To investigate the anti-apoptotic effects of HSP90 in *T. annulata* Ankara 288-infected cells.
- To investigate the functional effects of HSP90 in the proliferation of *T.annulata* Ankara 288-infected cells.
- To investigate the effect of HSP90 on the parasite stage progression.
- To analyse the differential expression profile of HSP90 by *T. annulata* Ankara 288-infected cells during stress conditions (treatment with GA or high temperature) as well as during developmental stages of the parasite.
- To identify and characterize *T.annulata* HSP90.

### 3 Materials and Methods

#### 3.1 Materials

##### 3.1.1 Cells and Cell lines

Table 1: List of cells and cell lines

Cells and cell line	Properties	Reference
<i>T. annulata</i> Ankara 288-infected cells (cell line)	Bovine lymphocyte cells infected with <i>T. annulata</i> were isolated from an infected animal (No. 288) from the region near Ankara, Turkey.	(Ahmed <i>et al.</i> , 1989)
BoMac	Bovine macrophage cell line immortalized by SV40 large T-antigen.	(Stabel and Stabel, 1995)
HeLa	Human cell line derived from a cervical cancer isolated in 1951 from the patient Henrietta Lacks.	(Puck <i>et al.</i> , 1956)
PBL	Peripheral blood leukocyte. The blood was collected from cattle.	

##### 3.1.2 Chemicals, reagents and Kits

Reagent	Company
10x T4 DNA ligase buffer (0.5ml)	Fermentas, Sankt Leon-Rot, Germany
2-Mercaptoethanol for RNA extraction	Carl Roth GmbH, Karlsruhe, Germany
2-Mercaptoethanol (50mM) for complete cell culture medium	Gibco®, Life Technologies, Darmstadt, Germany
6x Loading Dye Solution	Fermentas, Sankt Leon-Rot, Germany
Acrylamide/Bis-acrylamide	Bio-Rad Laboratories GmbH, München, Germany
Advantage® 2 PCR (High fidelity PCR)	Clontech, Saint-Germain-en-Laye, France
Agar Agar	Carl Roth GmbH, Karlsruhe, Germany
AnnexinV Apoptosis Detection Kit	Santa Cruz Biotechnology. Inc, Heidelberg, Germany
APS (ammonium persulfate)	Carl Roth GmbH, Karlsruhe, Germany
BCIP (5-bromo-4 chloro-3-indolyl phosphate)	Carl Roth GmbH, Karlsruhe, Germany
BioRAD Micro-DC Assay Kit	Bio-Rad Laboratories GmbH, München, Germany
Boric acid (H <sub>3</sub> BO <sub>3</sub> )	Carl Roth GmbH, Karlsruhe, Germany
Bromophenol blue	Sigma-Aldrich Chemie GmbH, Taufkirchen, Germany
BSA	PAA, Laboratories, Pasching, Austria
Carbenicillin (50mg/ml)	Carl Roth GmbH, Karlsruhe, Germany
Cell Trace™ CFSE Cell Proliferation Kit	Life Technologies GmbH, Darmstadt, Germany
Crystal Agarose (500g)	Biolab products GmbH, Göttingen, Germany
DABCO	Sigma-Aldrich Chemie GmbH, Taufkirchen, Germany
ddH <sub>2</sub> O	B. Braun Melsungen AG, Melsungen, Germany
D-Glucose (D-Glucose monohydrate C <sub>6</sub> H <sub>12</sub> O <sub>6</sub> ·H <sub>2</sub> O)	Merck Millipore, Darmstadt, Germany

Dimethylformamide	Merck Millipore, Darmstadt, Germany
DMEM high glucose (4.5g/l)	PAA, Laboratories, Pasching, Austria
DMSO	Carl Roth GmbH, Karlsruhe, Germany
DTT	Sigma-Aldrich Chemie GmbH, Taufkirchen, Germany
EDTA	Carl Roth GmbH, Karlsruhe, Germany
EGTA	Serva Electrophoresis GmbH, Heidelberg, Germany
Ethanol	Merck Millipore, Darmstadt, Germany
Fetal calf serum	Biochrom AG, Berlin, Germany
Geldanamycin (GA)	InvivoGen, San Diego, California, USA
GeneRuler™ 1kb Plus DNA Ladder	Fermentas, Sankt Leon-Rot, Germany
Glycerin	Carl Roth GmbH, Karlsruhe, Germany
Glycin	Carl Roth GmbH, Karlsruhe, Germany
H <sub>2</sub> O- (nuclease free)	Fermentas, Sankt Leon-Rot, Germany
Hepes (4-(2-hydroxyethyl)-1-Piperazineethanesulfonic acid)	Sigma-Aldrich Chemie GmbH, Taufkirchen, Germany
InnuPREP Plasmid Mini Kit	Analytik Jena, Life Science, Jena, Germany
IPTG (Isopropyl β-D-1-thiogalactopyranoside) 1M	PEQLAB Biotechnologie GmbH, Erlangen, Germany
Isopropanol	Merck Millipore, Darmstadt, Germany
Kanamycin	Carl Roth GmbH, Karlsruhe, Germany
KCl	Carl Roth GmbH, Karlsruhe, Germany
KH <sub>2</sub> PO <sub>4</sub>	Merck Millipore, Darmstadt, Germany
L-Glutamine (200 mM)	PAA, Laboratories, Pasching, Austria
Methanol	Merck Millipore, Darmstadt, Germany
MgCl <sub>2</sub>	Carl Roth GmbH, Karlsruhe, Germany
MgSO <sub>4</sub>	Merck Millipore, Darmstadt, Germany
Na <sub>2</sub> HPO <sub>4</sub>	Merck Millipore, Darmstadt, Germany
Na <sub>2</sub> HPO <sub>4</sub> ×2H <sub>2</sub> O	Merck Millipore, Darmstadt, Germany
NaCl (Sodium chloride)	Carl Roth GmbH, Karlsruhe, Germany
NaH <sub>2</sub> PO <sub>4</sub>	Carl Roth GmbH, Karlsruhe, Germany
NaH <sub>2</sub> PO <sub>4</sub> ×H <sub>2</sub> O	Carl Roth GmbH, Karlsruhe, Germany
NaOH	Carl Roth GmbH, Karlsruhe, Germany
NBT (nitro blue tetrazolium chloride)	Carl Roth GmbH, Karlsruhe, Germany
Ni-NTA columns	Qiagen, Hilden, Germany
Nocodazole	Sigma-Aldrich Chemie GmbH, Taufkirchen, Germany
Non-Essential Amino Acids (100x)	PAA, Laboratories, Pasching, Austria
Novobiocin	Santa Cruz Biotechnology. Inc, Heidelberg, Germany
PageBlue™ Protein Staining Solution	Thermo Scientific, Schwerte, Germany
PageRuler™ prestained protein ladder	Fermentas, Sankt Leon-Rot, Germany
Penicillin-Streptomycin (100x)	PAA, Laboratories, Pasching, Austria
Percoll (density = 1,131 g/ml)	GE Healthcare Bio-Sciences AB, Uppsala, Sweden
PFA (Paraformaldehyde)	Merck Millipore, Darmstadt, Germany
Phenol red	Sigma-Aldrich Chemie GmbH, Taufkirchen, Germany
Ponceau S red stain	Sigma-Aldrich Chemie GmbH, Taufkirchen, Germany
PVA (Polyvinyl alcohol)	Sigma-Aldrich Chemie GmbH, Taufkirchen, Germany

Pyronin Y	Serva Electrophoresis GmbH, Heidelberg, Germany
PCR Cloning Kit	Qiagen, Hilden, Germany
QIAquick Gel Extraction Kit	Qiagen, Hilden, Germany
QIAquick PCR Purification Kit	Qiagen, Hilden, Germany
RevertAid H Minus First Strand cDNA Synthesis Kit	Thermo Scientific, Schwerte, Germany
RNeasy® Mini Kit	Qiagen, Hilden, Germany
Roti®-ImmunoBlock (10x)	Carl Roth GmbH, Karlsruhe, Germany
RPMI 1640	PAA, Laboratories, Pasching, Austria
SDS (Dodecylsulfate-Na-salt)	Serva Electrophoresis GmbH, Heidelberg, Germany
Skimmed milk	Sigma-Aldrich Chemie GmbH, Taufkirchen, Germany
Sodium Pyruvate Solution (100 mM)	PAA, Laboratories, Pasching, Austria
T4 DNA ligase (200 units)	Fermentas, Sankt Leon-Rot, Germany
TEMED (N,N,N',N'-Tetramethylethylenediamine)	Merck Millipore, Darmstadt, Germany
Tris base (C <sub>4</sub> H <sub>11</sub> NO <sub>3</sub> )	Serva Electrophoresis GmbH, Heidelberg, Germany
Tris-Cl	Carl Roth GmbH, Karlsruhe, Germany
Trisodium citrate x2H <sub>2</sub> O	Carl Roth GmbH, Karlsruhe, Germany
Triton x-100	AppliChem GmbH, Darmstadt, Germany
Trypanblau 0.5% [w/v]	Biochrom AG, Berlin, Germany
Trypsin (10x)	PAA, Laboratories, Pasching, Austria
Trypton /Pepton	Carl Roth GmbH, Karlsruhe, Germany
Tryptone	Carl Roth GmbH, Karlsruhe, Germany
Tween® 20	Carl Roth GmbH, Karlsruhe, Germany
Urea	Carl Roth GmbH, Karlsruhe, Germany
X-Gal (5-bromo-4-chloro-3-indolyl-β-D-galactopyranoside) 40mg/ml	PEQLAB Biotechnologie GmbH, Erlangen, Germany
Yeast extract	Carl Roth GmbH, Karlsruhe, Germany

### 3.1.3 Buffers, solutions and media

Buffers, solutions and media	Components
0.25% Triton-X-100	0.25% (v/v) in PBS
1% Agarose gel	1% (w/v) Crystal agarose in 1xTBE buffer
10% APS buffer	10% (w/v) APS in H <sub>2</sub> O
10% BSA	10% BSA (w/v) in PBS
1x Assay buffer (Annexin V Apoptosis Detection Kit)	10% (v/v) 10x Assay buffer 90% (v/v) ddH <sub>2</sub> O
1x HEPES-EDTA	10 mM HEPES; 150 mM NaCl; 20 mM KCl; 5 mM EDTA; pH=7.4
1x HEPES-CaCl <sub>2</sub>	10mM HEPES; 150 mM NaCl; 20 mM KCl; 1 mM CaCl <sub>2</sub> ; pH=7.4
1x Roti-ImmunoBlock	10% (v/v) Roti®-ImmunoBlock (10x) 90% (v/v) TBS
1x TBE	89 mM Tris base; 89 mM Boric acid; 2 mM EDTA; pH=8
2% PFA	2% (w/v) PFA in PBS
20x HEPES	200 mM HEPES; 3M NaCl; 400 mM KCl; pH=7.4

20x SSC	3M NaCl; 340 mM Trisodium citrate.2H <sub>2</sub> O; pH=7.0
2x SDS-PAGE sample buffer	50% (v/v) 4x SDS-PAGE in ddH <sub>2</sub> O
2x SSC	1:10 20xSSC in H <sub>2</sub> O
3% BSA blocking buffer	3% (w/v) BSA in PBS
4% PFA	4% (w/v) PFA in PBS
4x SDS-PAGE sample buffer	180 mM Tris-HCl; 4% (w/v) SDS; 40% (v/v) Glycerin 0.04% (w/v) Bromophenol Blue; 100 mM DTT in ddH <sub>2</sub> O, pH= 6.8
5% BSA	5% BSA (w/v) in PBS
5% Skimmed milk	5% (w/v) Skimmed milk in PBS
50% Glycerin	50% (v/v) Glycerin in ddH <sub>2</sub> O
70% Ethanol	70% (v/v) Ethanol in ddH <sub>2</sub> O
AP buffer	100 mM Tris base; 100 mM NaCl; 5 mM MgCl <sub>2</sub> ; pH=9.5
BCIP stock solution	5% (w/v) BCIP (5-bromo-4 chloro-3-indolyl phosphate) in 100% Dimethylformamide
Blotting buffer (Wet blot)	20% (v/v) Methanol; 0.1% (v/v) SDS solution; 20 mM Tris base; 150 mM Glycine; pH= 8.3
Buffer B	100 mM NaH <sub>2</sub> PO <sub>4</sub> xH <sub>2</sub> O; 10 mM Tris-Cl; 8M Urea Adjust pH= 8.0 using NaOH
Buffer C	100 mM NaH <sub>2</sub> PO <sub>4</sub> xH <sub>2</sub> O; 10 mM Tris-Cl; 8M Urea Adjust pH= 6.3 using HCl
Buffer D	100 mM NaH <sub>2</sub> PO <sub>4</sub> xH <sub>2</sub> O; 10 mM Tris-Cl; 8M Urea Adjust pH= 5.9 using HCl
Buffer E	100 mM NaH <sub>2</sub> PO <sub>4</sub> xH <sub>2</sub> O; 10 mM Tris-Cl; 8M Urea Adjust pH= 4.5 using HCl
DABCO	2.5% (w/v) DABCO; 10 ml PBS; 90 ml Glycerin; pH = 8.6
Denaturing solution	0.5M NaOH ; 1.5M NaCl
LB Agar plates	1.5% (w/v) Agar agar in LB-Medium
LB medium	1% (w/v) tryptone / peptone; 0.5 % (w/v) yeast extract; 1% (w/v) NaCl in H <sub>2</sub> O; pH = 7.5
Lower phase Percoll (85%)	85% (v/v) Percoll; 5% (v/v) 20x Hepes; 10% (v/v) EDTA (50 mM)
Lower Tris buffer (pH=8.8)	1.5M Tris; 0.4% (w/v) SDS in H <sub>2</sub> O
NBT (Stock solution)	5% (w/v) NBT (nitro blue tetrazolium chloride) in 70% Dimethylformamide / ddH <sub>2</sub> O
NBT/ BCIP staining buffer	0.66% NBT; 0.33% BCIP in AP buffer
Neutralization solution	1.5M NaCl; 0.5M Tris-Cl; pH=7.4
PBS	154 mM NaCl; 8.00 mM Na <sub>2</sub> HPO <sub>4</sub> x2H <sub>2</sub> O; 2 mM KH <sub>2</sub> PO <sub>4</sub> ; pH=7.3
PBS (Flow cytometry)	9.1 mM Na <sub>2</sub> HPO <sub>4</sub> , 1.7 mM NaH <sub>2</sub> PO <sub>4</sub> and 150 mM NaCl; pH=7.4
Psi broth	4 mM MgSO <sub>4</sub> ; 10mM KCl; LB medium
Pyronin Y buffer	0.5M Tris-HCl; 10% (v/v) Glycerin; 0.4% (w/v) SDS; 0.01% (w/v) Pyronin Y in H <sub>2</sub> O
SDS running buffer	25 mM Tris, 192 mM glycine, 0.1% SDS
SDS solution	10% (w/v) Sodium dodecyl sulfate
SOC medium	2% (w/v) tryptone; 0.5% (w/v) yeast extract; 10 mM NaCl; 2.5 mM KCl; 10 mM MgCl <sub>2</sub> ; 10 mM MgSO <sub>4</sub> ; 20 mM glucose; ddH <sub>2</sub> O; pH=7.0
TBS buffer	10 mM Tris-Cl; 150 mM NaCl; pH=7.5
TBS-Tween buffer	10 mM Tris-Cl; 150 mM NaCl; 0.1% (v/v) Tween® 20; pH=7.5
TGE	107.8 mM NaCl; 2.05 mM Na <sub>2</sub> HPO <sub>4</sub> ; 1.58 KH <sub>2</sub> PO <sub>4</sub> ; 4.45 mM KCl; 5.5 mM D-Glucose; 22.28 Tris base; 0.025 mM Phenol red; 10% (v/v) Trypsin(10x); 1.05 mM EGTA and 0.01% (w/v) PVA (Dissolved in 1 liter ddH <sub>2</sub> O, pH=7.6)
Trypan blue working solution	1:3 (v/v) Trypan blue (0.5% [w / v] stock solution) in PBS
Upper phase Percoll (45%)	45% (v/v) Percoll; 5% (v/v) 20x Hepes; 10% (v/v) EDTA (50 mM); 40% (v/v) ddH <sub>2</sub> O
Upper Tris buffer (pH=6.8)	0.5M Tris; 0.4 % (w/v) SDS in H <sub>2</sub> O

### 3.1.4 Primers

All primers were ordered from Eurofins MWG operon, Ebersberg, Germany.

Table 2: List of primers

Name	Sequence (5'-3')	T <sub>m</sub> [°C]	Application
TaHSP90C1-1F	5'-ATGAAAGTTAGTTTACTCTTG-3'	50.1	PCR
TaHSP90C1-1R	5'-CTATAATTCATCATTGGACC-3'	51.2	PCR
TaHSP90C4-1F	5'-ATGAATCCTCGATTGGGT-3'	52.4	PCR
TaHSP90C4-1R	5'-TTATACAAGGTCTAGGGTG-3'	52.4	PCR
M13 forward	5' TGTA AACGACGGCCAGT -3'	53.7	M13 PCR
M13 reverse	5' CAGGAAACAGCTATGACC -3'	53.7	M13 PCR
TaHSP90C1-2F	5'-CCCGAACTTGATTGGTCAGT-3'	57.3	Sequencing
TaHSP90C1-2R	5'-ACAACCAACTGTGGCTCTTC-3'	57.3	Sequencing
TaHSP90C1-3F	5'-TAAACAGGAAGTAGGATGGG-3'	55.3	Sequencing
TaHSP90C1-3R	5'-CTTCTAACACGAAACCACTC -3'	55.3	Sequencing
TaHSP90C4-2F	5'-GGACAGTTCGGAGTTGGATT -3'	57.3	Sequencing
TaHSP90C4-2R	5'-CGAAATCTCCTCTTGGCGCT -3'	59.4	Sequencing
TaHSP90C4-3F	5'-AGGAATGACAGCAGAAGAAC-3'	55.3	Sequencing
TaHSP90C4-3R	5'-TGTTGCTTGATCTCTTCTCC -3'	55.3	Sequencing
TaHSP90C4-4F	5'-AAGAGAATAGCGAGCAAAGC-3'	55.3	Sequencing
TaHSP90C4-4R	5'- TCTACCAGCCTACTACTAAC -3'	55.3	Sequencing
TaHSP90-C1-XP2_F	5'TATGGATCCAAGAAGTTGAAGGATAAACA-3'	61.0	T4 Ligation
TaHSP90-C1-XP2_R	5'TATGTCGACAAGGTAGAGGAGTTTGAC-3'	63.4	T4 Ligation
TaHSP90-C4-XP1_F	5'-TATGGATCCAATCCTCGATT-3'	48.5	T4 Ligation
TaHSP90-C4-XP1_R	5'-TATAAGCTTTTATACAAGGTCT-3'	46.5	T4 Ligation
pQE-30 TypeIII/IV	5'- CGGATAACAATTTACACAG-3'	53.2	pQE-30
pQE-30 reverse	5'-GTTCTGAGGTCATTACTGG-3'	54.5	pQE-30

#### qRT- PCR primers and probes

Primers were ordered from Eurofins MWG operon, Ebersberg, Germany. The probes were ordered from Roche Diagnostic GmbH, Mannheim, Germany.

Table 3: List of qRT-PCR primers and probes

Name	Sequence (5'-3')	Tm [° C]	UPL Probe No	Parasite/ Host	Accession No	Target/ Reference gene
UPL-BHSP90 aa1-1F	5'-CAGGAGGGTCCTTCAC AGTAA-3'	59	2	Bovine HSP90	NM_00101267 0.2	Target
UPL-BHSP90 aa1-1R	5'-CAGAATAACCTTTGTT CCACGTC -3'	59	2	Bovine HSP90	NM_00101267 0.2	Target
UPL-BHSP90 ab1-1F	5'-TGTTTCGAAACTGCACT GCTC-3'	60	106	Bovine HSP90	NM_00107963 7.1	Target
UPL-BHSP90 ab1-1R	5'-GTAGATGCGGTTGGA GTGG-3'	59	106	Bovine HSP90	NM_00107963 7.1	Target
UPLTaHSP90 c1-1F	5'-ACTCCGACTCGTTCCC ATT-3'	59	84	<i>T.</i> <i>annulata</i>	XM_948749.1	Target
UPLTaHSP90 c1-1R	5'-CACACCTTTTTCCCA ATCA-3'	60	84	<i>T.</i> <i>annulata</i>	XM_948749.1	Target
UPLTaHSP90 c4-1F	5'-AAAGAGTGCCGGACG ATG-3'	59	11	<i>T.</i> <i>annulata</i>	XM_948193.1	Target
UPLTaHSP90 c4-1R	5'-TGCCTTTTCTTTGTTAC TGTCTTG-3'	59	11	<i>T.</i> <i>annulata</i>	XM_948193.1	Target
Tamr1-12-FW	5'-CCACTCCTGTAGCGGG TAAA-3'	59	12	<i>T.</i> <i>annulata</i>	XM_948695.1 (TA16685)	Target
Tamr1-12-RV	5'TTGTGGAGGTAAGTACC CAAA-3'	59	12	<i>T.</i> <i>annulata</i>	XM_948695.1 (TA16685)	Target
GAPDH-80- FW	5'-CACTCCCAACGTGTCT GTTG-3'	60	80	Bovine	NM_00103403 4.2	Reference
GAPDH-80- RV	5'-CTGCTTCACCACCTTC TTGA-3'	59	80	Bovine	NM_00103403 4.2	Reference
GAPDH-45-F	5'-CAACAGCGACTCAC TCTTCT-3'	59	45	Bovine	NM_00103403 4.2	Reference
GAPDH-45-R	5'-TGACAAAGTGGTCGTT GAGG-3'	59	45	Bovine	NM_00103403 4.2	Reference
TaActin-31- FW	5'-CGGAAGGGACCTGACT GAG-3'	60	31	<i>T.</i> <i>annulata</i>	XM_946720.1 (TA15750)	Reference
TaActin-31- RV	5'-CGGAAGGGACCTGACT GAG-3'	59	31	<i>T.</i> <i>annulata</i>	XM_946720.1 (TA15750)	Reference

### 3.1.5 Antibodies

Table 4: List of primary antibodies. WB: Western blotting, IF: Immunofluorescence

Antibody	Dilution	Company
Anti p53 DO7 p53 (DO-7) is a mouse monoclonal antibody epitope mapping between amino acids 1-45 of p53 human origin.	IF 1:50	Santa Cruz Biotechnology Inc., Heidelberg, Germany
Anti-Tamr1 (Bob E21) Polyclonal rabbit anti-Tamr1 Gene symbol: TA16685.	IF 1:2000	(Shiels <i>et al.</i> , 1994)
Anti-Tams1 (5E1) Monoclonal mouse anti-Tams1 Gene symbol: TA17050 and the sequence: LTVANGYRFKTLKVGQKT.	IF 1:10	(Shiels <i>et al.</i> , 1994)
Anti-TaSP Rabbit antiserum against the <i>T. annulata</i> surface protein.	IF 1:10,000	(Schnittger <i>et al.</i> , 2002)

## Materials and Methods

HSP90 $\alpha/\beta$ (F-8): sc-13119 Mouse monoclonal	WB 1:200 IF 1:250	Santa Cruz Biotechnology, Inc, Heidelberg, Germany
Mouse RGS-His antibody (100 $\mu\text{g}$ )	WB 1:1000	Qiagen, Hilden, Germany
Rabbit anti- <i>T. annulata</i> HSP90 antiserum	WB 1:250	(Mohammed <i>et al.</i> , 2013)

Table 5: List of secondary antibodies. WB: Western blotting, IF: Immunofluorescence

Antibody	Dilution	Company
Alexa Fluor® 488 Goat Anti-Mouse IgG (H+L)	IF 1:500	Life Technologies GmbH, Darmstadt, Germany
Alexa Fluor® 568 Goat Anti-Rabbit IgG (H+L)	IF 1:500	Life Technologies GmbH, Darmstadt, Germany
DAPI (4',6-Diamidine 2', phenylindole dihydrochlorid), DNA stain.	IF 1 $\mu\text{g}/\text{ml}$	Roche diagnostic, Mannheim, Germany
Goat anti-Mouse AP Alkaline phosphatase-conjugated IgG+ IgM (H+L)	WB 1:1000	Jackson ImmunoResearch Laboratories, Inc. West Grove, USA
Goat anti-Rabbit AP Alkaline phosphatase-conjugated IgG (H+L)	WB 1:1000	Jackson ImmunoResearch Laboratories, Inc. West Grove, USA
IRDye® 680RD Polyclonal Goat anti-Rabbit IgG (H+L)	WB 1:10,000	LI-COR Biosciences, Lincoln, USA
IRDye® 800CW Polyclonal Goat anti-Mouse IgG (H+L)	WB 1:10,000	LI-COR Biosciences, Lincoln, USA

### 3.1.6 Bacteria, vectors and enzymes

Bacteria / Vector	Company
10 x FastDigest® buffer	Fermentas, Sankt Leon-Rot, Germany
<i>E. coli</i> DH5 $\alpha$ Genotype: F' $\phi$ 80lacZ $\Delta$ M15 $\Delta$ (lacZYA-argF) <b>U169 recA1 endA1 hsdR17 (r<sub>k</sub><sup>-</sup>, m<sub>k</sub><sup>+</sup>) phoA supE44 <math>\lambda</math> thi<sup>1</sup> gyrA96 relA1</b>	Invitrogen Life Technologies GmbH, Darmstadt, Germany
<i>E. coli</i> M15 (pREP4)	Qiagen, Hilden, Germany
FastDigest®BamHI 5'...G↓G A T C C...3' 3'...C C T A G↑G...5'	Fermentas, Sankt Leon-Rot, Germany
FastDigest®EcoRI 5'...G↓A A T T C...3' 3'...C T T A A↑G...5'	Fermentas, Sankt Leon-Rot, Germany
FastDigest®HindIII 5'...A↓A G C T T...3' 3'...T T C G A↑A...5'	Fermentas, Sankt Leon-Rot, Germany
FastDigest®Sall 5'...G↓T C G A C...3' 3'...C A G C T↑G...5'	Fermentas, Sankt Leon-Rot, Germany
pDrive vector (50 ng/ $\mu\text{l}$ )	Qiagen, Hilden, Germany
pQE-30: belongs to the pDS plasmid family (Bujard <i>et al.</i> , 1987) and has a 6xHis-tag coding sequence in the N-terminus.	Qiagen, Hilden, Germany

### 3.1.7 Lab supplies

Item	Company
12 well cell culture Multiwell plate	Greiner Bio-One GmbH, Frickenhausen, Germany
24 well cell culture Multiwell plate	Greiner Bio-One GmbH, Frickenhausen, Germany
24 well Multiwell plate	Greiner Bio-One GmbH, Frickenhausen, Germany
5ml Polystyrene round bottom	BD Becton Dickinson GmbH, Heidelberg, Germany
96 Multiwell plate	Roche Diagnostic GmbH, Mannheim, Germany
Cell scraper (25cm, 39.4cm)	Sarstedt AG & Co, Nümbrecht, Germany
Culture flask canted neck	Corning Incorporated, USA
Gel blot paper (58cm x58cm)	Whatman GmbH, Dassel, Germany
Gel Drying Frames –MAXI (Spare pack of cellophane 24cmx24cm)	Carl Roth GmbH, Karlsruhe, Germany
Glass plates (10 cm x 11 cm) and (10 cm x 20 cm)	G&P Kunststofftechnik, Kassel, Germany
Microtiter plate (96 well plate)	Corning GmbH, Kaiserslautern, Germany
Neubauer chamber	Brand, Wertheim, Germany
Nitrocellulose membrane (0.2µM 300 mmx3m)	Whatman GmbH, Dassel, Germany
Pipette	Eppendorf, Hamburg, Germany
Polystyrene dish	Greiner Bio-One GmbH, Frickenhausen, Germany
Round coverslips, 15 mm diameter	Thermo Scientific, Schwerte, Germany
Scalpel	Bayha C. Bruno GmbH, Tuttlingen, Germany
Slides	Thermo Scientific, Schwerte, Germany
Spacers	G&P Kunststofftechnik, Kassel, Germany
SteriPettes™ (5ml, 10ml, 25ml)	Corning GmbH, Kaiserslautern, Germany
SuperFrost® Plus	Thermo Scientific, Schwerte, Germany
Syringe needles	BD Becton Dickinson GmbH, Heidelberg, Germany
Tube (0.5, 1.5, 2, 15 and 50 ml)	Sarstedt AG & Co, Nümbrecht, Germany
Ultracentrifuge tube, Ultra-Clear™ (14x95 mm)	Beckman Coulter Inc, Brea, USA

### 3.1.8 Equipment

Equipment	Company
Branson -250, sonifier TM 2	Branson Ultraschall, Dietzenbach, Germany
Centrifuge 5810R	Eppendorf, Hamburg, Germany
Confocal microscope, TCS SP5	Leica Microsystems GmbH, Wetzlar, Germany
Cytospin 3	Shandon, Pittsburgh, USA
Electrophoresis chamber (SDS gel)	G&P Kunststofftechnik, Kassel, Germany
Electrophoresis power supply	G&P Kunststofftechnik, Kassel, Germany
Electrophoresis, Mini (Agarose gel documentation)	G & P Kunststofftechnik, Kassel, Germany
ELISA reader	Expert 96, Asys Hitech GmbH, Eugendorf, Austria
FACS Calibur flow cytometry System	BD, Franklin Lakes, USA
Freezer (-20°C), Liebherr Comfort	Liebherr, Biberach an der Riss, Germany
Freezer (-70°C), Revco value plus	Thermo scientific, Schwerte, Germany
Gel dryer- Model 543	Bio-Rad Laboratories GmbH, München, Germany
HERAcell® 150, Cell incubator	Thermo scientific, Schwerte, Germany

## Materials and Methods

---

Heraeus B5025 , Incubator for Bacteria	Thermo scientific, Schwerte, Germany
LI-COR Odyssey®	Li-cor Biosciences GmbH, Bad Homburg, Germany
Light Cycler® 480 II system	Roche Diagnostic GmbH, Mannheim, Germany
Microcentrifuge, Centrifuge	Eppendorf, Hamburg, Germany
Mini Protean II™, Western transblot system	Bio-Rad Laboratories GmbH, München, Germany
NanoDrop 1000	PEQLAB, Biotechnologie GmbH, Erlangen, Germany
Retort Stand & Clamp	Carl Roth GmbH, Karlsruhe, Germany
Rocking platform shaker	Biometra GmbH, Goettingen, Germany
Rolling shaker 220V,50HZ	Glaswarenfabrik Karl Hecht GmbH & Co. KG, Sondheim vor der Rhön, Germany
Spectrophotometer	Eppendorf, Hamburg, Germany
Thermocycler, TProfessional TRIO	Biometra GmbH, Goettingen, Germany
Thermomixer 5436, Heating block	Eppendorf, Hamburg, Germany
Ultracentrifuge L7-65	Beckman Coulter GmbH, Krefeld, Germany
UVStar, UV light	Biometra GmbH, Goettingen, Germany
Vortex VF2	IKA®-Werke GmbH, Staufen, Germany
Water bath	GFL, Gesellschaft für Labortechnik GmbH, Burgwedel, Germany
Wilovert®, light microscope	Helmut Hund GmbH, Wetzlar, Germany

### 3.1.9 Software

Program	Application
Leica Application Suite, AF (V.1.8.2)	Imaging program for confocal microscope (Leica SP5)
MikroWin Version 4.06; licence Nr: 3205	Protein measurement
Universal Probe Library Probe Finder version 2.49 for other organism	qRT-PCR

## 3.2 Methods

### 3.2.1 Cell culture

#### 3.2.1.1 *T. annulata* Ankara 288-infected cells (cell line)

Cells were cultured in 25 cm<sup>2</sup>, 75 cm<sup>2</sup> or 175 cm<sup>2</sup> culture flasks in RPMI 1640 complete medium (RPMI 1640, 10% (v/v) heat-inactivated fetal calf serum, 4 mM L-glutamine, 100 U/ml penicillin, 100 U/ml streptomycin, 1 mM sodium pyruvate solution, 1% Non-Essential Amino Acids and 0.1 mM 2-Mercaptoethanol) and incubated at 37°C in a humidified atmosphere with 5% CO<sub>2</sub>.

#### 3.2.1.2 Bovine macrophage cell line (BoMac)

BoMac cells were cultured as mentioned above.

#### 3.2.1.3 HeLa cell line

HeLa cells were cultured in DMEM complete medium (DMEM, 10% (v/v), heat-inactivated fetal calf serum, 4 mM L-glutamine, and 100 U/ml penicillin and 100 U/ml streptomycin). The cell line was incubated at 37°C in a humidified atmosphere with 5% CO<sub>2</sub>.

### 3.2.2 Sub-culturing and cell counting

For all cell lines, medium was changed twice per week. First, cells were washed with 10 ml PBS and then trypsinized for 2 min using 1-3 ml TEG. The trypsinization was stopped by adding fresh RPMI 1640 complete medium or DMEM complete medium, respectively. To quantify the cells, 10 µl of the suspension were added to 190 µl of trypan blue working solution. After that, 10 µl from this solution were applied to a Neubauer chamber and the cells were counted under a light microscope according to the formula below:

$$\text{Number of cells / ml} = \frac{\Sigma \text{ of the cells of 4 large squares} \times 20 \text{ (dilution factor)} \times 10^4}{4}$$

4

For sub-culturing, 1x10<sup>6</sup> cells were transferred into a new 75 cm<sup>2</sup> culture flask containing fresh medium.

### **3.2.3 Molecular biological methods**

#### **3.2.3.1 Genetic information about *T. annulata* HSP90**

Information about the *T. annulata* HSP90 gene was obtained from Genbank (<http://www.ncbi.nlm.nih.gov/genbank/>) and GeneDB (<http://www.genedb.org>). Reference sequences of two isoforms were found; one located at chromosome one (accession no.: XM\_948749.1) named here TaHSP90-Chr1, and the second isoform located at chromosome four (accession no.: XM\_948193) named here TaHSP90-Chr4.

#### **3.2.3.2 RNA extraction**

Total RNA was extracted from *T.annulata* Ankara 288-infected cells using the RNeasy® Mini Kit according to the manufacturer's instructions. Briefly, *T.annulata* Ankara 288-infected cells as pellets (approximately  $10^7$  cells) were resuspended in 600  $\mu$ l of RLT buffer (containing 1% 2-Mercaptoethanol). The lysates were pipetted into a QIAshredder spin column placed in a 2 ml collection tube and centrifuged for 2 min at 12,000x g. 600  $\mu$ l of 70% ethanol were added to the flow-through (from the previous step) and mixed by pipetting. The homogenized samples were transferred into the RNeasy spin column and centrifuged for 15 s at 8,000x g. The RNeasy spin columns were washed using RW1 buffer for 15 s at 8,000x g and then the RNeasy spin columns were washed twice using RPE buffer for 15 s at 8,000x g and for 2 min at 8,000x g, respectively. The RNA was dissolved by adding 30-50  $\mu$ l RNase free water in the RNeasy spin column placed in a 1.5 ml RNase-free tube and incubated for 1 min at RT before being centrifuged for 1 min at 8,000x g. The concentration of RNA was measured by using the NanoDrop 1000 and the quality of RNA was evaluated by using electrophoresis. Briefly, 5  $\mu$ g of RNA were mixed with 1  $\mu$ l of 6 x Loading Dye Solution and loaded onto a 1% agarose gel. The RNA was stored at -70°C.

#### **3.2.3.3 Synthesis of cDNA**

For the synthesis of cDNA from RNA the RevertAid H Minus First Strand cDNA Synthesis Kit was used. First, the genomic DNA was removed from isolated RNA by using 1  $\mu$ l of RNase-free DNaseI and 1  $\mu$ l of 10x Reaction buffer (containing MgCl<sub>2</sub>) for 1  $\mu$ g of RNA. The mixture was incubated at 37°C for 30 min. One  $\mu$ l of 50 mM EDTA was added to the mixture and incubated at 65°C for 10 min.

For the synthesis of cDNA from mRNA the RevertAid H Minus M-Mul V Reverse Transcriptase enzyme was used. 5 µg of prepared RNA were used in a final reaction volume of 20 µl. To the RNA, 1 µl of oligo (dT)<sub>18</sub> primers, 4 µl of 5x reaction buffer, 2 µl of 10 mM dNTP mix, 1 µl of Ribolock RNase inhibitor (20 U/ µl) and 1 µl of RevertAid H Minus M-Mul V Reverse Transcriptase (200 U/ µl) were added. The mixture was incubated at 42°C for 60 min. The reaction was terminated by heating at 70 °C for 5 min and the prepared cDNA was stored at -20°C.

### **3.2.3.4 PCR**

#### **3.2.3.4.1 Conventional PCR**

Two primer pairs (TaHSP90C1-1F and TaHSP90C1-1R for TaHSP90-Chr1 and TaHSP90C4-1F and TaHSP90C4-1R for TaHSP90-Chr4) were designed based on the Genbank reference sequences (accession no.: XM\_948749.1 and XM\_948193) to amplify the full-length gene sequences. A high fidelity PCR was applied to amplify the desired fragments using cDNA, prepared from *T.annulata* Ankara 288- infected cells, as a template. PCR reactions were performed in 50 µl volume containing 40 µl of PCR-grade water, 5 µl of 10x PCR buffer, 1 µl of cDNA template (200 ng/µl), 1 µl of each primer (10 µM), 1 µl of 50x dNTP mix and 1 µl of the 50x polymerase mix. PCR program was comprised at 94°C for 3 min followed by 35 cycles of 94°C for 30 s, 52°C for 30 s, 72°C for 3.5 min and a final extension step at 72°C for 7 min. PCR products were separated on an 1% agarose gel.

#### **3.2.3.4.2 M13 PCR**

The colonies were tested for the correct insert in a M13 PCR reaction utilizing the M13 primers and 2 µl of purified plasmid prepared from individual clones as a template. The cycling program for M13 PCR was performed as follows: 94°C initial denaturation step for 3 min, 30 cycles of 94°C for 30 s, 55°C for 30 s and 72°C for 3 min followed by a final extension step at 72 °C for 7 min. The correct product size was determined as the original PCR product size plus 267 bp representing flanking vector sequences.

### 3.2.3.4.3 pQE PCR

PCR reaction was done to verify the presence of the TaHSP90-Chr1 and TaHSP90-Chr4 constructs in the pQE30 vector utilizing pQE primers (Type III/IV and reverse). The PCR conditions were performed as described in section (3.2.3.4.2) with an annealing temperature of 54°C for 30s.

### 3.2.3.4.4 Quantitative real-time polymerase chain reaction (qRT-PCR)

The effect of the HSP90 inhibitor Geldanamycin (GA) regarding gene expression of parasite or host HSP90 in *T. annulata* Ankara 288-infected cells was analysed using the qRT-PCR method. QRT-PCR was performed in 96 Multiwell plate format using the Light Cycler® 480 system. The assessment of gene expression was performed using primers and hydrolysis probes (also known as TaqMan probes). Hydrolysis probes are oligonucleotides of 8-9 nucleotides length that have a fluorophore covalently attached to the 5' end and a quencher to the 3' end. As long as the fluorophore and the quencher are in proximity, quenching inhibits any fluorescence signal. When the probe hybridizes to the target sequence, the 5'-nuclease activity of the polymerase cleaves the hydrolysis probe thus separating the fluorophore and quencher and allowing fluorescence of the fluorophore. With an increasing amount of target sequence during PCR, more probes are cleaved and the fluorescence signal of the unquenched reporter dye increases.

All primers and hydrolysis probes were chosen based on the bioinformatic results of the software ProbeFinder at <http://www.roche-applied-science.com>. The primers and probes were aligned using the ClustalW multiple alignment tool ([http://npsa-pbil.ibcp.fr/cgi-bin/align\\_clustalw.pl](http://npsa-pbil.ibcp.fr/cgi-bin/align_clustalw.pl)) and blasted ([blast.ncbi.nlm.nih.gov/](http://blast.ncbi.nlm.nih.gov/)) to verify the specificity of the primers and probes used for each gene (*T. annulata* HSP90 or bovine HSP90).

The expression of genes was analysed using qRT-PCR. The cells were prepared as described in section (3.2.10.1.2) and incubated in RPMI 1640 complete medium containing GA or DMSO as described in Table 19 and Table 20. The cells were gently scraped and harvested by centrifugation at 800x g for 5 min and the RNA was extracted as explained in section (3.2.3.2) and diluted in RNase free water at the ratio 1:3.

Using the Light Cycler® 480 Probes Master kit, the RT-PCR reaction was performed in 10 µl volume containing 5 µl of Light Cycler® 480 Probes Master (2x), 2.5 µl of H<sub>2</sub>O PCR grade,

0.1  $\mu$ l of probe, 2  $\mu$ l of diluted RNA and 0.4  $\mu$ l of primer mix (10  $\mu$ M from each). The mixture was transferred into a 96 Multiwell plate. The RT-PCR program was performed following the steps described in Table 6.

Table 6: The RT-PCR program

Step	Temperature (°C)	Time	Cycles
Pre-incubation	95	10 min	1
Amplification	95	10 s	50
	58	30 s	
	72	1 s	
Cooling	40	30 s	1

### 3.2.3.5 Purification of PCR products

The purification of PCR products was done using the QIAquick PCR Purification Kit according to the manufacturer's instructions. Briefly, 5 volumes of PB buffer were added to 1 volume of the PCR product and mixed together ( $\text{pH} \leq 7.5$ ). The mixture was applied into a QIAquick spin column placed in a 2 ml collection tube and centrifuged at 15,000x *g* for 1 min. The flow-through was discarded and the column was placed back into the same collection tube. The column was then washed by addition 0.75 ml of PE buffer and centrifuged at 15,000x *g* for 1 min. The flow-through was discarded and the column was placed back into the same collection tube and centrifuged for an additional 1 min at 15,000x *g*. The QIAquick spin column was placed in a 1.5 microcentrifuge tube and the DNA was eluted by addition 50  $\mu$ l of ddH<sub>2</sub>O to the column and then centrifuged at 15,000x *g* for 1 min.

### 3.2.3.6 Purification of DNA fragments

Purification of DNA fragments was done using the QIAquick Gel Extraction Kit according to the manufacturer's instructions. DNA bands were excised from the agarose gel with a sharp, clean scalpel and placed in a 2 ml tube. To solubilize the gel fragment, 3 volumes of QG buffer (in microliters) were added to 1 volume of gel (in milligram) and then incubated at 50°C for 10 min. After the gel was dissolved completely, 1 volume of isopropanol was added and mixed. To bind the DNA, the solution was applied into a QIAquick spin column placed in a 2 ml collection tube and centrifuged at 15,000x *g* for 1 min. The flow-through was discarded and the column was placed back into the same collection tube. The QIAquick spin column was washed by addition of 0.75 ml PE buffer and then centrifuged at 15,000x *g* for 1

min. The flow-through was discarded and the column was placed back into the same tube and centrifuged for an additional 1 minute as described above. After that, the column was placed into a clean 1.5 ml microcentrifuge tube and the DNA was eluted by adding 50  $\mu$ l of H<sub>2</sub>O to the centre of the QIAquick membrane and centrifuged at 15,000x g for 1 min.

### **3.2.3.7 Cloning of PCR products, transformation into *E. coli* and restriction digestion**

Cloning of PCR products was performed using the Qiagen PCR Cloning Kit according to the manufacturer's instructions. Briefly, 4  $\mu$ l of purified PCR product were mixed with 1  $\mu$ l pDrive cloning vector (50 ng/ $\mu$ l) and 5  $\mu$ l of 2x ligation master mix. The ligation reaction was incubated at 16°C for 18 h. Then the ligated product was transformed into *E. coli* DH5 $\alpha$  competent cells. Therefore, 5  $\mu$ l of the ligation reaction mixture were added to tube containing 100  $\mu$ l aliquot of competent cells, mixed gently and incubated on ice for 30 min. After that, cells were heat-shocked by placing the tubes in a 42°C heating block for 45 s without shaking followed by an incubation on ice for 2 min. 500  $\mu$ l of SOC medium were added to each tube before the tubes were shaken in a water bath for 1.5 h. Subsequently, the tubes were centrifuged at 10x g for 5 min, 500  $\mu$ l of the supernatant were removed and the pellets were resuspended gently in the remaining 100  $\mu$ l of the medium. Volumes of 20  $\mu$ l and 80  $\mu$ l from the tube's contents were plated onto LB agar plates containing carbenicillin (100  $\mu$ g/ml), 50  $\mu$ M IPTG and X-Gal (80  $\mu$ l/ml) and incubated at 37 °C overnight.

White colonies were picked and grown overnight in 5 ml of LB medium containing 100  $\mu$ g/ml carbenicillin at 37°C. After purification of the plasmid as described in section (3.2.3.8), the presence of insert was tested by using FastDigest® *EcoRI* (*BamHI* and *HindIII* in case of TaHSP90-Chr4) restriction enzymes. The FastDigest® restriction enzymes were used according to manufacturer's instructions. Briefly, 14-15  $\mu$ l of nuclease free-H<sub>2</sub>O, 2 $\mu$ l of 10x FastDigest® buffer and 1  $\mu$ l FastDigest® enzyme were added to 1 $\mu$ g of plasmid DNA and incubated at 37°C for 1 h. The products were run on an 1% agarose gel. Positive colonies were stored as glycerol stocks at -70 °C. Therefore, 500  $\mu$ l of overnight culture were mixed with 500  $\mu$ l of 50% glycerine.

### **3.2.3.8 Plasmid purification**

Plasmid purification of individual clones was performed using the innuPREP Plasmid Mini Kit. 5 ml of overnight bacterial culture were centrifuged at 11,000x g for 1 min and the supernatant was discarded. After that, the cell pellets were resuspended by adding 250  $\mu$ l of

Re-suspension buffer and then vortexed. 250 µl of Lysis buffer were added to the suspension and mixed by inverting the tubes 6-8 times. This step was followed by adding 350 µl of Neutralization buffer and mixed by inverting the tubes 6-8 times; the tubes were then centrifuged for 10 min at 12,000x g. The supernatant was decanted into a spin filter column and centrifuged at 11,000x g for 1 min. The flow-through was discarded and the column was washed twice using 500 µl of washing solution A for 1 min at 11,000x g and 700 µl of washing solution B for 1 min at 11,000x g, respectively. The column was centrifuged for additional 2 min to remove residual washing buffer. The elution step was performed by adding 50 µl of ddH<sub>2</sub>O on the spin filter membrane placed in a new 1.5 ml tube and centrifuged at 11,000x g for 1 min.

### 3.2.3.9 Sequencing and bioinformatics

Plasmids were sequenced (Eurofins MWG operon, Ebersberg, Germany). To verify the sequencing accuracy for TaHSP90-Chr1 and TaHSP90-Chr4, multiple alignments for sequenced clones of each isoform were performed using a ClustalW multiple alignment method ([http://npsa-pbil.ibcp.fr/cgi-bin/align\\_clustalw.pl](http://npsa-pbil.ibcp.fr/cgi-bin/align_clustalw.pl)).

The signal peptide was determined using SignalP 4.0 server (SignalP: <http://www.cbs.dtu.dk/services/SignalP/>). Amino acid sequence blast of TaHSP90-Chr1 and TaHSP90-Chr4 was carried out against other apicomplexa parasites ([blast.ncbi.nlm.nih.gov/](http://blast.ncbi.nlm.nih.gov/)) and a phylogenetic tree was constructed using a phylogeny analysis software (<http://www.phylogeny.fr/>). The determination of the HSP90 domain in TaHSP90-Chr1 and TaHSP90-Chr4 sequences was carried out using InterProScan, version 4.8 (<http://www.ebi.ac.uk>).

### 3.2.3.10 Generation of pQE30 expression constructs

The information obtained from bioinformatic analysis was used to generate pQE30 expression constructs. Clones showing 100% identity for each isoform were used to amplify the HSP90 domains (between amino acids 288 and 738) of TaHSP90-chr1 (55.9 kDa) and the full-length open reading frame (ORF) of TaHSP90-Chr4. First, PCR products were cloned into the pDrive vector as described in section (3.2.3.7), and then plasmids were purified as described previously (3.2.3.8). After that, 5 µg of plasmid DNA containing the TaHSP90-Chr1 or TaHSP90-Chr4 insert and the pQE30 empty vector were digested with restriction enzymes *BamHI* and *Sall* or *BamHI* and *HindIII* as described previously (3.2.3.7). After

digestion, the plasmid DNA was separated on an 1% agarose gel and then the correct fragments (size 2967 bp, 2742 bp and 3400 bp for TaHSP90-Chr1, TaHSP90-Chr4 and pQE-30, respectively) were cut out from the agarose gel and purified as described in section (3.2.3.6) and then the concentration was measured using NanoDrop 1000. The purified fragments (TaHSP90-Chr1, TaHSP90-Chr4) were ligated into the linearized pQE30 vector. The ligation was performed in 10 µl volume containing 50 ng of digested pQE-30, 100 ng of digested plasmid (TaHSP90-Chr1 or TaHSP90-Chr4), 1 µl of T4 DNA ligase, 1 µl of 10x T4 DNA ligase buffer and H<sub>2</sub>O-nuclease free. The ligation reaction was incubated at 16 °C for 18 h.

### **3.2.3.11 Transformation of M15 (pREP4) competent cells**

An aliquot containing 100 µl of the competent *E.coli* M15 (*pREP4*) cells was thawed on ice and gently resuspended. 5 µl of the ligation were added to the competent cells and mixed by gentle pipetting. After that, cells were kept on ice for 20 min and then heat-shocked by incubating at 42°C for 90 s. The cells were incubated on ice for 2 min before 200 µl of Psi broth medium were added to the cells. The tubes were incubated at 37°C for 1.5 h in a shaking water bath. Finally, volumes of 75 µl and 125 µl from each transformation were plated on LB-agar plates containing 25 µg/ml kanamycin and 100µg/ml carbenicillin then incubated at 37°C overnight.

## **3.2.4 Expression and purification of recombinant *T. annulata* HSP90**

### **3.2.4.1 Colony Blot**

The colony blot procedure was used to identify the clones expressing His-tagged protein according to the manufacturer's instructions (QIAGEN). The LB-agar plate containing the clones was removed from the incubator and opened to allow any condensation to dry for 10 min. After that, the nitrocellulose membrane positioned on the LB-agar for 1 min. The membrane and agar were pierced at the asymmetric position using a syringe needle to facilitate a proper alignment after staining. After that, the membrane (colony side up) was transferred onto a fresh agar plate containing 25 µg/ml kanamycin, 100µg/ml carbenicillin and 250 µM IPTG and incubated for 4 h at 37°C. The original plate was placed back in the incubator to allow the clones to regrow. A set of polystyrene dishes was prepared, whereby each dish contained a sheet of gel blot paper wetted with one of the following solutions: SDS

solution, denaturing solution, neutralization solution and 2xSSC. The membrane was placed (colony side up) on the gel blot paper in the following order: 10 min on the paper wetted with SDS solution, 5 min on the paper wetted with denaturing solution, 10 min on the paper wetted with neutralization solution and 15 min on the paper wetted with 2x SSC. All incubation steps were performed at RT. At the end, immunostaining of the membrane was performed as described in section (3.2.6.4.1) by using RGS-His antibody as primary antibody to detect His-tag positive clones.

#### **3.2.4.2 Protein expression**

For each construct (TaHSP90-Chr1 and TaHSP90-Chr4) several colonies were picked and each used to inoculate 7 ml LB broth medium containing 25 µg/ml kanamycin and 100 µg/ml carbenicillin and incubated overnight with gentle shaking in a water bath at 37°C. On the next day, 1 ml of overnight culture was added to 50 ml freshly prepared LB medium containing 25 µg/ml kanamycin and 100 µg/ml carbenicillin and grown at 37°C with gentle shaking in a water bath. At an OD<sub>600</sub> value of 0.6 (measured by spectrophotometer), IPTG was added with a final concentration of 2 mM to induce protein expression and the culture was incubated for further 4h. Finally, the bacterial cells were pelleted by centrifugation at 300x g for 1 min and stored at -20°C.

#### **3.2.4.3 Protein purification**

Recombinant proteins were purified under denaturing conditions using Ni-NTA columns following the manufacturer's instructions. First, the cell pellets were thawed on ice and resuspended in buffer B (5ml per gram-wet weight). The resuspended cells were lysed under rotation for 1.5 h at RT. The lysates were centrifuged at 10,000x g for 30 min at 4°C. After that, the supernatant was transferred into a clean tube and kept for protein purification. For SDS-PAGE analysis as described in section (3.2.5.3), 5 µl of 2x SDS-PAGE sample buffer were mixed with 5 µl of supernatant and stored at -20°C until use.

Before purification, the Ni-NTA columns were equilibrated with 0.5 ml buffer B and the flow-through was discarded. After that, the supernatants were applied to the Ni-NTA columns and mixed by rolling on a rotary shaker for 1 h at 4°C. By using a retort stand, the columns were fixed and the screw caps were removed. The flow-through was collected by gravity flow and kept for SDS-PAGE analysis. The columns were washed two times, each with 4ml of buffer C. Finally, the proteins were eluted by adding four times 0.5 ml buffer D

followed by four times each with 0.5 ml buffer E (each flow-through was collected by gravity flow and kept for SDS-PAGE analysis).

### **3.2.5 Protein analysis**

#### **3.2.5.1 Preparation of cell lysates**

Cells (*T. annulata* Ankara 288-infected cells, BoMac cells, Bovine Peripheral Blood Lymphocytes (PBL) and Hela cells) were counted as described in section (3.2.2) and  $5 \times 10^6$  cells were harvested by centrifugation at 600x g for 5 min then the pellet was resuspended in PBS. After that, cells were pelleted again at 600x g for 10 min at 4°C. The supernatants were discarded and the pellets were resuspended in 400 µl ddH<sub>2</sub>O by pipetting. Then, the cells were sonicated on ice using Branson -250 sonifier (settings: duty cycle= 30%, output control= 3) for 8 sequential cycles each consisting of 30 s sonication and 30 s pause. The lysates were centrifuged at 15,000x g for 10 min at 4°C and the supernatants were transferred into new 1.5 ml tubes. The protein concentration was measured using BioRAD Micro-DC Assay kit as described in section (3.2.5.2). The lysates were stored at -20°C.

#### **3.2.5.2 Protein quantification**

The protein concentration was measured using BioRAD Micro-DC Assay kit. As reference, a serial dilution of bovine serum albumin ranging between 2.0 and 0.2 mg/ml was used. The samples were diluted 1:5 and 1:10 in H<sub>2</sub>O. Five µl of BSA and the samples were pipetted into a microtiter plate and 25 µl of reagent A and 200 µl of reagent B were added. The plate was incubated for 30 min at RT in a dark place. Finally, the optical density values were read at 550 nm using an ELISA reader. The values were processed automatically using a computer program (MikroWin Version 4.06), where the concentrations were given in mg/ml.

#### **3.2.5.3 SDS-polyacrylamide gel electrophoresis (SDS-PAGE)**

SDS-PAGE was used to separate proteins according to their molecular size. The SDS-PAGE technique used here was similar to the method that described by Laemmli (1970). Briefly, two glass plates (10 cm x 11 cm) or (10 cm x 20 cm) were cleaned using 70 % ethanol and then assembled using spacers and fixed onto a clamping frame. The gel solution (7.5% resolving gel (lower gel) and 3% stacking gel (upper gel)) was prepared according to Table 7. First, the resolving gel was transferred into the assembled chamber then covered with 70 %

ethanol and allowed to polymerize for 45 min. After removing the ethanol, the stacking gel was transferred into the assembled chamber and then the combs were placed into the stacking gel between the glasses. The stacking gel was left to polymerize for 30 min. Ready gels were removed from the clamping frame and placed in the electrophoresis chamber filled with running buffer.

The samples were prepared by mixing 20 µg of protein with 5 µl of 4x SDS-PAGE sample buffer in a total volume of 20 µl and heated at 98°C for 10 min. Up to 20 µl of each sample were loaded per pocket. As a marker, 5 µl of PageRuler™ Prestained protein Ladder were used. Electrophoresis was carried out for 75 min as follows: 50 V for 5 min, 100 V for 10 min and 200 V for 1 h.

Table 7: Composition of resolving and stacking gel

Component	7.5% resolving gel	3% Stacking gel
H <sub>2</sub> O	6 ml	3 ml
Acrylamide/Bis-acrylamide (30%)	3 ml	0.5 ml
1.5M Tris (lower Tris buffer)	3 ml	-
0.5M Tris (upper Tris buffer)	-	1.25 ml
TEMED	10 µl	10 µl
10% APS	100 µl	30 µl
Pyronin Y buffer	-	10 µl

#### 3.2.5.4 Coomassie blue staining

PageBlue™ Protein Staining Solution was used to visualize the protein bands on acrylamide gels. First, the gel was washed 3 times using distilled water for 3 min at RT then was covered with PageBlue™ solution and incubated for 3 h at RT with gentle shaking. The washing steps were performed with distilled water, each for 10 min until the protein bands become visible. The gel was placed between cellophane papers and allowed to dry by using a vacuum gel dryer.

#### 3.2.5.5 Transfer of protein onto nitrocellulose membrane

SDS-PAGE separated proteins were transferred onto a nitrocellulose membrane following the wet blot method. The membrane was cut according to the gel size (7.5 cm x 9 cm for small gel, 7.5 cm x 17 cm for a large gel). Gel and the membrane were assembled as shown in (Figure 5) and then placed in the western transblot system. The chamber was filled with blotting buffer. The transfer was carried out overnight at 25 V, 50 mA and 300 W. Protein

transfer was checked using Ponceau S red stain. After that, the membrane was washed 3 times for 10 min with TBS buffer.

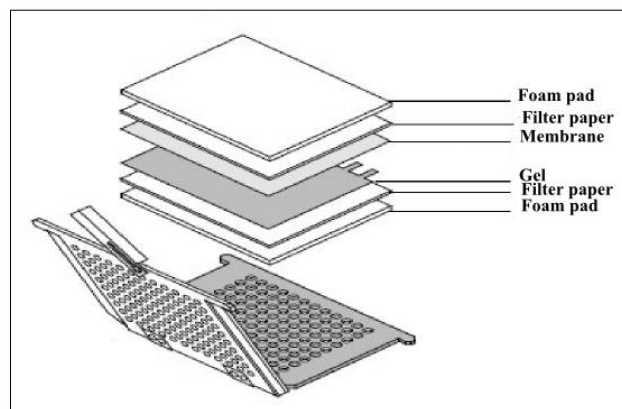


Figure 5: Preparation of the wet blot system.

Modified after ([http://www.biorad.com/webroot/web/images/lsr/products/electrophoresis/product\\_overlay\\_content/global/lsr\\_components\\_p3\\_of\\_trans\\_blot\\_cell\\_instructio.jpg](http://www.biorad.com/webroot/web/images/lsr/products/electrophoresis/product_overlay_content/global/lsr_components_p3_of_trans_blot_cell_instructio.jpg))

### 3.2.6 Generation of rabbit anti-*T. annulata* HSP90 antiserum

#### 3.2.6.1 Identification of antigenic peptides for immunization

Antigenic peptides were deduced from the sequence of TaHSP90-Chr1 and TaHSP90-Chr4 using the predication server Predicting Antigenic Peptides (<http://imed.med.ucm.es/Tools/antigenic.pl>). The peptide sequence of each isoform (TaHSP90-Chr1 and TaHSP90-Chr4) was aligned with bovine HSP90 (bovine HSP90-alpha, accession: BAC82487.1 and bovine HSP90-beta, accession: NP\_001073105.1) using ClustalW multiple alignment method (<http://www.ebi.ac.uk/Tools/msa/clustalw2>) to select the sequence region with the least identity between *T. annulata* HSP90 and bovine HSP90. Finally, the peptide sequence ELEKVKAVKEEKEWN was selected which is identical with amino acids 452-467 of TaHSP90-Chr1 and has 86% similarity with the corresponding region of TaHSP90-Chr4.

#### 3.2.6.2 Peptide synthesis

The selected peptide was synthesized by the Structural Biochemistry group at Research Centre Borstel. The name given for this peptide was TaHSP90C1\_C452-466.

### 3.2.6.3 Immunization of rabbits with a synthetic peptide

Two rabbits were immunized with the synthesized peptide TaHSP90C1\_C452-466 using an established immunization protocol (Charles River Laboratories, Germany). To enhance the immune response, 200 µg of peptide were mixed with complete or incomplete Freund's adjuvant. Starting from the third immunization, 10 ml of blood were taken from the ear vein 10 days after the immunization. After centrifugation of the blood (at 500×g for 30 min at 4°C), the serum (anti-*T. annulata* HSP90 antiserum) was tested for the presence of specific antibodies by using dot blot.

### 3.2.6.4 Immunodetection of proteins

#### 3.2.6.4.1 Western blot

The detection of proteins on nitrocellulose membranes was performed by using an antigen-specific antibody. First, the membrane was washed twice for 10 min each time with TBS buffer, then blocked with blocking buffer for 1 h at RT followed by three washing steps in TBS buffer each time for 10 min at RT. The primary antibody was applied to the membrane and incubated for 1-3 h at RT. Afterwards, the membrane was washed three times as described above. The secondary antibody was applied to the membrane and incubated for 1h at RT and the membrane was washed again as mentioned above. In case of using NBT/ BCIP staining buffer for detection, the membrane was equilibrated in AP buffer for 10 min. All incubation steps were performed under gentle shaking using a horizontal shaker.

Table 8: Primary and secondary antibodies used for western blot analysis.

Blocking buffer	3% BSA	5% skimmed milk	5% skimmed milk	5% skimmed milk
Primary antibody	RGS-His antibody (diluted in 3% BSA)	anti-HSP 90 $\alpha/\beta$ (F-8) (diluted in 5% skimmed milk)	anti- <i>T.annulata</i> HSP90 antiserum (diluted in 5% skimmed milk)	anti- <i>T.annulata</i> HSP90 antiserum and RGS-His antibody (diluted in 5% skimmed milk)
Secondary antibody	Goat anti mouse AP (diluted in 3% BSA)	Goat anti mouse AP (diluted in 5% skimmed milk)	Goat anti rabbit AP (diluted in 5% skimmed milk)	IRDye® 680RD goat anti rabbit and IRDye® 800W goat anti mouse (diluted in 1x Roti-ImmunoBlock buffer)
Substrate	NBT/ BCIP staining buffer	NBT/ BCIP staining buffer	NBT/ BCIP staining buffer	-
Detection	-	-	-	LI-COR Odyssey® scanner

#### **3.2.6.4.2 Dot blot**

To verify the efficiency of the obtained immune sera to detect *T. annulata* HSP90, the dot blot method was used. The peptide was dissolved in PBS to final concentrations of 2 µg/2 µl, 4 µg/2 µl and 8 µg/2 µl. Two microliters from each concentration were placed onto the membrane and dried overnight. Immunostaining was performed as described in section (3.2.6.4.1) by using anti-*T. annulata* HSP90 antiserum (1:100, 1:500 and 1:1000 diluted in 5% skimmed milk) as primary antibody.

#### **3.2.7 Isolation of *T.annulata* schizonts**

*T. annulata* schizonts were isolated according to a published protocol (Bakheit *et al.*, 2006). Briefly,  $5 \times 10^7$  cells were incubated in RPMI complete medium containing 10 µM nocodazole for 18 h at 37°C with 5% CO<sub>2</sub>. Cells were harvested by centrifugation at 650x g for 5 min at 4°C and then washed twice with cold PBS. The pellet was resuspended in 0.9 ml ice-cold 1x HEPES-CaCl<sub>2</sub> buffer. After adding proaerolysin at a final concentration of 30 µg/ml, the cells were incubated for 30 min under rotation at 4°C. After that, the cells were washed twice with ice-cold 1x HEPES-CaCl<sub>2</sub> at 650x g for 5 min at 4°C. The pellet was resuspended in 2 ml 1x HEPES-EDTA buffer and incubated for 15 min at 37 °C in a water bath. 2 ml of cell lysate were mixed with 7.6 ml of lower phase Percoll (85%) and the volume was adjusted to 10 ml by adding 1x HEPES- EDTA and mixed to obtain a final Percoll concentration of 64.6% (v/v). Each ultracentrifuge tube received 5 ml of the mixture and was layered with 7 ml of the upper phase Percoll (45%). The tubes were centrifuged at 85,000x g for 30 min at 12°C. The schizont layer between the two Percoll gradients (milky ring) was collected carefully and transferred into a 1.5 ml tube and washed twice with cold PBS at 2000x g for 5 min at 4°C. The schizont pellets were used either to prepare cytopsin slides or lysate.

#### **3.2.8 Cytopsin slides**

Cytopsin slides were prepared from isolated *T.annulata* schizonts (3.2.7) using Cytopsin-3. Since isolated schizonts tend to clump together, the appropriate dilution had to be determined empirically. The isolated schizonts were washed once using cold PBS and resuspended in 10% BSA. A volume of 100 µl suspension was loaded into each chamber placed on a slide (Super Frost® Plus) and spun at 60x g for 5 min. The slides were allowed to dry overnight at RT and stored at -70°C.

### 3.2.9 Immunocytochemistry

#### 3.2.9.1 Confocal microscopy

##### 3.2.9.1.1 Preparation of cells for immunofluorescence staining

*T. annulata* Ankara 288-infected cells and BoMac were grown under sterile conditions in 24 well cell culture Multiwell plate on round cover slips. Therefore,  $1 \times 10^5$  cells/2 ml RPMI 1640 complete medium were seeded per well and incubated at 37°C and 5% CO<sub>2</sub> overnight.

##### 3.2.9.1.2 Immunofluorescence staining

Cytospin slides (section 3.2.8) were fixed in 2% PFA at RT for 10 min. The fixation of *T. annulata* Ankara 288-infected cells and BoMac (section 3.2.9.1.1) was performed by adding 4% PFA directly to the medium at a ratio 1:1 (v/v) for 10 min at RT. Afterwards, the cover slips and slides were washed three times using PBS for 1 min and permeabilized in 0.25% Triton-X-100 for 10 min at RT followed by washing steps as described above. The specimens were blocked in 10% BSA for 1h and washed as described above. The primary antibodies were added and incubated for 2h at RT. After that, the cover slips and slides were washed three times with PBS and incubated with the appropriate secondary antibodies for 45 min at RT. The cover slips and slides were washed three times with PBS and fixed with 2% PFA for 4 min at RT. After a final washing step, specimens were mounted in DABCO mounting medium. The analysis was carried out under a confocal laser scanning microscope.

Table 9: Primary and secondary antibodies used for immunofluorescence staining.

Primary antibodies	anti- HSP 90 $\alpha/\beta$ (F-8) and anti-TaSP	anti-TaSP and anti p53 DO7
Secondary antibodies	Alexa Fluor® 488 Goat Anti-Mouse, Alexa Fluor® 568 Goat Anti-rabbit and DAPI	Alexa Fluor® 488 Goat Anti-Mouse, Alexa Fluor® 568 Goat Anti-rabbit and DAPI

##### 3.2.9.1.3 Immunofluorescence staining to quantify merozoites

*T.annulata*- infected cells were prepared as described in section (3.2.10.1.2) and incubated in RPMI 1640 complete medium containing GA or DMSO as described in Table 17. One day before staining, the cells were scraped gently and harvested by centrifugation at 850x g for 5 min and transferred into 24 well cell culture plate on round cover slips at a concentration of  $1.5 \times 10^5$  cells/2ml of RPMI 1640 complete medium per well containing the same concentration of GA or DMSO. The immunofluorescence staining was performed as

explained in Table 10. The cover slips were fixed on the slides using DABCO. The analysis was carried out under a confocal laser scanning microscope. Merozoites were counted and the percentage of merozoite-forming cells was calculated based on the total cell number.

Table 10: Staining procedure for cover slip to detect merozoites.

Step	Procedure*	Time
1	Fixation by adding 4% PFA directly the medium at a ratio of 1:1 (v/v).	10 min at RT
2	Permeabilization in 0.25% Triton-X-100.	10 min at RT
3	Blocking in 10% BSA.	1 h at RT
4	Incubation with anti-Tamr1 (diluted in 5 % BSA).	1 h at RT
5	Incubation with Alexa Fluor® 568 Goat Anti-rabbit (diluted in 5 %BSA).	30 min at RT
6	Fixation in 2% PFA	3 min at RT
7	Incubation with anti-Tams1 (diluted in 5 % BSA).	1 h at RT
8	Alexa Fluor® 488 Goat Anti-Mouse and DAPI (both diluted in 5%)	30 min at RT
9	Fixation in 2% PFA	4 min at RT

\* After each step the cover slips were washed 3 times using PBS.

### 3.2.9.2 Fluorescence Assays

#### 3.2.9.2.1 AnnexinV

Cells were stained with annexin V using the AnnexinV Apoptosis Detection Kit and apoptotic cells were identified and quantified by flow cytometry. Briefly, cells were prepared as described in section (3.2.10.1.2) and incubated in 15 ml of RPMI 1640 complete medium containing GA or DMSO as described in Table 14 and Table 15. The cells were gently scraped and harvested by centrifugation at 300x g for 5 min. Cell pellets were washed once with RPMI 1640 complete medium and once with PBS and resuspended in 400 µl 1x Assay buffer. 100 µl aliquots of cells were transferred into 5 ml polystyrene round bottom tubes and incubated with 1x Assay buffer, 1 µl (0.4 µg) of Annexin V -FITC and 5 µl propidium iodide (PI) for 15 min at RT in a dark place. 400 µl of 1x Assay buffer were added to the cells and vortexed gently. The assessment was performed using FACS Calibur flow cytometry.

#### 3.2.9.2.2 CFSE

Proliferation of *T.annulata* Ankara 288-infected cells was measured using the Cell Trace™ CFSE Cell Proliferation Kit. First, the cells were harvested and counted as explained in section (3.2.2) and resuspended in PBS at a concentration of  $1 \times 10^6$  cells /ml. 6 µM of CFSE

as final concentration were added. The cells were vortexed gently for 6 min at RT and then 1ml of ice-cold fetal calf serum was added to stop the reaction of CFSE labelling. After that, the cells were harvested by centrifugation at 350x g for 5 min at 4°C followed by two washing steps with PBS. The efficiency of the CFSE labelling was determined by using FACS Calibur flow cytometry. After CFSE labelling, the cells were grown under sterile conditions in 12 well cell culture plates at a concentration of  $2 \times 10^5$  cell /3 ml RPMI 1640 complete medium per well containing GA or DMSO as explained in Table 18. Proliferation of the cells was measured by FACS Calibur flow cytometry after 1, 3 and 5 or 6 days, respectively.

### 3.2.9.3 Flow cytometry

Results obtained with the Annexin V Apoptosis Kit as well as the CFSE labelling were analysed using FACS Calibur flow cytometry following the settings as described in Table 11 and Table 12.

Table 11: FACS Calibur settings for flow cytometry used to assess apoptosis

Detector	Voltage	Amplitude gain	Mode	Threshold
FSC	E00	1.49	Line	52
SSC	322	1.0	Line	
FL1	420	1.0	Log	
FL2	550	1.0	Log	
FL3	654	1.0	Log	

Table 12: FACS Calibur settings for flow cytometry used to assess cell proliferation

Detector	Voltage	Amplitude gain	Mode	Threshold
FSC	E00	1.49	Line	52
SSC	349	1.0	Line	
FL1	275	1.0	Log	
FL2	550	1.0	Log	
FL3	654	1.0	Log	

### 3.2.10 HSP90 inhibitors

#### 3.2.10.1 Geldanamycin (GA)

GA is a benzoquinone ansamycin antibiotic which binds to the ATP-binding pocket of HSP90 leading to an inhibition of the function of HSP90 (Whitesell *et al.*, 1994; Schulte *et al.*, 1998).

### 3.2.10.1.1 Preparation of geldanamycin (GA)

GA was supplied as a yellow powder (5mg). The stock solution was prepared by dissolving 1 mg of GA in 1 ml DMSO to get a 1.78 mM stock concentration and stored at -20°C.

### 3.2.10.1.2 Preparation of *T. annulata* Ankara 288-infected cells for GA treatment

One million cells were cultured in RPMI 1640 complete medium overnight in 75 cm<sup>2</sup> culture flasks at 37°C and 5% CO<sub>2</sub>. Next day, the medium was removed and the adherent cells were washed gently with warm PBS and new fresh RPMI 1640 complete medium containing GA or DMSO was added.

### 3.2.10.1.3 GA treatment conditions for *T. annulata* Ankara 288-infected cells

Table 13: Treatment conditions for *T.annulata* Ankara 288-infected cells to assess the cell viability using trypan blue.

Incubation Time	1 day	2 days
Temperature (°C)	37 °C	37 °C
Control (using an equal volume to that used in GA-treated cells)	DMSO	DMSO
GA (final concentration)	0.5µM, 1 µM 5 µM 10 µM	0.5 µM 1 µM 5 µM 10 µM

Table 14: Treatment conditions for *T.annulata* Ankara 288-infected cells to assess apoptosis using FACS Calibur flow Cytometry, covering GA concentrations  $\geq 0.5 \mu\text{M}$ .

Incubation Time	1 day	2 days	3 days*
Temperature (°C)	37 °C	37 °C	37 °C
Control (14µl DMSO/50ml RPMI 1640 complete medium)	DMSO	DMSO	DMSO
GA (final concentration)	0.5 µM 1 µM	0.5 µM 1 µM	0.5 µM 1 µM

\* After two days of incubation, the medium was replaced daily with fresh medium containing an equal GA or DMSO concentration.

Table 15: Treatment conditions for *T.annulata* Ankara 288-infected cells to assess apoptosis using FACS Calibur flow Cytometry, covering GA concentrations  $\leq 0.5 \mu\text{M}$ .

Incubation Time	1, 3 and 6 days*	1, 3 and 5 days*
Temperature (°C)	37 °C	41 °C
Control (14 $\mu\text{l}$ DMSO/50ml RPMI 1640 complete medium)	DMSO	DMSO
GA (final concentration)	0.001 $\mu\text{M}$	0.001 $\mu\text{M}$
	0.005 $\mu\text{M}$	0.005 $\mu\text{M}$
	0.01 $\mu\text{M}$	0.01 $\mu\text{M}$
	0.05 $\mu\text{M}$	0.05 $\mu\text{M}$
	0.1 $\mu\text{M}$	0.1 $\mu\text{M}$
	0.25 $\mu\text{M}$	
	0.5 $\mu\text{M}$	

\* After two days of incubation, the medium was replaced daily with fresh medium containing an equal GA or DMSO concentration.

Table 16: Treatment conditions for *T.annulata* Ankara 288-infected cells to assess apoptosis by using immunofluorescence staining.

Incubation Time	1, 3 and 6 day*	1, 3 and 5 days*
Temperature (°C)	37 °C	41 °C
Control (14 $\mu\text{l}$ DMSO/50 ml RPMI 1640 complete medium)	DMSO	DMSO
GA (final concentration)	0.25 $\mu\text{M}$	0.1 $\mu\text{M}$
	0.5 $\mu\text{M}$	

\* After two days of incubation, the medium was replaced daily with fresh medium containing an equal GA or DMSO concentration.

Table 17: The concentration of GA and DMSO and the incubation times used to induce merogony in *T. annulata* Ankara 288-infected cells.

Incubation Time	5 days*	6 days*
Temperature (°C)	41 °C	37 °C
Control (14 $\mu\text{l}$ DMSO/50ml RPMI 1640 complete medium)	DMSO	DMSO
GA (final concentration)	0.001 $\mu\text{M}$	0.001 $\mu\text{M}$
	0.005 $\mu\text{M}$	0.005 $\mu\text{M}$
	0.01 $\mu\text{M}$	0.01 $\mu\text{M}$
	0.05 $\mu\text{M}$	0.05 $\mu\text{M}$
	0.1 $\mu\text{M}$	0.1 $\mu\text{M}$

\* After two days of incubation, the medium was replaced daily with fresh medium containing an equal GA or DMSO concentration.

Table 18: The concentration of GA and DMSO and the incubation time used to assess proliferation in *T. annulata* Ankara 288-infected cells.

Incubation Time	1, 3 and 6 days*	1, 3 and 5 days*
Temperature (°C)	37 °C	41 °C
Control (14µl DMSO/50ml RPMI 1640 complete medium)	DMSO	DMSO
GA (final concentration)	0.01 µM	0.001 µM
	0.05 µM	0.005 µM
	0.1 µM	0.01 µM
	0.25 µM	0.05 µM
	0.5 µM	0.1 µM

\* After two days of incubation, the medium was replaced daily with fresh medium containing an equal GA or DMSO concentration.

Table 19: Showing the GA or DMSO concentrations used to analyse the expression of bovine HSP90 genes.

Incubation Time	1, 3 and 6 days*	2, 3 and 5 days*
Temperature (°C)	37 °C	41 °C
Control (14 µl DMSO/ 50 ml RPMI 1640 complete medium)	DMSO	DMSO
GA (final concentration)	0.01 µM	0.05µM
	0.05 µM	
	0.1 µM	
	0.25 µM	
	0.5 µM	

\* After two days of incubation, the medium was replaced daily with fresh medium containing an equal GA or DMSO concentration.

Table 20: Showing the GA or DMSO concentrations used to analyse the expression of *T. annulata* HSP90 and Tamr1 genes.

Incubation Time	2 days		3 days*		5 days*	6 days*
Temperature (°C)	37 °C	41 °C	37 °C	41 °C	41 °C	37 °C
Control (14 µl DMSO/50 ml RPMI 1640 complete medium)	DMSO	DMSO	DMSO	DMSO	DMSO	DMSO
GA** (final concentration)	0.05 µM					

\* After two days of incubation, the medium was replaced daily with fresh medium containing an equal GA or DMSO concentration. \*\* This concentration was selected depending on the result from the quantification of merozoites.

### **3.2.10.2 Novobiocin**

Several studies were done by using novobiocin as HSP90 inhibitor, which binds to the C-terminal of HSP90. Marcu and co-workers (2000) analysed several C-terminal fragments of HSP90 for novobiocin binding. These fragments revealed that novobiocin binds to a carboxyl-terminal HSP90 fragment containing amino acids 538–728. Moreover, within this region the removal of amino acids 657–677 (DLVILLYETALLSSGFSLEDP) severely compromised novobiocin binding (Marcu *et al.*, 2000).

Novobiocin was dissolving in DMSO to get a 100 mM stock solution. Cells were first prepared as described in section (3.2.9.1.1) and then were treated with novobiocin (0.05, 0.1, 0.5 and 1 mM) or DMSO (at the same volume, respectively). After treatment, the cells were incubated for 3 days at 37°C and 5% CO<sub>2</sub>. The indirect immunofluorescence assay was performed following the procedure as explained in section (3.2.9.1.2).

### **3.2.11 Statistical analysis and data management**

#### **3.2.11.1 General data management**

Data from the experiments were recorded in Excel (Microsoft Corporation, USA) and then figures and tables were prepared. The statistical analysis of the data was performed using SPSS Statistics 19 (IBM Corporation, Armonk, New York, USA) and Graph Pad software (Graph Pad Software, Inc., USA).

#### **3.2.11.2 Quantification of gene expression measured by qRT-PCR**

Changes in the mRNA levels were determined through the calculation of the relative expression. This method compares the expression of the target gene related to the expression of a reference gene (house keeping gene). House keeping genes are constitutively expressed independently of experimental conditions. The  $2^{-\Delta\Delta CT}$  method was used to calculate relative changes in gene expression determined from real-time quantitative PCR experiments and the statistical significance was calculated by using the REST 2009 program (relative expression software tool, Qiagen, Germany) and LightCycler 480 software from Roche (Roche Diagnostic GmbH, Mannheim, Germany).

### 3.2.11.3 Quantitative assessment of the cell proliferation and apoptosis

The amount of apoptotic cells or proliferating cells, respectively, was calculated using the CellQuest™ software (BD Becton Dickinson GmbH, Heidelberg, Germany) and the number of positive cells was given in percentage in correlation to the total cell number.

### 3.3 Plan of work

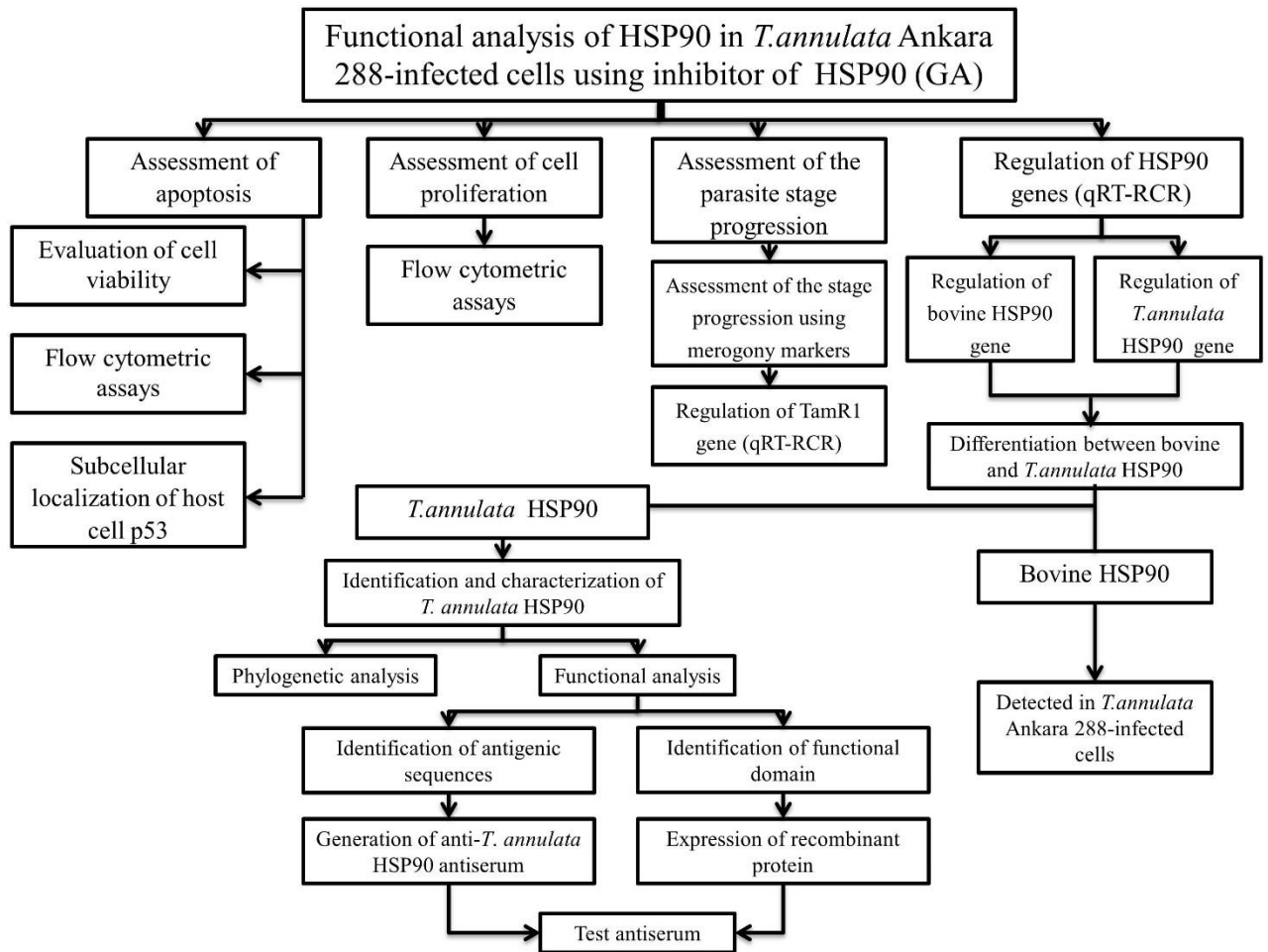


Figure 6: Diagram shows the plan of work.

## 4 Results

### 4.1 Functional analysis of HSP90 in *T.annulata* Ankara 288-infected cells

HSP90 is a unique molecular chaperone protein, which is involved in protein folding following stress. In addition to that, it is involved in chaperoning of important proteins such as kinases and transcription factors. Because HSP90 is involved in multiple cellular processes, the functions of HSP90 have been studied in different organisms using inhibitors. One of the best characterized HSP90 inhibitors is geldanamycin (GA), which inhibits HSP90 by binding to the unusual ADP/ATP-binding pocket of the protein (Schulte *et al.*, 1998).

In this study a functional analysis of HSP90 in *T.annulata* Ankara 288-infected cells was carried out using GA to examine the role of HSP90 in the cell viability, cell proliferation and on the parasite differentiation.

#### 4.1.1 Assessment of apoptosis

##### 4.1.1.1 Cell viability analysis using Trypan blue

In order to determine the number of dead cells in *T.annulata* Ankara 288-infected cells after treatment with GA, the dye exclusion test was applied. Cells were incubated in RPMI 1640 complete medium containing different concentrations of GA ranging between 0.5  $\mu$ M and 10  $\mu$ M as a final concentration. Because of GA was prepared in DMSO, the control cells were treated with the same volume of DMSO. The cells were incubated for 1 and 2 days at 37°C then stained with Trypan blue. The viability of cells was examined under light microscope.

As shown in Figure 7, more than 60% of the cells died after incubation for 1 day with GA (5  $\mu$ M or 10  $\mu$ M), which increased up to 100% after incubation for 2 days at both concentrations. Incubation of the cells with GA (0.5 $\mu$ M or 1 $\mu$ M) for 1 day showed that less than 20% dead cells, while this percentage increased up to 50% and 66% after 2 days incubation with GA 0.5  $\mu$ M and 1  $\mu$ M, respectively.

In all DMSO-treated groups, the percentages of dead cells were less than 10% regardless of the incubation time.

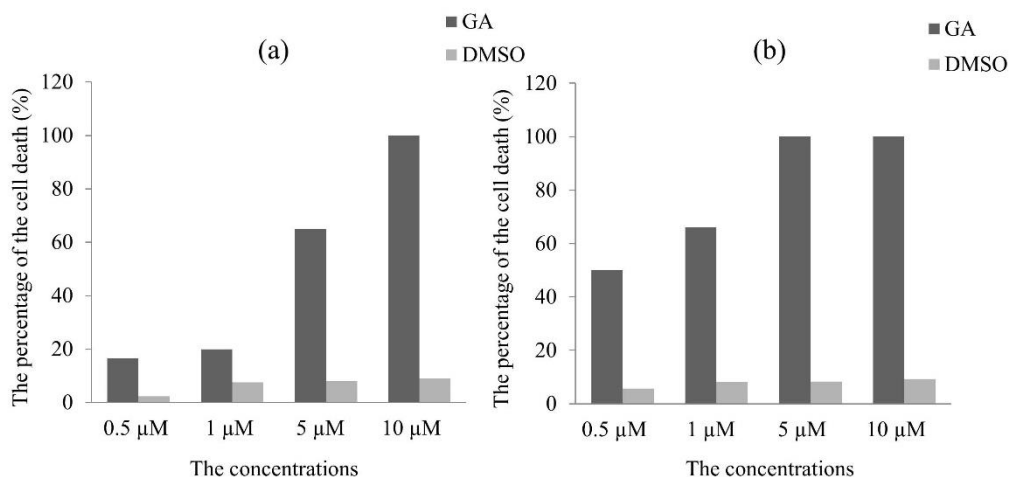


Figure 7: The percentages of dead cells (%) in *T. annulata* Ankara 288-infected cells.

Cells were treated with increasing doses of GA (0.5 µM, 1 µM, 5 µM and 10 µM). The control groups were treated with same volumes of DMSO. Cells were incubated for 1 day (a) and 2 days (b) at 37°C, and then stained with Trypan blue. The cell viability was determined visually under a light microscope.

#### 4.1.1.2 Flow cytometric analysis of apoptosis in *T. annulata* Ankara 288-infected cells incubated at 37°C

Flow cytometric assays for apoptosis are now in widespread use and provide a rapid and reliable means to quantify apoptosis. The results illustrated under 4.1.1.1 showed that GA reduced the cell viability in *T.annulata* Ankara 288-infected cells. In order to see whether the reduction in cell viability was due to apoptosis, the cells were stained with annexin V-FITC and PI and then analysed by flow cytometry. It is known that early apoptotic cells have increased annexin V staining, but not PI staining, while late apoptotic or necrotic cells are stained with both annexin V and PI.

##### 4.1.1.2.1 Treatment with GA ≥ 0.5 µM

Cells were first treated with GA (0.5 µM or 1µM) or DMSO (control groups) and incubated for 1, 2 and 3 days at 37°C. After that, the cells were stained with annexin V -FITC and PI and analysed by using CellQuest™ software (Becton-Dickinson).

Regardless of the incubation time, all DMSO-treated cells showed less than 10% apoptotic cells. In GA 0.5 µM-treated cells, the percentages of apoptotic cells increased to 23.2%, 45.9% and 55.4% after incubation for 1, 2 and 3 days at 37°C, respectively. The statistical analysis of these data revealed that treatment with 0.5 µM GA resulted in a significantly higher apoptotic cells compared with DMSO-treated cells ( $P \leq 0.028$ , Wilcoxon signed rank-

test). This result is in agreement with results obtained by using GA 1  $\mu\text{M}$ , in which the cells after incubation for 1, 2 and 3 days at 37°C showed apoptotic percentages of 35.4%, 55.8% and 70%, respectively ( $P \leq 0.028$ , Wilcoxon signed rank-test) (Figure 8).

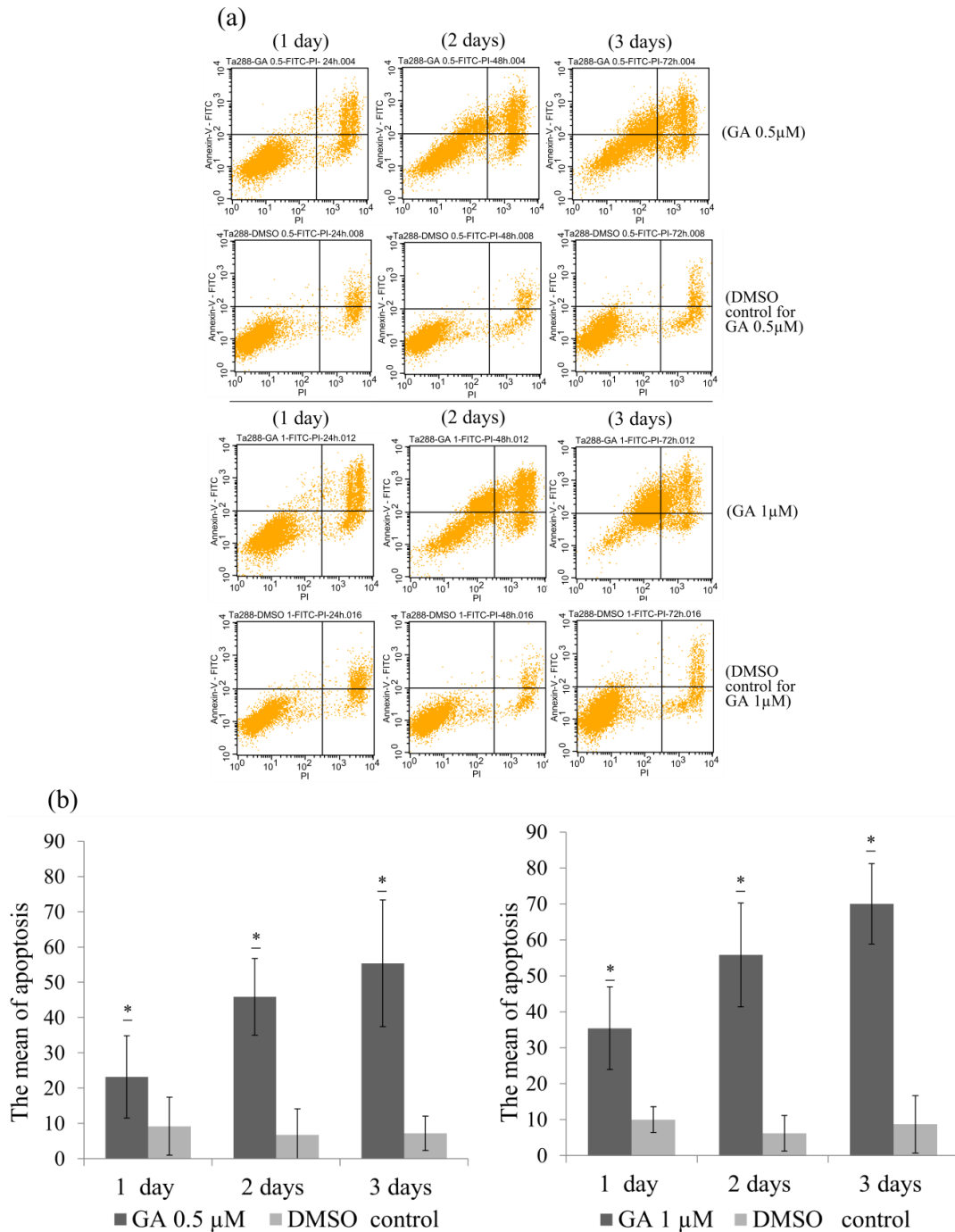


Figure 8: Flow cytometric analysis of apoptosis using Annexin V -FITC and PI staining in *T. annulata* Ankara 288-infected cells treated with GA  $\geq 0.5 \mu\text{M}$  and incubated at 37°C.

Cells were treated with GA (0.5  $\mu\text{M}$  and 1  $\mu\text{M}$ ) or DMSO (control group) and incubated for 1, 2 and 3 days at 37°C. The cells were harvested and stained with 2  $\mu\text{l}$  (0.4  $\mu\text{g}$ ) Annexin V- FITC and 10  $\mu\text{l}$  propidium iodide (PI) and then analysed by flow cytometry. (a) The data shown here represents one experiment of six independent experiments. (b) Mean  $\pm$  S.D (\* $P \leq 0.028$  for both GA concentrations compared with control group (DMSO), Wilcoxon signed rank-test),  $n = 6$ .

#### 4.1.1.2.2 Treatment with GA $\leq$ 0.5 $\mu$ M

The previous results have shown that using GA at concentrations more than 0.5  $\mu$ M induced a significant apoptosis in *T. annulata* Ankara 288-infected cells. Further investigations were performed to see if the lower concentrations of GA have similar effects or not. The cells were treated with DMSO (control group) or different concentrations of GA (0.001  $\mu$ M, 0.005  $\mu$ M, 0.01  $\mu$ M, 0.05  $\mu$ M, 0.1  $\mu$ M, 0.25  $\mu$ M and 0.5  $\mu$ M) and incubated for 1, 3 and 6 days at 37°C. The cells were then stained with annexin V -FITC and PI and analysed by flow cytometry.

As shown in Figure 9, after incubation for 1 day at 37°C, only GA 0.25  $\mu$ M- and 0.5  $\mu$ M-treated cells showed statistically a significant increase in apoptotic cells (3.9%, P = 0.006 and 15%, P=0.00039, respectively, Student's t-test) compared with the control group (1.4%). This result is in agreement with the results obtained after incubation for 3 days at 37°C, in which only treatment with GA 0.25  $\mu$ M and 0.5  $\mu$ M showed statistically a significant increase in apoptotic cells (6.1%, P=0.0002 and 40.1%, P=3.2E-5, respectively, Student's t-test), while in the control group the percentage of apoptotic cells was 2% (Figure 9).

After incubation with different concentrations of GA (0.001  $\mu$ M, 0.005  $\mu$ M, 0.01  $\mu$ M, 0.05  $\mu$ M, 0.1  $\mu$ M, 0.25  $\mu$ M and 0.5  $\mu$ M) for 6 days at 37°C, only GA 0.5  $\mu$ M-treated cells showed statistically a significant increase in apoptotic cells (76.2%, P=1.41E-5, Student's t-test) compared with the control group (2.9%) (Figure 9).

In summary, GA at concentration 0.25  $\mu$ M induced a significant apoptosis in *T.annulata* Ankara 288-infected cells incubated for 1 and 3 days, while GA at concentration 0.5  $\mu$ M induced a significant apoptosis in *T.annulata* Ankara 288-infected cells incubated for 1, 3 and 6 days.

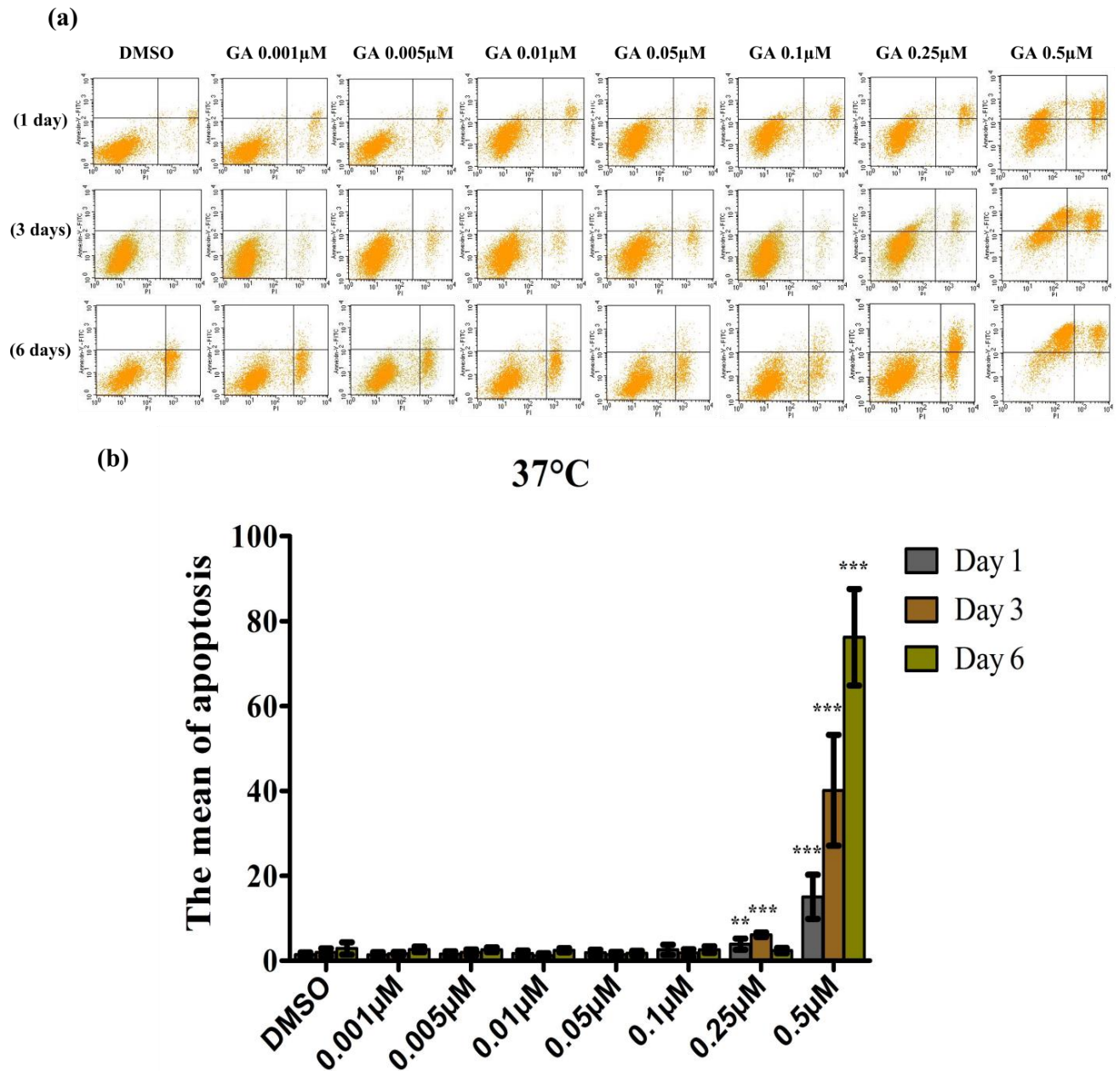


Figure 9: Flow cytometric analysis of apoptosis using Annexin V -FITC and PI staining in *T. annulata* Ankara 288-infected cells treated with GA  $\leq 0.5 \mu\text{M}$  and incubated at 37°C.

The cells were treated with DMSO (control group) or with different concentrations of GA (0.001  $\mu\text{M}$ , 0.005  $\mu\text{M}$ , 0.01  $\mu\text{M}$ , 0.05  $\mu\text{M}$ , 0.1  $\mu\text{M}$ , 0.25  $\mu\text{M}$  and 0.5  $\mu\text{M}$ ) then incubated for 1, 3 and 6 days at 37°C. Cells were harvested and stained with 2  $\mu\text{l}$  (0.4  $\mu\text{g}$ ) Annexin V-FITC and 10  $\mu\text{l}$  propidium iodide (PI) and then analysed by flow cytometry. (a) The data shown here represents one experiment of five independent experiments. (b) Mean  $\pm$  S.D (\*\*P  $\leq 0.01$ , \*\*\*P  $\leq 0.001$  for GA (0.25 $\mu\text{M}$  and 0.5 $\mu\text{M}$ ) -treated cells compared with control group, Student's t-test), n = 5.

#### **4.1.1.3 Flow cytometric analysis of apoptosis in *T. annulata* Ankara 288-infected cells treated with low GA concentration and incubated at 41°C**

In order to evaluate the anti-apoptotic function of HSP90 in *T. annulata* Ankara 288-infected cells exposed to high temperature, the cells were first treated with different concentrations of GA (0.001 µM, 0.005 µM, 0.01 µM, 0.05 µM and 0.1 µM) or DMSO (control group) and incubated for 1, 3 and 5 days at 41°C. After that, the cells were stained with annexin V -FITC and PI and analysed by using CellQuest™ software (Becton-Dickinson).

As shown in Figure 10, among all these concentrations only 0.1 µM GA induced a statistically significant increase in apoptosis percentage in the cells incubated for 3 and 5 days at 41°C (7.6% and 22.5%, respectively,  $P \leq 0.01$ , Student's t-test) compared with the control group (3.5%).

This experiment revealed that even low doses of GA can significantly induce apoptosis in cells incubated at elevated temperature.

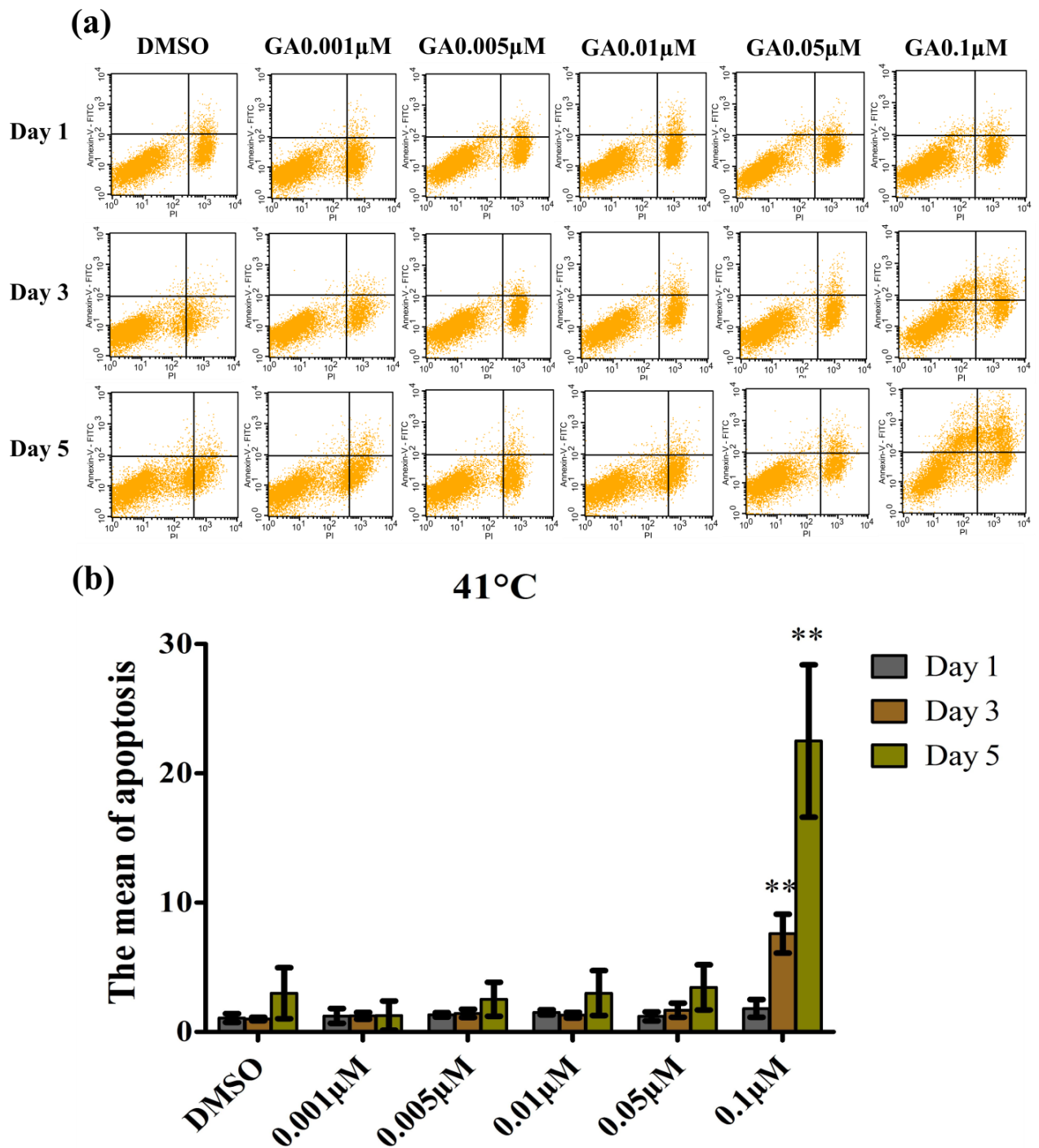


Figure 10: Flow cytometric analysis of apoptosis using Annexin V-FITC and PI staining in *T. annulata* Ankara 288-infected cells treated with GA  $\leq 0.1 \mu\text{M}$  and incubated at  $41^\circ\text{C}$ .

Cells were treated with DMSO (control group) or with different concentrations of GA (0.001  $\mu\text{M}$ , 0.005  $\mu\text{M}$ , 0.0  $\mu\text{M}$  1, 0.05  $\mu\text{M}$  and 0.1  $\mu\text{M}$ ) and incubated for 1, 3 and 5 days at  $41^\circ\text{C}$ . Cells were harvested and stained with 2  $\mu\text{l}$  (0.4  $\mu\text{g}$ ) Annexin V -FITC and 10  $\mu\text{l}$  propidium iodide (PI) and then analysed by flow cytometry. (a) The data shown here represents one experiment of four independent experiments. (b) Mean  $\pm$  S.D (\*\* $P \leq 0.01$  for GA 0.1  $\mu\text{M}$ - treated cells compared with control group (DMSO), Student's t-test),  $n = 4$ .

#### **4.1.1.4 The effect of GA treatment on the subcellular localization of host cell p53 in *T. annulata* Ankara 288-infected cells**

In a work of Haller *et al.*, p53 was used as a molecular marker for apoptosis in *T. annulata* Ankara 288-infected cells. They found that the major portion of p53 was localized in the host cell cytoplasm being closely associated with the parasite membrane. Elimination of the parasites from infected cells by the theilericidal drug buparvaquone leads to translocation of host cell p53 into the host cell nucleus, which in turn results in the upregulation of the pro-apoptotic proteins (Haller *et al.*, 2010).

In order to investigate whether inhibition of HSP90 has an influence on the subcellular localization of host cell p53, anti-p53 antibody was used. *T.annulata* Ankara 288-infected cells were treated with DMSO (control group) and GA (0.25  $\mu$ M, 0.5  $\mu$ M) and incubated for 1, 3 and 6 days at 37°C. Other groups of cells were treated with DMSO and GA 0.1  $\mu$ M and incubated for 1, 3 and 5 days at 41°C. The selection of these concentrations was based on the previous results obtained by flow cytometric analysis.

As shown in Figure 11, the confocal microscopic analysis indicated that in DMSO-treated cells the host cell p53 protein was largely located in the host cell cytoplasm and appeared to be associated with the macroschizont membrane.

In contrast, in GA-treated cells an obvious translocation of p53 into the host cell nucleus could be observed. This finding indicates that HSP90 may be involved in sequestration of p53 in the host cell cytoplasm, preventing p53 to exert apoptotic effects in *T. annulata* -infected cell line.

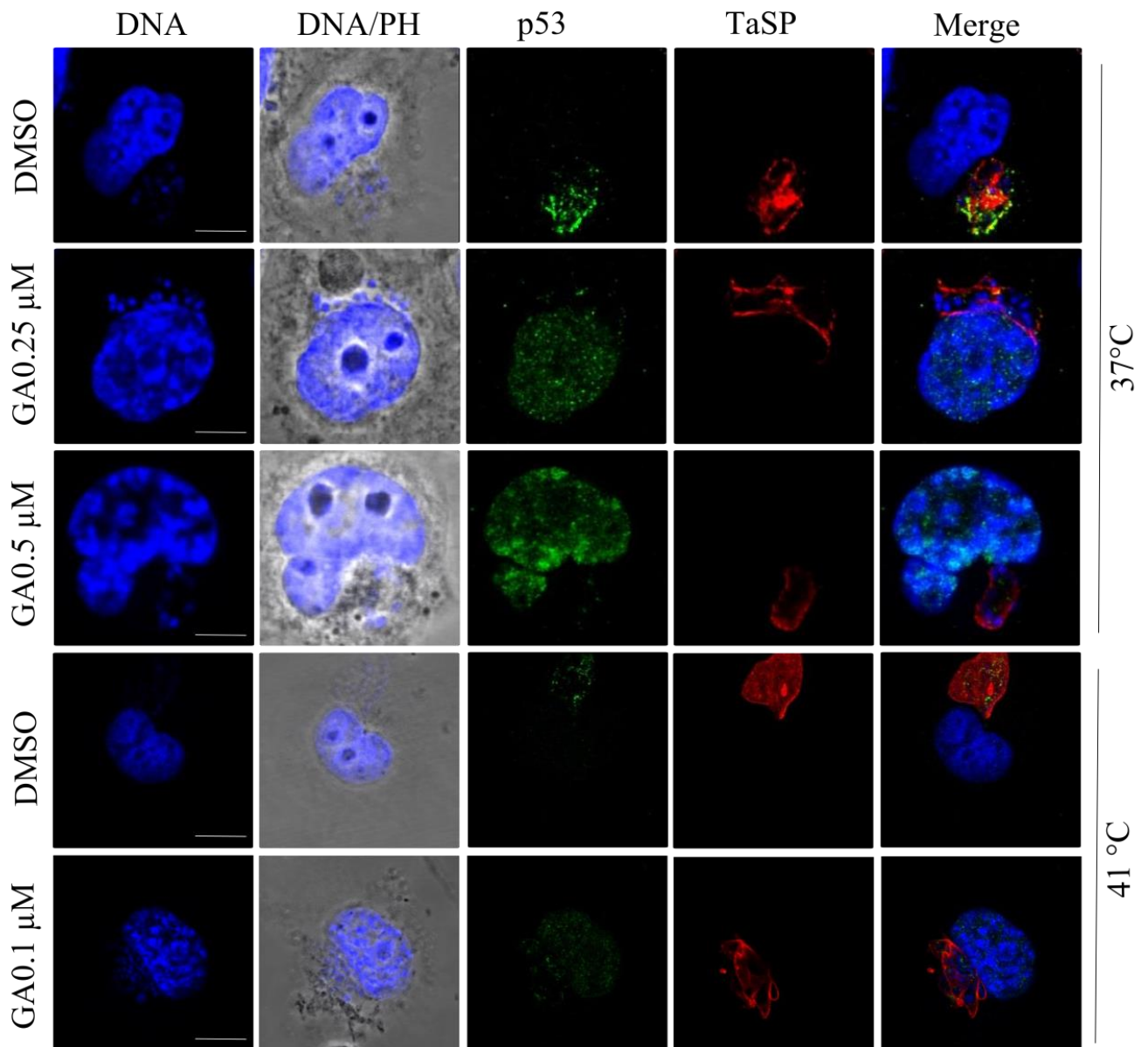


Figure 11: Subcellular localization of host cell p53 within *T. annulata* Ankara 288-infected cells treated with GA or DMSO.

Cells were treated with GA (0.25  $\mu\text{M}$ , 0.5  $\mu\text{M}$ ) or DMSO (control group) and incubated at 37°C. Other cells were treated with GA 0.1  $\mu\text{M}$  or DMSO and incubated at 41°C. Cells were subjected to immunostaining of nucleic acids (DAPI, blue), anti-p53 (Alexa-488, green) and anti-*T. annulata* surface membrane (TaSP) (Alexa-568, red). DNA/PH: Phase-contrast image plus DAPI staining. The data shown here represents one experiment.

#### **4.1.2 Quantitative assessment of the proliferation of *T. annulata* Ankara 288-infected cells**

To investigate the functional effects of HSP90 on the proliferation of *T.annulata* Ankara 288-infected cells, Cell Trace™ CFSE Cell Proliferation Kit was used.

After labelling with the CFSE, the cells were divided into two groups. The first group was incubated with GA (0.01 µM, 0.05 µM, 0.1 µM, 0.25 µM and 0.5 µM) or DMSO (control group) at 37°C for 1, 3 and 6 days. The second group was incubated with GA (0.001 µM, 0.005 µM, 0.01 µM, 0.05 µM and 0.1 µM) or DMSO (control group) at 41°C for 1, 3 and 5 days. The proliferation of the cells of both groups was measured by flow cytometry and the percentages of proliferating cells were calculated using CellQuest™ software (Becton-Dickinson).

##### **4.1.2.1 Cells incubated at 37°C**

As shown in Figure 12, after incubation for 1 day at 37°C, the inhibition of HSP90 by GA has no influence on the cell proliferation, since no difference was recorded between control and GA treated cells as more than 92.90% of the cells existed at the first cycle (M1).

A significant decrease in cell proliferation was reported in the cells incubated with GA  $\geq$  0.05 µM for 3 days at 37°C. More than 40% of the cells were arrested at the first cycle (M1), while in DMSO-treated cells only 6.59% of the cells showed a similar effect. Maximum reduction in proliferation was observed in cells incubated with GA 0.25 µM and 0.5 µM for 3 days, where 73.89% and 85.20% of the cells were arrested at the first cycle (M1), respectively ( $P \leq 0.001$ , Student's t- test) (Figure 12).

After incubation for 6 days at 37°C, a significant reduction in the cell proliferation was observed only in cells treated with GA 0.25 µM and GA 0.5 µM, where 35.67% and 65.40% of the cells were arrested at the first cycle (M1), respectively ( $P \leq 0.001$ , Student's t- test), while in DMSO-treated cells only 0.12% of the cells exhibited a similar effect (Figure 12).

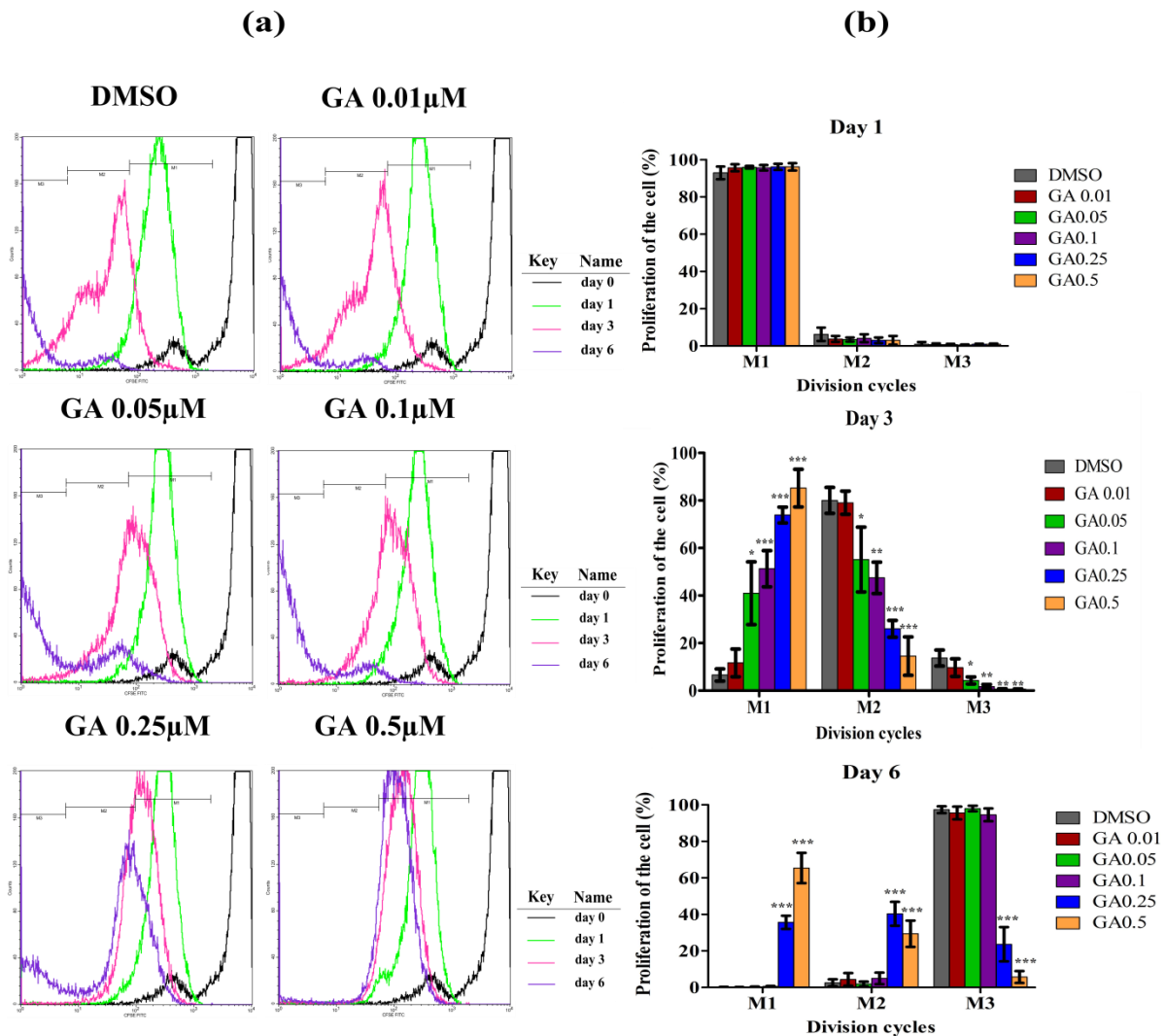


Figure 12: Quantitative assessment of the cell proliferation of *T. annulata* Ankara 288-infected cells incubated at 37°C.

The cells were labelled with 6 μM CFSE on day 0 and then incubated with different concentrations of GA (0.01 μM, 0.05 μM, 0.1 μM, 0.25 μM and 0.5 μM) or DMSO (control group) for 1, 3 and 6 days at 37°C. The proliferations of the cells were measured by flow cytometry. (A) Histogram plots of CFSE fluorescence of *T.annulata* infected-cells incubated with GA or DMSO for 1, 3 and 6 days. The data shown here represents one experiment of four independent experiments. The division cycles of *T.annulata* infected-cells were calculated by assessing the dilution of CFSE and each division is represented as (M). (B) Mean ± SD (\* $P \leq 0.05$ , \*\* $P \leq 0.01$ , \*\*\* $P \leq 0.001$ , Student's t- test)  $n=4$ .

#### 4.1.2.2 Cells incubated at 41°C

After incubation for 1 day at 41°C, GA has no influence on the cell proliferation, since both DMSO- and GA-treated cells showed more than 87.76 % of the cells existed at the first cycle (M1).

After 3 days incubation at 41°C, the cell proliferation was significantly decreased following treatment with GA  $\geq 0.05\mu\text{M}$  ( $P \leq 0.01$ , Student's t- test). More than 27.8% of the cells

## Results

were arrested at the first cycle (M1), while in DMSO-treated cells only 10.8% of the cells showed a similar effect (Figure 13).

After incubation for 5 days at 41°C, the significant reduction in the cell proliferation was observed also in the cells treated with GA  $\geq 0.05 \mu\text{M}$ , where more than 47.6% of the cells were arrested at the second cycle (M2) ( $P \leq 0.01$ , Student's t- test), while in DMSO-treated cells only 15.9% of the cells exhibited a similar effect (Figure 13).

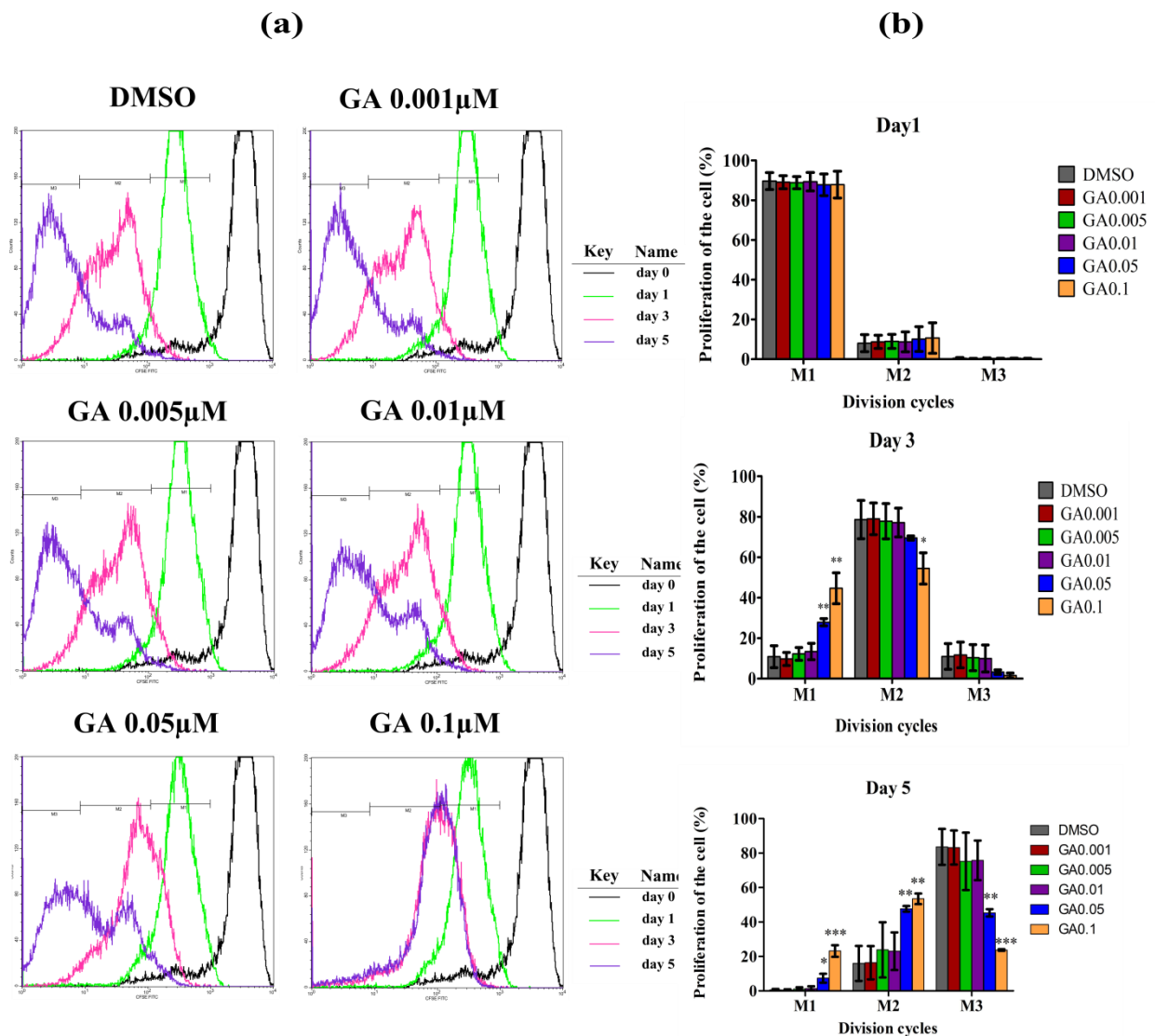


Figure 13: Quantitative assessment of the cell proliferation of *T. annulata* Ankara 288-infected cells incubated at 41°C.

The cells were labelled with 6  $\mu\text{M}$  CFSE on day 0 and incubated with different concentrations of GA (0.001  $\mu\text{M}$ , 0.005  $\mu\text{M}$ , 0.01  $\mu\text{M}$ , 0.05  $\mu\text{M}$  and 0.1  $\mu\text{M}$ ) or DMSO (control group) for 1, 3 and 5 days at 41°C. The proliferations of the cells were measured by flow cytometry. (A) Histogram plots of CFSE fluorescence of *T.annulata* infected-cells incubated with GA or DMSO for 1, 3 and 5 days, the data shown here represents one experiment of three independent experiments. The division cycles of *T.annulata* infected-cells were calculated by assessing the dilution of CFSE and each division is represented as (M). (B) Mean  $\pm$  SD (\* $P \leq 0.05$ , \*\* $P \leq 0.01$ , \*\*\* $P \leq 0.001$ , Student's t- test), n=3.

### **4.1.3 Quantitative assessment of the stage progression in *T. annulata* Ankara 288-infected cells treated with GA**

A fundamental biological aspect of protozoan parasites is the differentiation from one life cycle stage to another. It is known that differentiation frequently occurs following exposure to the extracellular stimuli such as temperature (Shiels *et al.*, 1994, 1998). However, the molecular events that regulate and trigger this process are not yet fully understood.

#### **4.1.3.1 Quantitative assessment of the stage progression using TamS1 and TamR1 (merogony markers)**

In order to evaluate the effect of HSP90 inhibition on the parasite stage progression, *T. annulata* Ankara 288-infected cells were divided into two groups. Both groups were treated with different concentrations of GA (0.001  $\mu$ M, 0.005  $\mu$ M, 0.01  $\mu$ M, 0.05  $\mu$ M and 0.1  $\mu$ M) and DMSO (control group). The first group was incubated for 5 days at 41°C, while the second group was incubated for 6 days at 37°C. The incubation time of this experiment was optimized after several trials using different time points starting from for 3 days until 7 days at both temperatures (data not shown).

The immunostaining of GA or DMSO-treated cells was performed using specific antibodies against TamS1 and TamR1 (merogony markers) to detect those cells undergoing differentiation into merozoites (Figure 15), which was calculated randomly using confocal microscope. More than 300 cells per each concentration were examined.

It was found that the number of cells undergoing merogony slightly increased in correlation with the increase of GA concentration in both groups (cells incubated at 37°C and 41°C). As shown in Figure 14, in the cells that were incubated for 6 days at 37°C, the percentages of cells undergoing merogony increased from 0.26% (DMSO-treated cells) to 0.28%, 0.34%, 0.51%, 0.88% and 0.84% at concentration 0.001  $\mu$ M, 0.005  $\mu$ M, 0.01  $\mu$ M, 0.05  $\mu$ M and 0.1  $\mu$ M GA, respectively. The statistical analysis of these data revealed a significant increase in the percentage of cells undergoing merogony in GA 0.01  $\mu$ M-, 0.05  $\mu$ M-, and 0.1 $\mu$ M-treated cells ( $P = 0.01$ ,  $P = 0.0004$  and  $P = 9.85E-5$ , respectively, Student's t-test) comparing with DMSO-treated cells (control group).

## Results

In the cells which were incubated for 5 days at 41°C, the percentages of cells undergoing merogony increased from 0.58% (DMSO-treated cells) to 0.64%, 0.95%, 1.3%, 1.48% and 1.52% at concentrations of 0.001  $\mu\text{M}$ , 0.005  $\mu\text{M}$ , 0.01  $\mu\text{M}$ , 0.05  $\mu\text{M}$  and 0.1  $\mu\text{M}$  GA, respectively. The statistical analysis of these data revealed a significant increase in the percentage of cells undergoing merogony in GA 0.005  $\mu\text{M}$ -, 0.01  $\mu\text{M}$ -, 0.05  $\mu\text{M}$ - and 0.1  $\mu\text{M}$ -treated cells ( $P = 0.028$ ,  $P = 0.0019$ ,  $P = 0.00024$  and  $P = 0.0037$ , respectively, Student's t-test).

In summary, the number of the cells undergoing merogony increased in *T. annulata* Ankara 288-infected cells treated with GA regardless of the incubation temperature.

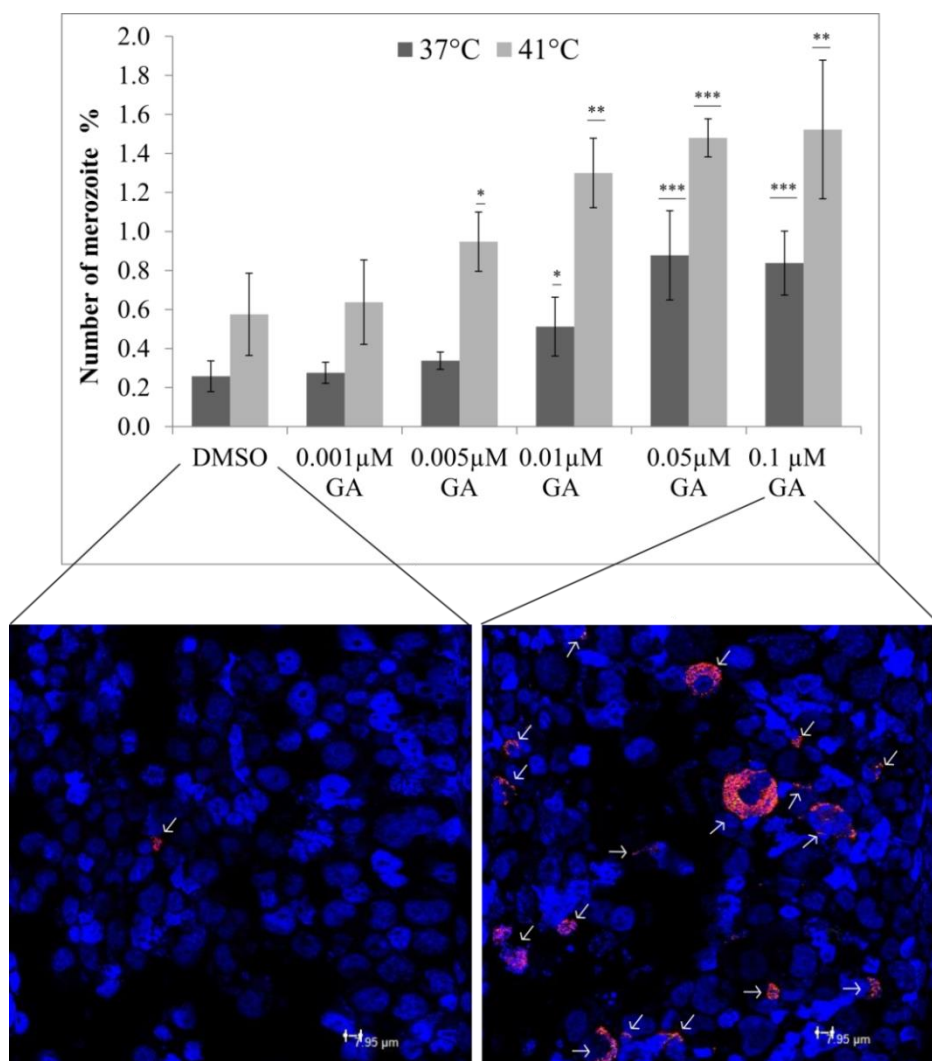


Figure 14: The percentages of the cells undergoing merogony in *T. annulata* Ankara 288-infected cells.

The cells were treated with GA (0.001  $\mu\text{M}$ , 0.005  $\mu\text{M}$ , 0.01  $\mu\text{M}$ , 0.05  $\mu\text{M}$  and 0.1  $\mu\text{M}$ ) or DMSO and incubated for 6 days at 37°C or for 5 days at 41 °C. Cells were subjected to immunostaining using TamS1 and TamR1 antibodies. The number of cells undergoing merogony in GA-treated cells or in DMSO-treated cells was estimated by counting (counting  $\geq 300$  cells per each concentration) (\* $P < 0.05$ , \*\* $P < 0.01$ , \*\*\* $P < 0.001$ , Student's t-test)  $n = 5$ .

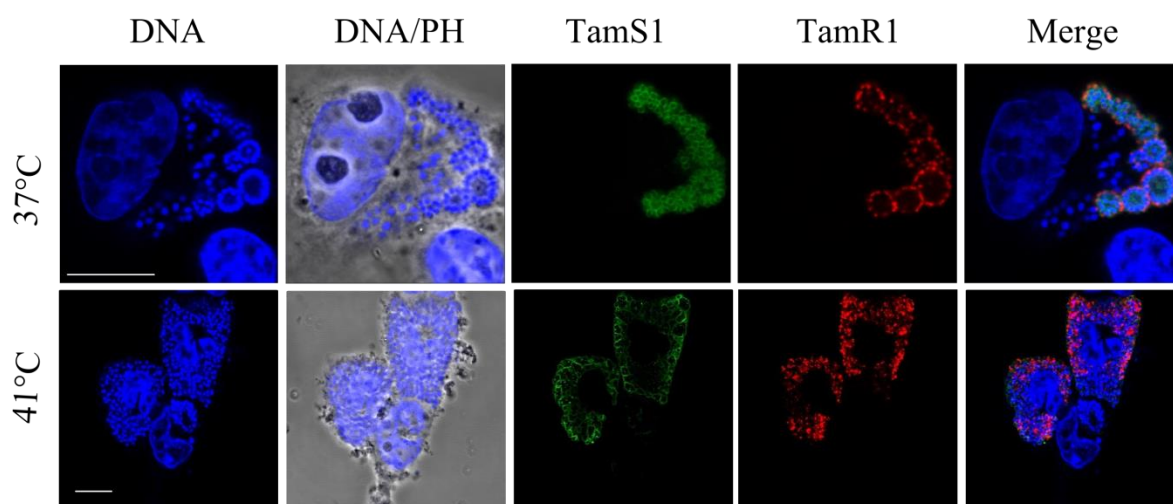


Figure 15: Immunostaining of the cells undergoing merogony in *T. annulata* Ankara 288-infected cells.

Cells were treated with GA 0.05  $\mu$ M and incubated for 6 days at 37°C (upper row) or for 5 days at 41°C (lower row). The cells were subjected to immunostaining of nucleic acids (DAPI, blue signals), TamS1 (Alexa-488, green) and TamR1 (Alexa-568, red). DNA/PH:Phase-contrast image plus DAPI staining .

#### 4.1.3.2 An increase in the number of the cells undergoing merogony after GA treatment correlates with expression of TamR1

The previous result has shown that the GA treatment leads to an increase in the number of merozoite in *T.annulata* Ankara 288-infected cells. According to this result, the expression of the genes encoding for merozoite polypeptides, such as TamR1, is supposed to increase. To verify this hypothesis, the expression level of TamR1 in *T.annulata* Ankara 288-infected cells during the parasite differentiation was evaluated by using qRT-PCR.

The cells were first treated with GA 0.05 $\mu$ M or DMSO (control group). After treatment, the cells were divided into two groups; the first group was incubated at 37°C, while the second group incubated at 41°C. The RNA was isolated after 2, 3 and 6 days from the first group and after 2, 3 and 5 days from the second group. The relative expression of TamR1 mRNA was normalized to the expression of the house keeping gene *Theileria annulata* actin 1 (accession no.: XM\_946720.1) (TaAct1).

As shown in Figure 16, incubation of *T. annulata* Ankara 288-infected cells with GA 0.05  $\mu$ M for 2 and 3 days at 37°C or 41°C leads to a gradual increase of TamR1 mRNA expression. However, this increase is statistically not significant. In the cells which were incubated for 6 days at 37°C or for 5 days at 41°C, the treatment with GA 0.05  $\mu$ M leads to a statistically significant increase of TamR1 mRNA expression (1.7 and 2.9 fold, respectively)

in comparison to the DMSO-treated cells (control group). This result confirms the previous findings obtained by using the confocal microscopy analysis.

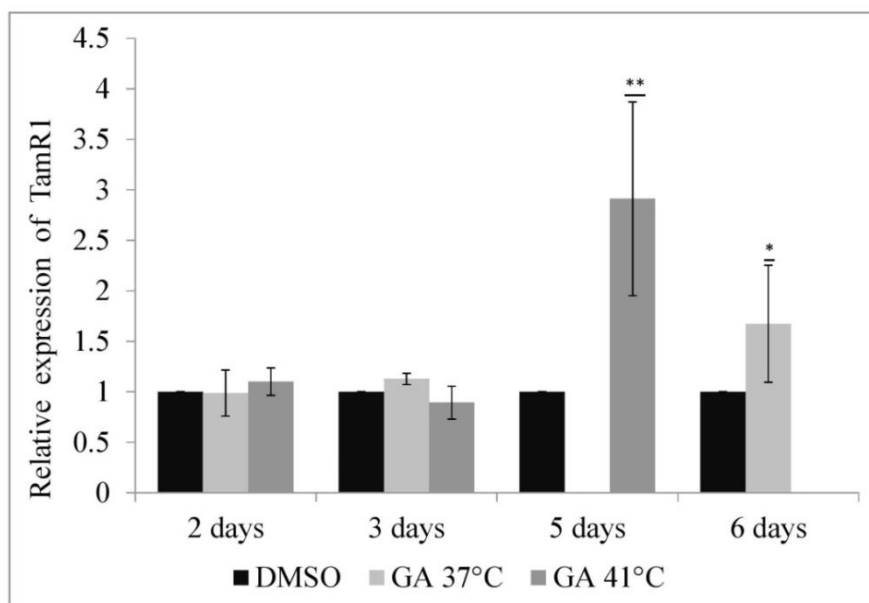


Figure 16: Relative expression of TamR1 mRNA in *T.annulata* Ankara 288-infected cells.

The cells were treated with GA 0.05  $\mu$ M or DMSO and incubated at 37°C or 41°C. RNA was isolated after 2, 3 and 5 or 6 days and the cDNA was synthesized. The qRT-PCR analysis for the mean  $\pm$  SD expression of TamR1 mRNA normalized to the house keeping gene TaAct1. DMSO-treated cells served as a control group (\* $P \leq 0.05$ , \*\* $P \leq 0.01$ , REST 2009), n=5.

## 4.2 The regulation of HSP90 in *T. annulata* Ankara 288-infected cells

Previous results have shown that inhibition of HSP90 in *T.annulata* Ankara 288-infected cells using GA reduces cell survival and cell proliferation, which in turn may be reflected in the upregulation of HSP90 to compensate these defects. To this end, it is not clear whether GA inhibits host, parasite HSP90 or both of them. To address this question, the following experiments were designed and performed.

### 4.2.1 The regulation of bovine HSP90 in GA-treated cells

#### Sequence data:

A search in the GenBank (<http://www.ncbi.nlm.nih.gov/genbank/>) was performed to determine the number of bovine HSP90 isoforms. Based on the phylogenetic analysis of the available sequence in Genbank (data not shown), two isoforms seem to be representative of all observed sequences. Therefore, I focused on these two reference sequences (isoform): the first isoform is Bos taurus heat shock protein 90kDa alpha (accession no.:

NM\_001012670.2), named here as BHSP90-alpha. The second isoform is Bos taurus heat shock protein 90kDa beta (accession no.: NM\_001079637.1), named here as BHSP90-beta. Both genes were analysed in the qRT-PCR analysis.

### **QRT-PCR analysis:**

In order to investigate the effect of HSP90 inhibition by GA on the regulation of bovine HSP90 (BHSP90-alpha and BHSP90-beta) mRNA, qRT-PCR analysis was used. *T. annulata* Ankara 288-infected cells were first treated with GA (0.01  $\mu$ M, 0.05  $\mu$ M, 0.1  $\mu$ M, 0.25  $\mu$ M and 0.5  $\mu$ M) or DMSO (control group), then incubated at 37°C. Finally, RNA was isolated from cells of these groups after 1, 3 and 6 days. The relative expression of BHSP90-alpha and BHSP90-beta mRNA was normalized to the expression of the house keeping gene Glyceraldehyde 3-phosphate dehydrogenase (GAPDH).

Generally, treatment of *T. annulata* Ankara 288-infected cells with GA leads to increased BHSP90-alpha mRNA and BHSP90-beta mRNA expression in a dose-dependent manner. The statistical analysis revealed that the BHSP90-alpha mRNA level was significantly up-regulated in cells incubated with GA 0.25  $\mu$ M for 3 days (2.53 fold) in comparison to the control group. A significant upregulation of BHSP90-alpha mRNA was also reported in cells incubated with GA 0.5  $\mu$ M for 3 and 6 days (2.37 and 2.57 fold, respectively) in comparison to the control group (Figure 17).

Regarding the BHSP90-beta isoform, the statistical analysis revealed significant upregulation of BHSP90-beta mRNA in cells incubated with GA 0.25  $\mu$ M for 1 and 3 days (1.73 and 1.74 fold, respectively) in comparison to the control group. The levels of BHSP90-beta mRNA were also significantly up-regulated in cells incubated with GA 0.5  $\mu$ M for 1, 3 and 6 days (1.86, 2.16 and 2.85 fold, respectively) (Figure 17).

In summary, the mRNA expression level of BHSP90-alpha isoform was significantly up-regulated after incubation for 3 days at concentration 0.25  $\mu$ M GA and after incubation for 3 and 6 days at concentration 0.5  $\mu$ M GA. In the case of BHSP90-beta isoform, a significant up-regulation was observed after incubation for 1 and 3 days at concentration 0.25  $\mu$ M GA and after incubation for 1, 3 and 6 days at concentration 0.5  $\mu$ M GA. These results suggest that there is a variation in the expression of bovine HSP90 isoforms.

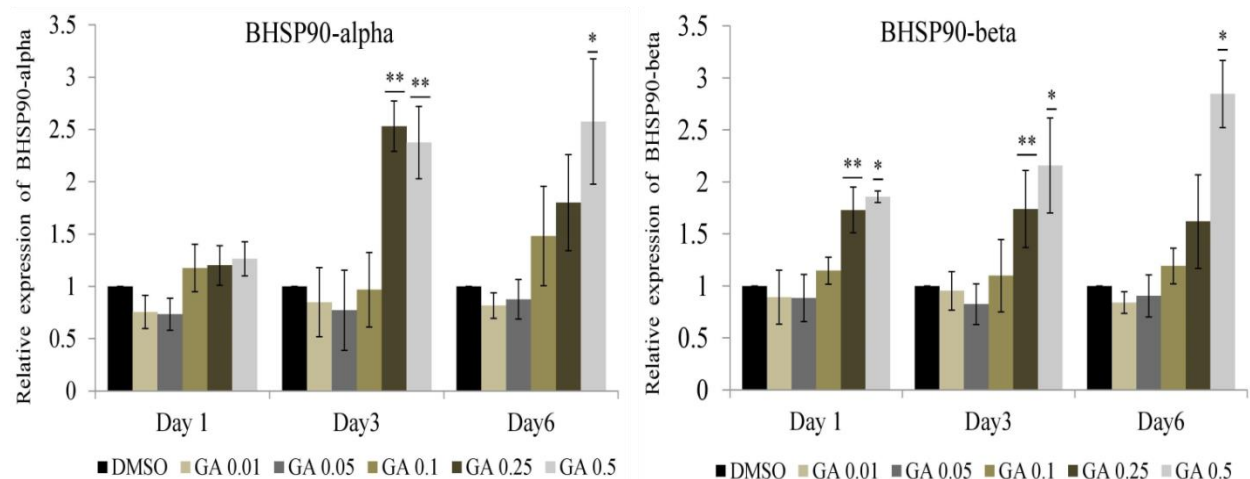


Figure 17: Relative expression of BHSP90-alpha mRNA and BHSP90-beta mRNA in *T.annulata* Ankara 288-infected cells at 37°C.

The cells were incubated with GA (0.01  $\mu$ M, 0.05  $\mu$ M, 0.1  $\mu$ M, 0.25  $\mu$ M and 0.5  $\mu$ M) or DMSO for 1, 3 and 6 days at 37°C. RNA was isolated and the cDNA was synthesized. The qRT-PCR analysis for the mean  $\pm$  SD expression of BHSP90-alpha mRNA and BHSP90-beta mRNA normalized to the house keeping gene GAPDH. DMSO-treated cells served as a control group (\* $P \leq 0.05$ , \*\* $P \leq 0.01$ , REST 2009), n=5.

### The effect of elevated temperature on the regulation of bovine HSP90 (BHSP90-alpha and -beta) in *T.annulata* Ankara 288-infected cells treated with GA

In order to investigate the effect of elevated temperature on the regulation of bovine HSP90 (BHSP90-alpha and -beta) mRNA in *T.annulata* Ankara 288- infected cells, the cells were first treated with GA and then incubated at 41°C for 1, 3 and 5 days. RNA of these cells were isolated and then analysed using qRT-PCR. The relative expression of BHSP90-alpha mRNA and BHSP90-beta mRNA was normalized to the expression of the house keeping gene GAPDH.

As shown in Figure 18, the elevation of the temperature to 41°C resulted in a gradual increase in the expression of BHSP90-alpha mRNA and BHSP90-beta mRNA in GA 0.05  $\mu$ M-treated cells incubated for 1 and 3 days. The increase of BHSP90-alpha mRNA and BHSP90-beta mRNA level became to be statistically significant after incubation with GA 0.05  $\mu$ M for 5 days at 41°C (1.6 and 1.85 fold, respectively) in comparison to the control group.

In summary, the data obtained showed that even low concentrations of GA can significantly increase the expression level of bovine HSP90 mRNA at 41°C.

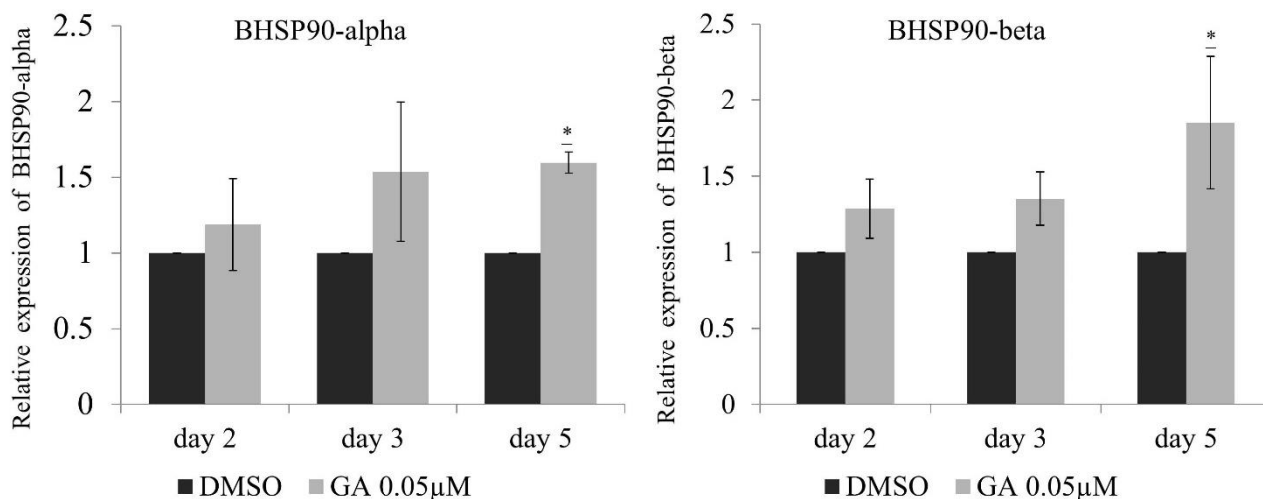


Figure 18: Relative expression of BHSP90-alpha mRNA and BHSP90-beta mRNA in *T. annulata* Ankara 288-infected cells incubated at 41°C.

The cells were incubated with GA 0.05 μM or DMSO for 2, 3 and 5 days at 41°C. RNA was isolated and the cDNA was synthesized. The qRT-PCR analysis for the mean  $\pm$  SD expression of BHSP90-alpha mRNA and BHSP90-beta mRNA normalized to the house keeping gene GAPDH. DMSO-treated cells served as a control group (\* $P \leq 0.05$ , REST 2009), n=5.

#### 4.2.2 The regulation of *T. annulata* HSP90 in GA-treated cells

##### Sequence data:

In order to obtain information on the number and positions of *T. annulata* HSP90 genes, a search in the GenBank (<http://www.ncbi.nlm.nih.gov/genbank>) and GeneDB (<http://www.genedb.org>) was performed. Reference sequences of the two isoforms were found: one located in chromosome one (accession no.: XM\_948749), given here the name TaHSP90-Chr1, and the second isoform located in chromosome four (accession no.: XM\_948193), named here as TaHSP90-Chr4. Both genes were analysed by qRT-PCR.

##### QRT-PCR analysis:

In order to investigate the effect of HSP90 inhibition by GA on the regulation of *T. annulata* HSP90, qRT-PCR analysis was performed. *T. annulata* Ankara 288-infected cells were treated with GA 0.05 μM or DMSO (control group). After treatment, the cells were divided into two groups. The first group was incubated at 37°C and the RNA was isolated after 2, 3 and 6 days. The second group was incubated at 41°C and the RNA was isolated after 2, 3 and 5 days. The relative expression of TaHSP90-Chr1 and TaHSP90-Chr4 mRNA was

## Results

normalized to the expression of the house keeping gene *Theileria annulata* actin 1 (accession no.: XM\_946720.1) TaAct1.

As shown in Figure 19, only a slight but not significant increase in the expression level of TaHSP90-Chr1 mRNA and TaHSP90-Chr4 mRNA was observed in *T. annulata* Ankara 288-infected cells incubated with GA 0.05  $\mu$ M for 2, 3 and 6 days at 37°C.

Although the treatment of the cells with GA 0.05  $\mu$ M for 2 days at 41°C led to increased expression level of TaHSP90-Chr1 mRNA and TaHSP90-Chr4 mRNA, the incubation for 3 and 5 days caused a down-regulation of TaHSM90-Chr1 mRNA and TaHSP90-Chr4 mRNA expression. The statistical analysis revealed that the down-regulation of TaHSP90-Chr1 mRNA and TaHSP90-Chr4 mRNA became significant in cells incubated with GA 0.05  $\mu$ M for 5 days at 41°C (0.61 and 0.5 fold, respectively) in comparison to the control group (Figure 19).

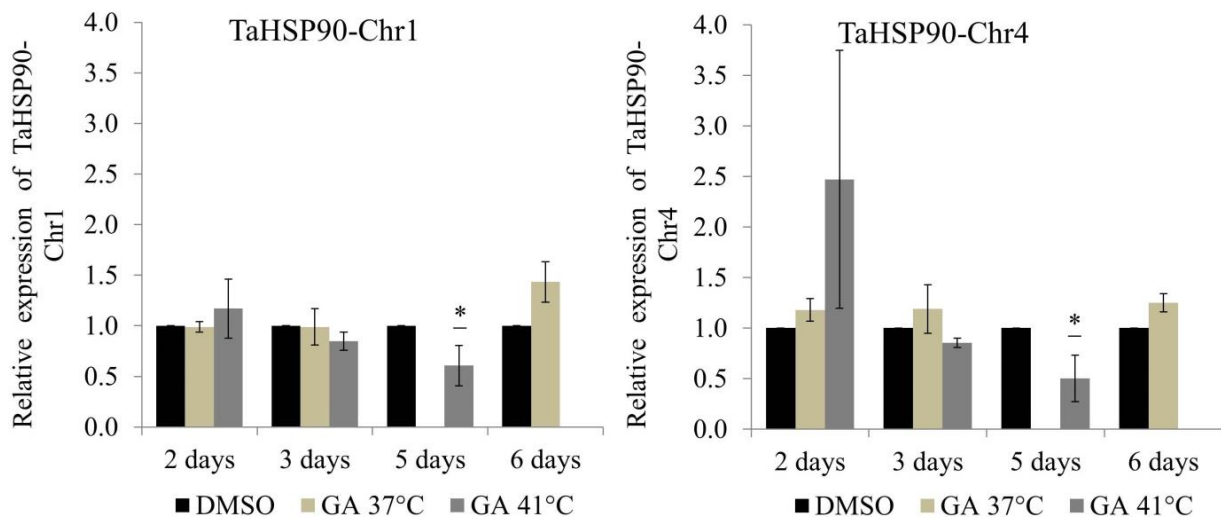


Figure 19: Relative expression of TaHSP90-Chr1 mRNA and TaHSP90-Chr4 mRNA in *T.annulata* Ankara 288-infected cells.

The cells were incubated with GA 0.05  $\mu$ M or DMSO for 2, 3 and 5 or 6 days at 37°C or 41°C. RNA was isolated and the cDNA was synthesized. The qRT-PCR analysis for the mean  $\pm$  SD expression of TaHSP90-Chr1 mRNA and TaHSP90-Chr4 mRNA normalized to the house keeping gene TaAct1. DMSO-treated cells served as a control group (\* $P \leq 0.05$ , REST 2009),  $n=5$ .

### 4.2.3 Comparison between the expression of bovine HSP90 and *T.annulata* HSP90 during the parasite differentiation.

In order to get a clear picture about the regulation of bovine HSP90 and *T.annulata* HSP90 during the parasite differentiation, the qRT-PCR analyses of TamrR1, bovine HSP90 and *T.annulata* HSP90 (section 4.1.3.2, 4.2.1 and 4.2.2) were compared to each other.

As shown in Figure 20, the expression profiles of bovine HSP90 (BHSP90-alpha and BHSP90-beta) and *T.annulata* HSP90 (TaHSP90-Chr1 and TaHSP90-Chr4) were slightly, but not significantly increased after incubation with GA 0.05  $\mu$ M for 6 days at 37°C, whereas the expression of TamR1 was significantly increased during the same time.

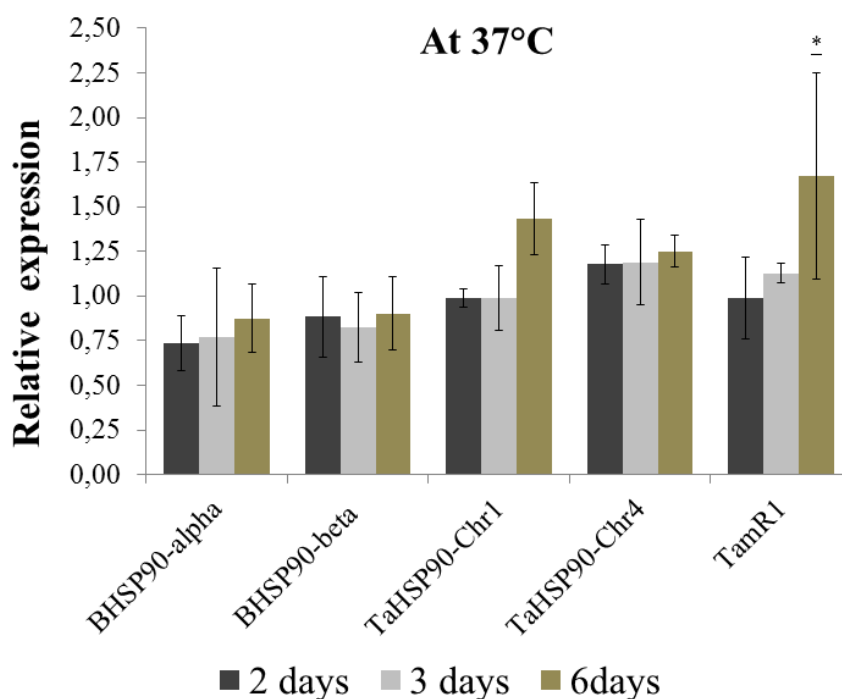


Figure 20: Relative expression of BHSP90-alpha mRNA, BHSP90-beta mRNA, TaHSP90-Chr1 mRNA, TaHSP90-Chr4 mRNA and TamR1 mRNA in *T.annulata* Ankara 288-infected cells at 37°C.

The cells were incubated with GA 0.05  $\mu$ M or DMSO for 2, 3 and 6 days at 37°C. RNA was isolated and the cDNA was synthesized. The qRT-PCR analysis for the mean  $\pm$  SD expression of TaHSP90-Chr1 mRNA, TaHSP90-Chr4 mRNA and TamR1 mRNA normalized to the house keeping gene TaAct1 and the expression of BHSP90-alpha mRNA and BHSP90-beta mRNA normalized to the house keeping gene GAPDH (\* $P \leq 0.05$ , REST 2009), n=5.

## Results

However, the expression profiles of bovine HSP90 mRNA (BHSP90-alpha and BHSP90-beta) and TamR1 mRNA were significantly increased after incubation with GA 0.05  $\mu$ M for 5 days at 41°C. Interestingly, the expression profiles of *T.annulata* HSP90 mRNA (TaHSP90-Chr1 and TaHSP90-Chr4) were significantly decreased during the same time. These results indicate that during parasite differentiation at 41°C, bovine HSP90 and *T.annulata* HSP90 are regulated in a different manner (Figure 21).

This observation raised an important question as to whether these HSP90s play different roles during parasite differentiation or not?

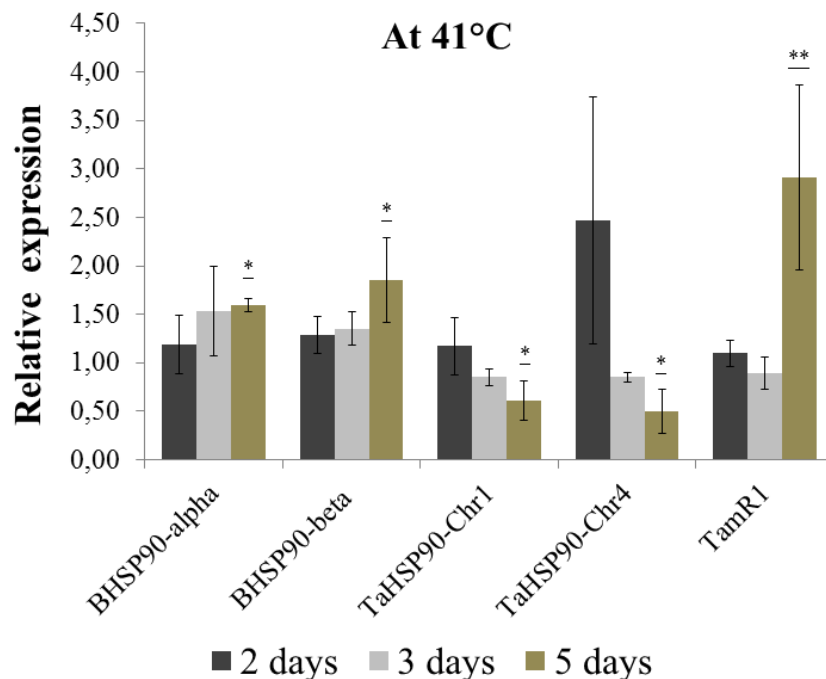


Figure 21: Relative expression of BHSP90-alpha mRNA, BHSP90-beta mRNA, TaHSP90-Chr1 mRNA, TaHSP90-Chr4 mRNA and TamR1 mRNA in *T.annulata* Ankara 288-infected cells at 41°C.

The cells were incubated with GA 0.05  $\mu$ M or DMSO for 2, 3 and 5 days at 41°C. RNA was isolated and the cDNA was synthesized. The qRT-PCR analysis for the mean  $\pm$  SD expression of TaHSP90-Chr1 mRNA, TaHSP90-Chr4 mRNA and TamR1 mRNA normalized to the house keeping gene TaAct1 and the expression of BHSP90-alpha mRNA and BHSP90-beta mRNA normalized to the house keeping gene GAPDH (\* $P \leq 0.05$ , REST 2009), n=5.

### 4.3 Detection of the bovine HSP90 protein

The amino acid alignment between bovine HSP90 and the amino acids 610-723 of HSP90  $\beta$  of human origin has shown 84% identity and 15% similarity (Appendix: Figure 43). Based on this information, anti-human HSP90 $\alpha/\beta$  (monoclonal antibody raised against amino acids

610-723 of HSP90  $\beta$  of human origin) was selected to specifically detect bovine HSP90 and to differentiate it from *T. annulata* HSP90.

Figure 22 illustrates results obtained by immunoblotting of the cell lysates of *T. annulata* Ankara 288- infected cells, BoMac, HeLa cells, PBL and isolated schizonts using the above mentioned anti-human HSP90 $\alpha/\beta$  antibody. This antibody recognized a strong band of approximately 90 kDa size in the lysates of *T. annulata* Ankara 288- infected cells, BoMac and HeLa cells but not in the lysates prepared from PBL or isolated schizonts.

The indirect immunofluorescence staining of *T.annulata* Ankara 288-infected cells, BoMac and isolated schizonts was performed using the same anti-human HSP90 $\alpha/\beta$ .

As shown in Figure 23 (a), a strong signal was observed in *T. annulata* Ankara 288-infected cells and BoMac, whereas this signal was absent in isolated schizonts. In addition, the bovine HSP90 was localized in the cytoplasm of the host cells, but not associated with the schizont as demonstrated by double staining of *T. annulata* infected cells on one hand with antibody against the surface membrane of the parasite (TaSP) and with anti-human HSP90 $\alpha/\beta$  antibody on the other hand (Figure 23 b).

Taken together, these results clearly confirm the specificity of anti-human HSP90 $\alpha/\beta$  for bovine HSP90 but not for the parasite HSP90.

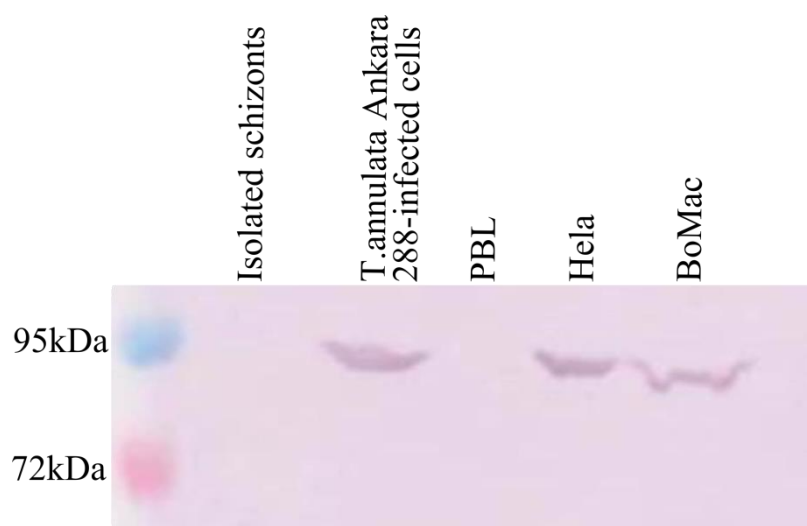


Figure 22: Detection of bovine HSP90

Lysates of *T. annulata* Ankara 288-infected cells, BoMac, HeLa cells, isolated schizonts and PBL were blotted and stained with anti-human HSP 90 $\alpha/\beta$  (HSP 90 90 $\alpha/\beta$  (F-8): sc-13119, Santa Cruz).

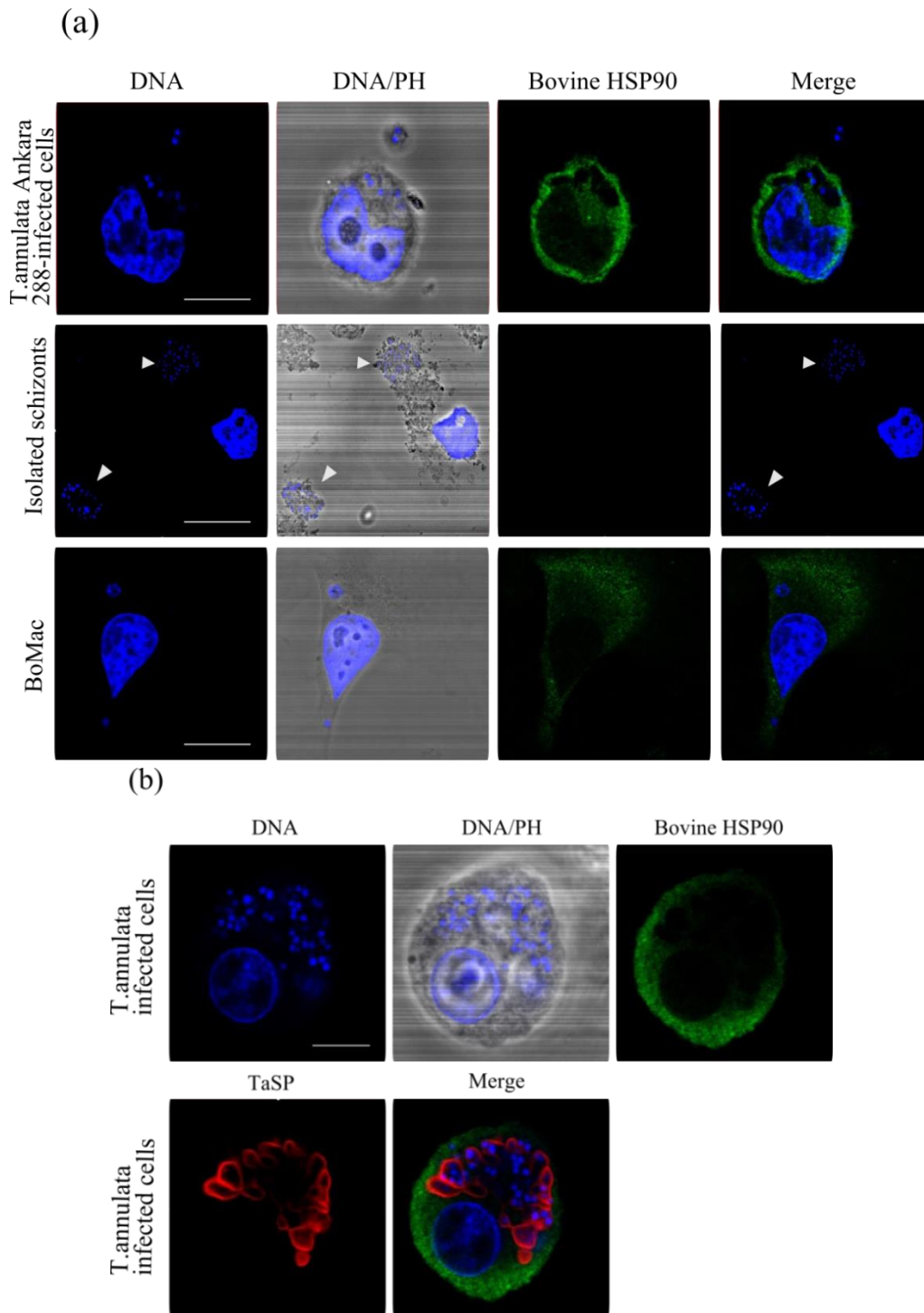


Figure 23: Subcellular localization of bovine HSP90.

(a) *T.annulata* Ankara 288-infected cells, isolated schizonts (arrow) and BoMac were subjected to immunostaining using an anti-human HSP90 $\alpha/\beta$  antibody (HSP90 $\alpha/\beta$  (F-8): sc-13119, Santa Cruz). DNA was visualized using DAPI (blue), bovine HSP90 was stained with anti-human HSP90 $\alpha/\beta$  and visualized using an Alexa-488 (green). DNA/PH shows the phase-contrast image plus DAPI. (b) Subcellular localization of bovine HSP90. *T.annulata* Ankara 288-infected cells were subjected to immunostaining with anti-human HSP90 $\alpha/\beta$  (HSP90 $\alpha/\beta$  (F-8): sc-13119, Santa Cruz) and anti *T.annulata* surface membrane (TaSP) antibodies. DNA was visualized using DAPI (blue), bovine HSP90 was stained with anti-human HSP90 $\alpha/\beta$  and visualized using an Alexa-488 (green), TaSP visualized using an Alexa-568 (red). DNA/PH: Phase-contrast image plus DAPI staining.

## 4.4 Identification and characterization of *T. annulata* HSP90

### 4.4.1 Detection of *T. annulata* HSP90 and cDNA cloning

As mentioned in section (4.2.2) a reference sequences of the two isoforms were found: the first isoform (TaHSP90-Chr1) located in chromosome one (accession no.: XM\_948749) with a size of 2967 base pairs (bp), and the second isoform (TaHSP90-Chr4) located in chromosome four (accession no.: XM\_948193) with a length of 3067 bp and a spliced length of 2742 bp. The primers were designed to amplify the full-length gene sequences of *T. annulata* HSP90 based on the Genbank reference sequence.

An amplificate of a correct fragment (size ~2967 bp) could be demonstrated with the cDNA template prepared from *T. annulata* Ankara 288-infected cells using specific primers designed to amplify TaHSP90-Chr1 (Figure 24, left panel). Additionally, another amplified fragment (~2742 bp) could also be obtained using specific primers designed to amplify TaHSP90-Chr4 with the same cDNA template (Figure 24, right panel). Thus, the PCR results confirmed the presence of two isoforms of *T. annulata* HSP90.

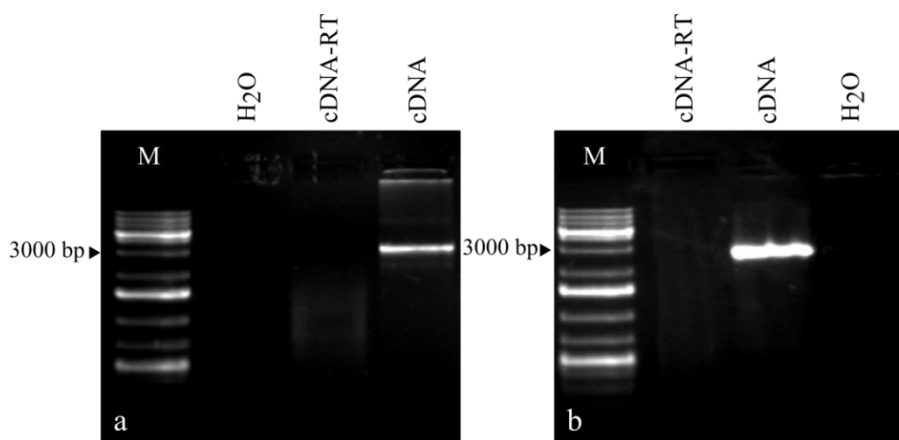


Figure 24: PCR amplification of mRNA transcripts of *T. annulata* HSP90 isoforms using *T. annulata* HSP90 specific primers.

(a) Detection of TaHSP90-Chr1, the cDNA template giving a PCR product of 2967 bp. (b) Detection of TaHSP90-Chr4, the cDNA template giving a PCR product of 2742 bp. M: molecular weight marker, H<sub>2</sub>O: Negative control.

In a further step, the PCR products of each isoform were ligated into pDrive cloning vector and then transferred into *E. coli* DH5 $\alpha$  to produce plasmid DNA copies of each PCR product. After purification, the plasmids were digested using the FastDigest® restriction enzymes to verify the presence of insert for both isoforms in the vector (Appendix: Figure 44).

## Results

To confirm the presence of the target sequences, M13 PCR was used. As shown in Figure 25, an amplificate of two correct sizes (~3234 bp and ~3009 bp representing TaHSP90-Chr1 and TaHSP90-Chr4 inserts, respectively) could be demonstrated. The size of the PCR product was determined as the original PCR product size, plus a 267 bp representing the total distance of the M13 primers annealing sites from the PCR insert in the pDrive sequence.

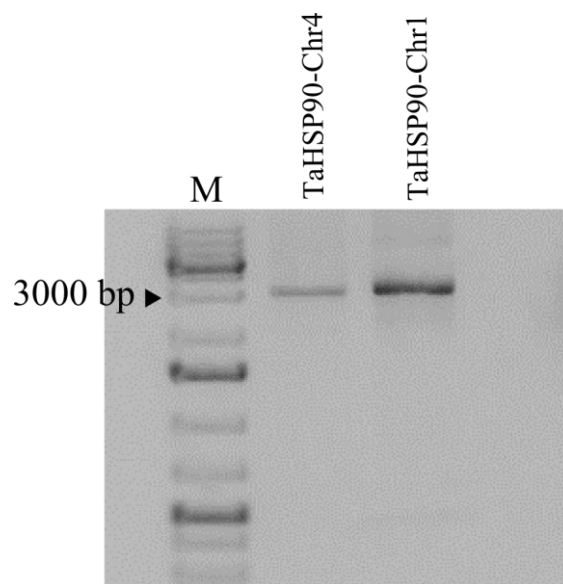


Figure 25: M13 PCR selection of positive pDrive clones of TaHSP90-Chr1 and TaHSP90-Chr4 construct.

M13 PCR was applied using purified plasmids from *E. coli* DH5 $\alpha$  competent cells as templates to detect TaHSP90-Chr4 or TaHSP90-Chr1 constructs into pDrive vector. The purified plasmid templates, giving a PCR product of 3009 bp and 3234 bp, respectively. M: molecular weight marker.

### 4.4.2 Sequencing and sequence analysis

The clones containing the correct insert were selected and sequenced. The sequences were first subjected to BLAST (Basic Local Alignment Search Tool, [www.ncbi.nlm.nih.gov/BLAST](http://www.ncbi.nlm.nih.gov/BLAST)) and then to ClustalW multiple alignment ([http://npsa-pbil.ibcp.fr/cgi-bin/align\\_clustalw.pl](http://npsa-pbil.ibcp.fr/cgi-bin/align_clustalw.pl)). As shown in Figure 26, the multiple sequence alignment of each gene (TaHSP90-Chr1 and TaHSP90-Chr4) revealed a variation in the nucleotide sequence between the clones. In addition, slight variations could also be observed in the nucleotide sequences of these clones compared with the reference sequence obtained from the Genbank. As a result of these variations more clones were picked and sequenced.

Eleven clones from TaHSP90-Chr1 and 7 clones from TaHSP90-Chr4 were sequenced to obtain two 100% identical sequences for each gene. Further alignment analyses were performed by using the 100% identical sequences of each gene. Comparison by alignment of TaHSP90-Chr1 and TaHSP90-Chr4 nucleotide sequence with the reference Genbank

accessions number XM\_948749.1 and XM\_948193.1 revealed identity of 97% and 98%, respectively. In addition, the nucleotide sequence identity and difference between the TaHSP90-Chr1 and TaHSP90-Chr4 were 42.2% and 57.8%, respectively.

(a)

	10	20	30	40	50	60
Clone (12)	TACCATTTTCGTATCATGTAATGAATCGGATGAACTGGAAGTAGTTGAGGATACAGTGAAC					
Clone (H)	TACCATTTTCGTATCATGTAATGAATCGGATGAACTGGAAGTAGTTGAGGATACAGTGAAC					
Clone (E)	TACCATTTTCGTATCATGTAATGAATCGGATGAACTGGAAGTAGTTGAGGATACAGTGAAC					
Clone (1)	TACCATTTTCGTATCATGTAATGAATCGGATGAACTGGAAGTAGTTGAGGATACAGTGAAC					
Clone (C-D)	TACCATTTTCGTATCATGTAATGAATCGGATGAACTGGAAGTAGTTGAGGATACAGTGAAC					
Clone (C-A)	TACCATTTTCGTATCATGTAATGAATCGGATGAACTGGAAGTAGTTGAGGATACAGTGAAC					
Clone (3)	TACCATTTTCGTATCATGTAATGAATCGGATGAACTGGAAGTAGTTGAGGATACAGTGAAC					
Clone (C-C)	TACCATTTTCGTATCATGTAATGAATCGGATGAACTGGAAGTAGTTGAGGATACAGTGAAC					
Genebank	TACCATTTTCGTATCATGTAATGAATCGGATGAACTGGAAGTAGTTGAGGATACAGTGAAC					
Clone (g-A)	TACCATTTTCGTATCATGTAATGAATCGGATGAACTGGAAGTAGTTGAGGATACAGTGAAC					
Clone (g-B)	TACCATTTTCGTATCATGTAATGAATCGGATGAACTGGAAGTAGTTGAGGATACAGTGAAC					
Clone (g-C)	TACCATTTTCGTATCATGTAATGAATCGGATGAACTGGAAGTAGTTGAGGATACAGTGAAC					

	70	80	90	100	110	120
Clone (12)	GTTGATGAGGACGTTACTGAGGAGCAAACACCCCTCTGAGCTTTCTGAGGAAGAAGTCCCTA					
Clone (H)	GTTGATGAGGACGTTACTGAGGAGCAAACACCCCTCTGAGCTTTCTGAGGAAGAAGTCCCTA					
Clone (E)	GTTGATGAGGACGTTACTGAGGAGCAAACACCCCTCTGAGCTTTCTGAGGAAGAAGTCCCTA					
Clone (1)	GTTGATGAGGACGTTACTGAGGAGCAAACACCCCTCTGAGCTTTCTGAGGAAGAAGTCCCTA					
Clone (C-D)	GTTGATGAGGACGTTACTGAGGAGCAAACACCCCTCTGAGCTTTCTGAGGAAGAAGTCCCTA					
Clone (C-A)	GTTGATGAGGACGTTACTGAGGAGCAAACACCCCTCTGAGCTTTCTGAGGAAGAAGTCCCTA					
Clone (3)	GTTGATGAGGACGTTACTGAGGAGCAAACACCCCTCTGAGCTTTCTGAGGAAGAAGTCCCTA					
Clone (C-C)	GTTGATGAGGACGTTACTGAGGAGCAAACACCCCTCTGAGCTTTCTGAGGAAGAAGTCCCTA					
Genebank	GTTGATGAGGACGTTACTGAGGAGCAAACACCCCTCTGAGCTTTCTGAGGAAGAAGTCCCTA					
Clone (g-A)	GTTGATGAGGACGTTACTGAGGAGCAAACACCCCTCTGAGCTTTCTGAGGAAGAAGTCCCTA					
Clone (g-B)	GTTGATGAGGACGTTACTGAGGAGCAAACACCCCTCTGAGCTTTCTGAGGAAGAAGTCCCTA					
Clone (g-C)	GTTGATGAGGACGTTACTGAGGAGCAAACACCCCTCTGAGCTTTCTGAGGAAGAAGTCCCTA					

	130	140	150	160	170	180
Clone (12)	GATAGGTCAGAAGATTCATCAGTGTTAACTAGCGAAAAATATTTTAAAGATTCACAAAA					
Clone (H)	GATAGGTCAGAAGATTCATCAGTGTTAACTAGCGAAAAATATTTTAAAGATTCACAAAA					
Clone (E)	GATAGGTCAGAAGATTCATCAGTGTTAACTAGCGAAAAATATTTTAAAGATTCACAAAA					
Clone (1)	GATAGGTCAGAAGATTCATCAGTGTTAACTAGCGAAAAATATTTTAAAGATTCACAAAA					
Clone (C-D)	GATAGGTCAGAAGATTCATCAGTGTTAACTAGCGAAAAATATTTTAAAGATTCACAAAA					
Clone (C-A)	GATAGGTCAGAAGATTCATCAGTGTTAACTAGCGAAAAATATTTTAAAGATTCACAAAA					
Clone (3)	GATAGGTCAGAAGATTCATCAGTGTTAACTAGCGAAAAATATTTTAAAGATTCACAAAA					
Clone (C-C)	GATAGGTCAGAAGATTCATCAGTGTTAACTAGCGAAAAATATTTTAAAGATTCACAAAA					
Genebank	GATAGGTCAGAAGATTCATCAGTGTTAACTAGCGAAAAATATTTTAAAGATTCACAAAA					
Clone (g-A)	GATAGGTCAGAAGATTCATCAGTGTTAACTAGCGAAAAATATTTTAAAGATTCACAAAA					
Clone (g-B)	GATAGGTCAGAAGATTCATCAGTGTTAACTAGCGAAAAATATTTTAAAGATTCACAAAA					
Clone (g-C)	GATAGGTCAGAAGATTCATCAGTGTTAACTAGCGAAAAATATTTTAAAGATTCACAAAA					

	190	200	210	220	230	240
Clone (12)	TCTGAAAAATACGAATACCAGGCAGAAGTTACAAGACTGCTTGACATTATCGTAAACTCA					
Clone (H)	TCTGAAAAATACGAATACCAGGCAGAAGTTACAAGACTGCTTGACATTATCGTAAACTCA					
Clone (E)	TCTGAAAAATACGAATACCAGGCAGAAGTTACAAGACTGCTTGACATTATCGTAAACTCA					
Clone (1)	TCTGAAAAATACGAATACCAGGCAGAAGTTACAAGACTGCTTGACATTATCGTAAACTCA					
Clone (C-D)	TCTGAAAAATACGAATACCAGGCAGAAGTTACAAGACTGCTTGACATTATCGTAAACTCA					
Clone (C-A)	TCTGAAAAATACGAATACCAGGCAGAAGTTACAAGACTGCTTGACATTATCGTAAACTCA					
Clone (3)	TCTGAAAAATACGAATACCAGGCAGAAGTTACAAGACTGCTTGACATTATCGTAAACTCA					
Clone (C-C)	TCTGAAAAATACGAATACCAGGCAGAAGTTACAAGACTGCTTGACATTATCGTAAACTCA					
Genebank	TCTGAAAAATACGAATACCAGGCAGAAGTTACAAGACTGCTTGACATTATCGTAAACTCA					
Clone (g-A)	TCTGAAAAATACGAATACCAGGCAGAAGTTACAAGACTGCTTGACATTATCGTAAACTCA					
Clone (g-B)	TCTGAAAAATACGAATACCAGGCAGAAGTTACAAGACTGCTTGACATTATCGTAAACTCA					
Clone (g-C)	TCTGAAAAATACGAATACCAGGCAGAAGTTACAAGACTGCTTGACATTATCGTAAACTCA					

## Results

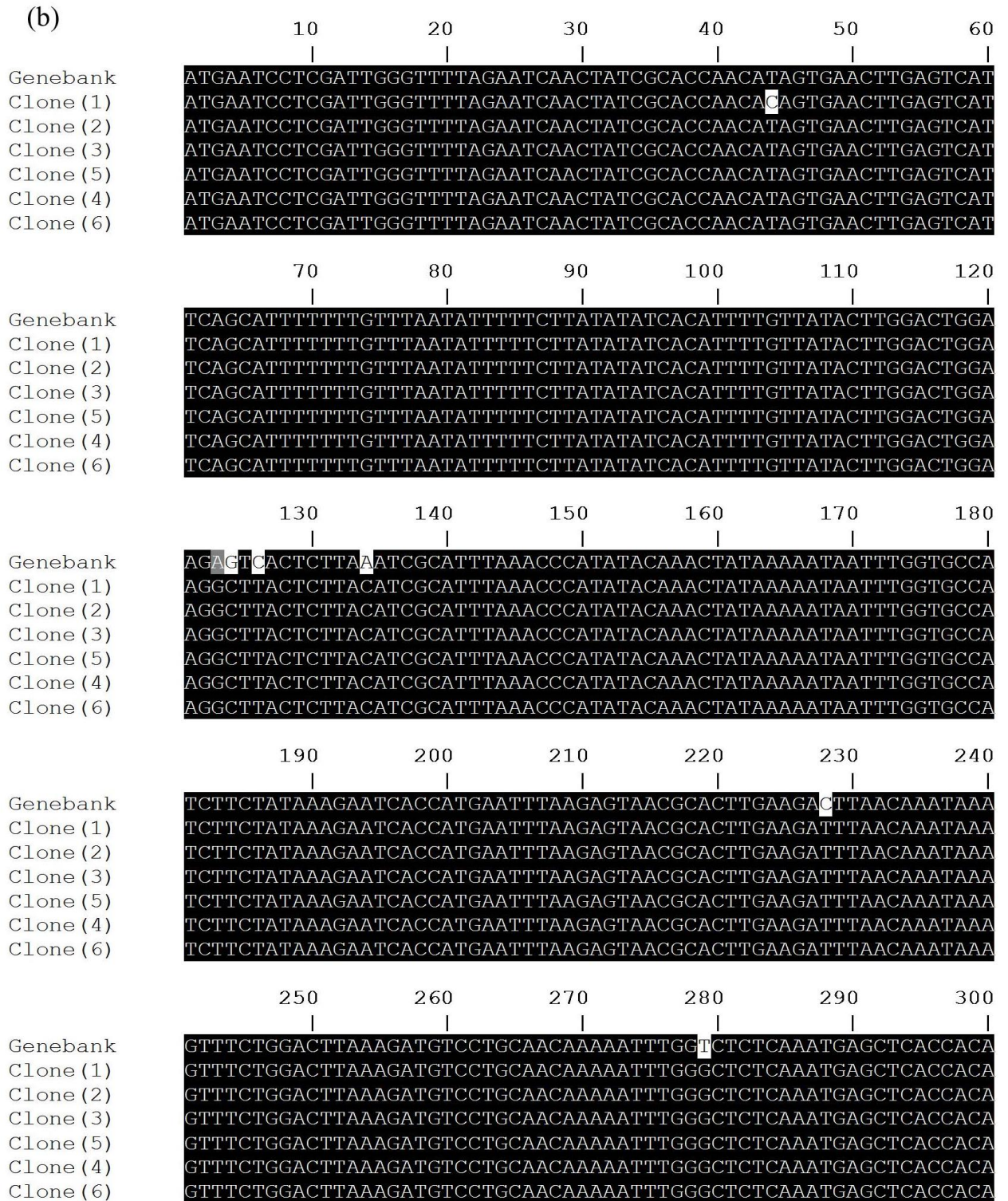


Figure 26: Alignment of the nucleotide sequence of TaHSP90-Chr1 and TaHSP90-Chr1

(a) Alignment of the nucleotide sequence of *T. annulata* TaHSP90-Chr1 sequenced clones (c-D, 1, c-A, g-B, g-A, C-C, 3, g-C, 12, H and E) with *T. annulata* HSP90 reference sequence (Accession: XM\_948749). (b) Alignment of the nucleotide sequence of *T. annulata* TaHSP90-Chr4 sequenced clones (1–6) with *T. annulata* HSP90 reference sequence (Accession: XM\_948193.1).

#### 4.4.3 Phylogenetic analysis

In order to determine the evolutionary relationships between TaHSP90-Chr1 and TaHSP90-Chr4 with other HSP90 family, the nucleotide sequence of these genes were translated into corresponding peptide sequences ([web.expasy.org/translate/](http://web.expasy.org/translate/)) and their phylogenetic relationship was determined using one click software (<http://www.phylogeny.fr/>).

As shown in Figure 27, a high identity was found between TaHSP90-Chr1 amino acid sequence with *T.parva* HSP90 (accession: XP\_766455.1) and *T.orientalis* molecular chaperone protein (accession: BAM39425.1) (E value = 0.0). In the case of TaHSP90-Chr4, a high identity was found with *T.parva* HSP90 (accession: XP\_764281.1), *T. orientalis* HSP90 (accession: BAM41905.1) and *Babesia bovis* HSP90 (accession: XP\_001611867.1) (E value = 0.0). The phylogenetic analysis revealed that TaHSP90-Chr1 and TaHSP90-Chr4 are more closely related to HSP90 from *Theileria* species and *Babesia bovis* than to HSP90 from human or bovine.

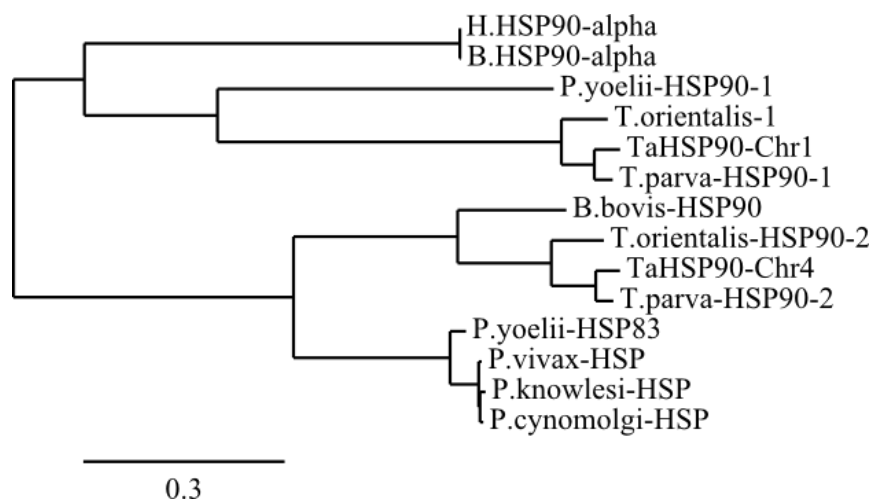


Figure 27: Phylogenetic relationship of *T. annulata* TaHSP90-Chr1 and TaHSP90-Chr4.

Sequences of *T. annulata* TaHSP90-Chr1 and TaHSP90-Chr4 were aligned with H. HSP90-alpha (*Human* HSP90a, accession: NP\_005339.3), B. HSP90-alpha (*Bovine* HSP90- alpha, accession: BAC82487.1), T. parva-HSP90-1 (*Theileria parva* HSP90, accession: XP\_766455.1), T. orientalis-1 (*Theileria orientalis*-molecular chaperone protein, accession: BAM39425.1), P. yoelii-HSP90-1 (*Plasmodium yoelii* HSP90, accession: XP\_725468.1), T. parva-HSP90-2 (*Theileria parva* HSP90, accession: XP\_764281.1), T. orientalis-HSP90-2 (*Theileria orientalis* HSP90, accession: BAM41905.1), B.bovis- HSP90 (*Babesia bovis* HSP90 accession: XP\_001611867.1), P.yoelii-HSP83 (*Plasmodium yoelii* HSP83 accession: XP\_729743.1), P.cynomolgi- HSP (*Plasmodium cynomolgi* HSP accession: GAB68147.1), P.knowlesi-HSP (*Plasmodium knowlesi* HSP accession: XP\_002260434.1) and P.vivax- HSP (*Plasmodium vivax* HSP accession: XP\_001615952.1). Alignment shows that TaHSP90-Chr1 is closely related to *Theileria parva* HSP90 (accession: XP\_766455.1) and *Theileria orientalis*-molecular chaperone protein (BAM39425.1), while TaHSP90-Chr4 is closely related to *Theileria parva* HSP90 (accession: XP\_764281.1), *Theileria orientalis* HSP90 (accession: BAM41905.1) and *Babesia bovis* HSP90 (accession: XP\_001611867.1).

## **4.5 Expression and purification of recombinant *T. annulata* HSP90**

### **4.5.1 Bioinformatic analysis of TaHSP90-Chr1 and TaHSP90-Chr4**

The open reading frame (ORF) of TaHSP90-Chr1 (2967 bp) encodes for a protein of 989 amino acids with a theoretical mass of 115.7 kDa, while the ORF of TaHSP90-Chr4 (~2742 bp) encodes for a protein of 913 amino acids with a theoretical mass of 104.1 kDa. The amino acid alignment between TaHSP90-Chr1 and TaHSP90-Chr4 revealed 46% difference (Figure 46, appendix).

Analysis using Signal P 4.0 server prediction showed that the TaHSP90-Chr1 contains a signal peptide with a most likely cleavage site between position 20 and 21, whereas TaHSP90-Chr4 with a probable cleavage site between amino acid 39 and 40.

In order to determine the functional domain of TaHSP90-Chr1 and TaHSP90-Chr4, the amino acid sequences of TaHSP90-Chr1 and TaHSP90-Chr4 were analysed using Conserved Domain Search Service (CD Search) (<http://www.ncbi.nlm.nih.gov/Structure/cdd/wrpsb.cgi>) and other programs (results in Table 21 and Table 22, appendix).

The functional HSP90 domain of TaHSP90-Chr1 was found to be located between the amino acids 288 and 738 with a calculated size of 55.9 kDa, while in TaHSP90-Chr4 this domain was found to be located between the amino acids 316 and 839 with a calculated size of 60.5 kDa.

### **4.5.2 Expression and purification of TaHSP90-Chr1 and TaHSP90-Chr4 recombinant protein**

First, in order to express TaHSP90-Chr1 recombinant protein, new primers were designed to express the functional domain of HSP90 (between amino acids 288 and 738) of TaHSP90-chr1 (55.9 kDa). Secondly, other primes were designed to express the full-length ORF of TaHSP90-Chr4 (the predicted signal peptide was excluded). Using these primes, PCR products were cloned first into the pDrive vector and then sub-cloned into pQE30 vector, which was used to transform *E. coli* M15 [pREP4] cells.

The colony blot procedure was applied as an initial screening test to identify the clones expressing the recombinant protein using anti-His-tagged antibody, which reacts only with TaHSP90-Chr1 and TaHSP90-Chr4 constructs in the pE30 vector. As shown in Figure 28, the majority of the clones reacted positively with anti-His-tagged antibody.

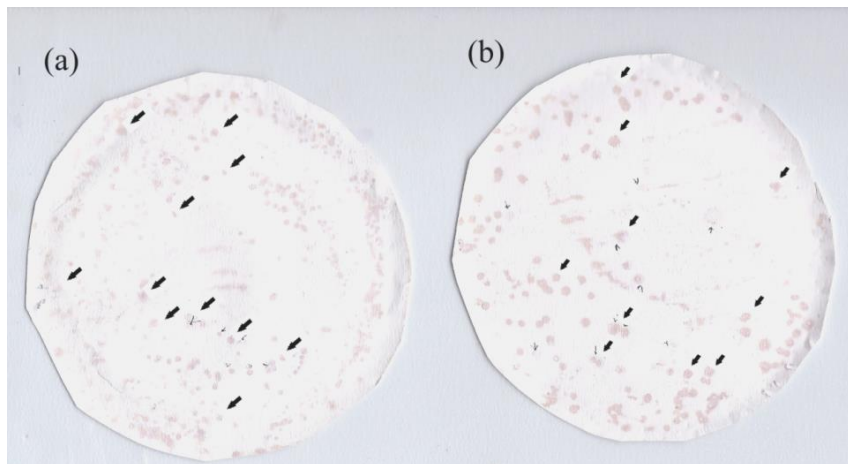


Figure 28: Plating and screening of the clones expressing the His-tagged protein using the colony blot method. Arrows indicate to the clones that were picked randomly. (a) Screening of the clones supposed to contain a TaHSP90-Chr1 insert. (b) Screening of the clones supposed to contain a TaHSP90-Chr4 insert.

Between 11 to 12 clones were picked from each transform (TaHSP9-Chr1 and TaHSP90-Chr4) and grown as individual clones in overnight cultures and their plasmid DNA was isolated. Figure 29 and Figure 30 show the PCR results using the pQE-30 primers to test the presence of the insert. After that, the plasmids DNA of these clones were sequenced to verify whether the insert integrated in the desired reading frame or not (data not shown).

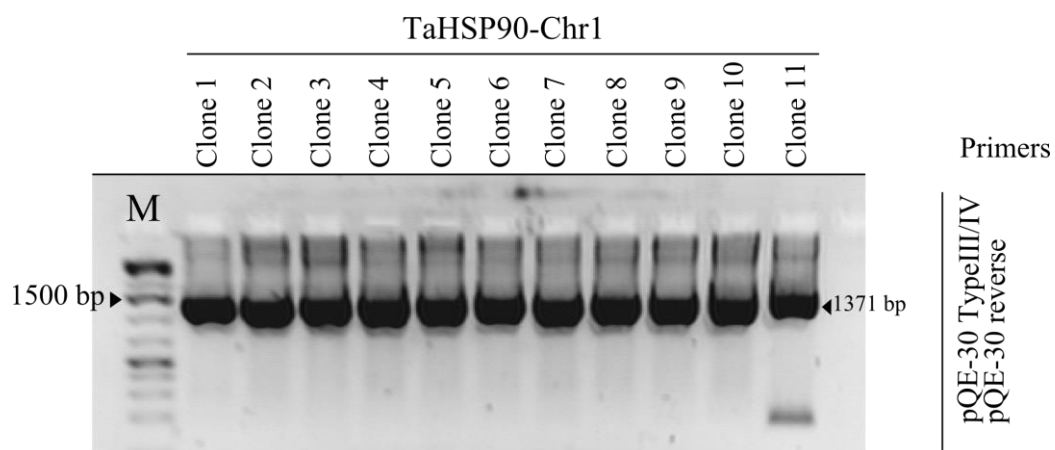


Figure 29: PQE-PCR and selection of recombinant pQE30 clones (TaHSP90-Chr1).

The PCR was performed using the primer pair pQE-30 Type III/IV and pQE-30 reverse, which bind to the sequences flanking of the pQE 30 vector (MCS) and giving PCR product of 1371 bp which representing the full sequence of TaHSP90-Chr1. M: molecular weight marker.

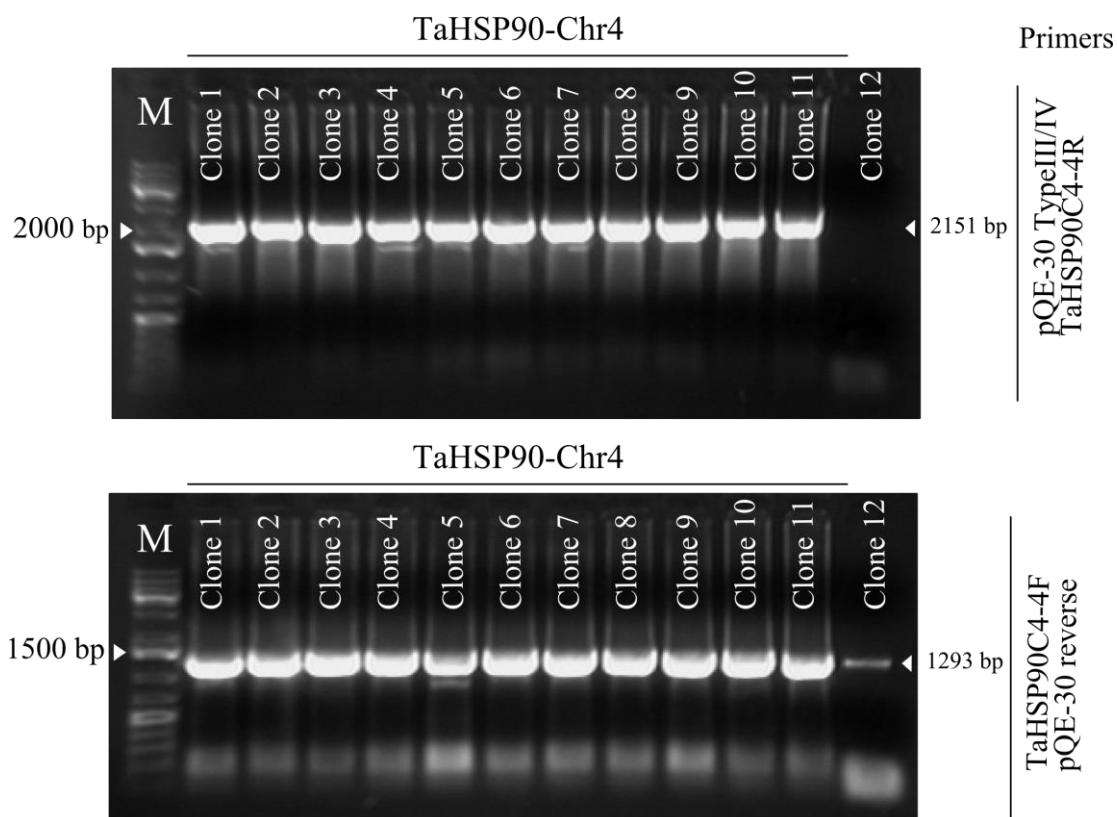


Figure 30: PQE-PCR and selection of recombinant pQE30 clones (TaHSP90-Chr4).

Upper row: The PCR was performed using the primer pair pQE TypeIII/IV and TaHSP90C4-4R which bind to the sequence of the pQE vector and the sequence of TaHSP90-Chr, 4 respectively, and giving a PCR product of 2151 bp, which representing a part of TaHSP90-Chr4 sequence. Lower row: The PCR was performed using the primer pair TaHSP90C4-4F and pQE-30 reverse, which bind to the sequence of the TaHSP90-Chr4 and the sequence of pQE vector, respectively, and giving a PCR product of 1293 bp, which representing a part of TaHSP90-Chr4 sequence. M: molecular weight marker.

After induction of expression by adding 2mM IPTG, proteins were separated on SDS-PAGE electrophoresis either by applying bacterial cell lysates directly or after purification of the proteins. Figure 31 shows results obtained using Coomassie stained SDS-gels of the bacterial cell lysates and immunoblotting of the purified products of TaHSP90-Chr1 and TaHSP90-Chr4. It was found that the anti-His-tagged antibody recognized a band of the correct size (approximately 55.5 kDa) representing the protein of the construct TaHSP90-Chr1, while the same antibody detected a band of approximate size of 170 kDa representing the protein of the construct TaHSP90-Chr4 (full-length ORF). However, it is apparent that the latter is greater than the calculated size. It is worth to say that, these bands were also observed in Coomassie stained SDS-gels of the bacterial cell lysates.

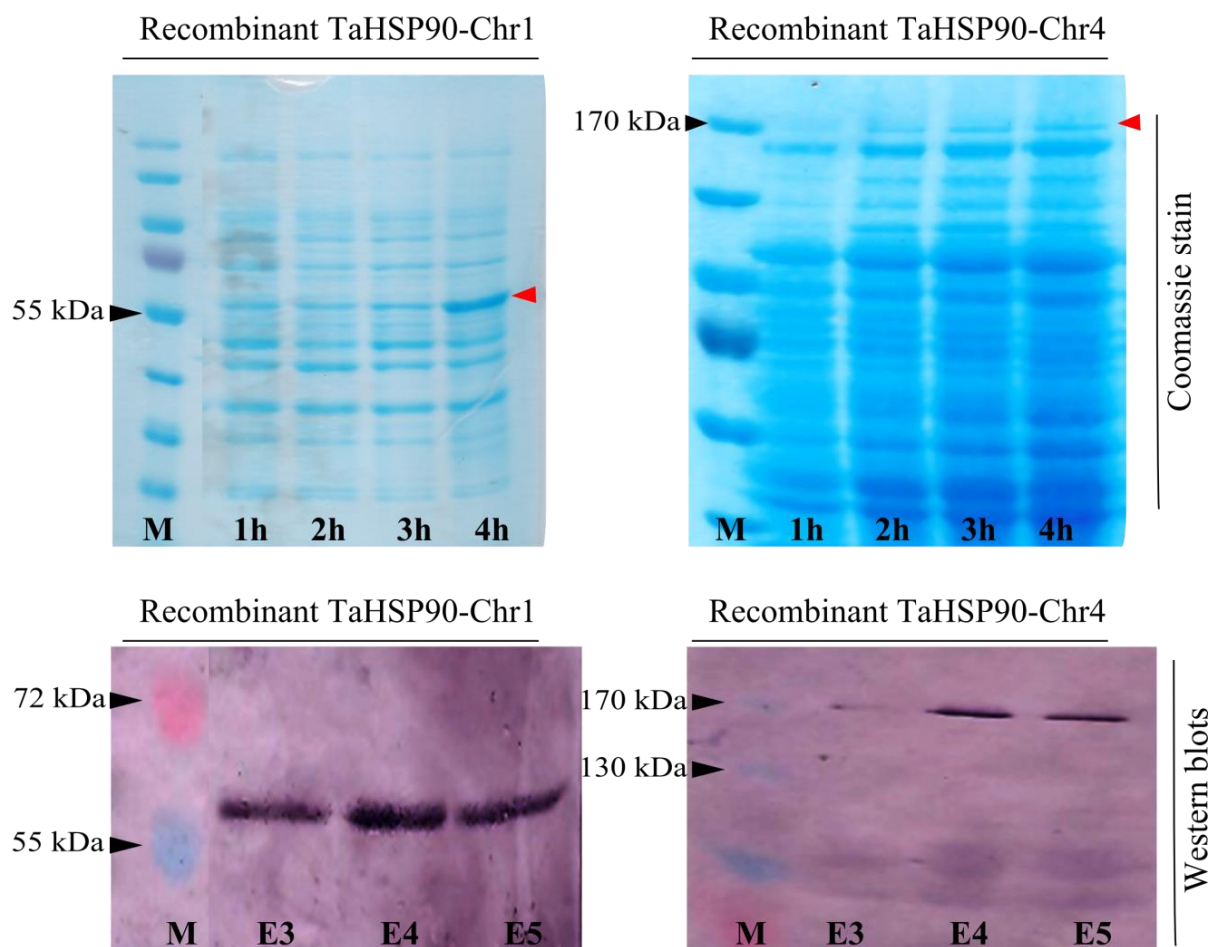


Figure 31: Recombinant expression and detection of *T. annulata* HSP90 proteins.

Upper row: SDS-PAGE gel of recombinant TaHSP90-Chr1 and TaHSP90-Chr4 after 1-4 hour of induction stained with Coomassie blue. Lower row: Recombinant proteins were expressed and purified under denaturing conditions, and then detected in western blots using an anti-His tag antibody (E3-E5 Collection of recombinant protein in the Elution buffer), M: molecular weight marker.

#### 4.6 Detection of *T. annulata* HSP90 protein

As mentioned before, bovine HSP90 can be recognized by using anti-human HSP 90 $\alpha/\beta$  (HSP 90 $\alpha/\beta$  (F-8): sc-13119, Santa Cruz), whereas an antibody against *T.annulata* HSP90 was not available. Consequently, an anti-serum against *T. annulata* HSP90 was generated by immunization of rabbits with a synthetic peptide prepared from the amino acid sequence of the parasite HSP90.

#### 4.6.1 Antigenic determinants of TaHSP90-Chr1 and TahSP90-Chr4

Antigenic determinants were deduced from the protein sequence of TaHSP90-Chr1 and TaHSP90-Chr4 using Predicting of Antigenic Peptides (<http://imed.med.ucm.es/Tools/antigenic.pl>) method of (Kolaskar and Tongaonkar, 1990), which is based on a table that reflects the occurrence of amino acid residues in experimentally known segmental epitopes.

As shown in Figure 32, a total of 32 and 30 antigenic determinants were deduced for TaHSP90-Chr1 and TaHSP90-Chr4, respectively.

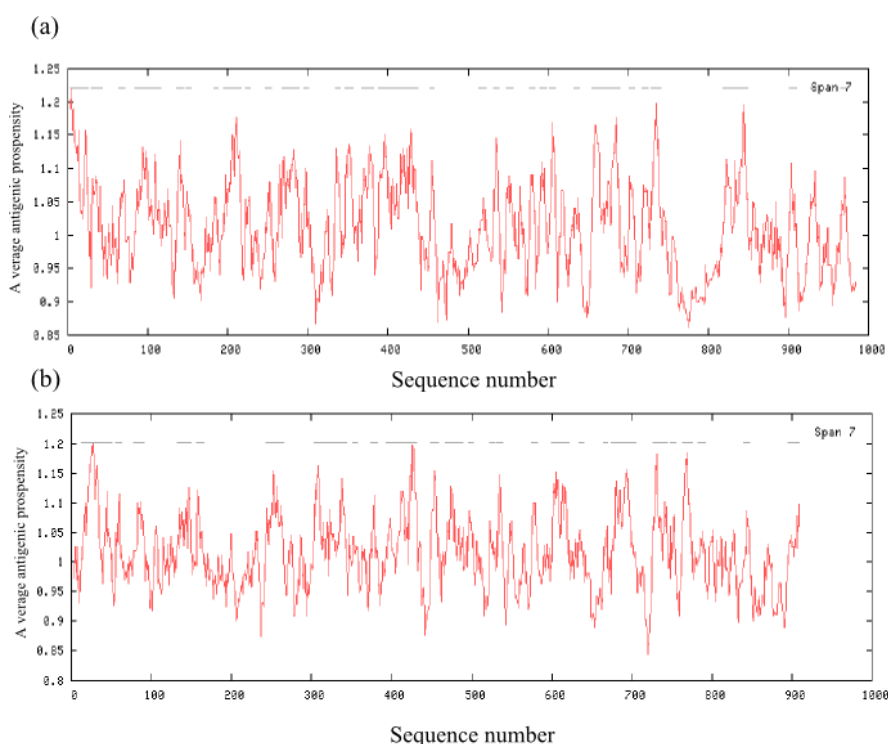


Figure 32: Distribution of the antigenic determinants sequence in the TaHSP90-Chr1 and TahSP90-Chr4.

(a) A total of 32 antigenic determinants were deduced for TaHSP90-Chr1. (b) A total of 30 antigenic determinants were deduced for TahSP90-Chr4.

One of these antigenic determinants was chemically synthesized as peptides: ELEKVKAVKEEKEWN. This peptide sequence is identical with amino acids 452–467 of TaHSP90-Chr1 and has an 86% similarity with the corresponding region of TahSP90-Chr4. In addition, this peptide sequence was selected based on an alignment of TaHSP90-Chr1, TahSP90-Chr4 and bovine HSP90 to avoid the region, where the *T.annulata* HSP90 and bovine HSP90 sequences are similar. Two rabbits were immunized with the synthesized peptide using an established immunization protocol (Charles River Laboratories).

To verify the efficiency of the immunization, dot blot was performed. The anti-*T. annulata* HSP90 antiserum used at the dilutions of 1:100, 1:500 and 1:1000 in the dot blot against the synthesized peptide at a concentration 2  $\mu$ g, 4  $\mu$ g and 8  $\mu$ g diluted in PBS. The serum obtained from rabbit before immunization was used as negative sera. As shown in Figure 33, the anti-*T. annulata* HSP90 antiserum reacted positively with all concentration of the synthesized peptide, while the negative sera showed no reactivity under the same conditions.

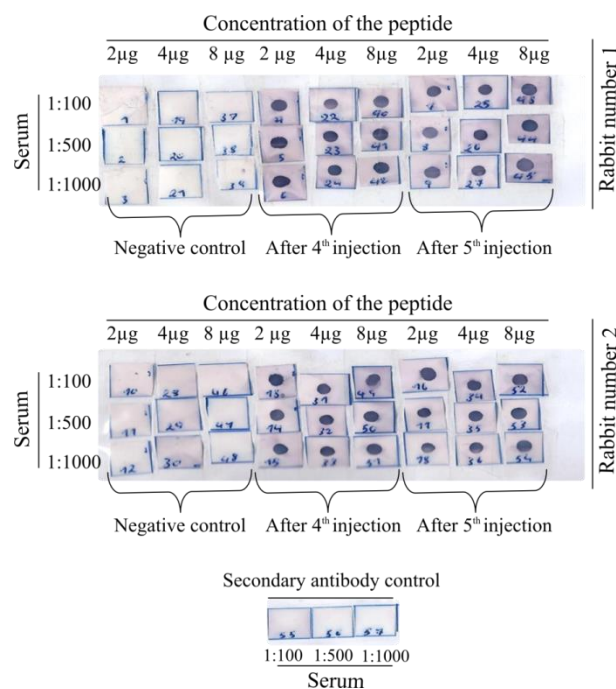


Figure 33: Dot blot testing the reactivity of anti-*T. annulata* HSP90 antiserum with peptide.

The peptide was dotted at a 2 fold dilution starting at 8  $\mu$ g per dot. The serum was obtained from two rabbits (rabbit number 1 and 2) before and after immunization. The sera were diluted 1:100, 1:500 and 1:1000 with 5% skimmed milk. The nitrocellulose membranes were incubated with; the serum obtained before immunization (negative control), the serum obtained after immunization (after 4<sup>th</sup> and 5<sup>th</sup> injection of the peptide) and with secondary antibody only (secondary antibody control).

#### 4.6.2 Detection of *T. annulata* HSP90 in cell lysates prepared from *T. annulata* Ankara 288-infected cells

An initial experiment was performed to test the reactivity of anti-*T. annulata* HSP90 antiserum against recombinant proteins (both isoforms, TaHSP90-Chr1 and TaHSP90-Chr4). As presented in Figure 34, TaHSP90-chr1 isoform (approximately 55.5 kDa) could be detected by anti-*T. annulata* HSP90 antiserum used in western blot. A similar band was also specifically recognized by anti-His-tagged antibody, indicating that this band was originating from the recombinant protein (TaHSP90-Chr1). However, attempts to detect a band

## Results

corresponding to the size of the purified recombinant TaHSP90-Chr4 protein were unsuccessful. Moreover, the same antibody failed to recognize the native form of parasite HSP90 in cells lysate or even by immunostaining of infected cells.

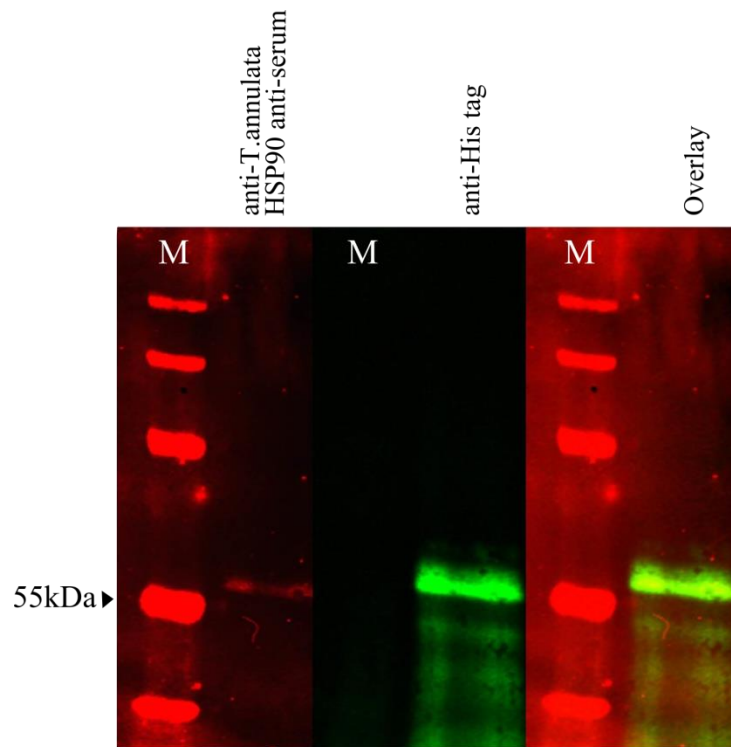


Figure 34: Recombinant expression and detection of TaHSP90-Chr1 protein.

Recombinant TaHSP90-Chr1 protein (59 kDa) was expressed and purified under denaturing conditions and then detected in western blots using an anti-His-tagged antibody and anti- *T. annulata* HSP90 antiserum. The analysis was performed using fluorescent secondary antibodies and the Licor Odyssey system.

Therefore, this antibody seems to be not suitable for use to differentiate between host and parasite HSP90. Accordingly, another approach must be used. To this end, it is known that there is a fine difference between the C-terminal sequence of host and parasite HSP90 novobiocin binding site (a specific sequence located at the C-terminal, which represents the specific binding site for novobiocin with HSP90).

The alignment of novobiocin binding site of bovine HSP90 and *T.annulata* HSP90 showed that the bovine HSP90 possesses a specific binding site for novobiocin (Figure 35 and Figure 36). This fact enables using novobiocin to interfere with bovine HSP90 function but not with the parasite. Based on these knowledge, I used novobiocin as a specific inhibitor for bovine HSP90.

```

                670      680      690      700      710      720
                |        |        |        |        |        |
BHSP90-alpha  KDLVILLYETALLSSGFSLEDPQTHANRIYRMIKLGIGIDEEDDPTADDSSAAVTEEMPPL
BHSP90-beta   KDLVVLLFETALLSSGFSLEDPQTHSNRIYRMIKLGIGIDEDEVTAEEPSAAVPDEIPPL
Novobiocin    -DLVILLYETALLSSGFSLEDP-----
                *****:*****

```

Figure 35: Alignment of the amino acid sequence of bovine HSP90 with novobiocin binding site.

Alignment of the amino acid sequences of BHSP90-alpha and BHSP90-beta with novobiocin binding site (amino acids 657-677 of chicken HSP90 $\beta$ , accession no.: NP\_001103255.1) showed 95% identity and 5% similarity.

```

                910      920      930      940      950      960
                |        |        |        |        |        |
Novobiocin    -----D-LVILLYETALLSSGFSLEDP-----
TaHSP90_Chr1  ELTEKKKKYMKRLDRLFKLLYNAAKLKSGFVLEEPQLVVVNYLYEKLNRSLGDFVEKDFEF
TaHSP90_Chr4  EKMLKVDSLDRMKEIAAQLLDVVSIQGGYSIEDPSSFAKGI IKLMQNEAKHYLNDPAET
                . : * :.. :..* : :*:

```

Figure 36: Alignment of the amino acid sequence of *T. annulata* HSP90 with novobiocin binding site.

Alignment of the amino acid sequences of TaHSP90-Chr1 and TaHSP90-Chr4 with novobiocin binding site (amino acids 657-677 of chicken HSP90 $\beta$ , accession no.: NP\_001103255.1) showed 19% identity and 28.6% similarity.

#### 4.7 Assessment of the effect of Novobiocin on *T. annulata* Ankara 288-infected cells

In order to investigate the effect of novobiocin on parasite and host cell HSP90, *T. annulata* Ankara 288-infected cells were treated with different concentrations of novobiocin (0.05 mM, 0.1 mM, 0.5 mM and 1mM) or DMSO (control group) then incubated for 3 days at 37°C.

Confocal microscopic analysis revealed that the treatment of *T. annulata* Ankara 288-infected cells using novobiocin (0.05 mM, 0.1 mM, 0.5 mM and 1 mM) led to the killing of the parasite, while the DMSO treated cells showed the presence of the parasite in the host cytoplasm (Figure 37).

In summary, neither anti- *T. annulata* HSP90 antiserum nor novobiocin helped to distinguish between the functional role of bovine HSP90 and *T. annulata* HSP90 during the parasite differentiation. Thereby, it will be helpful in the future to produce anti-*T. annulata* HSP90 antibody by using the recombinant protein.

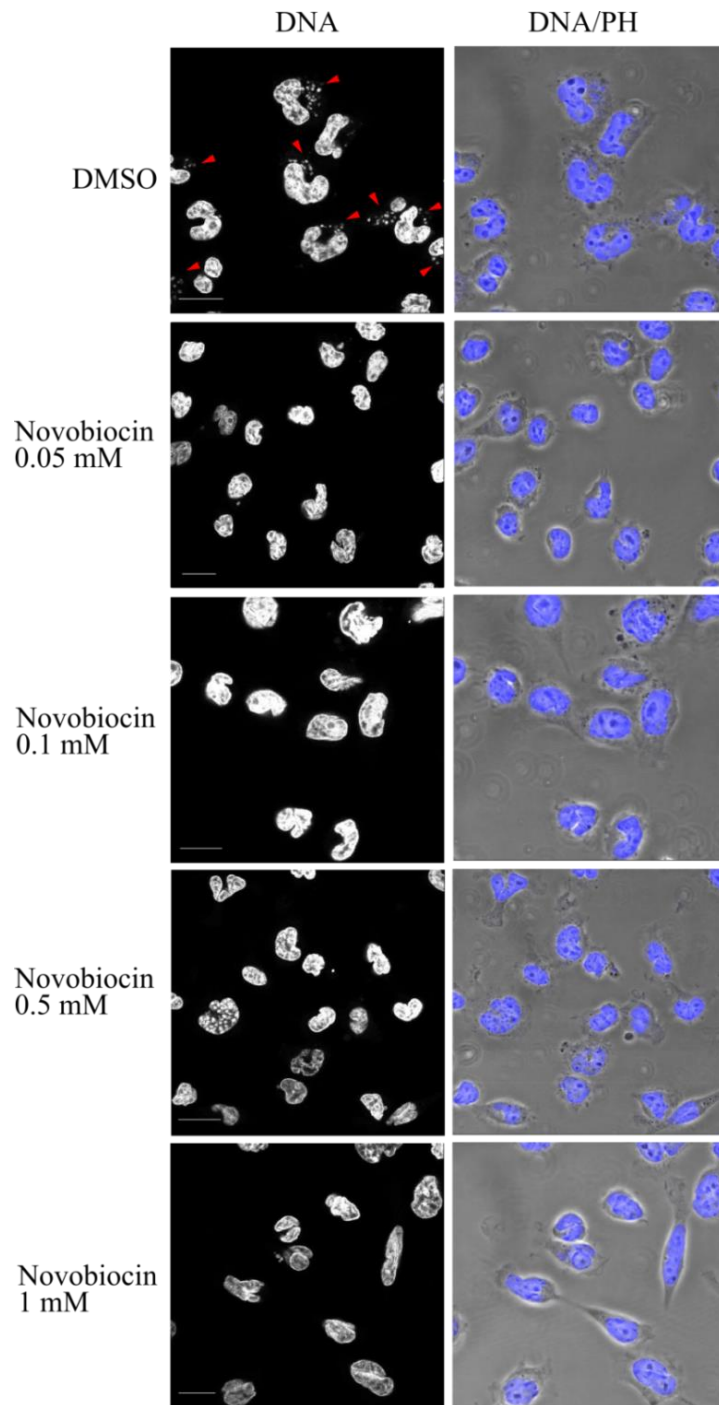


Figure 37: The effect of Novobiocin (Nb) on *T.annulata* Ankara 288-infected cells.

The cells were incubated with Nb (0.05 mM, 0.1 mM, 0.5 mM and 1mM) or DMSO for 3 days at 37°C. DNA was visualized using DAPI, DNA/PH: Phase-contrast image plus DAPI staining. As shown in the figure, the treatment of the cells using Nb led to the killing of the parasites, while in DMSO-treated cells the parasites still exists (arrow).

---

## 5 Discussion

### 5.1 The role of HSP90 in apoptosis and cell proliferation in *T.annulata* - infected cells

Many physiological processes such as tissue development and homeostasis need to keep the balance between apoptosis and cell proliferation, in which many genes are involved (Lawlor and Alessi, 2001; Alenzi, 2004). Among other factors, there is a link between HSP activities and apoptosis as well as cell proliferation.

The anti-apoptotic function of HSPs is partly mediated by the Fas death receptor and the caspase pathway (Parcellier *et al.*, 2003). For example, the expression of human HSP27 blocks the apoptotic process generated by the Fas receptor (Mehlen *et al.*, 1996). In another study, Pandey and co-workers investigated also the effect of HSP27 in another apoptotic pathway. They found that HSP27 acts as a negative regulator of cytochrome c- mediated activation of procaspase-3, where HSP27 inhibits caspase-3 activation and, thus, limiting the availability of procaspase-3 for cleavage (Pandey *et al.*, 2000b). Both HSP70 and HSP90 block apoptosis by interacting with Apaf-1, hence preventing the apoptotic function of caspases (Pandey *et al.*, 2000a; Parcellier *et al.*, 2003).

The close correlation between expression levels of HSPs and cell proliferation, especially in cancer cells, has been observed in various studies. For example, it was found that HSP90 was highly expressed in the leukemia cells compared with normal cells (Yufu *et al.*, 1992). Moreover, it has been shown that in breast cancer, the high expression of HSP70 is required for the cell proliferation (Vargas-Roig *et al.*, 1997). Taken together, it can be postulated that HSPs are involved in the regulation of cell proliferation and survival.

It is well known that *Theileria spp* (*T.annulata*, *T.parve*) have the ability to transform bovine leukocytes, which undergo a permanent proliferation similar to that of tumour cells (Heussler *et al.*, 1999). Moreover, in *Theileria* -infected cells, the apoptotic program is negatively affected by the presence of the parasite (Haller *et al.*, 2010).

A major aim of this study was to investigate the role of HSP90 in the viability and proliferation of *T.annulata* Ankara 288-infected cells using geldanamycin (GA), which is known as an inhibitor of HSP90.

The flow cytometric analysis of apoptosis showed that higher concentrations of GA (0.25  $\mu$ M, 0.5  $\mu$ M and 1  $\mu$ M) lead to a statistically significant increase in apoptotic cells at 37°C (Figure 8 and Figure 9), while the low concentration of GA (0.1  $\mu$ M) exhibited a similar effect in cells incubated at 41°C (Figure 10). However, in the case of incubation for a longer time (6 days) at 37°C, the treatment with GA 0.25  $\mu$ M becomes statistically less significant (Figure 9). This is probably due to the cell's ability to adapt themselves at 37°C through producing more level of HSP90.

Generally, GA induced apoptosis in *T.annulata*-infected cells in a time- and dose-dependent manner. Thus, treatment with GA at concentrations more than 0.05  $\mu$ M leads to a significant cell cycle arrest after incubation for 3 days at 37°C or for 3 and 5 days at 41°C. Five or 10 times more GA is required to achieve a similar effect, when the cells are incubated for a longer time at 37°C. These results indicated that HSP90 is required for the survival and proliferation of *T.annulata*-infected cells. In this context, these results are in agreement with results of experiments conducted by Li, who clearly showed that GA induces apoptosis in a dose- and time dependent manner in *L. donovani* promastigotes (Li *et al.*, 2009). Similarly, these results are in accordance with the finding of Graefe and Wiesgigl regarding the arrest of the proliferation of *T. cruzi* and *L. donovani*, respectively (Graefe *et al.*, 2002; Wiesgigl and Clos, 2001). Furthermore, a derivative of the antibiotic GA, 17-AAG, interferes also with cell cycle in malignant pleural mesothelioma as well as in breast cancer through inhibition of HSP90 (Münster *et al.*, 2001; Okamoto *et al.*, 2008).

There are a number of pathways through which HSP90 can exert its function:

- a) It is well known that the expression of HSP90 increases when the cells are exposed to a high temperature (Lindquist and Craig, 1988; Nathan and Lindquist, 1995). The increase in the expression level of HSP90 is required for proper folding of misfolded proteins, where exposure to high temperature leads to the accumulation of denatured or semi-denatured proteins (Latchman, 2001). In addition, higher concentrations of HSP90 are required for cell growth at higher temperatures (Borkovich *et al.*, 1989).

---

Thus, the imbalance in the function of this protein by using GA when the cells are exposed to elevated temperature leads to cell death.

- b) It was reported that, HSP90 regulates activities of a large number of client proteins (substrates) that are involved in the controlling of cell cycle progression and signal transduction pathways (Picard, 2002). The list of substrates modulated by HSP90 includes transcription factors such as cyclin-dependent kinase 1 (cdc2), Akt/PKB and p53 (Pratt and Toft, 2003). In this context, HSP90 can regulate the cell cycle via activation of cdc2, which plays a key role in the regulation of cell cycle (Kim *et al.*, 1999; García-Morales *et al.*, 2007).

HSP90 interacts also with phosphorylated serine/threonine kinase Akt/PKB, a protein that plays a major role in the cell cycle and survival. The binding of HSP90 with Akt/PKB protects Akt from the dephosphorylation and inactivation by protein phosphatase 2 (PPA2), this protection leads to inactivation of pro-apoptotic protein Bad (Sato *et al.*, 2000; Parcellier *et al.*, 2003). In addition, Akt can also activate I $\kappa$ B kinase (IKK), which in turn results in the activation of NF- $\kappa$ B (Ozes *et al.*, 1999). Furthermore, the activation of Akt/PKB leads to decreases in the cellular levels of cyclin-dependent kinase inhibitor 1B (p27<sup>Kip1</sup>), an enzyme that inhibits the cell cycle, thereby promoting the cell proliferation (Gesbert *et al.*, 2000; Lawlor and Alessi, 2001).

In *Theileria*-infected cells, it has been reported that the constitutive activation of PI-3K/Akt pathways is necessary for the permanent proliferation of infected cells (Baumgartner *et al.*, 2000).

Taken together, it can be postulated that HSP90 can regulate the cell cycle in *Theileria*-infected cells via activation of Akt/PKB. Further work is required to clarify this assumption.

- c) It has been demonstrated that p53 is arrested in the cytoplasm of *T.annulata*-infected cells and by this way is prevented to induce apoptosis in host cell (Haller *et al.*, 2010). Therefore, in my study I tested the possible role of HSP90 in arresting p53 in the cytoplasm of infected cells. Indeed, I could observe that the treatment of *T.annulata*-infected cells with GA leads to the translocation of p53 into the host cell nucleus. In contrast, p53 predominantly remains in the cytoplasm of DMSO-treated cells (Figure 11). This finding indicated that HSP90 function is essential for the stabilization of p53 in *T.annulata* Ankara 288-infected cells. These results clearly confirm the observation of Haller and co-workers, who found that the elimination of the parasite by

buparvaquone resulted in translocation of p53 into the host cell nucleus. Further, they found that the translocation of p53 into cell nucleus is associated with the upregulation of the pro-apoptotic Bax and Apaf-1 and the down-regulation of the anti-apoptotic Bcl-2 proteins (Haller *et al.*, 2010).

It has been shown that HSP90 binds tightly to mutated p53, where this binding interferes with the function of p53 proteins as tumour suppressors (Whitesell and Lindquist, 2005) by doing so, it contributes to the stabilization of p53 (Peng *et al.*, 2001).

Although p53 is not mutated in *T.annulata*-infected cells, HSP90 is still able to arrest p53 in the host cell cytoplasm as inhibition of HSP90 by GA clearly leads to the translocation of p53 into the host nucleus. However, how HSP90 arrests p53 is not known in *T.annulata*-infected cells and needs further investigations.

## 5.2 HSP90 and stage progression of the parasite

Parasite differentiation is a fundamental biological event that allows amplification, expansion and transmission of the parasite (Shiels *et al.*, 1994). Although it is known that differentiation frequently occurs in response to altered extracellular conditions (Shiels *et al.*, 1994, 1998), the molecules that regulate this process are not yet fully understood. Previous work carried out on *T. annulata* demonstrated that the differentiation or stage progression from schizont to merozoite can be induced in vitro by elevation of culture temperature to 41°C (Shiels *et al.*, 1992), and it is also known that heat shock genes are activated when a cell responds to stress, such as an increase in temperature (Lindquist and Craig, 1988). Based on this, HSPs may be involved directly or indirectly in the parasite differentiation. This assumption is supported by experiments showing that the expression level of HSP90 is increased during the differentiation process of *T. brucei* (Van der Ploeg *et al.*, 1985) and *T. gondii* (Echeverria *et al.*, 2005). Similarly, the inhibition of HSP90 by GA blocks the differentiation from ring stage to the trophozoite stage in *P. falciparum* (Banumathy *et al.*, 2003). In contrast to this, the disturbances of HSP90 homeostasis by GA in *L. donovani* are a signal for the onset of stage differentiation (Wiesgigl and Clos, 2001).

In the present study, I addressed the role of HSP90 in *T.annulata* stage differentiation and found that, inactivation of HSP90 by GA coincided with a significant increase in the number of cells in which *T. annulata* differentiates from schizont to merozoite, regardless of the

temperature used for the incubation of the cells. In addition, the qRT-PCR analysis showed a significant increase in the RNA level of the TamR1 gene during parasite differentiation. It is well known that TamR1 gene encodes a polypeptide that is present in the merozoite stage. Thus, the TamR1 is expressed at high level in the merozoite stage and at very low level in macroschizont stage (Shiels *et al.*, 1994).

In *T.annulata*-infected cells cultured at 37°C, host cell and parasite proliferation is synchronized and only a few parasites differentiate. This can change if the culture temperature is raised to 41°C. In this case, HSP90 of the parasite and bovine host cell is up-regulated as determined by qRT-PCR. In addition to this, the differentiation of the parasite is increased relative to the situation at 37°C. These findings are favouring the hypothesis that HSP90 is needed for parasite differentiation. However, when the cells are treated with GA  $\leq$  0.1 $\mu$ M and incubated at 37°C, only low numbers of merozoites are observed and neither apoptosis nor cell cycle arrest was found. Again, when GA-treated cells are cultivated at 41°C, a dramatic differentiation occurred, the host cell cycle is arrested, and when the duration of the incubation is extended the percentage of apoptotic cells is significantly increased (Figure 39). At the same time, the variation in the expression profile of parasite and bovine HSP90 occurs, where GA treatment led to down-regulation of the parasite HSP90 as measured by qRT-PCR, while bovine HSP90 increased. This means:

- 1) as by *L. donovani*, HSP90 has no effects on the parasite differentiation.
- 2) Although, more bovine HSP90 is produced the cells undergo cell cycle arrest and when incubated for longer time more apoptotic cells are observed. In this case, GA may interfere with bovine HSP90 through binding to the N-terminal domain of the protein.
- 3) As a consequence of the GA action, p53 is translocated to the host cell nucleus where it activates the pro-apoptotic proteins and inactivates anti-apoptotic proteins.

Shiels and colleagues found that there is a direct link between the cell proliferation and differentiation process (Shiels *et al.*, 1998). They clearly demonstrated that the proliferation rate of *T.annulata*-infected cells is reduced before the morphological differentiation can be detected. Moreover, blocking of the cell proliferation by aphidicolin, an inhibitor of the cell cycle, resulted in a significant increase in differentiation levels in *T.annulata*-infected cells (Shiels *et al.*, 1997). A similar mechanism may operate in GA-treated cells, in which the

reduction in the cell proliferation enhances the probability that parasite differentiation will occur.

### 5.3 The regulation of HSP90 in *T. annulata* Ankara 288-infected cells

As mentioned earlier, four major HSP90 isoforms were identified in *T.annulata* Ankara 288-infected cells; two of them belong to the bovine HSP90 (BHSP90-alpha and HSP90-beta) and the others belong to *T.annulata* HSP90 (TaHSP90-Chr1 and TaHSP90-Chr4) (Mohammed *et al.*, 2013).

My results showed that the expression levels of BHSP90-alpha and BHSP90-beta were significantly up-regulated in response to high concentrations of GA ( $\geq 0.25\mu\text{M}$ ) at 37°C (Figure 17). A significant effect of low concentration of GA (0.05  $\mu\text{M}$ ) on the expression level of BHSP90-alpha and BHSP90-beta was also reported at 41°C (Figure 18). Moreover, the qRT-PCR revealed that the response of BHSP90-beta isoform to GA treatment is faster than BHSP90-alpha isoform. This result may indicate that there is a variation in the expression profile of bovine HSP90 isoforms.

It is well known that HSP90 expression is enhanced when cells are incubated at higher temperature or infected with certain pathogen (Welch, 1992; Csermely *et al.*, 1998), such as *Plasmodium* (Banumathy *et al.*, 2003). Like many other intracellular parasites, *T. annulata* also encounters several stresses and adverse environment imposed by the host during its life cycle. On the other hand, the existences of *T. annulata* in the host cells is by itself a stress factor for the host cells and consequently an increase in the expression level of HSP90 in *T.annulata*-infected cells can be expected (Mohammed *et al.*, 2013)

The variation in the expression of HSP90 isoforms has also been reported (Csermely *et al.*, 1998; Chen *et al.*, 2005). Human HSP90 $\beta$  isoform is constitutively expressed, while HSP90 $\alpha$  isoform is typically expressed under stress conditions. It is quite likely that there is a substantial difference in the function of the HSP90 isoforms, which in turn leads to a variation in the expression of these isoforms (Csermely *et al.*, 1998).

As mentioned in the preceding section (5.2), unexpected decrease in the expression level of *T.annulata* HSP90 was observed in the cells incubated with GA at 41°C. This phenomenon may be similar to that reported in another study, where a part of HSP90, HSP70 was also decreased in *T.annulata*-infected cells incubated at 42°C as compared to the cells incubated

at 37°C (Schnittger et al., 2000). The drop of mRNA level of *T.annulata* HSP90 is most probably a mechanism, through which parasites can induce apoptosis in the host cells and then released themselves from the host cells after differentiation process. This assumption is supported by the results obtained by flow cytometric assays, which revealed a significant increase in apoptotic cells in *T.annulata* -infected cells incubated for a longer time at 41°C (Figure 39, appendix).

In summary, inactivation of HSP90 in *T.annulata* Ankara 288-infected cells is a signal for the induction of apoptosis and cell cycle arrest in a dose- and time dependent manner, probably through the binding of GA to the N-terminal domain of HSP90. Moreover, HSP90 does not seem to be involved in the parasite differentiation. However, this issue needs further investigation.

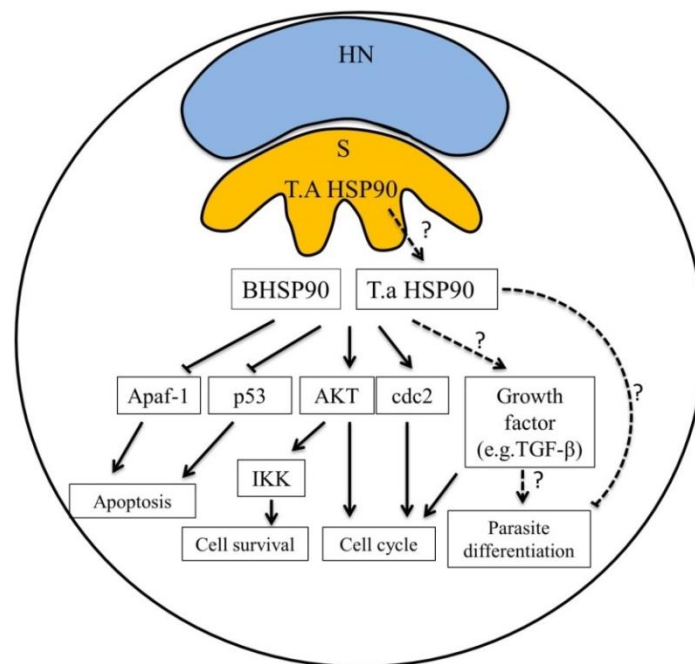


Figure 38: Model: The potential biological role of HSP90 (bovine/ parasite HSP90) in *T.annulata* Ankara 288-infected cells.

Illustrating the effects of HSP90, which stimulates the PI3K/Akt pathway, enhancing cdc2 activity, is essential for p53 stabilization and binds to Apaf-1 thereby resulting in inhibition of caspases activation. HSP90 may also stimulate the growth factors such as TGF- $\beta$ . HN: host nucleus, S: schizont, BHSP90: bovine HSP90, T.aHSP90: *T.annulata* HSP90.

#### 5.4 Identification and characterization of *T. annulata* HSP90

The existence of multiple HSP90 isoforms has been described in many eukaryotes. Humans have four isoforms of HSP90 (Chen *et al.*, 2005), while budding yeast has two isoforms (Millson *et al.*, 2007). The isoform specificity is not restricted to the biochemical level, but is extended to the functional role of HSP90 isoforms in cell differentiation and development (Sreedhar *et al.*, 2004). For example, in yeast and human, one isoform is constitutively expressed at high level (human HSP90 $\beta$  and yeast Hsc82), whereas the other isoform is strongly heat-inducible (human HSP90 $\alpha$  and yeast Hsp82) (Borkovich *et al.*, 1989; Millson *et al.*, 2007). Although, the identification and characterization of HSP90 were performed in various parasites species, such as *T. gondii* (Echeverria *et al.*, 2010), *P. falciparum* (Bonney *et al.*, 1994) and *L. donovani* (de Andrade *et al.*, 1992), the available information regarding its function in the parasites is extremely limited.

In the present study, two isoforms of *T. annulata* HSP90 were identified and characterized. These two isoforms are transcribed by two genes located in chromosome 1 and 4 (TaHSP90-Chr1 and TaHSP90-Chr4). The complete cDNA sequences of both transcripts were obtained and analysed. A comparison of nucleotide sequences of TaHSP90-Chr1 and TaHSP90-Chr4 with the reference Genbank accessions number XM\_948749.1 and XM\_948193.1 revealed identities of 97% and 98%, respectively. These findings indicate that the amplified products from cDNA belong to the *T.annulata* genes. Based on the signal peptide, both TaHSP90-Chr1 and TaHSP90-Chr4 are proposed to be secreted into the host cell and participate in the manipulation of the host cell environment.

Phylogenetic analysis of TaHSP90-Chr1 and TaHSP90-Chr4 based on the deduced protein sequence revealed that they are most closely related to that of HSP90 of *T.parva*, *T.orientalis* and *B. bovis* (Figure 27). Several studies have been performed to draw relationships across all HSP90 family members. However, due to the lack of genome-wide information and the limited number of sequences used for the determination of the phylogenetic relationships, this issue is still not completely solved (Chen *et al.*, 2006). Apparently, HSP90 is playing an important role in the folding of proteins and refolding of denatured proteins after stress across all eukaryotic cells (Pallavi *et al.*, 2010). Thereby, HSP90s from these organisms share a significant homology at the level of their primary structures, which is reflected in their function. Moreover, the overall amino acid sequence homology of members of the HSP90 family may reach 90% in certain conserved regions (Gerhards *et al.*, 1994).

Bioinformatic analysis of the protein sequence revealed the existence of ATP binding pocket in TaHSP90-Chr1 and TaHSP90-Chr4 (data not shown), which represents an important part for HSP90 activity (Young *et al.*, 2001). Moreover, the analysis of TaHSP90-Chr1 predicted a molecular mass of 55.9 kDa for the HSP90 domain, which is in agreement with the size of the expressed recombinant domain as detected by immunoblot analysis. Although, the analysis of TaHSP90-Chr4 predicted a molecular mass of 60.5 kDa for the HSP90 domain, the open read frame (ORF) of TaHSP90-Chr4 was expressed in order to test the ability of anti-*T. annulata* HSP90 antiserum to detect this isoform.

A theoretical molecular mass of TaHSP90-Chr4 protein (ORF) was 105.5 kDa, while the recombinant protein size as detected by immunoblot was approximately 170 kDa. This phenomenon was also reported in *T. annulata* surface protein (TaSP), which has a high amount of dipeptide repeats containing proline (X-Pro, especially Glu-Pro and Lys-Pro), which may lead to a retarded migration during electrophoresis (Brewer *et al.*, 1990). However, TaHSP90-Chr4 does not contain a high amount of dipeptide repeats, and the reasons for the retarded migration in SDS gel remain to be elucidated.

## 5.5 Detection of *T.annulata* HSP90 and bovine HSP90

The high degree of homology between bovine HSP90 and human HSP90 (Figure 43) gave a strong motive to use anti-human HSP 90 $\alpha/\beta$  as a specific antibody for bovine HSP90. Our results indicate that anti-human HSP 90 $\alpha/\beta$  can recognize bovine HSP90 in Western blots and also in indirect fluorescent antibody test. Interestingly, this antibody does not react with *T. annulata* HSP90.

Regarding *T.annulata* HSP90, an anti-serum against *T. annulata* HSP90 was generated by immunization of rabbits with a synthetic peptide ELEKVKAVKEEKEWN. The anti-*T. annulata* HSP90 anti-serum reacted strongly with a TaHSP90-Chr1 recombinant protein, indicating the efficiency of the immunization and the specificity of the immune serum. However, attempts to use this anti-serum to detect the native protein from lysates of *T. annulata* Ankara 288-infected cells or by using confocal microscopy were unsuccessful. Failure to detect the native protein could be due to a low amount of the protein in cell lysates compared with the recombinant protein or that the native protein normally present in a tertiary structure which might lead to difficulty in binding of the anti-*T. annulata* HSP90 anti-serum to small recognition site amino acids: ELEKVKAVKEEKEWN. Despite the high

similarity of the antigenic peptide sequences and the corresponding sequence in TaHSP90-Chr4, detection of this isoform was not successful using the anti-*T. annulata* HSP90 anti-serum.

## 5.6 Novobiocin

As mentioned in the preceding section, anti-*T. annulata* HSP90 anti-serum failed to detect *T.annulata* HSP90. Therefore, novobiocin was used as an alternative tool to distinguish between bovine HSP90 and *T.annulata* HSP90. Novobiocin inhibits HSP90 through binding to amino acids 538-728 of HSP90 (Marcu *et al.*, 2000). Furthermore, removal of amino acids 657-677 from the 538-728 of fragment resulted in a decline in novobiocin binding to HSP90. The alignment of this sequence (amino acids 657-677 of HSP90) with bovine HSP90 and *T.annulata* HSP90 showed 95% and 19% identity, respectively. This finding gave a strong motive to use novobiocin as a specific inhibitor of bovine HSP90.

Indeed, in my study novobiocin treatment killed the parasite in *T. annulata* Ankara 288-infected cells (Figure 37). Novobiocin has been reported to act as an inhibitor of bacterial DNA gyrase, particular gyraseB (GyrB) subunit (Maxwell, 1999). Although DNA gyrase commonly exists in prokaryotes, some studies show the presence of bacterial-like DNA gyrase activity in apicomplexan protozoa (García-Estrada *et al.*, 2010). In an vitro study, novobiocin was able to inhibit *P. falciparum* GyrB ATPase activity and to kill the parasite (Raghu Ram *et al.*, 2007). I suppose that novobiocin likewise uses a similar mechanism in *T. annulata* Ankara 288-infected cells. However, further investigations are required to proof this hypothesis.

---

## 5.7 Conclusion

*Theileria* parasites are obligate intracellular pathogens and are unique in their capacity to induce the transformation of their host cells, which acquire some characteristics of cancer cells such as clonal expansion and metastasis. Although, a number of parasite and host cell molecules have been identified which might be involved in this cell transformation, the exact mechanisms(s) are still unknown.

In the present study, the possible role of HSP90 in cell survival and parasite stage differentiation was investigated. It was found that treatment of parasitized cells with an HSP90 inhibitor, GA, led to host cell cycle arrest and apoptosis in a dose- and time-dependent manner.

After treatment with GA, the number of the cells undergoing merogony increased in *T. annulata* Ankara 288-infected cells regardless of the incubation temperature, albeit much stronger at 41°C.

The expression level of TaHSP90-Chr1 mRNA and TaHSP90-Chr4 mRNA differed in relation to the incubation temperature. Thus, while the mRNA of both parasite HSP90 isoforms were slightly, but not significantly up-regulated after GA treatment at 37°C, there was a significant decrease in the expression level of TaHSM90-Chr1 and TaHSP90-Chr4 in cells incubated with GA at 41°C. This surprising finding probably has a direct association with the release of the parasite from host cell after differentiation process.

Taken together, HSP90 seems to play an important role, at least, in the maintenance of host cell transformation, as its inhibition by GA results in host cell arrest and apoptosis. However, its role in the process of parasite stage differentiation needs more investigations.

Another interesting finding was that treating of the infected cells with novobiocin resulted in the killing of the parasites and in apoptotic morphological changes in the host cells. This substance may have potential as a novel drug against *Theileria*.

## 6 Summary

*Theileria annulata* is an obligate intracellular parasite that causes great health problems in cattle and domestic buffalo in tropical and subtropical areas. The parasite is transmitted transstadially by several species of *Hyalomma* ticks.

*T. annulata* has a unique ability to transform and to induce a permanent proliferation of bovine leukocytes in a similar manner as tumor cells do. Among others, this transformation results in clonal expansion and metastasis of the infected cells in various organs of the affected animal. The mechanism (s) underlying the transformation process is still not entirely clear.

However, in the last years, it has been found that a number of genes are involved in the regulation of cell proliferation and / or apoptosis such as NF- $\kappa$ B, PI-3k/Akt and Heat shock proteins (HSPs). Moreover, HSP90 has been shown to be involved in the host cell proliferation/apoptosis as well as in stage differentiation of parasites.

Accordingly, this work was designed:

- i) To investigate the functional role of HSP90 in the maintenance of the cell viability and proliferation
- ii) To analyse the differential expression profile of HSP90 in *T. annulata* Ankara 288-infected cells under stress conditions
- iii) To investigate the role of HSP90 during the developmental stages of the parasite.

In a number of studies, geldanamycin (GA) was used to inhibit the HSP90 function in cell proliferation and survival. In the present work, I also used this drug to dissect a possible impact of the HSP90 on the host-parasite interaction in *Theileria*-transformed bovine cells.

As a first step, the effect of HSP90 inhibition by GA on the cell viability was examined at 37°C by Trypan blue test. The percentages of dead cells were determined and was less than 20% in the cells incubated with GA (0.5  $\mu$ M or 1 $\mu$ M) for 1 day, while this percentage increased up to 66% after 2 days. The treatment with GA  $\geq$  5 $\mu$ M showed more than 60% of dead cells after 1 day and increased up to 100% after 2 days. The flow cytometric assays for

apoptosis was carried out on one hand, to verify the previous result and on the other hand, to investigate the effect of GA (0.001 $\mu$ M-0.5 $\mu$ M) at 37°C and 41°C. The analysis revealed that GA induced significant apoptosis in *T. annulata* Ankara 288- infected cells in a dose- and time- dependent manner. The effect of GA depended also on the incubation temperature, where low concentrations of GA could significantly induce apoptosis at 41°C.

These findings were confirmed by the immunofluorescence staining of host cell p53 as a great accumulation of p53 was observed in the host cell nucleus after treatment with GA.

The cell proliferation analysis by flow cytometry showed a significant reduction in the cell proliferation after treatment with GA  $\geq$  0.05  $\mu$ M for 3 days, while after 6 days incubation at 37°C only GA  $\geq$  0.25  $\mu$ M has a similar effect.

The effect of HSP90 inhibition on the parasite differentiation in *T. annulata* Ankara 288- infected cells was evaluated by using two different methods. The first method was immunofluorescence staining using specific antibodies against TamS1 and TamR1, which can detect those cells in which schizonts differentiate to merozoites. The qRT-PCR was applied as another method to evaluate the expression level of TamR1 gene during the parasite differentiation. Both methods revealed that the number of the cells undergoing merogony increased in *T. annulata* Ankara 288-infected cells after GA treatment regardless of the incubation temperature.

The regulation of bovine HSP90 genes (BHSP90-alpha and BHSP90-beta) and *T. annulata* HSP90 genes (TaHSP90-Chr1 and TaHSP90-Chr4) in *T. annulata* Ankara 288-infected cells was evaluated by qRT-PCR. The qRT-PCR analysis showed that the mRNA expression levels of BHSP90-alpha and BHSP90-beta were significantly up-regulated after treatment with GA in a dose- and time dependent manner. In agreement with a previous result, the expression levels of TaHSP90-Chr1 mRNA and TaHSP90-Chr4 mRNA were slightly up-regulated after GA treatment at 37°C. An interesting finding was the significant decrease in the expression level of TaHSM90-Chr1 and TaHSP90-Chr4 in the cells incubated with GA at 41°C. This variance raised an important requirement for tools to distinguish between *T. annulata* HSP90 and bovine HSP90.

As mentioned above, reference sequences of two isoforms of *T. annulata* HSP90 were found and named TaHSP90-Chr1 and TaHSP90-Chr4. Characterization of TaHSP90-Chr1 and TaHSP90-Chr4 gene and its protein forms was carried out using molecular biological

methods and bioinformatic analysis. Phylogenetic tree analysis indicated that TaHSP90-Chr1 and TaHSP90-Chr4 are more closely related to HSP90 from *Theileria* species and *B. bovis* than to HSP90 from human or bovine. Both TaHSP90-Chr1 and TaHSP90-Chr4 showed most of the characteristics reported for HSP90 e.g. the presence of ATP sequence, the presence of the functional HSP domain and the existence of a signal sequence located in the N-terminal sequence of the TaHSP90-Chr1 and TaHSP90-Chr4.

Antigenic peptides were deduced from the sequence of TaHSP90-Chr1 and TaHSP90-Chr4 using the predication server Predicting Antigenic Peptides (<http://imed.med.ucm.es/Tools/antigenic.pl>). The selected peptide was synthesized and used to immunize two rabbits. However, the anti- *T. annulata* HSP90 antiserum failed to recognize *T. annulata* HSP90 (native protein).

Regarding bovine HSP90, immunoblotting staining carried out using anti-human HSP 90 $\alpha$ / $\beta$  (HSP 90 $\alpha$ / $\beta$  (F-8): sc-13119, Santa Cruz) showed the ability of anti-human HSP 90 $\alpha$ / $\beta$  to detect bovine HSP90 in the cell lysates. Moreover, the immunofluorescence staining of *T.annulata* Ankara 288-infected cells showed the specificity of this antibody.

Novobiocin was used as an alternative method to distinguish between the role of bovine HSP90 and *T. annulata* HSP90. Although, novobiocin was utilized as a specific inhibitor of bovine HSP90, the novobiocin treatment resulted in death of the parasites also. Whether this was a direct effect on the parasite or rather on the host cell is not clear.

Nevertheless, the results of this study showed that the inactivation of HSP90 in *T. annulata* Ankara 288-infected cells leads to cell cycle arrest, apoptosis and differentiation of the schizonts to merozoites.

## 7 Zusammenfassung

### **Die Rolle des Hitze-Schock-Proteins 90 (HSP90) in der Transformation von *T. annulata*-infizierten Zellen und der Differenzierung von Parasiten-Stadien.**

*Theileria annulata* gehört zu den lymphoproliferativen Theilerien des Rindes. Der Parasit wird durch Hyalomma-Zecken transstadial übertragen und verursacht bei Tieren die Tropische Theileriose in subtropischen und tropischen Regionen.

Eine wichtige Eigenschaft dieser Erkrankung ist die unkontrollierte Proliferation/Transformation der befallenen Leukozyten infizierter Wirte, die einige Eigenschaften der Tumorzellen erlangen, wie z. B. „Clonal Expansion“ und „Metastasis“ der infizierten Zellen in verschiedenen Organen des betroffenen Wirtes. Die der Transformation der Wirtszellen zugrunde liegenden molekularen Mechanismen sind noch weitgehend ungeklärt.

In den letzten Jahren wurden einige Wirts- und Parasitenmoleküle identifiziert, die möglicherweise an der Wirtszellproliferation bzw. -apoptose beteiligt sind, wie zB. NF $\kappa$ B und P53. Es wird zunehmend auf die Rolle der Hitzeschockproteine (HSP) bei der Regulation der Zellapoptose hingewiesen. Darüber hinaus wird über die Bedeutung von HSP90 bei der Differenzierung bestimmter Parasitenstadien berichtet.

Die Hauptziele der vorliegenden Doktorarbeit waren:

- i) Die Rolle von HSP90 bei der Aufrechterhaltung der Vitalität und Proliferation *T. annulata*-infizierter Zellen zu untersuchen,
- ii) das Expressionsprofil von HSP90 unter Stressbedingungen in *T. annulata*-infizierten Zellen zu analysieren und
- iii) die Bedeutung von HSP90 bei der Differenzierung der Schizonten zu Merozoiten zu klären.

In eine Reihe von Untersuchungen wurde Geldanamycin (GA) benutzt, um die Funktion von HSP90 zu inhibieren und dessen Einfluss auf Proliferation und Vitalität der Zellen zu untersuchen. In der vorliegenden Arbeit wurde GA auch verwendet, um einen möglichen Einfluss von HSP90 auf die Wirt-Parasiten-Interaktion in *Theileria*-transformierten bovinen Zellen zu untersuchen.

Zu nächst wurden die parasitenhaltigen Zellen mit verschiedenen Konzentrationen von Geldanamycin (GA) behandelt und anschließend für unterschiedliche Zeiten bei 37°C inkubiert. Der Effekt wurde mit dem Trypan-Blau-Test untersucht.

Bei einer GA Konzentration von 0.5 µM und 1µM und einer Inkubationszeit von einem Tag bei 37°C, lag der prozentuale Anteil toter Zellen bei weniger als 20%. Diese Zahl stieg jedoch breits nach zwei Tagen auf 66%. Mehr als 60% der für einen Tag mit  $\geq 5\mu\text{M}$  GA behandelten Zellen waren tot. Bei einer Verlängerung der Inkubationszeit auf 2 Tage waren alle Zellen abgestorben.

Zur Klärung der Frage, ob die Apoptose ursächlich für den Tod der Zellen verantwortlich ist, wurde eine Durchfluss-Zytometrie zur Erfassung apoptotischer Zellen durchgeführt. Darüber hinaus wurde das gleiche Verfahren zur Untersuchung des Effektes von geringeren Konzentrationen von GA (0.001 µM-0.5 µM) bei 37°C und 41°C eingesetzt. Die Analyse der erzielten Ergebnisse zeigte, dass GA die Apoptose in *T. annulata* Ankara288-infizierten Zellen in Abhängigkeit von Dosis und Inkubationszeit signifikant induzieren kann. Der Effekt von GA hing dabei auch von der Inkubationstemperatur ab, wobei auch niedrige Konzentrationen von GA bei 41°C eine Apoptose signifikant induzieren konnten.

Diese Ergebnisse wurden durch eine Immunofluoreszenz-Färbung des Wirtszellproteins p53 bestätigt. Hierbei wurde eine hohe Akkumulation von p53 im Wirtszellkern nach der Behandlung mit GA nachgewiesen.

Die Analyse der Zellproliferation mit Hilfe der Durchfluss-Zytometrie zeigte eine signifikante Reduzierung der Zellproliferation nach der Behandlung mit  $\text{GA} \geq 0.05\mu\text{M}$  für 3 Tage. Ein ähnlicher Effekt wurde mit einer Inkubationszeit von 6 Tagen und einer Konzentration von  $\text{GA} \geq 0.25\mu\text{M}$  erzielt.

Der Effekt von HSP90 auf die Differenzierung der Parasitenstadien wurde mit Hilfe zweier Methoden untersucht. So wurde zum einen eine Immunofluoreszenz-Färbung mit den spezifischen Merozoiten-Markern TamS1 und TamR1 durchgeführt. Zum anderen wurde eine qRT-PCR zur Bestimmung der Höhe der Genexpression von TamR1 durchgeführt. Beide Methoden zeigten, dass die Anzahl der Zellen in Merogonie nach der Behandlung mit GA steigt, unabhängig von der Inkubationstemperatur.

Die Regulation des bovinen HSP90-Gens (BHSP90-alpha und BHSP90-beta) sowie des *T. annulata* HSP90-Gens (TaHSP90-Chr1 und TaHSP90-Chr4) wurde mit Hilfe einer qRT-PCR evaluiert. Beide Isoformen des bovinen Gens zeigten eine signifikante Hochregulation nach der Behandlung mit GA in einer konzentrations- und inkubationszeitabhängigen Weise.

Die Expression der TaHSP90-Chr1 mRNA und TaHSP90-Chr4 mRNA war auch von der Inkubationstemperatur abhängig. Während die Expression der mRNA beider Parasiten-HSP90-Isoformen nach der Behandlung der Zellen mit GA bei 37°C leicht, jedoch nicht signifikant hochreguliert war, nahm die Expression der mRNA dieser Gene bei 41°C signifikant ab. Dieses überraschende Ergebnis kann möglicherweise mit der Freisetzung der Parasiten aus den Wirtszellen während der Differenzierung der Schizonten zu Merozoiten assoziiert sein.

Die Charakterisierung der TaHSP90-Chr1 und TaHSP90-Chr4 Gen- und Proteinformen wurde mittels molekularer Methoden sowie mit Hilfe bioinformatischer Analysen durchgeführt. Eine Analyse der Phylogenie deutete darauf hin, dass beide Isoformen mit dem HSP90 von *Theileria annulata* und *Babesia ovis* näher verwandt sind als mit dem humanen bzw. dem bovinen HSP90. Beide hier untersuchten Isoformen zeigten die Eigenschaften von HSP90, wie z. B. die Anwesenheit einer ATP-Sequenz, die Anwesenheit einer funktionalen HSP-Domäne sowie die Existenz einer Signal-Sequenz in der N-terminalen Sequenz.

Antigene Peptide wurden mit Hilfe der Internetseite „Predicting Antigenic Peptides“ (<http://imed.med.ucm.es/Tools/antigenic.pl>) aus der Sequenz von TaHSP90-Chr1 und TaHSP90-Chr4 abgeleitet. Die selektierten Peptide wurden synthetisiert und genutzt, um zwei Kaninchen zu immunisieren. Leider erkannte das anti-*T. annulata* HSP90-Antiserum das native HSP90 Protein nicht.

In Bezug auf das bovine HSP90 wurde eine Immunoblot-Färbung unter Verwendung des anti-humanen HSP90 $\alpha/\beta$  (HSP 90 $\alpha/\beta$  (F-8): sc-13119, Santa Cruz) durchgeführt. Hier wurde gezeigt, dass ein Antiserum gegen das humane HSP 90 $\alpha/\beta$  das bovine HSP90 im Zelllysat detektieren kann. Darüber hinaus wurde die Spezifität dieses Antikörpers nachgewiesen.

Als alternative Methode für die Unterscheidung zwischen dem Einfluss des bovinen und des *T-annulata* HSP90 wurde Novobiocin herangezogen. Obwohl Novobiocin als spezifischer Inhibitor des bovinen HSP90 eingesetzt wird, zeigte sich nach der Behandlung mit Novobiocin jedoch, dass auch die Parasiten starben. Ob Novobiocin jedoch einen direkten Einfluss auf den Parasiten hat, oder dieser Effekt mit dem Tod der Wirtszellen zusammenhängt, ist jedoch unklar.

Zusammenfassend zeigen die Ergebnisse der vorliegenden Doktorarbeit, dass die Inaktivierung der Funktion von HSP90 durch Geldanamycin zu Zellzyklusarrest, Apoptose und möglicherweise zur Differenzierung der Schizonten zu Merozoiten in *T. annulata* Ankara 288-infizierten Wirtszellen führt.

## 8 Reference

- Ahmed, J.S., Glass, E.J., Salih, D.A., and Seitzer, U. (2008). Innate immunity to tropical theileriosis. *Innate Immun.* **14**, 5–12.
- Ahmed, J.S., and Mehlhorn, H. (1999). Review: the cellular basis of the immunity to and immunopathogenesis of tropical theileriosis. *Parasitol. Res.* **85**, 539–549.
- Ahmed, J.S., Rothert, M., Steuber, S., and Schein, E. (1989). In vitro proliferative and cytotoxic responses of PBL from *Theileria annulata*-immune cattle. *J. Vet. Med. B.* **36**, 584–592.
- Akarid, K., Arnoult, D., Micic-Polianski, J., Sif, J., Estaquier, J., and Ameisen, J.C. (2004). *Leishmania major*-mediated prevention of programmed cell death induction in infected macrophages is associated with the repression of mitochondrial release of cytochrome c. *J. Leukoc. Biol.* **76**, 95–103.
- Alenzi, F.Q.B. (2004). Links between apoptosis, proliferation and the cell cycle. *Br. J. Biomed. Sci.* **61**, 99–102.
- Ameyar, M., Wisniewska, M., and Weitzman, J.B. (2003). A role for AP-1 in apoptosis: the case for and against. *Biochimie.* **85**, 747–752.
- Atkinson, E.A., Barry, M., Darmon, A.J., Shostak, I., Turner, P.C., Moyer, R.W., and Bleackley, R.C. (1998). Cytotoxic T lymphocyte-assisted suicide. Caspase 3 activation is primarily the result of the direct action of granzyme B. *J. Biol. Chem.* **273**, 21261–21266.
- Bakheit, M.A., Endl, E., Ahmed, J.S., and Seitzer, U. (2006). Purification of macroschizonts of a Sudanese isolate of *Theileria lestoquardi* (*T. lestoquardi* [Atbara]). *Ann. N. Y. Acad. Sci.* **1081**, 453–462.
- Banumathy, G., Singh, V., Pavithra, S.R., and Tatu, U. (2003). Heat Shock Protein 90 Function Is Essential for *Plasmodium falciparum* Growth in Human Erythrocytes. *J. Biol. Chem.* **278**, 18336–18345.
- Baumgartner, M., Chaussepied, M., Moreau, M.F., Werling, D., Davis, W.C., Garcia, A., and Langsley, G. (2000). Constitutive PI3-K activity is essential for proliferation, but not survival, of *Theileria parva*-transformed B cells. *Cell. Microbiol.* **2**, 329–339.
- Bielefeldt Ohmann, H., Campos, M., Snider, M., Rapin, N., Beskorwayne, T., Popowych, Y., Lawman, M.J., Rossi, A., and Babiuk, L.A. (1989). Effect of chronic administration of recombinant bovine tumor necrosis factor to cattle. *Vet. Pathol.* **26**, 462–472.
- Bishop, R., Musoke, A., Morzaria, S., Gardner, M., and Nene, V. (2004). *Theileria*: intracellular protozoan parasites of wild and domestic ruminants transmitted by ixodid ticks. *Parasitology.* **129** Suppl, S271–S283.

- Bonnefoy, S., Attal, G., Langsley, G., Tekai, F., and Mercereau-Puijalon, O. (1994). Molecular characterization of the heat shock protein 90 gene of the human malaria parasite *Plasmodium falciparum*. *Mol. Biochem. Parasitol.* **67**, 157–170.
- Borkovich, K.A., Farrelly, F.W., Finkelstein, D.B., Taulien, J., and Lindquist, S. (1989). hsp82 is an essential protein that is required in higher concentrations for growth of cells at higher temperatures. *Mol. Cell. Biol.* **9**, 3919–3930.
- Botteron, C., and Dobbelaere, D. (1998). AP-1 and ATF-2 are constitutively activated via the JNK pathway in *Theileria parva*-transformed T-cells. *Biochem. Biophys. Res. Commun.* **246**, 418–421.
- Brewer, S., Tolley, M., Trayer, I.P., Barr, G.C., Dorman, C.J., Hannavy, K., Higgins, C.F., Evans, J.S., Levine, B.A., and Wormald, M.R. (1990). Structure and function of X-Pro dipeptide repeats in the TonB proteins of *Salmonella typhimurium* and *Escherichia coli*. *J. Mol. Biol.* **216**, 883–895.
- Broemer, M., Krappmann, D., and Scheidereit, C. (2004). Requirement of Hsp90 activity for I $\kappa$ B kinase (IKK) biosynthesis and for constitutive and inducible IKK and NF- $\kappa$ B activation. *Oncogene.* **23**, 5378–5386.
- Brown, D.J., Campbell, J.D., Russell, G.C., Hopkins, J., and Glass, E.J. (1995). T cell activation by *Theileria annulata*-infected macrophages correlates with cytokine production. *Clin. Exp. Immunol.* **102**, 507–514.
- Buchner, J. (1999). Hsp90 & Co. - a holding for folding. *Trends Biochem. Sci.* **24**, 136–141.
- Bujard, H., Gentz, R., Lanzer, M., Stueber, D., Mueller, M., Ibrahimi, I., Haeuptle, M.T., and Dobberstein, B. (1987). A T5 promoter-based transcription-translation system for the analysis of proteins in vitro and in vivo. *Methods Enzymol.* **155**, 416–433.
- Campbell, J.D., Howie, S.E., Odling, K.A., and Glass, E.J. (1995). *Theileria annulata* induces aberrant T cell activation in vitro and in vivo. *Clin. Exp. Immunol.* **99**, 203–210.
- Campbell, J.D.M., Brown, D.J., Nichani, A.K., Howie, S.E.M., Spooner, R.L., and Glass, E.J. (1997). A non-protective T helper 1 response against the intra-macrophage protozoan *Theileria annulata*. *Clin. Exp. Immunol.* **108**, 463–470.
- Chaussepied, M., and Langsley, G. (1996). *Theileria* transformation of bovine leukocytes: a parasite model for the study of lymphoproliferation. *Res. Immunol.* **147**, 127–138.
- Chen, B., Piel, W.H., Gui, L., Bruford, E., and Monteiro, A. (2005). The HSP90 family of genes in the human genome: insights into their divergence and evolution. *Genomics* **86**, 627–637.
- Chen, B., Zhong, D., and Monteiro, A. (2006). Comparative genomics and evolution of the HSP90 family of genes across all kingdoms of organisms. *BMC Genomics.* **7**, 156.

- Chuenkova, M.V., and Pereira, M.A. (2000). A trypanosomal protein synergizes with the cytokines ciliary neurotrophic factor and leukemia inhibitory factor to prevent apoptosis of neuronal cells. *Mol. Biol. Cell.* **11**, 1487–1498.
- Ciocca, D.R., and Calderwood, S.K. (2005). Heat shock proteins in cancer: diagnostic, prognostic, predictive, and treatment implications. *Cell Stress Chaperones.* **10**, 86–103.
- Conroy, S.E., and Latchman, D.S. (1996). Do heat shock proteins have a role in breast cancer? *Br. J. Cancer.* **74**, 717–721.
- Csermely, P., Schnaider, T., Soti, C., Prohászka, Z., and Nardai, G. (1998). The 90-kDa molecular chaperone family: structure, function, and clinical applications. A comprehensive review. *Pharmacol. Ther.* **79**, 129–168.
- Datta, S.R., Dudek, H., Tao, X., Masters, S., Fu, H., Gotoh, Y., and Greenberg, M.E. (1997). Akt phosphorylation of BAD couples survival signals to the cell-intrinsic death machinery. *Cell.* **91**, 231–241.
- De Andrade, C.R., Kirchhoff, L.V., Donelson, J.E., and Otsu, K. (1992). Recombinant *Leishmania* Hsp90 and Hsp70 are recognized by sera from visceral leishmaniasis patients but not Chagas' disease patients. *J. Clin. Microbiol.* **30**, 330–335.
- Dobbelaere, D., and Heussler, V. (1999). Transformation of leukocytes by *Theileria parva* and *T. annulata*. *Annu. Rev. Microbiol.* **53**, 1–42.
- Dobbelaere, D.A., Fernandez, P.C., and Heussler, V.T. (2000). *Theileria parva*: taking control of host cell proliferation and survival mechanisms. *Cell. Microbiol.* **2**, 91–99.
- Dobbelaere, D.A.E., and Küenzi, P. (2004). The strategies of the *Theileria* parasite: a new twist in host-pathogen interactions. *Curr. Opin. Immunol.* **16**, 524–530.
- Dolan, T.T. (1989). Theileriosis : a comprehensive review. *Rev Sci Tech Int Epizoot.* **8**, 11–36.
- D' Oliveira, C., van der Weide, M., Habela, M.A., Jacquiet, P., and Jongejan, F. (1995). Detection of *Theileria annulata* in blood samples of carrier cattle by PCR. *J. Clin. Microbiol.* **33**, 2665–2669.
- Downward, J. (1998). Mechanisms and consequences of activation of protein kinase B/Akt. *Curr. Opin. Cell Biol.* **10**, 262–267.
- Echeverria, P.C., Figueras, M.J., Vogler, M., Kriehuber, T., de Miguel, N., Deng, B., Dalmasso, M.C., Matthews, D.E., Matrajt, M., Haslbeck, M., Buchner, J., and Angel, S.O. (2010). The Hsp90 co-chaperone p23 of *Toxoplasma gondii*: Identification, functional analysis and dynamic interactome determination. *Mol. Biochem. Parasitol.* **172**, 129–140.

- Echeverria, P.C., Matrajt, M., Harb, O.S., Zappia, M.P., Costas, M.A., Roos, D.S., Dubremetz, J.F., and Angel, S.O. (2005). *Toxoplasma gondii* Hsp90 is a potential drug target whose expression and subcellular localization are developmentally regulated. *J. Mol. Biol.* **350**, 723–734.
- Eichhorn, M., and Dobbelaere, D.A. (1994). Induction of signal transduction pathways in lymphocytes infected by *Theileria parva*. *Parasitol. Today.* **10**, 469–472.
- Fawcett, D.W., Conrad, P.A., Grootenhuis, J.G., and Morzaria, S.P. (1987). Ultrastructure of the intra-erythrocytic stage of *Theileria* species from cattle and waterbuck. *Tissue Cell.* **19**, 643–655.
- Forsyth, L.M., Minns, F.C., Kirvar, E., Adamson, R.E., Hall, F.R., McOrist, S., Brown, C.G., and Preston, P.M. (1999). Tissue damage in cattle infected with *Theileria annulata* accompanied by metastasis of cytokine-producing, schizont-infected mononuclear phagocytes. *J. Comp. Pathol.* **120**, 39–57.
- García-Estrada, C., Prada, C.F., Fernández-Rubio, C., Rojo-Vázquez, F., and Balaña-Fouce, R. (2010). DNA topoisomerases in apicomplexan parasites: promising targets for drug discovery. *Proc. Biol. Sci.* **277**, 1777–1787.
- García-Morales, P., Carrasco-García, E., Ruiz-Rico, P., Martínez-Mira, R., Menéndez-Gutiérrez, M.P., Ferragut, J.A., Saceda, M., and Martínez-Lacaci, I. (2007). Inhibition of Hsp90 function by ansamycins causes downregulation of cdc2 and cdc25c and G(2)/M arrest in glioblastoma cell lines. *Oncogene.* **26**, 7185–7193.
- Gerhards, J., Ebel, T., Dobbelaere, D.D., Morzaria, S.P., Musoke, A.J., Williams, R.O., and Lipp, J. (1994). Sequence and expression of a 90-kilodalton heat-shock protein family member of *Theileria parva*. *Mol. Biochem. Parasitol.* **68**, 235–246.
- Gesbert, F., Sellers, W.R., Signoretti, S., Loda, M., and Griffin, J.D. (2000). BCR/ABL Regulates Expression of the Cyclin-dependent Kinase Inhibitor p27Kip1 through the Phosphatidylinositol 3-Kinase/AKT Pathway. *J. Biol. Chem.* **275**, 39223–39230.
- Glass, E.J. (2001). The balance between protective immunity and pathogenesis in tropical theileriosis: what we need to know to design effective vaccines for the future. *Res. Vet. Sci.* **70**, 71–75.
- Glass, E.J., Craigmile, S.C., Springbett, A., Preston, P.M., Kirvar, E., Wilkie, G.M., Eckersall, P.D., Hall, F.R., and Brown, C.G.D. (2003). The protozoan parasite, *Theileria annulata*, induces a distinct acute phase protein response in cattle that is associated with pathology. *Int. J. Parasitol.* **33**, 1409–1418.
- Graefe, S.E.B., Wiesgigl, M., Gaworski, I., Macdonald, A., and Clos, J. (2002). Inhibition of HSP90 in *Trypanosoma cruzi* induces a stress response but no stage differentiation. *Eukaryot. Cell.* **1**, 936–943.

- Grover, A., Shandilya, A., Agrawal, V., Pratik, P., Bhasme, D., Bisaria, V.S., and Sundar, D. (2011). Hsp90/Cdc37 chaperone/co-chaperone complex, a novel junction anticancer target elucidated by the mode of action of herbal drug Withaferin A. *BMC Bioinformatics*. **12** Suppl 1, S30.
- Gupta, R.S. (1995). Phylogenetic analysis of the 90 kD heat shock family of protein sequences and an examination of the relationship among animals, plants, and fungi species. *Mol. Biol. Evol.* **12**, 1063–1073.
- Haller, D., Mackiewicz, M., Gerber, S., Beyer, D., Kullmann, B., Schneider, I., Ahmed, J.S., and Seitzer, U. (2010). Cytoplasmic sequestration of p53 promotes survival in leukocytes transformed by *Theileria*. *Oncogene*. **29**, 3079–3086.
- Heussler, V.T. (2002). *Theileria* survival strategies and host cell transformation In: *Theileria*, Dobbelaere DAE, McKeever DJ (eds) World Class Parasites, Kluwer, Boston, London, pp. 69–84.
- Heussler, V.T., Küenzi, P., Fraga, F., Schwab, R.A., Hemmings, B.A., and Dobbelaere, D.A. (2001a). The Akt/PKB pathway is constitutively activated in *Theileria*-transformed leucocytes, but does not directly control constitutive NF-kappaB activation. *Cell. Microbiol.* **3**, 537–550.
- Heussler, V.T., Küenzi, P., and Rottenberg, S. (2001b). Inhibition of apoptosis by intracellular protozoan parasites. *Int. J. Parasitol.* **31**, 1166–1176.
- Heussler, V.T., Machado, J., Fernandez, P.C., Botteron, C., Chen, C.G., Pearse, M.J., and Dobbelaere, D.A.E. (1999). The intracellular parasite *Theileria parva* protects infected T cells from apoptosis. *Proc. Natl. Acad. Sci. USA*. **96**, 7312–7317.
- Hippe, D., Lytovchenko, O., Schmitz, I., and Lüder, C.G.K. (2008). Fas/CD95-mediated apoptosis of type II cells is blocked by *Toxoplasma gondii* primarily via interference with the mitochondrial amplification loop. *Infect. Immun.* **76**, 2905–2912.
- Hisaeda, H., Sakai, T., Ishikawa, H., Maekawa, Y., Yasutomo, K., Good, R.A., and Himeno, K. (1997). Heat shock protein 65 induced by gammadelta T cells prevents apoptosis of macrophages and contributes to host defense in mice infected with *Toxoplasma gondii*. *J. Immunol.* **159**, 2375–2381.
- Innes, E.A., Millar, P., Brown, C.G., and Spooner, R.L. (1989). The development and specificity of cytotoxic cells in cattle immunized with autologous or allogeneic *Theileria annulata*-infected lymphoblastoid cell lines. *Parasite Immunol.* **11**, 57–68.
- Johnson, J.L., and Brown, C. (2009). Plasticity of the Hsp90 chaperone machine in divergent eukaryotic organisms. *Cell Stress Chaperones*. **14**, 83–94.
- Kerr, J.F., Wyllie, A.H., and Currie, A.R. (1972). Apoptosis: a basic biological phenomenon with wide-ranging implications in tissue kinetics. *Br. J. Cancer*. **26**, 239–257.
- Kim, H.R., Lee, C.H., Choi, Y.H., Kang, H.S., and Kim, H.D. (1999). Geldanamycin induces cell cycle arrest in K562 erythroleukemic cells. *IUBMB Life*. **48**, 425–428.

- Kim, J.Y., Ahn, M.H., Jun, H.S., Jung, J.W., Ryu, J.S., and Min, D.Y. (2006). *Toxoplasma gondii* inhibits apoptosis in infected cells by caspase inactivation and NF-kappaB activation. *Yonsei Med. J.* **47**, 862–869.
- Kischkel, F.C., Hellbardt, S., Behrmann, I., Germer, M., Pawlita, M., Krammer, P.H., and Peter, M.E. (1995). Cytotoxicity-dependent APO-1 (Fas/CD95)-associated proteins form a death-inducing signaling complex (DISC) with the receptor. *EMBO J.* **14**, 5579–5588.
- Kolaskar, A.S., and Tongaonkar, P.C. (1990). A semi-empirical method for prediction of antigenic determinants on protein antigens. *FEBS Lett.* **276**, 172–174.
- Kroemer, G., Galluzzi, L., and Brenner, C. (2007). Mitochondrial membrane permeabilization in cell death. *Physiol. Rev.* **87**, 99–163.
- Laemmli, U.K. (1970). Cleavage of structural proteins during the assembly of the head of bacteriophage T4. *Nature.* **227**, 680–685.
- Latchman, D.S. (2001). Heat shock proteins and cardiac protection. *Cardiovasc. Res.* **51**, 637–646.
- Lawlor, M.A., and Alessi, D.R. (2001). PKB/Akt: a key mediator of cell proliferation, survival and insulin responses? *J. Cell Sci.* **114**, 2903–2910.
- Lee, H.H., Dadgostar, H., Cheng, Q., Shu, J., and Cheng, G. (1999). NF-kappaB-mediated up-regulation of Bcl-x and Bfl-1/A1 is required for CD40 survival signaling in B lymphocytes. *Proc. Natl. Acad. Sci. USA.* **96**, 9136–9141.
- Leirião, P., Albuquerque, S.S., Corso, S., van Gemert, G.J., Sauerwein, R.W., Rodriguez, A., Giordano, S., and Mota, M.M. (2005). HGF/MET signalling protects *Plasmodium*-infected host cells from apoptosis. *Cell. Microbiol.* **7**, 603–609.
- Levine, N.D., Corliss, J.O., Cox, F.E., Deroux, G., Grain, J., Honigberg, B.M., Leedale, G.F., Loeblich, A.R., 3rd, Lom, J., Lynn, D., Merinfeld, E.G., Page, F.C., Poljansky, G., Sprague, V., Vavra, J., and Wallace, F.G. (1980). A newly revised classification of the protozoa. *J. Protozool.* **27**, 37–58.
- Li, Q., Zhou, Y., Yao, C., Ma, X., Wang, L., Xu, W., Wang, Z., and Qiao, Z. (2009). Apoptosis caused by Hsp90 inhibitor geldanamycin in *Leishmania donovani* during promastigote-to-amastigote transformation stage. *Parasitol. Res.* **105**, 1539–1548.
- Li, Z., and Srivastava, P. (2004). Heat-shock proteins. *Curr. Protoc. Immunol.* Appendix 1, Appendix 1T.
- Lindquist, S., and Craig, E.A. (1988). The heat-shock proteins. *Annu. Rev. Genet.* **22**, 631–677.
- Lizundia, R., Sengmanivong, L., Guergnon, J., Müller, T., Schnelle, T., Langsley, G., and Shorte, S.L. (2005). Use of micro-rotation imaging to study JNK-mediated cell survival in *Theileria parva*-infected B-lymphocytes. *Parasitology.* **130**, 629–635.

- Marcu, M.G., Chadli, A., Bouhouche, I., Catelli, M., and Neckers, L.M. (2000). The Heat Shock Protein 90 Antagonist Novobiocin Interacts with a Previously Unrecognized ATP-binding Domain in the Carboxyl Terminus of the Chaperone. *J. Biol. Chem.* **275**, 37181–37186.
- Maxwell, A. (1999). DNA gyrase as a drug target. *Biochem. Soc. Trans.* **27**, 48–53.
- Mehlen, P., Schulze-Osthoff, K., and Arrigo, A.P. (1996). Small stress proteins as novel regulators of apoptosis. Heat shock protein 27 blocks Fas/APO-1- and staurosporine-induced cell death. *J. Biol. Chem.* **271**, 16510–16514.
- Mehlhorn, H. (2008). Theileriosis. *Encyclopedia of parasitology*, 3rd Edition, pp1370-1372.
- Mehlhorn, H., and Schein, E. (1984). The piroplasms: life cycle and sexual stages. *Adv. Parasitol.* **23**, 37–103.
- Meyer, K.J., and Shapiro, T.A. (2013). Potent antitrypanosomal activities of heat shock protein 90 inhibitors in vitro and in vivo. *J. Infect. Dis.* **208**, 489–499.
- Millson, S.H., Truman, A.W., Rácz, A., Hu, B., Panaretou, B., Nuttall, J., Mollapour, M., Söti, C., and Piper, P.W. (2007). Expressed as the sole Hsp90 of yeast, the alpha and beta isoforms of human Hsp90 differ with regard to their capacities for activation of certain client proteins, whereas only Hsp90beta generates sensitivity to the Hsp90 inhibitor radicicol. *FEBS J.* **274**, 4453–4463.
- Mohammed, S.B., Bakheit, M.A., Ernst, M., Ahmed, J.S., and Seitzer, U. (2013). Identification and Characterization of *Theileria annulata* Heat-Shock Protein 90 (HSP90) Isoforms. *Transbound. Emerg. Dis.* **60**, 137–149.
- Molestina, R.E., Payne, T.M., Coppens, I., and Sinai, A.P. (2003). Activation of NF-kappaB by *Toxoplasma gondii* correlates with increased expression of antiapoptotic genes and localization of phosphorylated IkappaB to the parasitophorous vacuole membrane. *J. Cell Sci.* **116** (Pt 21), 4359–4371.
- Montagna, G.N., Buscaglia, C.A., Münter, S., Goosmann, C., Frischknecht, F., Brinkmann, V., and Matuschewski, K. (2012). Critical role for heat shock protein 20 (HSP20) in migration of malarial sporozoites. *J. Biol. Chem.* **287**, 2410–2422.
- Morgensztern, D., and McLeod, H.L. (2005). PI3K/Akt/mTOR pathway as a target for cancer therapy. *Anticancer. Drugs.* **16**, 797–803.
- Morrison, W.I., MacHugh, N.D., and Lalor, P.A. (1996). Pathogenicity of *Theileria parva* is influenced by the host cell type infected by the parasite. *Infect. Immun.* **64**, 557–562.
- Morzaria, S. (1989). Identification of *Theileria* species and characterization of *Theileria parva* stocks. In *Theileriosis in Eastern, Central and Southern Africa: Proceedings of a Workshop on East Coast Fever Immunization*, Held in Lilongwe, Malawi 20-22 September 1988, T.T. Dolan, ed. (The international laboratory for research on animal diseases), pp. 102–110.

- Müller, L., Schaupp, A., Walerych, D., Wegele, H., and Buchner, J. (2004). Hsp90 regulates the activity of wild type p53 under physiological and elevated temperatures. *J. Biol. Chem.* **279**, 48846–48854.
- Mun, H.S., Aosai, F., Norose, K., Chen, M., Hata, H., Tagawa, Y.I., Iwakura, Y., Byun, D.S., and Yano, A. (2000). *Toxoplasma gondii* Hsp70 as a danger signal in *Toxoplasma gondii*-infected mice. *Cell Stress Chaperones.* **5**, 328–335.
- Münster, P.N., Srethapakdi, M., Moasser, M.M., and Rosen, N. (2001). Inhibition of heat shock protein 90 function by ansamycins causes the morphological and functional differentiation of breast cancer cells. *Cancer Res.* **61**, 2945–2952.
- Nathan, D.F., and Lindquist, S. (1995). Mutational analysis of Hsp90 function: interactions with a steroid receptor and a protein kinase. *Mol. Cell. Biol.* **15**, 3917–3925.
- Norval, R.A.I., Perry, B.D., and Young, A.S. (1992). The epidemiology of theileriosis in Africa. London:Academic Press, 481.
- Ogata, M., Naito, Z., Tanaka, S., Moriyama, Y., and Asano, G. (2000). Overexpression and localization of heat shock proteins mRNA in pancreatic carcinoma. *J. Nippon Med. Sch.* **67**, 177–185.
- Okamoto, J., Mikami, I., Tominaga, Y., Kuchenbecker, K.M., Lin, Y.C., Bravo, D.T., Clement, G., Yagui-Beltran, A., Ray, M.R., Koizumi, K., He, B., and Jablons, D.M.. (2008). Inhibition of Hsp90 leads to cell cycle arrest and apoptosis in human malignant pleural mesothelioma. *J. Thorac. Oncol.* **3**, 1089–1095.
- Ozes, O.N., Mayo, L.D., Gustin, J.A., Pfeffer, S.R., Pfeffer, L.M., and Donner, D.B. (1999). NF-kappaB activation by tumour necrosis factor requires the Akt serine-threonine kinase. *Nature.* **401**, 82–85.
- Pallavi, R., Roy, N., Nageshan, R.K., Talukdar, P., Pavithra, S.R., Reddy, R., Venketesh, S., Kumar, R., Gupta, A.K., Singh, R.K., Yadav, S.C., and Tatu, U. (2010). Heat shock protein 90 as a drug target against protozoan infections: biochemical characterization of HSP90 from *Plasmodium falciparum* and *Trypanosoma evansi* and evaluation of its inhibitor as a candidate drug. *J. Biol. Chem.* **285**, 37964–37975.
- Palmer, G.H., Machado, J.Jr, Fernandez, P., Heussler, V., Perinat, T., and Dobbelaere, D.A. (1997). Parasite-mediated nuclear factor kappaB regulation in lymphoproliferation caused by *Theileria parva* infection. *Proc. Natl. Acad. Sci. USA.* **94**, 12527–12532.
- Pandey, P., Farber, R., Nakazawa, A., Kumar, S., Bharti, A., Nalin, C., Weichselbaum, R., Kufe, D., and Kharbanda, S. (2000b). Hsp27 functions as a negative regulator of cytochrome c-dependent activation of procaspase-3. *Oncogene.* **19**, 1975–1981.
- Pandey, P., Saleh, A., Nakazawa, A., Kumar, S., Srinivasula, S.M., Kumar, V., Weichselbaum, R., Nalin, C., Alnemri, E.S., Kufe, D., and Kharbanda, S. (2000a). Negative regulation of cytochrome c-mediated oligomerization of Apaf-1 and activation of procaspase-9 by heat shock protein 90. *EMBO J.* **19**, 4310–4322.

## Reference

---

- Parcellier, A., Gurbuxani, S., Schmitt, E., Solary, E., and Garrido, C. (2003). Heat shock proteins, cellular chaperones that modulate mitochondrial cell death pathways. *Biochem. Biophys. Res. Commun.* **304**, 505–512.
- Parsell, D.A., and Lindquist, S. (1993). The function of heat-shock proteins in stress tolerance: degradation and reactivation of damaged proteins. *Annu. Rev. Genet.* **27**, 437–496.
- Pearl, L.H., and Prodromou, C. (2006). Structure and mechanism of the Hsp90 molecular chaperone machinery. *Annu. Rev. Biochem.* **75**, 271–294.
- Pearl, L.H., Prodromou, C., and Workman, P. (2008). The Hsp90 molecular chaperone: an open and shut case for treatment. *Biochem. J.* **410**, 439–453.
- Peng, Y., Chen, L., Li, C., Lu, W., and Chen, J. (2001). Inhibition of MDM2 by hsp90 contributes to Mutant p53 Stabilization. *J. Biol. Chem.* **276**, 40583–40590.
- Péroval, M., Péry, P., and Labbé, M. (2006). The heat shock protein 90 of *Eimeria tenella* is essential for invasion of host cell and schizont growth. *Int. J. Parasitol.* **36**, 1205–1215.
- Petersen, C.A., Krumholz, K.A., Carmen, J., Sinai, A.P., and Burleigh, B.A. (2006). *Trypanosoma cruzi* infection and nuclear factor kappa B activation prevent apoptosis in cardiac cells. *Infect. Immun.* **74**, 1580–1587.
- Picard, D. (2002). Heat-shock protein 90, a chaperone for folding and regulation. *Cell. Mol. Life Sci.* **59**, 1640–1648.
- Pratt, W.B., and Toft, D.O. (2003). Regulation of signaling protein function and trafficking by the hsp90/hsp70-based chaperone machinery. *Exp. Biol. Med (Maywood)*. **228**, 111–133.
- Preston, P.M., Brown, C.G., Bell-Sakyi, L., Richardson, W., and Sanderson, A. (1992). Tropical theileriosis in *Bos taurus* and *Bos taurus* cross *Bos indicus* calves: response to infection with graded doses of sporozoites of *Theileria annulata*. *Res. Vet. Sci.* **53**, 230–243.
- Preston, P.M., Brown, C.G., Entrican, G., Richardson, W., and Boid, R. (1993). Synthesis of tumour necrosis factor-alpha and interferons by mononuclear cells from *Theileria annulata*-infected cattle. *Parasite Immunol.* **15**, 525–534.
- Preston, P.M., Hall, F.R., Glass, E.J., Campbell, J.D., Darghouth, M.A., Ahmed, J.S., Shiels, B.R., Spooner, R.L., Jongejan, F., and Brown, C.G. (1999). Innate and adaptive immune responses co-operate to protect cattle against *Theileria annulata*. *Parasitol. Today*. **15**, 268–274.
- Puck, T.T., Marcus, P.I., and Cieciura, S.J. (1956). Clonal growth of mammalian cells in vitro; growth characteristics of colonies from single HeLa cells with and without a feeder layer. *J. Exp. Med.* **103**, 273–283.

- Raghu Ram, E.V.S., Kumar, A., Biswas, S., Kumar, A., Chaubey, S., Siddiqi, M.I., and Habib, S. (2007). Nuclear gyrB encodes a functional subunit of the *Plasmodium falciparum* gyrase that is involved in apicoplast DNA replication. *Mol. Biochem. Parasitol.* **154**, 30–39.
- Saksouk, N., Bhatti, M.M., Kieffer, S., Smith, A.T., Musset, K., Garin, J., Sullivan, W.J., Jr, Cesbron-Delauw, M.F., and Hakimi, M.A. (2005). Histone-modifying complexes regulate gene expression pertinent to the differentiation of the protozoan parasite *Toxoplasma gondii*. *Mol. Cell. Biol.* **25**, 10301–10314.
- Samali, A., and Cotter, T.G. (1996). Heat shock proteins increase resistance to apoptosis. *Exp. Cell Res.* **223**, 163–170.
- Sato, S., Fujita, N., and Tsuruo, T. (2000). Modulation of Akt kinase activity by binding to Hsp90. *Proc. Natl. Acad. Sci. USA.* **97**, 10832–10837.
- Schmitt, E., Gehrman, M., Brunet, M., Multhoff, G., and Garrido, C. (2007). Intracellular and extracellular functions of heat shock proteins: repercussions in cancer therapy. *J. Leukoc. Biol.* **81**, 15–27.
- Schnittger, L., Katzer, F., Biermann, R., Shayan, P., Boguslawski, K., McKellar, S., Beyer, D., Shiels, B.R., and Ahmed, J.S. (2002). Characterization of a polymorphic *Theileria annulata* surface protein (TaSP) closely related to PIM of *Theileria parva*: implications for use in diagnostic tests and subunit vaccines. *Mol. Biochem. Parasitol.* **120**, 247–256.
- Schnittger, L., Shayan, P., Biermann, R., Mehlhorn, H., Gerdes, J., and Ahmed, J.S. (2000). Molecular genetic characterization and subcellular localization of *Theileria annulata* mitochondrial heat-shock protein 70. *Parasitol. Res.* **86**, 444–452.
- Schulte, T.W., Akinaga, S., Soga, S., Sullivan, W., Stensgard, B., Toft, D., and Neckers, L.M. (1998). Antibiotic radicicol binds to the N-terminal domain of Hsp90 and shares important biologic activities with geldanamycin. *Cell Stress Chaperones.* **3**, 100–108.
- Shaw, M.K. (1997). The same but different: the biology of *Theileria* sporozoite entry into bovine cells. *Int. J. Parasitol.* **27**, 457–474.
- Shaw, M.K. (2002). *Theileria* development and host cell invasion. In: *Theileria*, Dobbelaere DAE, McKeever DJ (eds) World Class Parasites, Kluwer, Boston, London, pp. 1–22.
- Shaw, M.K. (2003). Cell invasion by *Theileria* sporozoites. *Trends Parasitol.* **19**, 2–6.
- Shaw, M.K., and Tilney, L.G. (1992). How individual cells develop from a syncytium: merogony in *Theileria parva* (Apicomplexa). *J. Cell Sci.* **101**, 109–123.
- Shaw, M.K., and Tilney, L.G. (1995). The entry of *Theileria parva* merozoites into bovine erythrocytes occurs by a process similar to sporozoite invasion of lymphocytes. *Parasitology.* **111** (Pt 4), 455–461.

- Shi, L., Kam, C.M., Powers, J.C., Aebersold, R., and Greenberg, A.H. (1992a). Purification of three cytotoxic lymphocyte granule serine proteases that induce apoptosis through distinct substrate and target cell interactions. *J. Exp. Med.* **176**, 1521–1529.
- Shi, L., Kraut, R.P., Aebersold, R., and Greenberg, A.H. (1992b). A natural killer cell granule protein that induces DNA fragmentation and apoptosis. *J. Exp. Med.* **175**, 553–566.
- Shiels, B., Aslam, N., McKellar, S., Smyth, A., and Kinnaird, J. (1997). Modulation of protein synthesis relative to DNA synthesis alters the timing of differentiation in the protozoan parasite *Theileria annulata*. *J. Cell Sci.* **110** (Pt 13), 1441–1451.
- Shiels, B., Kinnaird, J., McKellar, S., Dickson, J., Miled, L.B., Melrose, R., Brown, D., and Tait, A. (1992). Disruption of synchrony between parasite growth and host cell division is a determinant of differentiation to the merozoite in *Theileria annulata*. *J. Cell Sci.* **101** (Pt 1), 99–107.
- Shiels, B., Langsley, G., Weir, W., Pain, A., McKellar, S., and Dobbelaere, D. (2006). Alteration of host cell phenotype by *Theileria annulata* and *Theileria parva*: mining for manipulators in the parasite genomes. *Int. J. Parasitol.* **36**, 9–21.
- Shiels, B., Swan, D., McKellar, S., Aslam, N., Dando, C., Fox, M., Ben-Miled, L., and Kinnaird, J. (1998). Directing differentiation in *Theileria annulata*: old methods and new possibilities for control of apicomplexan parasites. *Int. J. Parasitol.* **28**, 1659–1670.
- Shiels, B.R. (1999). Should I stay or should I go now? A stochastic model of stage differentiation in *Theileria annulata*. *Parasitol. Today.* **15**, 241–245.
- Shiels, B.R., Smyth, A., Dickson, J., McKellar, S., Tetley, L., Fujisaki, K., Hutchinson, B., and Kinnaird, J.H. (1994). A stoichiometric model of stage differentiation in the protozoan parasite *Theileria annulata*. *Mol. Cell. Differ.* **2**, 101–125.
- Silva, N.M., Gazzinelli, R.T., Silva, D.A., Ferro, E.A., Kasper, L.H., and Mineo, J.R. (1998). Expression of *Toxoplasma gondii*-specific heat shock protein 70 during *In vivo* conversion of bradyzoites to tachyzoites. *Infect. Immun.* **66**, 3959–3963.
- Spooner, R.L., Innes, E.A., Glass, E.J., and Brown, C.G. (1989). *Theileria annulata* and *T. parva* infect and transform different bovine mononuclear cells. *Immunology.* **66**, 284–288.
- Sreedhar, A.S., Kalmár, E., Csermely, P., and Shen, Y.F. (2004). Hsp90 isoforms: functions, expression and clinical importance. *FEBS Lett.* **562**, 11–15.
- Stabel, J.R., and Stabel, T.J. (1995). Immortalization and characterization of bovine peritoneal macrophages transfected with SV40 plasmid DNA. *Vet. Immunol. Immunopathol.* **45**, 211–220.
- Swan, D.G., Phillips, K., McKellar, S., Hamilton, C., and Shiels, B.R. (2001). Temporal coordination of macroschizont and merozoite gene expression during stage differentiation of *Theileria annulata*. *Mol. Biochem. Parasitol.* **113**, 233–239.

- Terasawa, K., Minami, M., and Minami, Y. (2005). Constantly updated knowledge of Hsp90. *J. Biochem.* **137**, 443–447.
- Thomson, B.J. (2001). Viruses and apoptosis. *Int. J. Exp. Pathol.* **82**, 65–76.
- Tripathi, A.K., Sha, W., Shulaev, V., Stins, M.F., and Sullivan, D.J.Jr (2009). *Plasmodium falciparum*-infected erythrocytes induce NF-kappaB regulated inflammatory pathways in human cerebral endothelium. *Blood.* **114**, 4243–4252.
- Uilenberg, G. (1981). *Theileria* species of domestic livestock. In *Advances in the Control of theileriosis*. Irvin, A.D., Cunningham, M.P., and Young, A.S. (Eds). Martinus Nijhoof Publishers, pp. 4–37.
- Van der Ploeg, L.H., Giannini, S.H., and Cantor, C.R. (1985). Heat shock genes: regulatory role for differentiation in parasitic protozoa. *Science.* **228**, 1443–1446.
- Vargas-Roig, L.M., Fanelli, M.A., López, L.A., Gago, F.E., Tello, O., Aznar, J.C., and Ciocca, D.R. (1997). Heat shock proteins and cell proliferation in human breast cancer biopsy samples. *Cancer Detect. Prev.* **21**, 441–451.
- Vargas-Roig, L.M., Gago, F.E., Tello, O., Aznar, J.C., and Ciocca, D.R. (1998). Heat shock protein expression and drug resistance in breast cancer patients treated with induction chemotherapy. *Int. J. Cancer.* **79**, 468–475.
- Vogelstein, B., Lane, D., and Levine, A.J. (2000). Surfing the p53 network. *Nature.* **408**, 307–310.
- Vousden, K.H., and Vande Woude, G.F. (2000). The ins and outs of p53. *Nat. Cell Biol.* **2**, E178–E180.
- Weiss, L.M., Ma, Y.F., Takvorian, P.M., Tanowitz, H.B., and Wittner, M. (1998). Bradyzoite development in *Toxoplasma gondii* and the hsp70 stress response. *Infect. Immun.* **66**, 3295–3302.
- Welch, W.J. (1992). Mammalian stress response: cell physiology, structure/function of stress proteins, and implications for medicine and disease. *Physiol. Rev.* **72**, 1063–1081.
- Whitesell, L., and Lindquist, S.L. (2005). HSP90 and the chaperoning of cancer. *Nat. Rev. Cancer.* **5**, 761–772.
- Whitesell, L., Mimnaugh, E.G., De Costa, B., Myers, C.E., and Neckers, L.M. (1994). Inhibition of heat shock protein HSP90-pp60v-src heteroprotein complex formation by benzoquinone ansamycins: essential role for stress proteins in oncogenic transformation. *Proc. Natl. Acad. Sci. USA.* **91**, 8324–8328.
- Wiesiggl, M., and Clos, J. (2001). Heat shock protein 90 homeostasis controls stage differentiation in *Leishmania donovani*. *Mol. Biol. Cell.* **12**, 3307–3316.
- Wong, R.S.Y. (2011). Apoptosis in cancer: from pathogenesis to treatment. *J. Exp. Clin. Cancer Res.* **30**, 87.

- Workman, P., Burrows, F., Neckers, L., and Rosen, N. (2007). Drugging the cancer chaperone HSP90: combinatorial therapeutic exploitation of oncogene addiction and tumor stress. *Ann. N. Y. Acad. Sci.* **1113**, 202–216.
- Wu, X., Wanders, A., Wardega, P., Tinge, B., Gedda, L., Bergstrom, S., Sooman, L., Gullbo, J., Bergqvist, M., Hesselius, P., Lennartsson, J., and Ekman, S. (2009). Hsp90 is expressed and represents a therapeutic target in human oesophageal cancer using the inhibitor 17-allylamino-17-demethoxygeldanamycin. *Br. J. Cancer.* **100**, 334–343.
- Xu, Z.S., Li, Z.Y., Chen, Y., Chen, M., Li, L.C., and Ma, Y.Z. (2012). Heat shock protein 90 in plants: molecular mechanisms and roles in stress responses. *Int. J. Mol. Sci.* **13**, 15706–15723.
- Yamada, T., Tomita, T., Weiss, L.M., and Orlofsky, A. (2011). *Toxoplasma gondii* inhibits granzyme B-mediated apoptosis by the inhibition of granzyme B function in host cells. *Int. J. Parasitol.* **41**, 595–607.
- Yang, S., and Parmley, S.F. (1997). *Toxoplasma gondii* expresses two distinct lactate dehydrogenase homologous genes during its life cycle in intermediate hosts. *Gene* **184**, 1–12.
- Young, J.C., Moarefi, I., and Hartl, F.U. (2001). Hsp90: a specialized but essential protein-folding tool. *J. Cell Biol.* **154**, 267–273.
- Yufu, Y., Nishimura, J., and Nawata, H. (1992). High constitutive expression of heat shock protein 90 alpha in human acute leukemia cells. *Leuk. Res.* **16**, 597–605.
- Zagouri, F., Bournakis, E., Koutsoukos, K., and Papadimitriou, C.A. (2012). Heat shock protein 90 (hsp90) expression and breast cancer. *Pharm (Basel).* **5**, 1008–1020.
- Zong, W.X., Edelstein, L.C., Chen, C., Bash, J., and Gélinas, C. (1999). The prosurvival Bcl-2 homolog Bfl-1/A1 is a direct transcriptional target of NF- $\kappa$ B that blocks TNF $\alpha$ -induced apoptosis. *Genes Dev.* **13**, 382–387.

## 9 Appendix

### 9.1 Flow cytometric analysis of apoptosis in *T. annulata*-infected cells incubated with GA 0.05 $\mu\text{M}$ at 41°C

Further assessment of apoptosis was conducted at 41°C by increasing the incubation time to determine whether the down-regulation of *T.annulata* HSP90 has significant influence in the occurrence of apoptosis. In order to perform that, *T. annulata* Ankara 288-infected cells treated with DMSO (control group) or GA 0.05 $\mu\text{M}$  then incubated for 5, 6 and 7 days at 41°C then analysed by flow Cytometry. As shown in Figure 39, the percentages of apoptotic cells were increased in the cells incubated with GA 0.05  $\mu\text{M}$  for 5, 6 and 7 days at 41°C (3.38%, 5.78% and 11.29%, respectively), while in DMSO-treated cells the percentages of apoptotic cells were 2.98%, 3.29% and 4.34%, respectively. The statistical analysis of these data revealed a significant increase in apoptotic cells in GA0.05  $\mu\text{M}$ -treated cells incubated for 7 days ( $P \leq 0.01$ , Student's t-test).

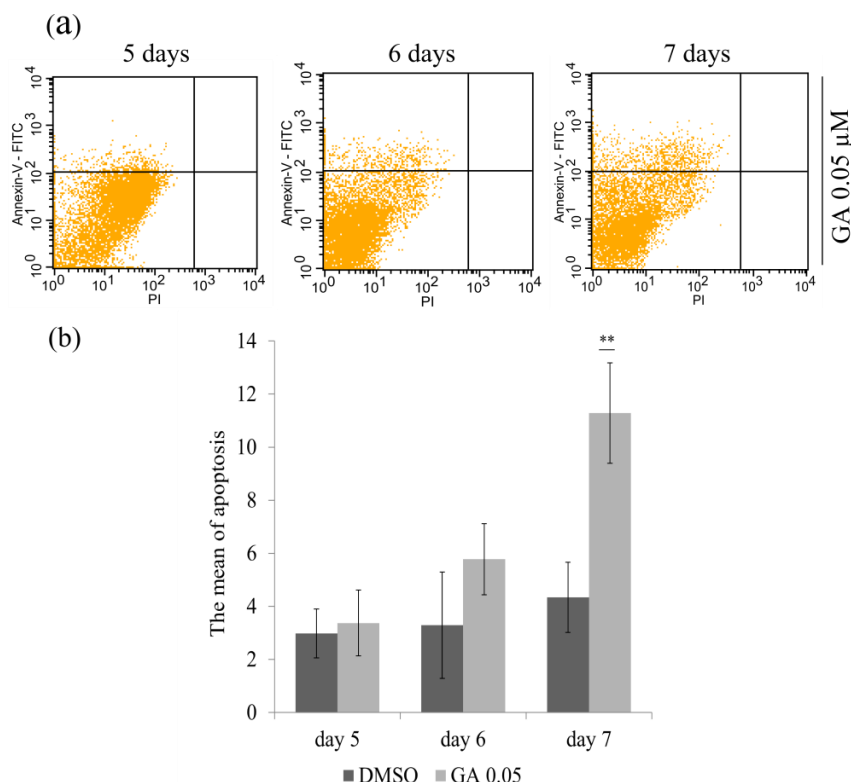


Figure 39: Flow cytometric analysis of apoptosis using Annexin V-FITC in *T. annulata* Ankara 288-infected cells treated with GA 0.05  $\mu\text{M}$  and incubated at 41°C for 5, 6 and 7 days.

Cells were treated with DMSO (control group) or GA 0.05  $\mu\text{M}$  and incubated for 5, 6 and 7 days at 41°C. The cells were harvested and stained with 2  $\mu\text{l}$  (0.4  $\mu\text{g}$ ) Annexin V- FITC then analysed by flow cytometric. (a) The data shown here represents one experiment of four independent experiments. (b) Mean  $\pm$  S.D, (\*\* $p \leq 0.01$ ) n=4.

## 9.2 Quantitative assessment of the stage progression in *T. annulata* Ankara 288-infected cells treated with GA using TamS1 and TamR1

The number of the cells undergoing merogony was increased in correlation with the increase of GA concentration.

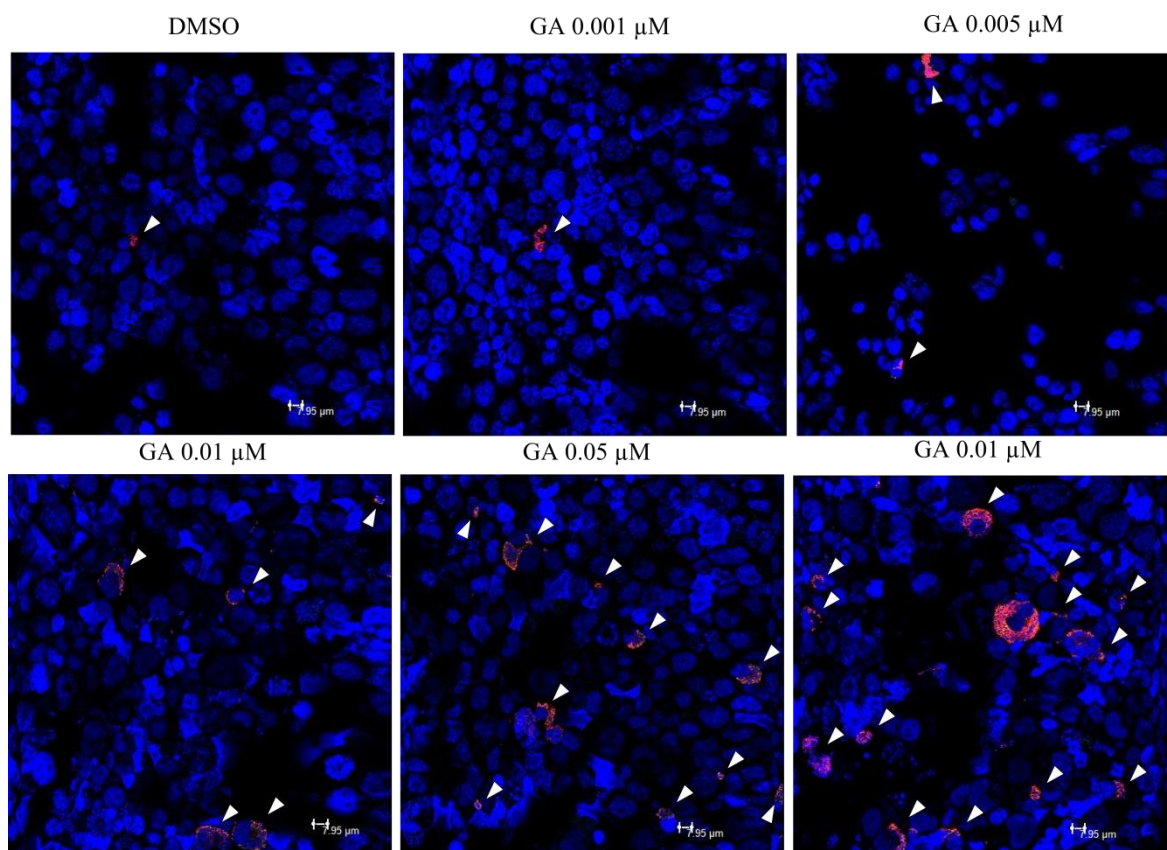


Figure 40: An increase in the number of the cells undergoing merogony after treatment with GA.

*T.annulata* Ankara 288-infected cells were incubated with GA (0.001 μM, 0.005 μM, 0.01 μM, 0.05 μM and 0.1μM) or DMSO for 5 days at 41°C. The cells were subjected to immunostaining using TamS1 and TamR1 antibodies. The number of the cells undergoing merogony was increased in correlation with the increase of GA concentration.

## 9.3 Quantitative real-time polymerase chain reaction (qRT-PCR)

In order to test the specificity of the qRT- PCR primers, a high fidelity PCR was applied to amplify cDNA prepared from *T. annulata* Ankara 288-infected cells or cDNA prepared from BoMac (as control). PCR reactions were performed as described in section 3.2.3.4 using the Advantage® 2 PCR kit.

As shown in Figure 41, an amplificate of fragment (size ~100 bp) could be demonstrated with the cDNA template prepared from *T. annulata* Ankara 288-infected cells and from BoMac using specific primers designed to amplify mRNA transcripts of BHSP90-alpha and

BHSP90-beta. These results showed the ability of these primers (UPL-BHSP90aa1 and UPL-BHSP90ab1) to amplify mRNA transcripts, which related to the bovine HSP90 genes.

On the other hand, an amplificate of 100 bp could be obtained with the cDNA template prepared from *T. annulata* Ankara 288-infected cells using specific primers (UPL-TaHSP90c1 and UPL-TaHSP90c4), which designed to amplify mRNA transcripts of TaHSP90-Chr1 and TaHSP90-Chr4, respectively. In contrast, these primers failed to obtain amplificate with the cDNA template prepared from BoMac, which confirmed the specificity of these primers (Figure 41).

As illustrated in Figure 42, both TaActin-31 and TamR1 can amplify fragments from the cDNA template prepared from RNA isolated from *T.annulata* Ankara 288-infected cells, but not from the cDNA template prepared from BoMac (negative control).

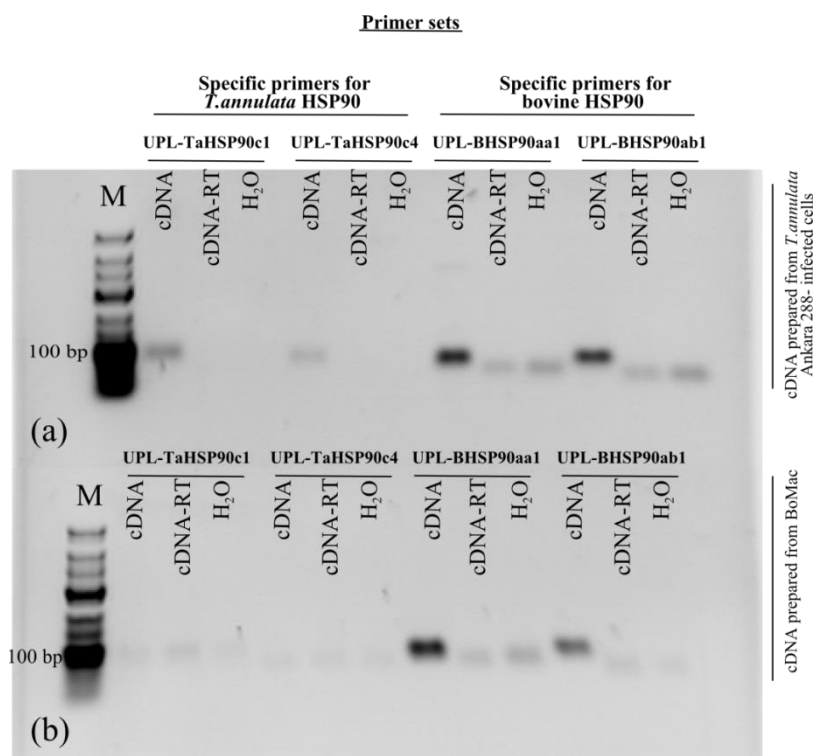


Figure 41: Specificity of the qRT-PCR primers used to detect TaHSP90-Chr1, TaHSP90-Chr4, BHSP90-alpha and BHSP90-beta.

(a) PCR amplification products of mRNA transcripts of *T.annulata* Ankara 288-infected cells. b) PCR amplification products of mRNA transcripts of BoMac. The primers were designed specifically to amplify mRNA transcripts of each gene, UPL-TaHSP90c1 primers were designed to amplify mRNA transcripts of TaHSP90-Chr1, UPL-TaHSP90c4 primers were designed to amplify mRNA transcripts of TaHSP90-Chr4, UPL-BHSP90aa1 primers were designed to amplify mRNA transcripts of BHSP90-alpha and UPL-BHSP90ab1 primers were designed to amplify mRNA transcripts of BHSP90-beta. Lanes M: molecular weight marker. The cDNA templates giving a PCR product of ~ 100bp.

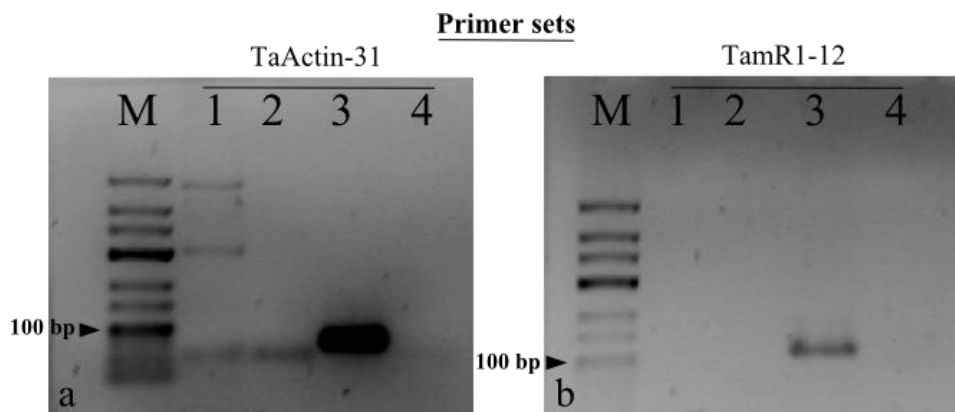


Figure 42: Specificity of the qRT-PCR primers used to detect TaAct1 and TamR1.

a) The amplification products were obtained by using TaActin-31 primers, which designed specifically to amplify mRNA transcripts of *Theileria annulata* actin 1 (TaAct1). b) The amplification products were obtained by using TamR1 primers, which designed specifically to amplify mRNA transcripts of TamR1. Lanes M: molecular weight marker; 1: cDNA prepared from BoMac; 2: cDNA-RT prepared from BoMac; 3: cDNA prepared from *T.annulata* Ankara 288-infected cells; 4: cDNA-RT prepared from *T.annulata* Ankara 288-infected cells.

### 9.4 The alignment of bovine HSP90 with HSP90 β of human

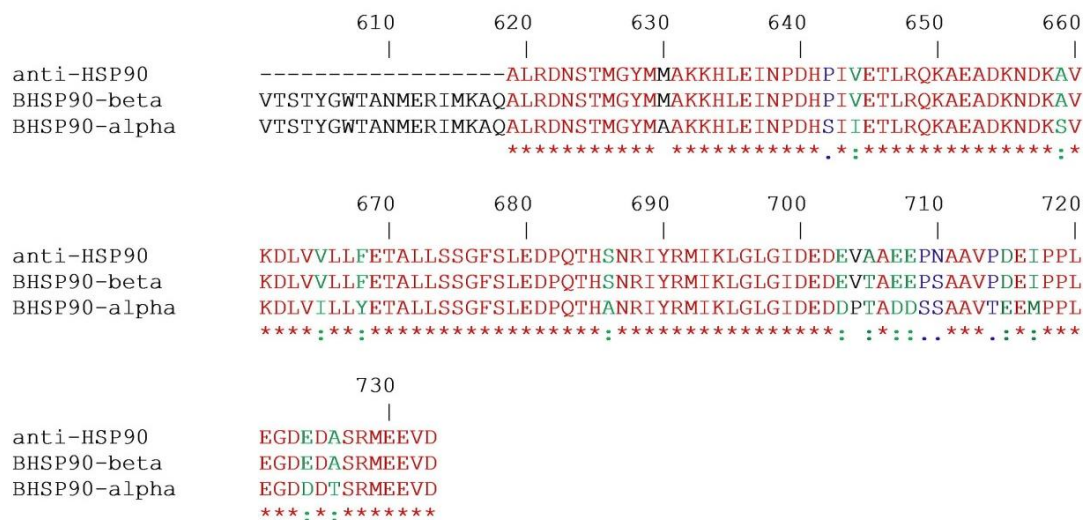


Figure 43: The alignment of bovine HSP90 with amino acids 610-723 of HSP90 β of human origin.

The anti-human HSP 90α/β antibody (HSP 90α/β (F-8): sc-13119, Santa Cruz) raised against amino acids 610-723 of HSP 90β of human. The alignment of BHSP90-alpha and BHSP90-beta with HSP90 β of human origin (amino acids 610-723) has shown 84% identity and 15% similarity.

## 9.5 FastDigest® restriction enzymes of purified plasmids from *E. coli* DH5α competent cell

These enzymes have the ability to cut the pDrive vector at promoter side and separate the insert from the vector. As shown in Figure 44, some of these clones contained the insert which included two fragments; one belong to pDrive vector (3850 bp) and the other belong to TaHSP90-Chr1 (2967 bp) or TaHSP90-Chr4 (2742 bp) insert.

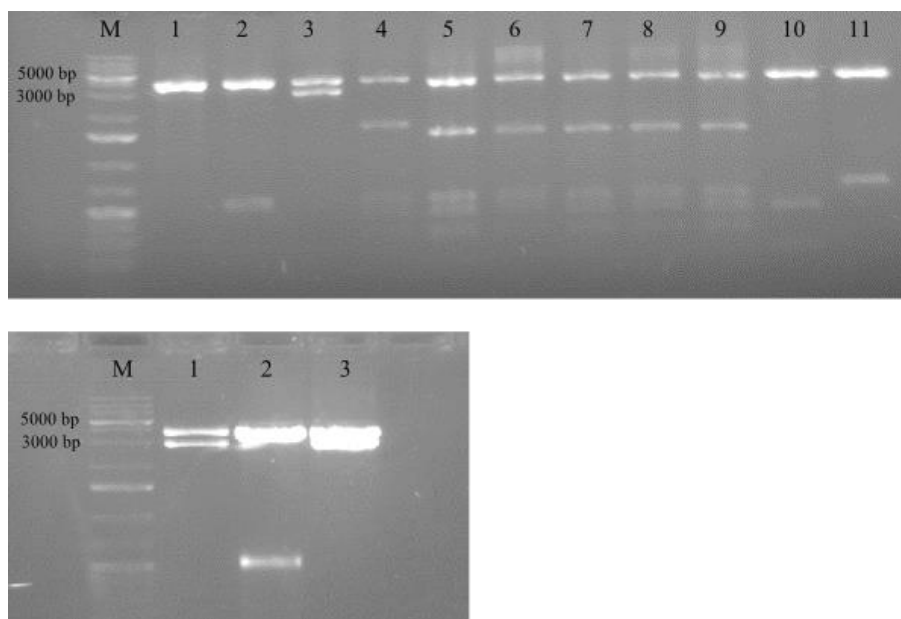


Figure 44: FastDigest® restriction enzymes of purified plasmids from *E. coli* DH5α competent cell.

Upper figure: screening for the presence of TaHSP90-Chr1 insert into pDrive vector using FastDigest® EcoRI, M: molecular weight marker, 3: detection of TaHSP90-Chr1 insert (2967 bp, lower fragment) into pDrive vector (upper fragment,) 1-11: purified plasmids from different clones showed the presence of different insert which are not in a correct size.

Lower figure: screening for the presence of TaHSP90-Chr4 insert into pDrive vector using FastDigest® BamHI and HindIII, M: molecular weight marker, 1: detection of TaHSP90-Chr4 insert (2742bp, lower fragment) into pDrive vector (upper fragment,) 2-3: purified plasmids from different clones showed the presence of different insert which are not in a correct size.

## 9.6 Alignment of the amino acid sequence of TaHSP90-Chr1 and TaHSP90-Chr4

### 9.6.1 Comparison of the deduced amino acid sequences of the clones

Eleven clones from TaHSP90-Chr1 and seven clones from TaHSP90-Chr4 were sequenced (fully or partially) to obtain two 100% identical sequences for each gene.

(a)

	10	20	30	40	50	60
Clone (1)	-----	YHFVSCNESG	GELEVVEDTVNVDE	VDVTEEQT	PSELSEEE	ELL
Clone (c_D)	-----	YHFVSCNESG	GELEVVEDTVNVDE	VDVTEEQT	PSELSEEE	ELL
Clone (c_A)	-----	YHFVSCNESG	GELEVVEDTVNVDE	VDVTEEQT	PSELSEEE	ELL
Clone (g_B)	-----	YHFVSCNESDE	LEVVEDTVNVDE	VDVTEEQT	PSELSEEE	ELL
Clone (g_A)	-----	YHFVSCNESDE	LEVVEDTVNVDE	VDVTEEQT	PSELSEEE	ELL
Clone (C_C)	-----	YHFVSCNESDE	LEVVEDTVNVDE	VDVTEEQT	PSELSEEE	ELL
Clone (3)	MKVSLLLLIKLFFILQLNKG	YHFVSCNESG	GELEVVEDTVNVDE	VDVTEEQT	PSELSEEE	ELL
Clone (g_C)	-----	YHFVSCNESDE	LEVVEDTVNVDE	VDVTEEQT	PSELSEEE	ELL
Clone (12)	MKVSLLLLIKLFFILQLNKG	YHFVSCNESDE	LEVVEDTVNVDE	VDVTEEQT	PSELSEEE	ELL
Clone (H)	MKVSLLLLIKLFFILQLNKG	YHFVSCNESDE	LEVVEDTVNVDE	VDVTEEQT	PSELSEEE	ELL
Clone (E)	MKVSLLLLIKLFFILQLNKG	YHFVSCNESDE	LEVVEDTVNVDE	VDVTEEQT	PSELSEEE	ELL
Genebank	MKVSLLLLIKLFFILQLNKG	YHFVSCNESDE	LEVVEDTVNVDE	VDVTEEQT	PSELSEEE	ELL

	70	80	90	100	110	120
Clone (1)	DRSEDSSVLTSEKLFK	DKSTKSEKYEYQAE	VRLLLDIIVNSLY	SSKDI	FLRELVSNSADAL	
Clone (c_D)	DRSEDSSVLTSEKLFK	DKSTKSEKYEYQAE	VRLLLDIIVNSLY	SSKDI	FLRELVSNSADAL	
Clone (c_A)	DRSEDSSVLTSEKLFK	DKSTKSEKYEYQAE	VRLLLDIIVNSLY	SSKDI	FLRELVSNSADAL	
Clone (g_B)	DRSEDSSVLTSEKLFK	DKSTKSEKYEYQAE	VRLLLDIIVNSLY	SSKDI	FLRELVSNSADAL	
Clone (g_A)	DRSEDSSVLTSEKLFK	DKSTKSEKYEYQAE	VRLLLDIIVNSLY	SSKDI	FLRELVSNSADAL	
Clone (C_C)	DRSEDSSVLTSEKLFK	DKSTKSEKYEYQAE	VRLLLDIIVNSLY	SSKDI	FLRELVSNSADAL	
Clone (3)	DRSEDSSVLTSEKLFK	DKSTKSEKYEYQAE	VRLLLDIIVNSLY	SSKDI	FLRELVSNSADAL	
Clone (g_C)	DRSEDSSVLTSEKLFK	DKSTKSEKYEYQAE	VRLLLDIIVNSLY	SSKDI	FLRELVSNSADAL	
Clone (12)	DRSEDSSVLTSEKLFK	DKSTKSEKYEYQAE	VRLLLDIIVNSLY	SSKDI	FLRELVSNSADAL	
Clone (H)	DRSEDSSVLTSEKLFK	DKSTKSEKYEYQAE	VRLLLDIIVNSLY	SSKDI	FLRELVSNSADAL	
Clone (E)	DRSEDSSVLTSEKLFK	DKSTKSEKYEYQAE	VRLLLDIIVNSLY	SSKDI	FLRELVSNSADAL	
Genebank	DRSEDSSVLTSEKLFK	DKSTKSEKYEYQAE	VRLLLDIIVNSLY	SSKDI	FLRELVSNSADAL	

	130	140	150	160	170	180
Clone (1)	EKYKITALQKNYRDK	DDVELFVRI	RSYPKRRLLTI	WDNGVGMTKTE	LMNNLGTIAK	SGTA
Clone (c_D)	EKYKITALQKNYRDK	DDVELFVRI	RSYPKRRLLTI	WDNGVGMTKTE	LMNNLGTIAK	SGTA
Clone (c_A)	EKYKITALQKNYRDK	DDVELFVRI	RSYPKRRLLTI	WDNGVGMTKTE	LMNNLGTIAK	SGTA
Clone (g_B)	EKYKITALQKNYRDK	DDVELFVRI	RSYPKRRLLTI	WDNGVGMTKTE	LMNNLGTIAK	SGTA
Clone (g_A)	EKYKITALQKNYRDK	DDVELFVRI	RSYPKRRLLTI	WDNGVGMTKTE	LMNNLGTIAK	SGTA
Clone (C_C)	KKYKITALQKNYRDK	DDVELFVRI	RSYPKRRLLTI	WDNGVGMTKTE	LMNNLGTIAK	SGTA
Clone (3)	EKYKITALQKNYRDK	DDVELFVRI	RSYPKRRLLTI	WDNGVGMTKTE	LMNNLGTIAK	SGTA
Clone (g_C)	EKYKITALQKNYRDK	DDVELFVRI	RSYPKRRLLTI	WDNGVGMTKTE	LMNNLGTIAK	SGTA
Clone (12)	EKYKITALQKNYRDK	DDVELFVRI	RSYPKRRLLTI	WDNGVGMTKTE	LMNNLGTIAK	SGTA
Clone (H)	EKYKITALQKNYRDK	DDVELFVRI	RSYPKRRLLTI	WDNGVGMTKTE	LMNNLGTIAK	SGTA
Clone (E)	EKYKITALQKNYRDK	DDVELFVRI	RSYPKRRLLTI	WDNGVGMTKTE	LMNNLGTIAK	SGTA
Genebank	EKYKITALQKNYRDK	DDVELFVRI	RSYPKRRLLTI	WDNGVGMTKTE	LMNNLGTIAK	SGTA

	190	200	210	220	230	240
Clone (1)	NFLDLSKAGSDPNLI	GQFGVGFYSAFL	VADTVLVQSKNY	DDKQYVWRSSA	ANNYELYED	
Clone (c_D)	NFLDLSKAGSDPNLI	GQFGVGFYSAFL	VADTVLVQSKNY	DDKQYVWRSSA	ANNYELYED	
Clone (c_A)	NFLDLSKAGSDPNLI	GQFGVGFYSAFL	VADTVLVQSKNY	DDKQYVWRSSA	ANNYELYED	
Clone (g_B)	NFLDLSKAGSDPNLI	GQFGVGFYSAFL	VADTVLVQSKNY	DDKQYVWRSSA	ANNYELYED	
Clone (g_A)	NFLDLSKAGSDPNLI	GQFGVGFYSAFL	VADTVLVQSKNY	DDKQYVWRSSA	ANNYELYED	
Clone (C_C)	NFLDLSKAGSDPNLI	GQFGVGFYSAFL	VADTVLVQSKNY	DDKQYVWRSSA	ANNYELYED	
Clone (3)	NFLDLSKAGSDPNLI	GQFGVGFYSAFL	VADTVLVQSKNY	DDKQYVWRSSA	ANNYELYED	
Clone (g_C)	NFLDLSKAGSDPNLI	GQFGVGFYSAFL	VADTVLVQSKNY	DDKQYVWRSSA	ANNYELYED	
Clone (12)	NFLDLSKAGSDPNLI	GQFGVGFYSAFL	VADTVLVQSKNY	DDKQYVWRSSA	ANNYELYED	
Clone (H)	NFLDLSKAGSDPNLI	GQFGVGFYSAFL	VADTVLVQSKNY	DDKQYVWRSSA	ANNYELYED	
Clone (E)	NFLDLSKAGSDPNLI	GQFGVGFYSAFL	VADTVLVQSKNY	DDKQYVWRSSA	ANNYELYED	
Genebank	NFLDLSKAGSDPNLI	GQFGVGFYSAFL	VADTVLVQSKNY	DDKQYVWRSSA	ANNYELYED	

(a)

	250	260	270	280	290	300
Clone (1)	TDNSLGDHGTLLITLLELREDSTEYLKTDVLENLVKKYSQFVRYPIQLYKKLKDKQEVGWVK					
Clone (c_D)	TDNSLGDHGTLLITLLELREDSTEYLKTDVLENLVKKYSQFVRYPIQLYKKLKDKQEVGWVK					
Clone (c_A)	TDNSLGDHGTLLITLLELREDSTEYLKTDVLENLVKKYSQFVRYPIQLYKKLKDKQEVGWVK					
Clone (g_B)	TDNSLGDHGTLLITLLELREDSTEYLKTDVLENLVKKYSQFVRYPIQLYKKLKDKQEVGWVK					
Clone (g_A)	TDNSLGDHGTLLITLLELREDSTEYLKTDVLENLVKKYSQFVRYPIQLYKKLKDKQEVGWVK					
Clone (C_C)	TDNSLGDHGTLLITLLELREDSTEYLKTDVLENLVKKYSQFVRYPIQLYKKLKDKQEVGWVK					
Clone (3)	TDNSLGDHGTLLITLLELREDSTEYLKTDVLENLVKKYSQFVRYPIQLYKKLKDKQEVGWVK					
Clone (g_C)	TDNSLGDHGTLLITLLELREDSTEYLKTDVLENLVKKYSQFVRYPIQLYKKLKDKQEVGWVK					
Clone (12)	TDNSLGDHGTLLITLLELREDSTEYLKTDVLENLVKKYSQFVRYPIQLYKKLKDKQEVGWVK					
Clone (H)	TDNSLGDHGTLLITLLELREDSTEYLKTDVLENLVKKYSQFVRYPIQLYKKLKDKQEVGWVK					
Clone (E)	TDNSLGDHGTLLITLLELREDSTEYLKTDVLENLVKKYSQFVRYPIQLYKKLKDKQEVGWVK					
Genebank	TDNSLGDHGTLLITLLELREDSTEYLKTDVLENLVKKYSQFVRYPIQLYKKLKDKQEVGWVK					

	310	320	330	340	350	360
Clone (1)	VNETQQIWRNKNTITEEEYNQFYKTI SGKNDEPLTHVHFTAEGDGVDFKALLYIPSSPPG					
Clone (c_D)	VNETQQIWRNKNTITEEEYNQFYKTI SGKNDEPLTHVHFTAEGDGVDFKALLYIPSSPPG					
Clone (c_A)	VNETQQIWRNKNTITEEEYNQFYKTI SGKNDEPLTHVHFTAEGDGVDFKALLYIPSSPPG					
Clone (g_B)	VNETQQIWRNKNTITEEEYNQFYKTI SGKNDEPLTHVHFTAEGDGVDFKALLYIPSSPPG					
Clone (g_A)	VNETQQIWRNKNTITEEEYNQFYKTI SGKNDEPLTHVHFTAEGDGVDFKALLYIPSSPPG					
Clone (C_C)	VNETQQI-----					
Clone (3)	-----					
Clone (g_C)	RP-----					
Clone (12)	VNETQQIWRNKNTITEEEYNQFYKTI SGKNDEPLTHVHFTAEGDGVDFKALLYIPSSPPG					
Clone (H)	VNETQQIWRNKNTITEEEYNQFYKTI SGKNDEPLTHVHFTAEGDGVDFKALLYIPSSPPG					
Clone (E)	VNETQQIWRNKNTITEEEYNQFYKTI SGKNDEPLTHVHFTAEGDGVDFKALLYIPSSPPG					
Genebank	VNETQQIWRNKNTITEEEYNQFYKTI SGKNDEPLTHVHFTAEGDGVDFKALLYIPSSPPG					

	370	380	390	400	410	420
Clone (1)	MYFSTESVGHNVKLYSRRVLVSQEMKDFIPRYLFSIYGVVSDSDFPLNVSREYLQQSKLV					
Clone (c_D)	MYFSTESVGHNVKLYSRRVLVSQEMKDFIPRYLFSIYGVVSDSDFPLNVSREYLQQSKLV					
Clone (c_A)	MYFSTESVGHNVKLYSRRVLVSQEMKDFIPRYLFSIYGVVSDSDFPLNVSREYLQQSKLV					
Clone (g_B)	MYFSTESVGHNVKLYSRRVLVSQEMKDFIPRYLFSIYGVVSDSDFPLNVSREYLQQSKLV					
Clone (g_A)	MYFSTESVGHNVKLYSRRVLVSQEMKDFIPRYLFSIYGVVSDSDFPLNVSREYLQQSKLV					
Clone (C_C)	-----					
Clone (3)	-----					
Clone (g_C)	-----					
Clone (12)	MYFSTESVGHNVKLYSRRVLVSQEMKDFIPRYLFSIYGVVSDSDFPLNVSREYLQQSKLV					
Clone (H)	MYFSTESVGHNVKLYSRRVLVSQEMKDFIPRYLFSIYGVVSDSDFPLNVSREYLQQSKLV					
Clone (E)	MYFSTESVGHNVKLYSRRVLVSQEMKDFIPRYLFSIYGVVSDSDFPLNVSREYLQQSKLV					
Genebank	MYFSTESVGHNVKLYSRRVLVSQEMKDFIPRYLFSIYGVVSDSDFPLNVSREYLQQSKLV					

	430	440	450	460	470	480
Clone (1)	KLIGKKVVRTVLDTLYDVMKKSQEDVKETEAELEKVKAVKEEKWNSYKKDWKKRNEVEY					
Clone (c_D)	KLIGKKVVRTVLDTLYDVMKKSQEDVKETEAELEKVKAVKEEKWNSYKKDWKKRNEVEY					
Clone (c_A)	KLIGKKVVRTVLDTLYDVMKKSQEDVKETEAELEKVKAVKEEKWNSYKKDWKKRNEVEY					
Clone (g_B)	KLIGKKVVRTVLDTLYDVMKKSQEDVKETEAELEKVKAVKEEKWNSYKKDWKKRNEVEY					
Clone (g_A)	KLIGKKVVRTVLDTLYDVMKKSQEDVKETEAELEKVKAVKEEKWNSYKKDWKKRNEVEY					
Clone (C_C)	-----					
Clone (3)	-----					
Clone (g_C)	-----					
Clone (12)	KLIGKRWREQFHCYTKNHKKLRRKQSWRRRO-----RRRKNWNSYKKDWKKRNEVEY					
Clone (H)	KLIGKKVVRTVLDTLYDVMKKSQEDVKE-----DSRVGE-----G--E-----G					
Clone (E)	KTDWEKGGENSFR--YIVRDEKITRRIGDSRVGE-----G--E-----G					
Genebank	KLIGKKVVRTVLDTLYDVMKKSQEDVKETEAELEKVKAVKEEKWNSYKKDWKKRNEVEY					

(a)

	490	500	510	520	530	540
Clone (1)	KEFEESAKKETDKEAKDKKSSWSSDLEKRKKKLEKCLKDVKYTKFYNGFKGSLKVGCYD					
Clone (c_D)	KEFEESAKKETDKEAKDKKSSWSSDLEKRKKKLEKCLKDVKYTKFYNGFKGSLKVGCYD					
Clone (c_A)	KEFEESAKKETDKEAKDKKSSWSSDLEKRKKKLEKCLKDVKYTKFYNGFKGSLKVGCYD					
Clone (g_B)	KEFEESAKKETDKEAKDKKSSWSSDLEKRKKKLEKCLKDVKYTKFYNGFKGSLKVGCYD					
Clone (g_A)	KEFEESAKKETDKEAKDKKSSWSSDLEKRKKKLEKCLKDVKYTKFYNGFKGSLKVGCYD					
Clone (C_C)	-----					
Clone (3)	-----					
Clone (g_C)	-----					
Clone (12)	KEFEESAKKETDKEAKDKKSSWSSDLEKRKKKLEKCLKDVKYTKFYNGFKGSLKVGCYD					
Clone (H)	SEGGEGMELEGLEKEKGGIRIRVSKERNRGSRKEFMVKFGKEKEGIGEEIKGCRIHEVLQ					
Clone (E)	SEGGEGMELEGLEKEKGGIRIRVSKERNRGSRKEFMVKFGKEKEEIGEEIKGCRIHEVLQ					
Genebank	KEFEESAKKETDKEAKDKKSSWSSDLEKRKKKLEKCLKDVKYTKFYNGFKGSLKVGCYD					

	550	560	570	580	590	600
Clone (1)	DDQNRKKIARLLRYKTLFSEKELTFDEYVEKMPPEEQTEIYYVTNENYDDLKQLPHIQGLK					
Clone (c_D)	DDQNRKKIARLLRYKTLFSEKELTFDEYVEKMPPEEQTEIYYVTNENYDDLKQLPHIQGLK					
Clone (c_A)	DDQNRKKIARLLRYKTLFSEKELTFDEYVEKMPPEEQTEIYYVTNENYDDLKQLPHIQGLK					
Clone (g_B)	DDQNRKKIARLLRYKTLFSEKELTFDEYVEKMPPEEQTEIYYVTNENYDDLKQLPHIQGLK					
Clone (g_A)	DDQNRKKIARLLRYKTLFSEKELTFDEYVEKMPPEEQTEIYYVTNENYDDLKQLPHIQGLK					
Clone (C_C)	-----					
Clone (3)	-----					
Clone (g_C)	-----					
Clone (12)	DDQNRKKIARLLRYKTLFSEKELTFDEYVEKMPPEEQTEIYYVTNENYDDLKQLPHIQGLK					
Clone (H)	WIQGKFEGRLRPE--QENCKTIKVDVVKGAYIVCENARGTNDILRNKKLRPTVASHS					
Clone (E)	WIQGKFEGRLRPE--QENCKTIKVDVVKGAYIVCENARGTNDILRNKKLRPTVASHS					
Genebank	DDQNRKKIARLLRYKTLFSEKELTFDEYVEKMPPEEQTEIYYVTNENYDDLKQLPHIQGLK					

	610	620	630	640	650	660
Clone (1)	KRKYDVLYLHDTMDEGCLTKLEEHHGKKFKNVQKADLNLKLTDEEQKEEERK--ETKYKP					
Clone (c-D)	KRKYDVLYLHDTMDEGCLTKLEEHHGKKFKNVQKADLNLKLTDEEQKEEERK--ETKYKP					
Clone (c_A)	KRKYDVLYLHDTMDEGCLTKLEEHHGKKFKNVQKADLNLKLTDEEQKEEERK--ETKYKP					
Clone (g_B)	KRKYDVLYLHDTMDEGCLTKLEEHHGKKFKNVQKADLNLKLTDEEQKEEERK--ETKYKP					
Clone (g_A)	KRKYDVLYLHDTMDEGCLTKLEEHHGKKFKNVQKADLNLKLTDEEQKEEERK--ETKYKP					
Clone (C_C)	-----					
Clone (3)	-----					
Clone (g_C)	-----					
Clone (12)	KRKYDVLYLHDTMDEGCLTKLEEHHGKKFKNVQKADLNLKLTDEEQKEEERK--ETKYKP					
Clone (H)	RPEEKVCAIPSRHNRGGLDKTGAQQEVOQKRPKGRLEPKTDGTEGRTEGDVAAPFVP					
Clone (E)	RPEEKVCAIPSRHNRGGLDKTGAQQEVOQKRPKGRLEPKTDGTEGRTEGDVAAPFVP					
Genebank	KRKYDVLYLHDTMDEGCLTKLEEHHGKKFKNVQKADLNLKLTDEEQKEEERK--ETKYKP					

	670	680	690	700	710	720
Clone (1)	LLLYLKDLLPETSQVGLSRRLVEDPCTVVASEWSMPSHMEKLMKSYAVHRDSSFDMFNKL					
Clone (c_D)	LLLYLKDLLPETSQVGLSRRLVEDPCTVVASEWSMPSHMEKLMKSYAVHRDSSFDMFNKL					
Clone (c_A)	LLLYLKDLLPETSQVGLSRRLVEDPCTVVASEWSMPSHMEKLMKSYAVHRDSSFDMFNKL					
Clone (g_B)	LLLYLKDLLPETSQVGLSRRLVEDPCTVVASEWSMPSHMEKLMKSYAVHRDSSFDMFNKL					
Clone (g_A)	LLLYLKDLLPETSQVGLSRRLVEDPCTVVASEWSMPSHMEKLMKSYAVHRDSSFDMFNKL					
Clone (C_C)	-----VEDPCTVVASEWSMPSHMEKLMKSYAVHRDSSFDMFNKL					
Clone (3)	-----CTVVASEWSMPSHMEKLMKSYAVHRDSSFDMFNKL					
Clone (g_C)	-----VHSGCLRNVNVI SHGKAHEVLCSSQRRO----FDMFNKL					
Clone (12)	LLLYLKDLLPETSQVGLSRRLVEDPCTVVASEWSMPSHMEKLMKSYAVHRDSSFDMFNKL					
Clone (H)	QGSFARNLW---SVVKKACRFVHSGCLRNVNVI SHGKAHEVLCSS---QRQFHVQQTQQ					
Clone (E)	QGSFARNLW---SVVKKACRFVHSGCLRNVNVI SHGKAHEVLCSS---QRQFHVQQTQQ					
Genebank	LLLYLKDLLPETSQVGLSRRLVEDPCTVVASEWSMPSHMEKLMKSYAVHRDSSFDMFNKL					

(a)

	730	740	750	760	770	780
Clone (1)	NSKVLELNPDPHPIMVKLLYLTYTQTKLDKVDKKDEQKDKSVEKEEESKEDESKDKDKETK					
Clone (c_D)	NSKVLELNPDPHPIMVKLLYLTYTQTKLDKVDKKDEQKDKSVEKEEESKEDESKDKDKETK					
Clone (c_A)	NSKVLELNPDPHPIMVKLLYLTYTQTKLDKVDKKDEQKDKSVEKEEESKEDESKDKDKETK					
Clone (g_B)	NSKVLELNPDPHPIMVKLLYLTYTQTKLDKVDKKDEQKDKSVEKEEESKEDESKDKDKETK					
Clone (g_A)	NSKVLELNPDPHPIMVKLLYLTYTQTKLDKVDKKDEQKDKSVEKEEESKEDESKDKDKETK					
Clone (C_C)	NSKVLELNPDPHPIMVKLLYLTYTQTKLDKVDKKDEQKDKSVEKEEESKEDESKDKDKETK					
Clone (3)	NSKVLELNPDPHPIMVKLLYLTYTQTKLDKVDKKDEQKDKSVEKEEESKEDESKDKDKETK					
Clone (g_C)	NSKVLELNPDPHPIMVKLLYLTYTQTKLDKVDKKDEQKDKSVEKEEESKEDESKDKDKETK					
Clone (12)	NSKVLELNPDPHPIMVKLLYLTYTQTKLDKVDKKDEQKDKSVEKEEESKEDESKDKDKETK					
Clone (H)	GTRTSPSN--HGQTPLFLYNSKTRSGKGTKRKCRKGRKGRVRRRNARNIEFRKGNIR					
Clone (E)	GTRTSPSN--HGQTPLFLYNSKTRSGKGTKRKCRKGRKGRVGRRNARNIEFRKGNIR					
Genebank	NSKVLELNPDPHPIMVKLLYLTYTQTKLDKVEKKDEQKDKSVEKEEESKEDESKDKNEETK					

	790	800	810	820	830	840
Clone (1)	EDETksKEDESKDKETESKDEKELEEKrkELTEKkkkYMKRLDRlFKLLYNAAKLKSGFV					
Clone (c_D)	EDETksKEDESKDKETESKDEKELEEKrkELTEKkkkYMKRLDRlFKLLYNAAKLKSGFV					
Clone (c_A)	EDETksKEDESKDKETESKDEKELEEKrkELTEKkkkYMKRLDRlFKLLYNAAKLKSGFV					
Clone (g_B)	EDETksKEDESKDKETESKDEKELEEKrkELTEKkkkYMKRLDRlFKLLYNAAKLKSGFV					
Clone (g_A)	EDETksKEDESKDKETESKDEKELEEKrkELTEKkkkYMKRLDRlFKLLYNAAKLKSGFV					
Clone (C_C)	EDETksKEDESKDKETESKDEKELEEKrkELTEKkkkYMKRLDRlFKLLYNAAKLKSGFV					
Clone (3)	EDETksKEDESKDKETESKDEKELEEKrkELTEKkkkYMKRLDRlFKLLYNAAKLKSGFV					
Clone (g_C)	EDETksKEDESKDKETESKDEKELEEKrkELTEKkkkYMKRLDRlFKLLYNAAKLKSGFV					
Clone (12)	EDETksKEDESKDKETESKDEKELEEKrkELTEKkkkYMKRLDRlFKLLYNAAKLKSGFV					
Clone (H)	-----KRIGREKKGINREEEKVYEEIG--IVVIVRSQVKEWFR					
Clone (E)	-----KRIGREKKGINREEEKVYEEIG--IVVIVRSQVKEWFR					
Genebank	-DETksKEDESKDKETESKDEKELEEKrkELTEKkkkYMKRLDRlFKLLYNAAKLKSGFV					

	850	860	870	880	890	900
Clone (1)	LEEPQLVVNYLYEKLNRS LGDFVEKDFEFTKNLTLDDFEVEKEEVKEPDSVENLEGQKKM					
Clone (c_D)	LEEPQLVVNYLYEKLNRS LGDFVEKDFEFTKNLTLDDFEVEKEEVKEPDSVENLEGQKKM					
Clone (c_A)	LEEPQLVVNYLYEKLNRS LGDFVEKDFEFTKNLTLDDFEVEKEEVKEPDSVENLEGQKKM					
clone (g_B)	LEEPQLVVNYLYEKLNRS LGDFVEKDFEFTKNLTLDDFEVEKEEVKEPDSVENLEGQKKM					
clone (g_A)	LEEPQLVVNYLYEKLNRS LGDFVEKDFEFTKNLTLDDFEVEKEEVKEPDSVENLEGQKKM					
Clone (C_C)	LEEPQLVVNYLYEKLNRS LGDFVEKDFEFTKNLTLDDFEVEKEEVKEPDSVENLEGQKKM					
Clone (3)	LEEPQLVVNYLYEKLNRS LGDFVEKDFEFTKNLTLDDFEVEKEEVKEPDSVENLEGQKKM					
Clone (g_C)	LEEPQLVVNYLYEKLNRS LGDFVEKDFEFTKNLTLDDFEVEKEEVKEPDSVENLEGQKKM					
clone (12)	LEEPQLVVNYLYEKLNRS LGDFVEKDFEFTKNLTLDDFEVEKEEVKEPDSVENLEGQKKM					
Clone (H)	VR--RATVGC LLVKAQVIGRF CRKRLVYQK---SDTRRLGKGGSK-----G-ACRKSRR					
Clone (E)	VR--RATVGC LLVKAQVIGRF CRKRLVYQK---SDTRRLGKGGSK-----G-ACRKSRR					
Genebank	LEEPQLVVNYLYEKLNRS LGDFVEKDFEFTKNLTLDDFEVEKEEVKEPDSVENLEGQKKM					

	910	920	930	940	950	960
Clone (1)	DDEDVFKLDEVEY PGKEDEKTPEERKKQLEEASVDLKEILQGRGPEGFDLTGGTVGDTGG					
Clone (c_D)	DDEDVFKLDEVEY PGKEDEKTPEERKKQLEEASVDLKEILQGRGPEGFDLTGGTVGDTGG					
Clone (c_A)	DDEDVFKLDEVEY PGKEDEKTPEERKKQLEEASVDLKEILQGRGPEGFDLTGGTVGDTGG					
Clone (g_B)	DDEDVFKLDEVEY PGKEDEKTPEERKKQLEEASVDLKEILQGRGPEGFDLTGGTVGDTGG					
Clone (g_A)	VDEDVFKLDEVEY PGKEDEKTPEERKKQLEEASVDLKEILQGRGPEGFDLTGGTVGDTGG					
Clone (C_C)	DDEDVFKLDEVEY PGKEDEKTPEERKKQLEEASVDLKEILQGRGPEGFDLTGGTVGDTGG					
Clone (3)	DDEDVFKLDEVEY PGKEDEKTPEERKKQLEEASVDLKEILQGRGPEGFDLTGGTVGDTGG					
Clone (g_C)	DDEDVFKLDEVEY PGKEDEKTPEEGKKQLEEASVDLKEILQGRGPEGFDLTGGTVGDTGG					
Clone (12)	DDEDVFKLDEVEY PGKEDEKTPEERKKQLEEASVDLKEILQGRGPEGFDLTGGTVGDTGG					
Clone (H)	TEENGRRCIQVRSRISRKRKNTRRKEKTTGRCRSKRNF-ARGSRRI-LNRRNCWHRRR					
Clone (E)	TEENGRRCIQVRSRISRKRKNTRRKEKTTGRCRSKRNF-ARGSRRIWLNRRNCWRRRR					
Genebank	DDEDVFKLDEVEY PGKEDEKTPEERKKQLEEASVDLKEILQGRGPEGFDLTGGTVGDTGG					

(b)

	10	20	30	40	50	60
Clone (1)	MNPRLGFRINRYRTNIVNLSHSAFFCLIFFFLYITFCYWTWGRLTLTSHLNPTYNYKNNLVP					
Clone (3)	MNPRLGFRINRYRTNIVNLSHSAFFCLIFFFLYITFCYWTWGRLTLTSHLNPTYNYKNNLVP					
Clone (5)	MNPRLGFRINRYRTNIVNLSHSAFFCLIFFFLYITFCYWTWGRLTLTSHLNPTYNYKNNLVP					
Clone (4)	MNPRLGFRINRYRTNIVNLSHSAFFCLIFFFLYITFCYWTWGRLTLTSHLNPTYNYKNNLVP					
Clone (6)	MNPRLGFRINRYRTNIVNLSHSAFFCLIFFFLYITFCYWTWGRLTLTSHLNPTYNYKNNLVP					
Clone (2)	MNPRLGFRINRYRTNIVNLSHSAFFCLIFFFLYITFCYWTWGRLTLTSHLNPTYNYKNNLVP					
Genebank	MNPRLGFRINRYRTNIVNLSHSAFFCLIFFFLYITFCYWTWGRLTLTSHLNPTYNYKNNLVP					
	70	80	90	100	110	120
Clone (1)	SSIKNHHEFKSNALEDLTNKVSGLKDVLQKQKFGLSNELTTTDNAQVSKYEGERPAEPKKE					
Clone (3)	SSIKNHHEFKSNALEDLTNKVSGLKDVLQKQKFGLSNELTTTDNAQVSKYEGERPAEPKKE					
Clone (5)	SSIKNHHEFKSNALEDLTNKVSGLKDVLQKQKFGLSNELTTTDNAQVSKYEGERPAEPKKE					
Clone (4)	SSIKNHHEFKSNALEDLTNKVSGLKDVLQKQKFGLSNELTTTDNAQVSKYEGERPAEPKKE					
Clone (6)	SSIKNHHEFKSNALEDLTNKVSGLKDVLQKQKFGLSNELTTTDNAQVSKYEGERPAEPKKE					
Clone (2)	SSIKNHHEFKSNALEDLTNKVSGLKDVLQKQKFGLSNELTTTDNAQVSKYEGERPAEPKKE					
Geneban	SSIKNHHEFKSNALEDLTNKVSGLKDVLQKQKFGLSNELTTTDNAQVSKYEGERPAEPKKE					
	130	140	150	160	170	180
Clone (1)	EAQELTSLSGEQTYPFQAEVSRVMDIVNSLYTDRDIFLRELVSNSADALDKRRLKADPEE					
Clone (3)	EAQELTSLSGEQTYPFQAEVSRVMDIVNSLYTDRDIFLRELVSNSADALDKRRLKADPEE					
Clone (5)	EAQELTSLSGEQTYPFQAEVSRVMDIVNSLYTDRDIFLRELVSNSADALDKRRLKADPEE					
Clone (4)	EAQELTSLSGEQTYPFQAEVSRVMDIVNSLYTDRDIFLRELVSNSADALDKRRLKADPEE					
Clone (6)	EAQELTSLSGEQTYPFQAEVSRVMDIVNSLYTDRDIFLRELVSNSADALDKRRLKADPEE					
Clone (2)	EAQELTSLSGEQTYPFQAEVSRVMDIVNSLYTDRDIFLRELVSNSADALDKRRLKADPEE					
Genebank	EAQELTSLSGEQTYPFQAEVSRVMDIVNSLYTDRDIFLRELVSNSADALDKRRLKADPEE					
	190	200	210	220	230	240
Clone (1)	KIPKEAFGGIRIMPKNKELSTLTIEDDGIGMTAEELKTNLGTIAESGTAKFLEQIEITGNN					
Clone (3)	KIPKEAFGGIRIMPKNKELSTLTIEDDGIGMTAEELKTNLGTIAESGTAKFLEQIEITGNN					
Clone (5)	KIPKEAFGGIRIMPKNKELSTLTIEDDGIGMTAEELKTNLGTIAESGTAKFLEQIEITGNN					
Clone (4)	KIPKEAFGGIRIMPKNKELSTLTIEDDGIGMTAEELKTNLGTIAESGTAKFLEQIEITGNN					
Clone (6)	KIPKEAFGGIRIMPKNKELSTLTIEDDGIGMTAEELKTNLGTIAESGTAKFLEQIEITGNN					
Clone (2)	KIPKEAFGGIRIMPKNKELSTLTIEDDGIGMTAEELKTNLGTIAESGTAKFLEQIEITGNN					
Genebank	KIPKEAFGGIRIMPKNKELSTLTIEDDGIGMTAEELKTNLGTIAESGTAKFLEQIEITGNN					
	250	260	270	280	290	300
Clone (1)	NLIGQFGVGFYSSYLVSNNKVEVFSRAYGQENGPVYRWKSDSNGTYTIGKVENQELNEKFM					
Clone (3)	NLIGQFGVGFYSSYLVSNNKVEVFSRAYGQENGPVYRWKSDSNGTYTIGKVENQELNEKFM					
Clone (5)	NLIGQFGVGFYSSYLVSNNKVEVFSRAYGQENGPVYRWKSDSNGTYTIGKVENQELNEKFM					
Clone (4)	NLIGQFGVGFYSSYLVSNNKVEVFSRAYGQENGPVYRWKSDSNGTYTIGKVENQELNEKFM					
Clone (6)	NLIGQFGVGFYSSYLVSNNKVEVFSRAYGQENGPVYRWKSDSNGTYTIGKVENQELNEKFM					
Clone (2)	NLIGQFGVGFYSSYLVSNNKVEVFSRAYGQENGPVYRWKSDSNGTYTIGKVENQELNEKFM					
Genebank	NLIGQFGVGFYSSYLVSNNKVEVFSRAYGQENGPVYRWKSDSNGTYTIGKVENQELNEKFM					
	310	320	330	340	350	360
Clone (1)	KCGTRIVLHLKPECDDYLEDYKLELLRKYSEFIRFPIQVWVERIEYERVPDDATIVDGK					
Clone (3)	KCGTRIVLHLKPECDDYLEDYKLELLRKYSEFIRFPIQVWVERIEYERVPDDATIVDGK					
Clone (5)	KCGTRIVLHLKPECDDYLEDYKLELLRKYSEFIRFPIQVWVERIEYERVPDDATIVDGK					
Clone (4)	KCGTRIVLHLKPECDDYLEDYKLELLRKYSEFIRFPIQVWVERIEYERVPDDATIVDGK					
Clone (6)	KCGTRIVLHLKPECDDYLEDYKLELLRKYSEFIRFPIQVWVERIEYERVPDDATIVDGK					
Clone (2)	KCGTRIVLHLKPECDDYLEDYKLELLRKYSEFIRFPIQVWVERIEYERVPDDATIVDGK					
Genebank	KCGTRIVLHLKPECDDYLEDYKLELLRKYSEFIRFPIQVWVERIEYERVPDDATIVDGK					

(b)

	370	380	390	400	410	420
Clone (1)	AGRYKTVTKKRHEWEVNTQLPIWRRDQATIKPEDYISFYKSTFKAYEDPLSYIHFKVEG					
Clone (3)	AGRYKTVTKKRHEWEVNTQLPIWRRDQATIKPEDYISFYKSTFKAYEDPLSYIHFKVEG					
Clone (5)	AGRYKTVTKKRHEWEVNTQLPIWRRDQATIKPEDYISFYKSTFKAYEDPLSYIHFKVEG					
Clone (4)	AGRYKTVTKKRHEWEVNTQLPIWRRDQATIKPEDYISFYKSTFKAYEDPLSYIHFKVEG					
Clone (6)	AGRYKTVTKKRHEWEVNTQLPIWRRDQATIKPEDYISFYKSTFKAYEDPLSYIHFKVEG					
Clone (2)	AGRYKTVTKKRHEWEVNTQLPIWRRDQATIKPEDYISFYKSTFKAYEDPLSYIHFKVEG					
Genebank	AGRYKTVTKKRHEWEVNTQLPIWRRDQATIKPEDYISFYKSTFKAYEDPLSYIHFKVEG					

	430	440	450	460	470	480
Clone (1)	QVEFTCLLFVPGTLPWELSRNMFDEESRGIRLYVKRVFINDKFSSEI PRWLT FVRGVVDS					
Clone (3)	QVEFTCLLFVPGTLPWELSRNMFDEESRGIRLYVKRVFINDKFSSEI PRWLT FVRGVVDS					
Clone (5)	QVEFTCLLFVPGTLPWELSRNMFDEESRGIRLYVKRVFINDKFSSEI PRWLT FVRGVVDS					
Clone (4)	QVEFTCLLFVPGTLPWELSRNMFDEESRGIRLYVKRVFINDKFSSEI PRWLT FVRGVVDS					
Clone (6)	QVEFTCLLFVPGTLPWELSRNMFDEESRGIRLYVKRVFINDKFSSEI PRWLT FVRGVVDS					
Clone (2)	QVEFTCLLFVPGTLPWELSRNMFDEESRGIRLYVKRVFINDKFSSEI PRWLT FVRGVVDS					
Genebank	QVEFTCLLFVPGTLPWELSRNMFDEESRGIRLYVKRVFINDKFSSEI PRWLT FVRGVVDS					

	490	500	510	520	530	540
Clone (1)	DELSLVGREYLQRTKALTVINKRIASKAIDMLKNLKNKPRFQKFCENYGKYIKIGVVE					
Clone (3)	DELSLVGREYLQRTKALTVINKRIASKAIDMLKNLKNKPRFQKFCENYGKYIKIGVVE					
Clone (5)	DELSLVGREYLQRTKALTVINKRIASKAIDMLKNLKNKPRFQKFCENYGKYIKIGVVE					
Clone (4)	DELSLVGREYLQRTKALTVINKRIASKAIDMLKNLKNKPRFQKFCENYGKYIKIGVVE					
Clone (6)	DELSLVGREYLQRTKALTVINKRIASKAIDMLKNLKNKPRFQKFCENYGKYIKIGVVE					
Clone (2)	DELSLVGREYLQRTKALTVINKRIASKAIDMLKNLKNKPRFQKFCENYGKYIKIGVVE					
Genebank	DELSLVGREYLQRTKALTVINKRIASKAIDMLKNLKNKPRFQKFCENYGKYIKIGVVE					

	550	560	570	580	590	600
Clone (1)	DRDNQQELASLTTFRSTKEKSTLLDDYIQRMKKQPAIYFISADSEQSAQNSPSLEKFNQ					
Clone (3)	DRDNQQELASLTTFRSTKEKSTLLDDYIQRMKKQPAIYFISADSEQSAQNSPSLEKFNQ					
Clone (5)	DRDNQQELASLTTFRSTKEKSTLLDDYIQRMKKQPAIYFISADSEQSAQNSPSLEKFNQ					
Clone (4)	DRDNQQELASLTTFRSTKEKSTLLDDYIQRMKKQPAIYFISADSEQSAQNSPSLEKFNQ					
Clone (6)	DRDNQQELASLTTFRSTKEKSTLLDDYIQRMKKQPAIYFISADSEQSAQNSPSLEKFNQ					
Clone (2)	DRDNQQELASLTTFRSTKEKSTLLDDYIQRMKKQPAIYFISADSEQSAQNSPSLEKFNQ					
Genebank	DRDNQQELASLTTFRSTKEKSTLLDDYIQRMKKQPAIYFISADSEQSAQNSPSLEKFNQ					

	610	620	630	640	650	660
Clone (1)	LDYEVLYSLEPVDEFCLSSLMASKYKGIMIQDVNKHDKVIGESKSLTETSTTEGKTKEAP					
Clone (3)	LDYEVLYSLEPVDEFCLSSLMASKYKGIMIQDVNKHDKVIGESKSLTETSTTEGKTKEAP					
Clone (5)	LDYEVLYSLEPVDEFCLSSLMASKYKGIMIQDVNKHDKVIGESKSLTETSTTEGKTKEAP					
Clone (4)	LDYEVLYSLEPVDEFCLSSLMASKYKGIMIQDVNKHDKVIGESKSLTETSTTEGKTKEAP					
Clone (6)	LDYEVLYSLEPVDEFCLSSLMASKYKGIMIQDVNKHDKVIGESKSLTETSTTEGKTKEAP					
Clone (2)	LDYEVLYSLEPVDEFCLSSLMASKYKGIMIQDVNKHDKVIGESKSLTETSTTEGKTKEAP					
Genebank	LDYEVLYSLEPVDEFCLSSLMASKYKGIMIQDVNKHDKVIGESKSLTETSTTEGKTKEAP					

	670	680	690	700	710	720
Clone (1)	RGDFEMLCNWLKTTFFPERVQEVKVSRLVESPALLVQADFGLSPSMQKYMRRQATSAGMN					
Clone (3)	RGDFEMLCNWLKTTFFPERVQEVKVSRLVESPALLVQADFGLSPSMQKYMRRQATSAGMN					
Clone (5)	RGDFEMLCNWLKTTFFPERVQEVKVSRLVESPALLVQADFGLSPSMQKYMRRQATSAGMN					
Clone (4)	RGDFEMLCNWLKTTFFPERVQEVKVSRLVESPALLVQADFGLSPSMQKYMRRQATSAGMN					
Clone (6)	RGDFEMLCNWLKTTFFPERVQEVKVSRLVESPALLVQADFGLSPSMQKYMRRQATSAGMN					
Clone (2)	RGDFEMLCNWLKTTFFPERVQEVKVSRLVESPALLVQADFGLSPSMQKYMRRQATSAGMN					
Genebank	RGDFEMLCNWLKTTFFPERVQEVKVSRLVESPALLVQADFGLSPSMQKYMRRQATSAGMN					

(b)

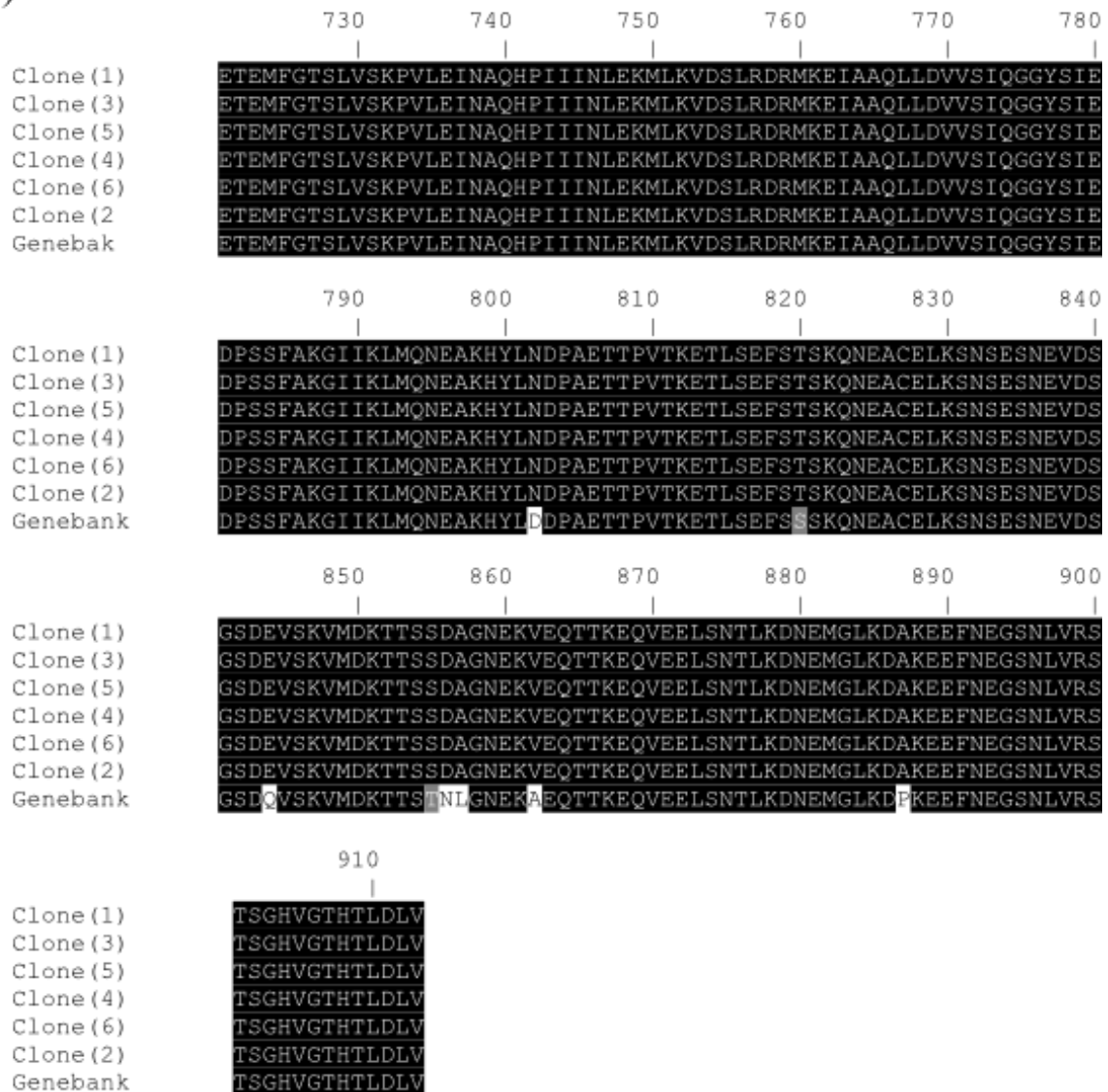


Figure 45: Alignment of the amino acid sequence of the clones of TaHSP90-Chr1 and TaHSP90-Chr4.

(a) Alignment of the amino acid sequence of *T. annulata* TaHSP90-Chr1 sequenced clones (c-D, 1, c-A, g-B, g-A, C-C, 3, g-C, 12, H and E) with *T.annulata* HSP90 reference sequence (Accession: XM\_948749).

(b) Alignment of the amino acid sequence of *T. annulata* TaHSP90-Chr4 sequenced clones (1–6) with *T. annulata* HSP90 from the reference sequence (Accession: XM\_948193.1).

## 9.6.2 Comparison of the deduced amino acid sequences of TaHSP90-Chr1 with TaHSP90-Chr4

```

          10      20      30      40      50      60
          |      |      |      |      |      |
TaHSP90_Chr1 -----MKVSLLLLIKLFILQLNKGYHFVS-----
TaHSP90_Chr4 MNPRLGFRINRYRTNIVNLSHSAFFCLIFFLYITFCYTWGTGRLTLTSHLNPYTNKNNLVP
          : : * : : * : * : * : . * : : .
          70      80      90      100     110     120
          |      |      |      |      |      |
TaHSP90_Chr1 -----CNESGELEVVEDTVNVEDVTEEQTPSELSEEEELLDRSEDSSVLTS
TaHSP90_Chr4 SSIKNHHEFKSNALEDLTNKNVSGLKDVLLQKQFGLSNELTTTDNAQVSKYEGEPAEPKQVE
          : : : : : : * : : : . : : : * * : : : : : . : . : . : .
          130     140     150     160     170     180
          |      |      |      |      |      |
TaHSP90_Chr1 EKLFKDSTKSEKYEQAEVTRLLDIIVNSLYSSKDI FLRELVSNSADALEKYKITALQKN
TaHSP90_Chr4 EAQELTLSGEQTYPFQAEVSRVMDIIVNSLYTDRDI FLRELVSNSADALDKRRLKADPE-
          * : : : * : * * * : * : * * * * * : : * * * * * * * * * * * : : : * :
          190     200     210     220     230     240
          |      |      |      |      |      |
TaHSP90_Chr1 YRDKDDVELFVRI RSYPKK--RL LTIW DNGVGMTKTEL MNNLGTIAKSGTANFLDSL SKA
TaHSP90_Chr4 --EKIPKEAFGGIRIMP NKELSTLTI EDDGIGMTAEELKTNLGTIAESGTAKFLEQIEIT
          : * * * * * * * * * * * * * * * * * * * * * * * * * * * * * : : : :
          250     260     270     280     290     300
          |      |      |      |      |      |
TaHSP90_Chr1 GSDPNLIGQFGVGFYS AFLVADTVLVQSKNYDDKQ---YVWRSSAANNYEL----YEDTD
TaHSP90_Chr4 GNN-NLIGQFGVGFYSSYLVS NKVEVFSRAYGQENGPVYRWKSDSNGTYTIGKVENQELN
          * : : * * * * * * * * * * * * * * * * * * * * * * * * * * * * * : : :
          310     320     330     340     350     360
          |      |      |      |      |      |
TaHSP90_Chr1 NSLGDHGT LITLELREDSTEY LKTDVLENLVKKYSQFVRYPIQLYKCLKDKQEVG-----
TaHSP90_Chr4 EKFMKCGTRIVLHLKPECD DYLEDYK LKELLRKYSEFIRFPIQVWVERIEYERVPDDATI
          : : : . * * * . * . * : : : * * : * : * : * * * * * * * * * * : : : *
          370     380     390     400     410     420
          |      |      |      |      |      |
TaHSP90_Chr1 -----WVKVNETQQI WTRNKNTIT EEEYNQFYKTISGKNDEPLTHVHF
TaHSP90_Chr4 VDGKAGRYKTVTKKRHEW EVVNTQLPI WRRDQATIKPEDYISFYKSTFKAYEDPLSYIHF
          * * * * * * * * * * * * * * * * * * * * * * * * * * * * *
          430     440     450     460     470     480
          |      |      |      |      |      |
TaHSP90_Chr1 TAEGDVDFKALLYIPSS PPGMYFS--TESVGHNVKLYSRRVLVSQEMKDFIPRYLFSIYG
TaHSP90_Chr4 KVEGQVEFTCLL FVPGTLPWELSRNMFDEESRGIRLYVKRVFINDKFSSESIPRWLTFVRG
          . . * * * : * . * * : * : * : : : * * * * * * * * * * * * * * * * : *
          490     500     510     520     530     540
          |      |      |      |      |      |
TaHSP90_Chr1 VVDSDFSPLNVSREYLQ QSKLVK LIGKVVRTVLD TLYDVMKKSQEDVKETEAELEKVKVA
TaHSP90_Chr4 VVDSDELSLNVGREYLQ RTKALT VINKRIASKAIDMLKNLKN-----N-----
          * * * * * : : * * * * * * * * * * * * * * * * * * * * * * * * *

```



## 9.7 Bioinformatic analysis of TaHSP90-Chr1 and TaHSP90-Chr4

Bioinformatic analysis of the deduced amino acid sequence of TaHSP90-Chr1 and TaHSP90-Chr4 was performed using different websites to determine the functional domain.

Table 21: Bioinformatic analysis of TaHSP90-Chr1.

Website	Start*	End*
<a href="http://www.sanger.ac.uk/">http://www.sanger.ac.uk/</a>	288	738
<a href="http://www.ncbi.nlm.nih.gov/Structure/cdd/wrpsb.cgi">http://www.ncbi.nlm.nih.gov/Structure/cdd/wrpsb.cgi</a>	76 262 523	445 433 736
<a href="http://swissmodel.expasy.org/workspace/index.php?func=workspace&amp;templateidentification&amp;userid=swissmodel@unibas.ch&amp;token=TOKEN&amp;key=2f7914bb182975ff86cab493b454c88d&amp;prjid=P003340#I PF02518">http://swissmodel.expasy.org/workspace/index.php?func=workspace&amp;templateidentification&amp;userid=swissmodel@unibas.ch&amp;token=TOKEN&amp;key=2f7914bb182975ff86cab493b454c88d&amp;prjid=P003340#I PF02518</a>	301	736
<a href="http://www.genedb.org">http://www.genedb.org</a>	300	736
<a href="http://www.ebi.ac.uk/Tools/services/web_iprscan/toolresult.ebi?tool=iprscan&amp;jobId=iprscan-I20120606-090445-0662-44269786-oy">http://www.ebi.ac.uk/Tools/services/web_iprscan/toolresult.ebi?tool=iprscan&amp;jobId=iprscan-I20120606-090445-0662-44269786-oy</a>	288	738

\* Positions of amino acid at which the HSP90 domain starts and ends.

Table 22: Bioinformatic analysis of TaHSP90-Chr4.

Website	Start*	End*
<a href="http://www.sanger.ac.uk/">http://www.sanger.ac.uk/</a>	316	839
<a href="http://www.ncbi.nlm.nih.gov/Structure/cdd/wrpsb.cgi">http://www.ncbi.nlm.nih.gov/Structure/cdd/wrpsb.cgi</a>	128	793
<a href="http://swissmodel.expasy.org/workspace/index.php?func=workspace&amp;templateidentification&amp;userid=swissmodel@unibas.ch&amp;token=TOKEN&amp;key=2f7914bb182975ff86cab493b454c88d&amp;prjid=P003340#I PF02518">http://swissmodel.expasy.org/workspace/index.php?func=workspace&amp;templateidentification&amp;userid=swissmodel@unibas.ch&amp;token=TOKEN&amp;key=2f7914bb182975ff86cab493b454c88d&amp;prjid=P003340#I PF02518</a>	316	839
<a href="http://www.genedb.org">http://www.genedb.org</a>	315	839
<a href="http://www.ebi.ac.uk/Tools/services/web_iprscan/toolresult.ebi?tool=iprscan&amp;jobId=iprscan-I20120606-090445-0662-44269786-oy">http://www.ebi.ac.uk/Tools/services/web_iprscan/toolresult.ebi?tool=iprscan&amp;jobId=iprscan-I20120606-090445-0662-44269786-oy</a>	316	823

\*Positions of amino acid at which the HSP90 domain starts and ends.

## 10 List of publications

- 1- **Mohammed, S.B.**, Bakheit, M.A., Ernst, M., Ahmed, J.S., and Seitzer, U. (2013). Identification and Characterization of *Theileria annulata* Heat-Shock Protein 90 (HSP90) Isoforms. *Transbound. Emerg. Dis.* **60**, 137–149.

## 11 Acknowledgements

It would not have been possible to finish this doctoral thesis without the help and support of the kind people around me. Above all, I would like to express my sincere gratitude to my supervisor Prof. Dr. Jabbar Sabir Ahmed for the opportunity to carry out my PhD in his division at the Research Center Borstel, and for his support, great patience and enormous motivation during my work. I am extremely grateful for his encouragement.

My greatest appreciation goes to Prof. Dr. Ulrike Seitzer for being an excellent supervisor, for many great ideas and suggestions and for her support during the first stages of my PhD work. I would like to express my deepest thanks to Dr. Mohammed Bakheit for providing me with many ideas when designing the experimental setup and for his constant scientific advice. In addition, many thanks to Dr. Monika Mackiewicz for her technical and editorial advice greatly improve the content of this thesis. Her helpful and constructive comments on this written work. For this, I am very grateful.

I extend my sincere thanks to all members of the Division of Veterinary Infection-Biology and –Immunology, Research Central Borstel for help with experimental setup and general advice; in particular, I would like to acknowledge the technical help of Ms. Birgit Kullmann and Ms. Doreen Beyer. My thanks also go to my colleagues Dr. Stefanie Renneker, Junlong Liu, Bogdan Oltean and Susan Tschischmann for numerous stimulating discussions.

I am very grateful to Dr. Martin Ernst, Rajia Bahri and Diego Goyeneche for their patience and excellent technical assistance with FACS Calibur System and Light Cycler® 480 system.

I would like to express my gratitude to DAAD for giving me the financial support during my study in Germany.

This work was partially funded by DFG ‘Molecular epidemiology network for promotion and support of delivery of live vaccines against *Theileria parva* and *Theileria annulata* infection in Eastern and Northern Africa’ - project no:AH41/7-1 and EU Project Pirovac ‘Improvement of current and development of new vaccines for theileriosis and babesiosis of small ruminants’ – Grant agreement no: 245145.

## Acknowledgements

---

My deepest appreciation and thanks goes to Ms. Birgit Kullmann and Ms. Doreen Beyer for their great help in many aspects of daily life in Germany. Thank you so much.

I am grateful to all friends and colleagues in Borstel for the friendly atmosphere they provided.

I would like to convey my heartfelt thanks to my parents, brothers, sisters, mother-in-law, brothers-in-law and sisters-in-law for their moral support and patience. Specifically, I would like to thank my husband Dr. AbdElrahman and my kids Hussam and Muram for their unconditional love, support, patience and encouragement.

---

**Declaration of authorship:**

I hereby declare that this thesis is my own work and effort, and I have used only the specified sources and aids. Part of this work has been published in the following publication:

Mohammed, S.B., Bakheit, M.A., Ernst, M., Ahmed, J.S., and Seitzer, U. (2013). Identification and Characterization of *Theileria annulata* Heat-Shock Protein 90 (HSP90) Isoforms. *Transbound. Emerg. Dis.* **60**, 137–149.

Place, date: Borstel, 11.02.2015

Sara Basher Taha Mohammed

---

**Selbständigkeitserklärung:**

Hiermit bestätige ich, dass ich die vorliegende Arbeit selbständig angefertigt habe. Ich versichere, dass ich ausschließlich die angegebenen Quellen und Hilfen Anspruch genommen habe.

Ort, den: Borstel, 11.02.2015

Sara Basher Taha Mohammed